



THE JOURNAL OF PHYSICAL CHEMISTRY

(Registered in U. S. Patent Office)

Founded by Wilder D. Bancroft

SYMPOSIUM ON RADIATION CHEMISTRY, CLEVELAND, OHIO, APRIL 11, 1951

Milton Burton: Symposium on Radiation Chemistry: Introduction.....	545
Frederick F. Morehead, Jr., and Farrington Daniels: Storage of Radiation Energy in Crystalline Lithium Fluoride and Metamict Minerals.....	546
J. A. Ghormley and H. A. Levy: Some Observations of Luminescence of Alkali Halide Crystals Subjected to Ionizing Radiation.....	548
John L. Magee: Elementary Processes in Radiation Chemistry. III. Charge Transfer Mechanisms.....	555
J. P. Manion and Milton Burton: Radiolysis of Hydrocarbon Mixtures.....	560
Lewis H. Gevantman and Russell R. Williams, Jr.: Detection and Identification of Free Radicals in the Radiolysis of Alkanes and Alkyl Iodides.....	569
A. O. Allen, C. J. Hochanadel, J. A. Ghormley and T. W. Davis: Decomposition of Water and Aqueous Solutions under Mixed Fast Neutron and γ -Radiation.....	575
C. J. Hochanadel: Effects of Cobalt γ -Radiation on Water and Aqueous Solutions.....	587
Edwin J. Hart: The Radical Pair Yield of Ionizing Radiation in Aqueous Solutions of Formic Acid.....	594
Samuel Yosim and T. H. Davies: Recoil Atoms from Slow Neutron Capture by Gold and Indium Surfaces.....	599

CONTRIBUTED PAPERS

Samuel Kaufman and C. R. Singletary: The Reaction between Tertiary Amines and Organic Acids in Non-polar Solvents.....	604
Hitosi Hagihara: Surface Oxidation of Galena in Relation to its Flotation as Revealed by Electron Diffraction....	610
Hitosi Hagihara: Mono- and Multilayer Adsorption of Aqueous Xanthate on Galena Surfaces.....	616
S. E. S. El Wakkad and T. M. Salem El Wakkad: Oxide Film Formation on the Surface of Metallic Mercury in Aqueous Solutions and the Anomaly between its Potential and that of the Mercury-Mercuric Oxide Electrode..	621
Hiroshi Fujita: On the Distribution of Liquid Ascending in a Filter Paper.....	625
Sterling B. Olsen: Measurement of Surface Phosphate on Hydroxylapatite and Phosphate Rock with Radiophosphorus.....	630
R. P. Mitra and H. B. Mathur: Titration Curves of the Clay Minerals Attapulgit and Nontronite.....	633
George A. Last and Melvin A. Cook: Collector-Depressant Equilibria in Flotation. I. Inorganic Depressants for Metal Sulfides.....	637
George A. Last and Melvin A. Cook: Collector-Depressant Equilibria in Flotation. II. Depressant Action of Tannic Acid and Quebracho.....	643
Ruth E. Benesch and Reinhold Benesch: The Role of Adsorption in the Reduction of Organic Mercury Compounds at the Dropping Mercury Electrode.....	648
Kenneth T. Waldock and Laurence D. Frizzell: A Study of the Functional Groups of Cationic Exchangers by Infra-red Absorption.....	654
F. H. Buttner, E. R. Funk and H. Udin: Adsorption of Oxygen on Silver.....	657
S. Chu Liang: Low Vapor Pressure Measurement and Thermal Transpiration.....	660
C. S. Rohrer, R. C. Christena and O. W. Brown: The Catalytic Activity of Some Reduced Vanadate Salts.....	662

Founded by Wilder D. Bancroft

THE JOURNAL OF PHYSICAL CHEMISTRY

(Registered in U. S. Patent Office)

W. ALBERT NOYES, JR., EDITOR

ALLEN D. BLISS

ASSISTANT EDITORS

ARTHUR C. BOND

EDITORIAL BOARD

R. P. BELL
E. J. BOWEN
G. E. BOYD

MILTON BURTON
E. A. HAUSER
C. N. HINSHELWOOD
S. C. LIND

W. O. MILLIGAN
J. R. PARTINGTON
J. W. WILLIAMS

Published monthly (except July, August and September) by the American Chemical Society at 20th and Northampton Sts., Easton, Pa.

Entered as second-class matter at the Post Office at Easton, Pennsylvania.

The *Journal of Physical Chemistry* is devoted to the publication of selected symposia in the broad field of physical chemistry and to other contributed papers.

Manuscripts originating in the British Isles, Europe and Africa should be sent to F. C. Tompkins, The Faraday Society, 6 Gray's Inn Square, London W. C. 1, England.

Manuscripts originating elsewhere should be sent to W. Albert Noyes, Jr., Department of Chemistry, University of Rochester, Rochester 3, N. Y.

Correspondence regarding accepted copy, proofs and reprints should be directed to Assistant Editor, Allen D. Bliss, Department of Chemistry, Simmons College, 300 The Fenway, Boston 15, Mass.

Business Office: American Chemical Society, 1155 Sixteenth St., N. W., Washington 6, D. C.

Advertising Office: American Chemical Society, 332 West 42nd St., New York 18, N. Y.

Articles must be submitted in duplicate, typed and double spaced. They should have at the beginning a brief Abstract, in no case exceeding 300 words. Original drawings should accompany the manuscript. Lettering at the sides of graphs (black on white or blue) may be pencilled in, and will be typeset. Figures and tables should be held to a minimum consistent with adequate presentation of information. Photographs will not be printed on glossy paper except by special arrangement. All footnotes and references to the literature should be numbered consecutively and placed on the manuscript at the proper places. Initials of authors referred to in citations should be given. Nomenclature should conform to that used in *Chemical Abstracts*, mathematical characters marked for italic, Greek letters carefully made or annotated, and subscripts and superscripts clearly shown. Articles should be written as briefly as possible consistent with clarity and should avoid historical background unnecessary for specialists.

Symposium papers should be sent in all cases to Secretaries of Divisions sponsoring the symposium, who will be responsible for their transmittal to the Editor. The Secretary of the Division by agreement with the Editor will specify a time after which symposium papers cannot be accepted. The Editor reserves the right to refuse to publish symposium articles, for valid scientific reasons. Each symposium paper may not exceed four printed pages (about sixteen double spaced typewritten pages) in length except by prior arrangement with the Editor.

Remittances and orders for subscriptions and for single copies, notices of changes of address and new professional connections, and claims for missing numbers should be sent to the American Chemical Society, 1155 Sixteenth St., N. W., Washington 6, D. C. Changes of address for the *Journal of Physical Chemistry* must be received on or before the 30th of the preceding month.

Claims for missing numbers will not be allowed (1) if received more than sixty days from date of issue (because of delivery hazards, no claims can be honored from subscribers in Central Europe, Asia, or Pacific Islands other than Hawaii) (2) if loss was due to failure of notice of change of address to be received before the date specified in the preceding paragraph, or (3) if the reason for the claim is "missing from files."

Annual Subscription: \$8.00 to members of the American Chemical Society, \$10.00 to non-members. Postage free to countries in the Pan American Union; Canada, \$0.40; all other countries, \$1.20. Single copies, \$1.25; foreign postage, \$0.15; Canadian postage \$0.05.

The American Chemical Society and the Editors of the *Journal of Physical Chemistry* assume no responsibility for the statements and opinions advanced by contributors to THIS JOURNAL.

The American Chemical Society also publishes *Journal of the American Chemical Society*, *Chemical Abstracts*, *Industrial and Engineering Chemistry*, *Chemical and Engineering News* and *Analytical Chemistry*. Rates on request.

* * * (Continued from first page of cover) * * *

F. E. Bartell and D. Joseph Donahue: Preferential Capillary Adsorption of Water from Solutions of Alcohols by Silica Gel.....	665
W. D. Robertson: Precipitation of Colloidal Ferric Oxide by Corrosion Inhibitor Ions.....	671
College Chemistry. By Linus Pauling. Review by Geoffrey Wilkinson.....	672

THE JOURNAL OF PHYSICAL CHEMISTRY

(Registered in U. S. Patent Office) (Copyright, 1952, by the American Chemical Society)

Founded by Wilder D. Bancroft

VOLUME 56

MAY 15, 1952

NUMBER 5

SYMPOSIUM ON RADIATION CHEMISTRY: INTRODUCTION

BY MILTON BURTON

Department of Chemistry, University of Notre Dame, Notre Dame, Indiana

Received February 25, 1952

Radiation characteristic of nuclear energy presents problems of protection and of possibility of technological application. Evidence has been adduced that certain compounds may protect others and that certain groupings within compounds also confer special resistivity to radiation. Conversely, other compounds and groupings have special features of reactivity. Details of the elementary and gross physical and chemical phenomena ensuing on absorption of radiation must be more thoroughly understood for interpretation of such results and for advancement of this exciting field.

The papers on the present program are a sampling of work in progress and represent merely fragments of the most recent developments of theory and results of experiments in a wide diversity of radiation-chemical studies.

The papers by Morehead and Daniels and by Ghormley and Levy are concerned with details of ionic crystals. They appear recondite but the results of the former may have very important consequences and applications in prospecting for

ore. The paper by Magee is a theoretical examination of some possible phenomena in mixtures and the paper by Manion and myself involves experimental evidence of such phenomena as well as an indication of an important elementary process of excitation transfer, implications of which have not been extensively considered hitherto. In particular, it is shown that under certain conditions the components of a mixture may protect each other. The paper by Williams and Gevantman shows how they have employed radioiodine for tracing details of radiation chemical phenomena in organic systems. The group of three papers by Allen, Hocharadel, Ghormley and Davis, by Hocharadel, and by Hart show how study of a variety of effects in aqueous solution have served both to clarify the phenomena there occurring and to pose some new and unsuspected problems. Finally, the paper by Yosim and Davies takes up one phase of phenomena occurring in pure metals and puts us on the doorstep of what in the past we have considered purely physical phenomena.

STORAGE OF RADIATION ENERGY IN CRYSTALLINE LITHIUM FLUORIDE AND METAMICT MINERALS¹

BY FREDERICK F. MOREHEAD, JR., AND FARRINGTON DANIELS

Chemistry Department of the University of Wisconsin, Madison, Wisconsin

Received February 26, 1962

Measurements have been made on the energy of thermoluminescence obtained when lithium fluoride is exposed to 30,000 roentgens of γ -radiation and then heated to 500°. The bluish light emitted is equivalent to 1.5×10^{-6} calorie per gram and amounts to a storage in electron traps of about 0.005% of the γ -radiation. Metamict minerals have their crystal lattices so damaged by alpha rays from radioactive elements for millions of years that they fail to exhibit an X-ray diffraction pattern. When the temperature is raised to 450°, however, the crystal lattice is restored and at the same time, it has been found in this investigation that there is an evolution of about 25 calories of heat per gram, as measured with a thermal analysis apparatus.

The mechanism by which energy from α -, β - and γ -rays is stored in a crystal lattice is a matter of theoretical interest for studying the nature of the solid state, and it is a matter of practical importance for developing materials for nuclear reactors which will withstand the intense radiation.

When a crystal or semi-conductor is subjected to γ -rays or X-rays part of the energy is absorbed in displacing electrons from their atoms. Some electrons return immediately to their normal positions giving off fluorescent light; others become trapped in lattice imperfections or holes. The trapped electrons give rise to the so-called F-centers which absorb definite wave lengths of light. When the crystals are heated, the increased kinetic energy drives the electrons out of their traps from which they fall eventually to positions of lower energy with the emission of light, a phenomenon known as thermoluminescence.

The thermoluminescence of rocks, which contain uranium, and alkali halides which have been exposed to γ -radiation, has been under investigation in this Laboratory in an attempt to understand better the various ways in which the energy of radiation can be stored. Lithium fluoride has been studied thoroughly and the absolute energy of its thermoluminescence is reported here. It is small, 1.5×10^{-6} calorie per gram, amounting to 0.005% of the γ -radiation absorbed. Although the energy stored in trapped electrons is small it seemed likely that the atoms of the lattice might be displaced also and that this displacement would involve much more energy. In general, where there is light there is apt to be more energy present in the form of heat, but the measurement of small amounts of heat is much more difficult than the measurement of an equivalent amount of light energy. In order to study the storage of energy in crystal lattices attention was turned to metamict minerals which have been exposed for millions of years to α -particles from the considerable amounts of uranium and thorium which they contain. The crystal lattice of metamict minerals has been so damaged by radioactivity that the minerals do not show an X-ray diffraction pattern, but the pattern is easily restored by heating to a sufficiently high temperature. The evolution of energy by the restoration of atoms to their normal positions in the crystal lattice should evolve more heat than is evolved by

the release of trapped electrons. Energy storage as large as 25 calories per gram was found, and other minerals will be examined in the hope of finding still larger amounts of stored energy.

Measurements of Thermoluminescence.—The apparatus for measuring thermoluminescence^{2,3} consists of a light-tight box containing an electrical plate heated at the rate of 1° per second, a photomultiplier tube (RCA 1 P21) and a suitable optical system. The current through the photomultiplier tube is amplified and recorded with a potentiometer in which the intensity of the light is plotted automatically as a function of the time. The temperature of the hot-plate as recorded by a thermocouple is automatically plotted on the same graph, and the heating current is controlled so as to give a linear rise in temperature.

The light intensity as recorded by the photomultiplier tube was calibrated with monochromatic light from an AH-4 mercury lamp at a distance of 25 meters. The energy of this light in turn was calibrated at a distance of one meter with a thermopile which in turn was calibrated with a standard carbon filament lamp provided by the Bureau of Standards. Application of the inverse square law showed that for blue light at 4300 Å. the highest sensitivity for one recorder gave a deflection amounting to 4.1×10^8 divisions per erg per second, and for a second recorder 1.1×10^6 divisions. Farrand interference filters were used with the mercury lamp for 4300 and 5500 Å. and the ratio of the calibrations at these two wave lengths (2.36) agreed within 4% with the ratio of relative values given by the manufacturers.

The crystals of lithium fluoride, 1 cm. square and 1 mm. thick, were obtained from large, clear crystals grown from the molten material by the Harshaw Chemical Company. They were irradiated in a hollow aluminum cylinder surrounded by cobalt powder which had been exposed in the pile of the Oak Ridge National Laboratory and calibrated directly with ionization meters as will be described in a later communication. The density of γ -radiation within the cylinder was 6000 roentgens per hour as determined by three different methods which gave an average deviation of less than 10%.

A spectrogram of the weak thermoluminescent light extends from about 4005 to 4823 Å. It shows regions of varying intensity but no structure can be detected with the instruments used. The midpoint of the emission is taken as 4400 Å.

The sensitivity of the recorder is such as to give a deflection of 1.1×10^6 divisions for one erg per second. The graph paper travels at the rate of 1 inch in 40 seconds. Since there are nine divisions per inch on the recording graph paper, one square inch under the thermoluminescent curve corresponds to $9 \times 40 / 1.1 \times 10^6$ or 3.3×10^{-4} erg. The lens which focuses the light from the crystal onto the photomultiplier tube is 4.5 cm. in diameter and 10.5 cm. from the crystal. Assuming that there is no reflection from the perfect crystal, the total light in all directions for each square inch under the curve of thermoluminescent light intensity, as recorded on the graph paper, is—

$$\frac{4\pi(10.5)^2}{\pi(4.5)^2/4} \times 3.3 \times 10^{-4} = 2.9 \times 10^{-2} \text{ erg}$$

(1) Further details of this research may be obtained from the Master's thesis of Frederick F. Morehead filed in the Library of the University of Wisconsin, June, 1951.

(2) F. Urbach, *Weiner Ber.*, **139**, 353 (1930).

(3) C. A. Boyd, *J. Chem. Phys.*, **17**, 1221 (1949).

For crystals which had a γ -ray exposure of exactly 5 hours, amounting to 30,000 roentgens, the area under the thermoluminescent curve was 2000 square inches per gram when converted to the highest sensitivity. The total light energy emitted is then $2000 \times 2.9 \times 10^{-2}$ erg or 58 ergs or 1.4×10^{-6} calorie. Assuming that the energy of the trapping level is about 10 electron volts above the highest ground level in lithium fluoride, as it is in sodium chloride, the energy of one 4400 Å. photon is 4.5×10^{-12} erg, the number of photons emitted per gram is 1.3×10^{13} , we find that the energy stored by the trapped electrons is 5×10^{-6} cal./g.

Lattice Displacements in Metamict Minerals.—Differential thermal analysis, long used for studying cooling and heating curves in metallurgy, has found extensive use recently in the analysis of clays. The ceramic material can be identified by means of heat effects at definite temperatures due to the melting or oxidation of some of the ingredients. An instrument manufactured by the Eberbach Company was modified for the present investigation. It consists of a metallic block 3 cm. in diameter which contains two cylindrical holes, one for the inert or deactivated (heated) material and the other for the material under investigation. A chromel-“P”-alumel thermocouple measures the difference in temperature between the two, and a second thermocouple measures the temperature of the metal block. A furnace with nichrome coils fits over the metal block and heats it by radiation while the energy input is kept constant by a voltage regulator. A sensitive galvanometer was substituted for the millivoltmeter, and the whole furnace and block was mounted in a gas-tight box so that oxygen could be removed by evacuation or by displacement with nitrogen. The return of the displaced atoms to their normal positions in the lattice at a definite temperature evolves heat, and the object of the experiment is to measure this heat. It is necessary then to eliminate all other sources of exothermic heat such as the oxidation of sulfides.

When there is no evolution or absorption of heat the differential thermocouple reads zero, but if there is a lattice transition, a fusion, or a chemical reaction in one of the two samples of material there will be a galvanometer deflection indicating the absorption of heat or evolution. If one plots this temperature difference against the temperature for a given rate of heating, a minimum in the curve indicates the temperature of heat absorption such as fusion, and a maximum indicates the evolution of heat.

A simple mathematical analysis¹ shows that the area under the curve in which temperature differences are plotted against temperature, is nearly proportional to the heat evolved by the active material. The area under such a curve within a definite temperature range is calibrated in terms of calories with materials of known heats of fusion as follows: tin at 232°, bismuth at 268°, lead at 327°, zinc at 419° and lead chloride at 485°.

A given weight of one of these powdered metals or salts was mixed with inert lithium fluoride powder in one of the holes in the heated block. The calibrations ranged from 2.19×10^{-3} calorie per cm. deflection (scale division) \times degrees at 232° to 3.49×10^{-3} at 485°.

Two radioactive minerals were studied exhaustively by this method. One a polycrase mineral (a titanio-niobate) designated as D-100 was a metamict mineral supplied by Dr. J. C. Rabbitt of the U. S. Geological Survey. The thermal analysis curve for this mineral is shown in the upper half of Fig. 1. The other mineral, shown in the lower half of Fig. 1, came from a radioactive inclusion in a quartz core of pegmatite collected in Ontario by Dr. Donald F. Saunders. It exhibited radial cracks with decreasingly intense smoky color with increasing distance from the radioactive inclusion. The metamict minerals have complex lattice structures containing rare-earth elements.

The metamict mineral shows an exothermic peak at 460° which was the same in air, in nitrogen and in a vacuum of 4 mm., thus showing that it does not involve air-oxidation. The fact that it involves a true change in the crystal lattice is proved by the fact that X-ray diffraction measurements of the mineral showed no patterns with the original mineral, but did show patterns corresponding to a definite crystal lattice after heating above 460°. This peak has an area equivalent to 2700 cm. degrees for a sample weighing 0.5 g. and the energy evolved is $2700 \times 3.5 \times 10^{-3}/0.5$ or 21 calories per gram.

Holland and Kulp⁴ have reported the evolution of heat on heating a metamict crystal.

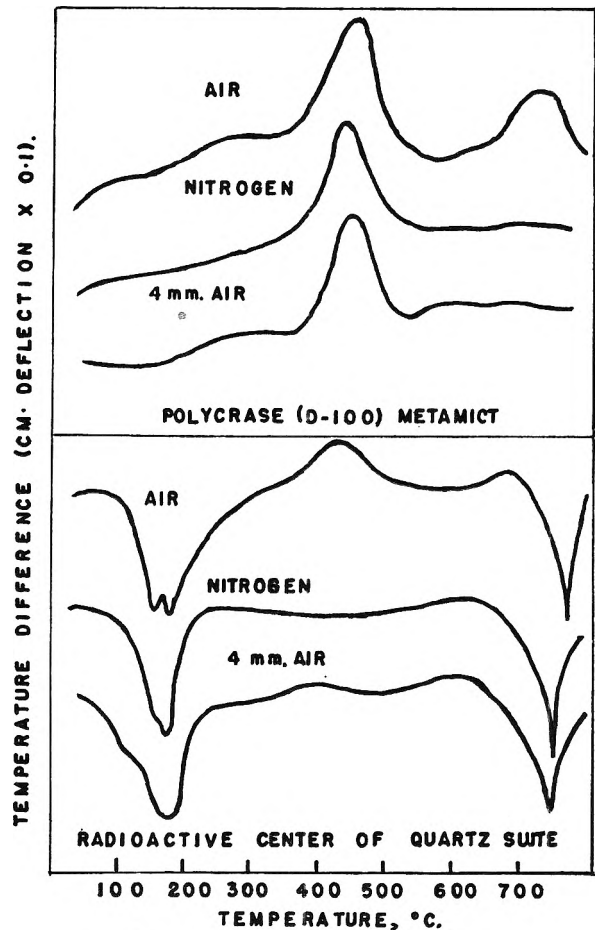


Fig. 1.—Thermal analysis curves.

In the sample of radiation-damaged quartz there are two endothermic transitions or fusions clearly evident but the exothermic peak at about 440° in air disappears when the heating is carried out in nitrogen or in a vacuum. It is probably due to the oxidation of iron or sulfur, and is similar to the peak found by Rowland and Lewis⁵ in the thermal analysis of certain pyritic clays. There is no evidence for exothermic changes in the crystal lattice. It is highly important to exclude the possibility of chemical reactions, particularly air-oxidations, when looking for heat effects which are due to radioactive damage of the crystal lattice.

The present equipment is not sensitive to less than about 1 calorie per gram and all attempts failed to measure the heat evolved when an irradiated crystal of lithium fluoride was heated. One crystal was irradiated with the high voltage electron accelerator at Brookhaven National Laboratory through the courtesy of Dr. A. O. Allen. Although this crystal was nearly black in color it failed to give a measurable quantity of heat when tested in a manner similar to that used for the metamict mineral.

Two additional metamict minerals supplied by Dr. J. C. Rabbitt were run by Mr. Warren E. Thompson in this Laboratory. One (samarskite) gave no evolution of heat; the other (eschybitic-prionite) gave about 20 calories per gram.

Conclusions

The amount of energy stored as trapped electrons in lithium fluoride is very small— 5×10^{-6} calorie or 0.005% of the 30,000 roentgen exposure. This corresponds to 1.3×10^{13} photons of blue light per gram or 4×10^{14} photons per mole. Optical and density measurements of crystals exposed to γ -radiation for long periods of time lead to esti-

(5) R. A. Rowland and D. R. Lewis, *American Mineralogist*, **36**, 80 (1951).

(4) H. D. Holland and J. L. Kulp, *Science*, **111**, 132 (1950)

mates of a saturated value of about 10^{18} trapped electrons per mole. It is not clear why the stored energy capable of producing thermoluminescence is only about one ten-thousandth of the amount expected on the basis of F-center studies. It will be shown in a later communication that thermoluminescence in lithium fluoride does not reach saturation until about 100,000 roentgens and an exposure to γ -radiation much in excess of 32,500 roentgens would have given somewhat greater thermoluminescence, but not more than three times as much. The extremely low efficiency is comparable in magnitude to the efficiency of the production of X-rays by means of electron bombardment of a metal target.

It has been calculated¹ from the geometry of the cobalt source with 6000 roentgens per hour that 4.8×10^7 photons of γ -rays were absorbed per second by the lithium fluoride crystal 1 cm. square and 1 mm. thick. This is equivalent to 0.33×10^{13} photons absorbed per gram during the 5.00 hour exposure of 30,000 roentgens. Since 1.3×10^3 photons of blue thermoluminescent light were emitted, it is seen that 5 photons of thermoluminescent light are emitted for every photon of γ -radiation absorbed.

The experiments with metamict minerals show that the storage of energy from radioactivity, mostly from α -particles, can be very much greater. The mechanism of energy storage is quite different. Although the samples studied thus far give a maximum of 25 calories per gram, other samples of old minerals rich in uranium or thorium will be

studied to ascertain if still greater amounts of energy can be stored under certain conditions. The possible storage of radioactive energy in rocks is a matter of interest in geology.

This investigation was carried out as a cooperative research with the U. S. Atomic Energy Commission under contract number AT(11-1)-27.

REMARKS

Professor Daniels, in reply to a question by Professor Burton concerning the thickness of the lithium fluoride crystals which were used for the dosimeter tests, said: The crystals were 1 cm. square and 3 mm. thick. It is true that in very thin crystals a considerable amount of energy may be lost by the escape of electrons released by γ -rays. In these experiments, however, crystals three mm. in thickness were stacked up in a pile inside the cobalt γ -irradiator, and so the thin crystals were behaving essentially as thick crystals and any loss of electron energy from one crystal was offset by a similar addition of energy from the adjoining crystal.

Professor Daniels, in reply to a question concerning the effect of impurities, said: The presence of impurities in the crystal lattice is certainly a factor in the thermoluminescence glow curves. Sometimes, however, impure crystals give nearly the same glow curves as purer crystals. Unfortunately the thermoluminescence can be so much more sensitive than other physical or chemical tests that it is difficult to connect the thermoluminescent glow curve peaks with traces of specific impurities. Sometimes samples from the same crystal 2 cm. apart will vary by 50% in their thermoluminescent intensity, presumably due to different amounts of trace impurities.

The areas under the peaks are proportional to the number of electrons released from traps. If the peaks are narrow, the peak heights are nearly proportional to the areas. A rapid rate of heating produces sharp narrow peaks, a slow rate gives broad flat peaks but the areas are practically the same.

SOME OBSERVATIONS OF LUMINESCENCE OF ALKALI HALIDE CRYSTALS SUBJECTED TO IONIZING RADIATION

By J. A. GHORMLEY AND H. A. LEVY

Chemistry Division, Oak Ridge National Laboratory,¹ Oak Ridge, Tennessee, and the Department of Chemistry, University of Tennessee, Knoxville, Tennessee

Received February 26, 1952

Luminescence phenomena of some alkali halides subjected to ionizing radiation under a variety of conditions have been measured and interpreted on an elementary level in terms of trapped electrons and positive holes. The observations include fluorescence and phosphorescence (primarily glow-curves for thermoluminescence) and spectral distribution of the emitted light in the range 2300 to 12,000 Å. Infrared emission has been observed from γ -irradiated and additively colored potassium chloride during the exposure to F-band light. This emission is interpreted as associated with a transition from the excited state of F-centers to their ground state. Glow curves for infrared emission during heating of additively colored potassium chloride following exposure at low temperatures to F-band light exhibit five peaks between -196 and $+25^\circ$, indicating five types of electron traps. Glow curves obtained simultaneously for different emission bands indicate that at least two types of processes requiring activation energy may occur, and a single type of activation step can lead to more than one spectral emission band. Sodium chloride and lithium fluoride crystals irradiated at 4°K . and allowed to warm give maximum emission at 66 and 135°K ., respectively, with little phosphorescence below these temperatures. These emission peaks are thought to arise from release of self-trapped electrons. A temperature-independent afterglow observed in alkali halides is attributed to tunnelling of trapped electrons to trapped holes.

1. Introduction

The effects of ionizing radiation on alkali halides have received considerable attention in the past twenty-five years. Most of this attention has been directed toward the study of color centers, and some of the observed phenomena are thought to be relatively well understood.² A fairly specific

picture of the nature of these changes has been developed and provides a basis for interpretation of phosphorescence.

The luminescence of irradiated alkali halides has also been studied. The complex nature of emission spectra and glow curves causes difficulty in interpretations of observations in this field. The low intensity of emitted light from pure alkali halides makes measurements of phosphorescence spectra impossible except with the most sensitive light detecting techniques.

(1) This work was performed for the Atomic Energy Commission under the resident graduate program of the University of Tennessee and the Oak Ridge National Laboratory.

(2) F. Seitz, *Rev. Modern Phys.*, **18**, 384 (1946).

Urbach³ has subjected alkali halides to radium irradiation and has studied phosphorescence stimulated in them by infrared radiation, heat and pressure. Urbach and Schwarz⁴ studied thermoluminescence of alkali halides, especially the effects of time of irradiation, time lapse before heating, exposure to light, and mechanical stress applied either before or after irradiation. Kats⁵ has reported different temperatures of maximum emission for visible and for ultraviolet thermoluminescence following X-ray irradiation of sodium chloride, potassium chloride and potassium bromide at liquid air temperature, and has attributed visible emission to the transition occurrent in formation of F-centers by electrons from the conduction band. He postulates that ultraviolet emission results from recombination of electrons of F-centers with positive holes migrating to them. Our observations lead to an interpretation somewhat different with respect to the transitions leading to visible and ultraviolet emission.

According to the current picture, when ionizing radiation is absorbed in a crystal, some electrons are excited into the conduction energy band, in which state they may diffuse through the crystal. An electron may remain mobile until it comes into a region where an electron is missing from the filled band (a positive hole) or becomes trapped at a position of relative stability, for example at a lattice imperfection. At a sufficiently low temperature the electron may become localized by polarizing its surroundings, that is, displacing the surrounding ions, to give a self-trapped electron predicted by Landau.⁶ For each type of trap, there is a characteristic activation energy for release of the electron. As an irradiated crystal is heated, electrons are released from their traps by thermal activation and migrate through the crystal until they combine with a positive hole or again become trapped. Either of these processes may lead to light emission; therefore when light emission is measured during heating of an irradiated crystal several temperatures of maximum emission are observed, each related to the activation energy for release of electrons from traps of some specific configuration. Exposure to light of appropriate wave lengths may also cause release of electrons from traps and thus give rise to light emission. The behavior of positive holes is parallel to that of excited electrons: they may diffuse through the crystal (actually the surrounding electrons are mobile) and may become trapped, for example, at positive ion vacancies. Their release may also lead to light emission when the hole subsequently meets an excited electron, or possibly when it becomes retrapped.

We describe here some measurements of light emission by alkali halide crystals subjected to ionizing radiation and subsequently heated or exposed to light. Both intensities and spectral distributions in the range 2300 to 12,000 Å. have been studied. The phenomena are interpreted on an

elementary level in terms of trapped electrons and positive holes as described above.

2. Apparatus

The 300-curie cobalt-60 γ -ray source used in the present work is described elsewhere.⁷ A block diagram of the apparatus used for measuring emitted light is shown in Fig. 1. A Beckman quartz spectrophotometer was used in some experiments for obtaining emission spectra and in other experiments as a source of monochromatic light for illuminating samples. For most of the phosphorescence measurements, crystals were irradiated in a dewar flask of liquid nitrogen, then transferred to a copper block in a silica dewar flask of liquid nitrogen, then transferred to a copper block in a silica dewar flask having an unsilvered band for optical measurements. A heater and thermocouple junctions for controlling and recording temperature were attached to the copper block. The sample in the dewar flask was placed directly in front of what is normally the exit slit of the spectrophotometer and light emerging from what is normally the entrance slit fell on the photocathode of a photomultiplier at liquid nitrogen temperature. Two types of photomultipliers were used, a 1P28 for the range 2300 to 6000 Å. and a C7050^{7a} for red and infrared to 12,000 Å. A pulse counting technique gave maximum sensitivity for light detection. We estimate that a minimum of 10 photons per second was required for measurements with the 1P28 photomultiplier. The usual background was about 1 count per second with the amplifier sensitivity adjusted to count nearly every photoelectron from the cathode. Pulses were amplified with a high-gain preamplifier and linear amplifier⁸ and fed into a logarithmic count rate meter⁹ permitting continuous recording of the light intensity on a logarithmic scale.

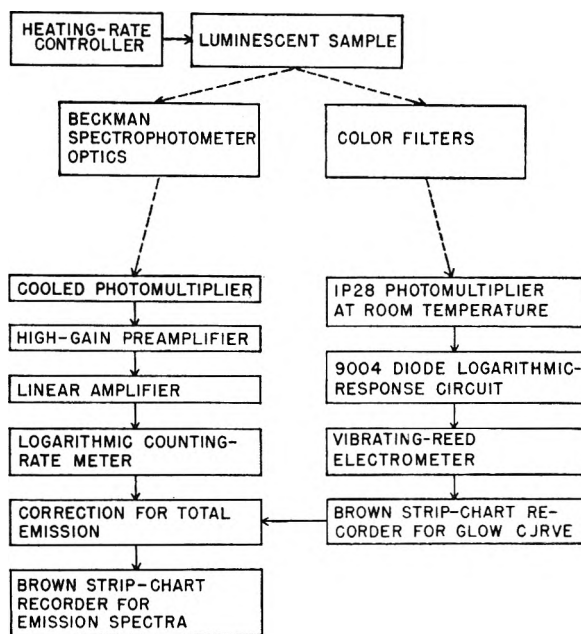


Fig. 1.—Apparatus for light emission measurements. Optical links are indicated by dashed lines and electrical links by solid lines.

Another 1P28 photomultiplier at room temperature was connected with a circuit which permitted continuous recording of the logarithm of total light intensity or of spectral bands isolated by filters.

For control of temperature during thermoluminescence

(3) F. Urbach, *Sitzb. Akad. Wiss. Wien. Abt. IIa*, **139**, 353, 363 (1930).

(4) F. Urbach and G. Schwarz, *ibid.*, **483** (1930).

(5) M. L. Kats, *J. Exp. Theoret. Phys. (U. S. S. R.)*, **18**, 501 (1948).

(6) L. Landau, *Physik. Z. Sowjetunion*, **3**, 664 (1933).

(7) J. A. Ghormley and C. J. Eochanadel, *Rev. Sci. Instruments*, **22**, 473 (1951).

(7a) We are indebted to R. W. Engstrom of RCA for the loan of this developmental-type infrared-sensitive photomultiplier.

(8) W. H. Jordan and P. R. Bell, *Rev. Sci. Instruments*, **18**, 703 (1947).

(9) W. G. James, A. E. C. Report, ORNL-413.

measurements, the desired temperature (in terms of thermocouple e.m.f.) change as a function of time was laid out as a broad conducting line on the strip chart of a Speedomax recorder. The e.m.f. from a thermocouple was fed into this recorder and deviation of its indicator from one edge of the conducting line controlled the heater. For this purpose the recorder was modified by substituting for the pen a platinum contact point connected to a vacuum tube relay which turned the heater on or off.

3. Experimental

3.1 Role of Impurities.—In any investigation of luminescence of pure materials the influence of inevitable impurities must be considered. Methods for determining the effects of impurities include (1) observations on relatively pure samples before and after further purification, (2) study of effects of added impurities and (3) comparison of luminescence properties of samples from various sources. We have observed that in some samples the impurities present have a large effect on the magnitude and spectral distribution of the emitted light although the temperatures and relative heights of the glow curve peaks are not significantly affected by the impurities. For example, air-grown and vacuum-grown single crystals of lithium fluoride (Harshaw Chemical Company) gave very similar glow curves below room temperature, except that the magnitude of emission at any temperature was ten times greater for the purer vacuum-grown crystals. Addition of a trace of copper to relatively pure potassium bromide or to sodium chloride produced a significant change in the emission spectra but had little effect on the glow curves except for about a hundred-fold displacement in the direction of greater light emission. We conclude from these and other experiments that most of the glow curves we have observed are characteristic of pure alkali halides with naturally occurring lattice imperfections serving as electron (or hole) traps whose affinities for electrons (or holes) determine the temperatures at which the glow-curve peaks are observed. Emission spectra may be more strongly influenced by presence of impurities. However, we believe the significant features of those described below to be characteristic of pure alkali halides.

3.2 Fluorescence of Color Centers.—Mott and Gurney¹⁰ have concluded from theoretical considerations that the transition from the excited state of an F-center to the ground state should result in emission of light and have suggested a search for near-infrared fluorescence in alkali

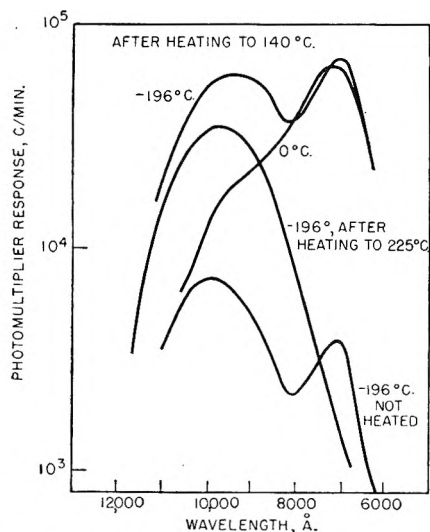


Fig. 2.—Fluorescence spectra of γ -irradiated lithium fluoride excited by 4500 Å. light at temperatures indicated, after γ -irradiation of 2×10^7 r. in 24 hr. at -196° (emission at 7000 Å. during heating shown for same sample in Fig. 3).

(10) N. F. Mott and R. W. Gurney, "Electronic Processes in Ionic Crystals," Oxford University Press, London, 1940, p. 136.

halides illuminated in the F-band. Both Molnar¹¹ and Klick¹² have observed fluorescence, peaked around 7000 Å., attributed to the M-band in LiF (absorption peak at 4500 Å.), but have not observed F-center fluorescence.

As shown in Fig. 2, we also have observed the emission peak at 7000 Å. and in addition a peak at 10,000 Å. during illumination of a γ -irradiated lithium fluoride crystal with 4500 Å. light isolated with filters. The lower curve of Fig. 2 shows the fluorescence emission spectrum of the crystal while still at liquid nitrogen temperature. The two upper curves show the emission spectrum observed after heating the crystal to 140° and cooling to 0° and -196° , respectively, for fluorescence measurements. As has been pointed out by Pringsheim and Yuster¹³ the 4500 Å. absorption band in lithium fluoride irradiated at low temperature does not reach a maximum until the crystal has been heated to room temperature or above. We have carried out an experiment to determine whether 7000 Å. fluorescence in lithium fluoride irradiated at -196° and heated during excitation by 4500 Å. light also reaches a maximum above room temperature. The results are shown in Fig. 3. The dashed portion of the curve probably represents thermoluminescence rather than fluorescence. Emission increased by a factor of ten between 50 and 130° then dropped rapidly above 200° . After heating the crystal to 225° and cooling to -196° , fluorescence excited by 4500 Å. light showed only the 10,000 Å. band. Most of the 4500 Å. absorption band anneals out below 225° so the 10,000 Å. fluorescence must be associated with relatively weak absorption in the 4500 Å. region.

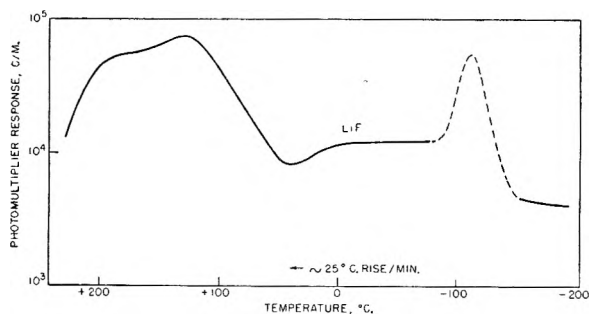


Fig. 3.—Emission at 7000 Å. from lithium fluoride excited by 4500 Å. light after γ -irradiation of 2×10^7 r. at -196° . Dashed portion of curve is probably thermoluminescence but emission at other temperatures is fluorescence (curve traced directly from recorder chart).

Figure 4 shows infrared emission resulting from absorption of F-band light in potassium chloride which contains F-centers. (The shapes of the emission curves shown are determined to a great extent by the sensitivity of the photocathode; the actual peaks would appear at wave lengths greater than 10,000 Å.) It is not possible to determine from available data whether the emission is true F-center fluorescence or results from formation

(11) J. P. Molnar, The Absorption Spectra of Trapped Electrons in Alkali Halides, Thesis, Massachusetts Institute of Technology, 1940.

(12) C. C. Klick, *Phys. Rev.*, **79**, 894 (1950).

(13) P. Pringsheim and P. Yuster, *ibid.*, **78**, 293 (1950).

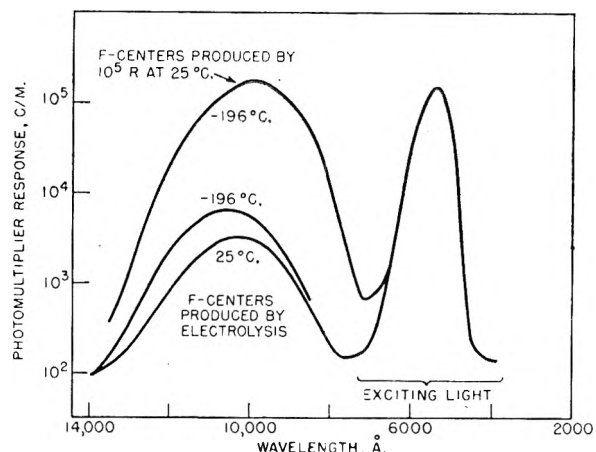


Fig. 4.—Spectra of fluorescence excited by light absorbed by F-centers of potassium chloride.

of other centers such as M-centers. The amount of light absorbed by F-centers in the additively colored sample (F-centers produced by electrolysis with pointed cathode) and in the irradiated sample was about the same; for most of the incident light was absorbed, yet the emission at 10,000 Å. was much greater in the irradiated sample. We have no explanation for this difference.

Similar infrared emission spectra were observed during γ irradiation of sodium chloride and potassium chloride. This emission is also assumed to arise from transitions occurring in the formation of F-centers or other centers.

3.3 Phosphorescence

3.3.1 Glow Curves for Electron Trapping.

When additively colored alkali halides absorb light in the F-band at appropriate temperatures, F-centers disappear and F'-centers are formed.¹ F'-centers in potassium chloride are thermally unstable at room temperature, F-centers being reformed as F'-centers disappear. If luminescence is a consequence of a transition which occurs during or immediately subsequent to electron capture with accompanying formation of F-centers (or perhaps other stable trapped-electron centers), it should be observable on warming an additively colored crystal after exposure to F-band light at temperatures at which F'-centers are thermally

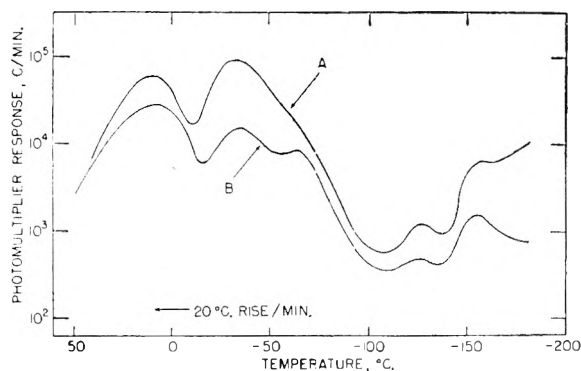


Fig. 5.—Glow curves for infrared emission from additively colored KCl following exposure to F-band light at -196° : curve A, exposed 10 minutes to 5500 Å; curve B, exposed 2 minutes to 5500 Å.

stable. Figure 5 shows glow curves obtained from such experiments.

Instead of a single peak in the infrared glow curves corresponding with thermal dissociation of F'-centers, five distinct peaks are observed, of which four must be due to release of electrons from other types of traps. The last peak at just above 0° may correspond with release of electrons from F'-centers since this temperature corresponds closely to their stability limit. The latter are probably formed following release of electrons from each of the less stable types of traps. No luminescence was detectable with the 1P28 photomultiplier (range 2300–6000 Å.); therefore, the visible thermoluminescence from irradiated potassium chloride does not accompany formation of color centers as proposed by Kats.⁵

3.3.2 Simultaneous Glow Curves for Different Spectral Bands. a. Potassium Bromide.

Figure 6 shows some typical phosphorescence spectra of irradiated potassium bromide thermostimulated at three temperatures and photostimulated with infrared (Tungsten lamp with 2550 Corning glass color filter) at -196° . These curves are not corrected for changes in total emission rate during progress of the measurement; consequently the positions of the peaks in the broad visible bands may be shifted by these changes and are subject to some uncertainty. Two distinct bands are observed in the ultraviolet at 3200 and 2900 Å., respectively. The 2900 Å. band appears in thermoluminescence only at about -10° . A number of potassium bromide samples from several different sources all gave the 3200 Å. peak in their emission spectra, although glow curves for this emission were not the same for the different samples. In all

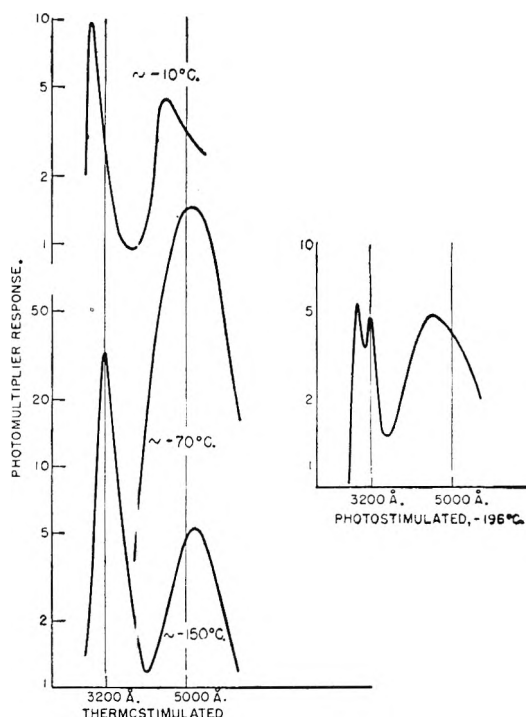


Fig. 6.—Typical phosphorescence spectra of fused potassium bromide after 10 minutes irradiation at 2000 r./min. and -196° .

samples glow-curve peaks for 3200 Å. emission appeared at temperatures different from those for visible emission, indicating that the activation processes resulting in 3200 Å. and in visible emission are different.

If one assumes that one type of emission, either visible or ultraviolet, follows release of trapped electrons and their migration to trapped holes, and the other type of emission follows release of trapped holes and their migration to trapped electrons, it is possible experimentally to determine the source of the visible and ultraviolet emission. Electrons in stable traps (F-centers) and positive holes in stable traps (V-centers) may be produced in a crystal by γ -irradiation at room temperature. This crystal may then be cooled and exposed to light absorbed by F-centers to give electrons in less stable traps, as indicated by observations discussed in the previous section. On warming, some of the electrons released from shallow traps will migrate to trapped holes and the observed thermoluminescence will be characteristic of the resulting transitions. Similarly, absorption of light by V-centers in a crystal at low temperature might be expected to yield holes trapped in less stable configurations, and upon subsequent warming to give thermoluminescence characteristic of the combination of free holes with trapped electrons. This sort of experiment would, however, not be conclusive as far as emission resulting from freed holes is concerned, as Seitz¹⁴ has pointed out that V-center light may excite but not free the trapped holes.

Results of an experiment to determine the origin of visible and ultraviolet emission from potassium bromide are shown in Fig. 7. A sample was γ -irradiated with 25,000 r. at room temperature, then cooled in the dark to -196° and exposed

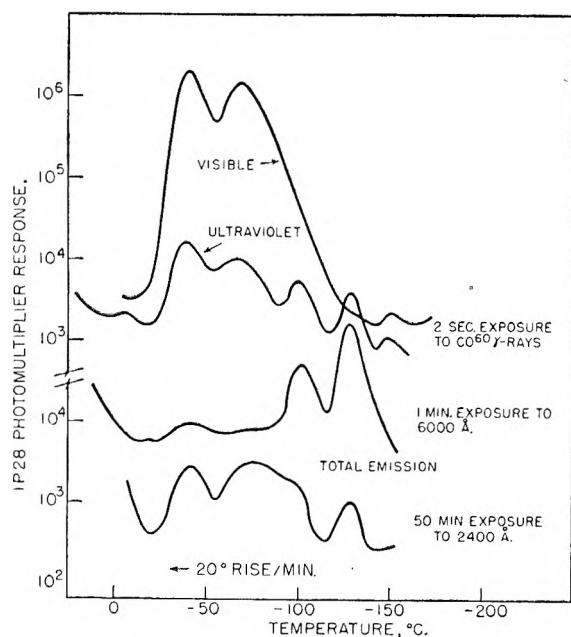


Fig. 7.—Glow curves for a sample of potassium bromide γ -irradiated with 25,000 r. at 25° , then exposed at -196° to each of three types of radiation and heated to 25° for observation of thermoluminescence after each exposure.

(14) F. Seitz, *Phys. Rev.*, **79**, 529 (1950).

to 50 r. Visible and ultraviolet emission isolated by filters (Corning glass filters, No. 9863 for ultraviolet and No. 3850 for visible) was measured as the crystal was warmed to room temperature, by inserting first one filter then the other between sample and photomultiplier for alternate 12 second periods during the heating, giving the two upper curves of Fig. 6. The crystal was again cooled to -196° and exposed this time to 6000 Å. light (the wavelength of the F-band peak) isolated with the spectrophotometer. As seen in Fig. 7 the subsequent glow curve for total light shows predominantly temperature peaks characteristic of the ultraviolet and not the peaks characteristic of visible emission. It was not convenient to isolate the two spectral regions because of the low intensity. Following exposure to 2400 Å. (the absorption band with peak at 2320 Å. termed the V_3 -band by Casler, Pringsheim and Yuster¹⁵ absorbs in this region) the glow curve for total emission exhibited peaks characteristic of both visible and ultraviolet emission. The result of the experiment involving F-band irradiation indicates that thermal release of trapped electrons leads to ultraviolet emission from irradiated potassium bromide. Visible emission must then follow from some other type of activation process, possibly from thermal release of trapped holes. A different picture was given by Kats,⁵ who postulated that ultraviolet emission accompanies the combination of F-center electrons with positive holes which have been thermally freed and have diffused to the F-center locality. This interpretation is not supported by our foregoing observations.

b. Lithium Fluoride.—The phosphorescence (thermostimulated) spectrum of gamma irradiated lithium fluoride is characterized by two broad bands with peaks at about 2700 and 4400 Å., respectively (see Fig. 12). Figure 8 shows glow curves obtained simultaneously (by alternating the wave length setting of the spectrophotometer

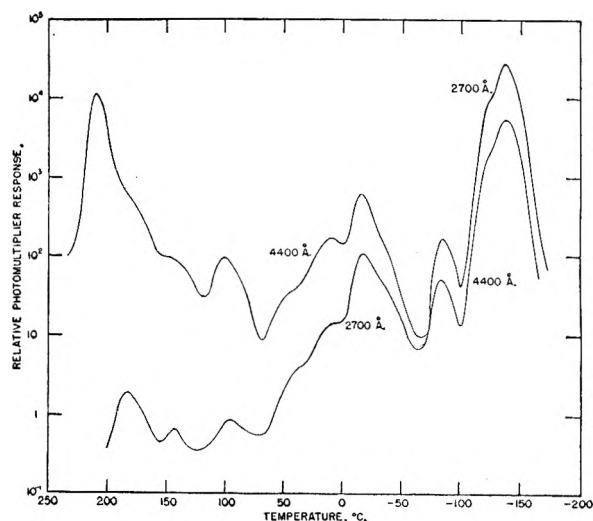


Fig. 8.—Glow curves for the two emission bands LiF after 40 min. exposure to 2000 r./min. Co^{60} γ -rays at -196° . Heating rate $8^\circ/\text{min}$.

(15) R. Casler, P. Pringsheim and P. Yuster, *J. Chem. Phys.*, **18**, 1564 (1950).

between the two wave lengths) for the peaks of the two bands. With the possible exception of the last (high temperature) peak, the difference between the two curves is only a gradual change in ratio of intensities of the two bands as the temperature increases; each peak of one curve appears also in the other. We assume that the particular wave lengths selected for examination in the glow curves are each representative of their bands. The width of the bands does not represent a composite of essentially different phenomena but the fact that the processes themselves are not precisely defined; *e.g.*, the initial or terminal energies or both may not be sharply fixed. The two emission bands show that two different capture-emission processes are involved—whatever they may be. The peaks in the glow curves indicate that a variety of activation energies is required to release the species later captured to give the observed emission. The identities of the peaks in the two glow curves indicate that they represent the release of identically trapped species. Since the temperature peaks are identical for both emission bands, each such peak corresponds to the release of one species later captured to give the emission. It can be reasonably assumed that a specific emission band corresponds to only one process; *i.e.*, the capture of a single species at a single trap. Thus, we conclude that either initially trapped electrons or initially trapped holes are involved—but not both, and that this species is released from a variety of traps of different energy depth. The emission processes yielding 2700 and 4400 Å. light involve capture of the released species at two different emission sites. The shift in relative intensity of the two bands as a function of temperature indicates a gradual change in the relative probabilities of the two emission processes as the crystal is warmed. The relative probabilities of emission may not be the same as the relative probabilities of capture.

3.3.3 Self-Trapped Electrons.—The general shape of all the glow curves for alkali halides irradiated at liquid nitrogen temperature was the same, namely, about eight peaks between -196 and $+250^\circ$. The glow curve for lithium fluoride was exceptional in that the first peak was much higher than any other peak observed in alkali halides. This feature was thought to be significant because of the calculation of Markham and Seitz¹⁶ that self-trapped electrons should be stable in lithium fluoride at liquid nitrogen temperature. The calculations also showed that in sodium chloride and presumably in all other alkali halides they would be stable only at lower temperatures. At the beginning of an irradiation of a crystal at a temperature where self-trapped electrons are stable nearly every ionization event should result in an electron which polarizes its surrounding ions and becomes self-trapped. Thus at sufficiently low temperatures very little phosphorescence should occur, because electrons will not be able to move through the crystal to the holes.

We have carried out an experiment to determine whether phosphorescence does occur in lithium fluoride at lower temperatures. A crystal was

(16) J. J. Markham and F. Seitz, *Phys. Rev.*, **74**, 1014 (1948).

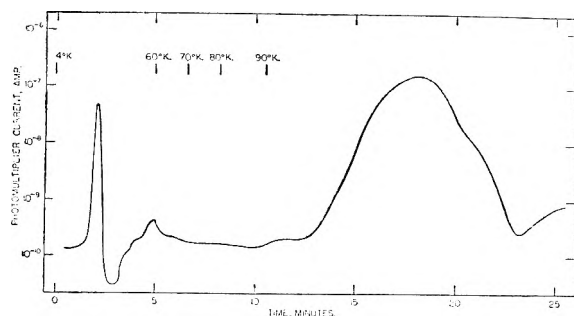


Fig. 9.—Glow curve for visible and ultraviolet emission from lithium fluoride following 4000 r. γ -irradiation at 4°K . Temperature measurements were made with a carbon resistor calibrated only in the range indicated.

irradiated at liquid helium temperature and phosphorescence observed while the sample was warming after irradiation. As shown in Fig. 9, very little phosphorescence was observed below 90°K ., but the intense peak at 135°K . appeared just as it did after irradiations at liquid nitrogen temperature (Fig. 8). Figure 10 shows the results of a similar experiment revealing release of self-trapped electrons in sodium chloride at a much lower temperature. An intense peak in the glow curve was observed at 66°K . with practically no emission below this temperature.

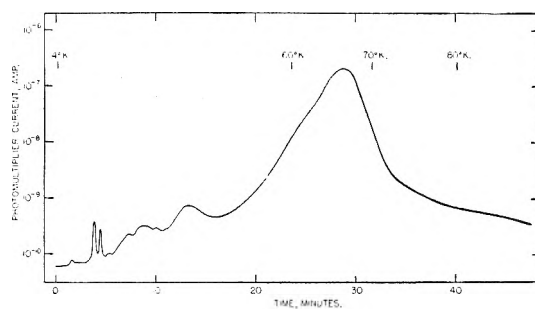


Fig. 10.—Glow curve for visible and ultraviolet emission from sodium chloride following 4000 r. γ -irradiation at 4°K .

The calculations of energy depths of electron traps from temperatures of the corresponding glow-curve peaks has been discussed by Randall and Wilkins.¹⁷ For a rigorous calculation, a number of variables must be evaluated, the most important of which is the probability of retrapping following thermal release of a self-trapped electron. We have not attempted to estimate this probability. A rough calculation of the trap depth which ignores the effect of retrapping is given by the expression $E = 25kT$; this formula yields the values 0.32 and 0.14 eV. for the traps giving rise to the predominant peaks in lithium fluoride and sodium chloride, respectively. The values predicted by Markham and Seitz for self-trapping in these materials are 0.3 and $0.13 (\pm 25\%)$. Thus, the theory is consistent with the interpretation that these glow curve peaks result from release of self-trapped electrons.

3.4 Temperature-independent Afterglow ("Tunnelling Phosphorescence").—In some experiments,

(17) J. T. Randall and M. H. F. Wilkins, *Proc. Roy. Soc. (London)*, **A184**, 366 (1945).

it is possible to separate glow curve peaks by first heating the sample until the thermoluminescence of one peak is nearly exhausted then quenching and heating again at a constant rate through the following peak. In this way the glow curve on the low temperature side of a peak may be observed without interference from preceding peaks. Figure 11 shows an attempted application of this technique to lithium fluoride. On first warming the irradiated sample from liquid nitrogen temperature a shoulder appeared on the glow curve at about -180° followed by a rapid rise of emission into the first peak. Upon reaching -156° , the temperature at which the emission was about one-tenth of the maximum, the crystal was quenched rapidly with liquid nitrogen. As shown in Fig. 11, the emission did not drop as expected to a low value at -196° but was actually higher than the initial emission at that temperature. When the crystal was allowed to warm a second time, the emission did not start to increase until the temperature reached -180° and no shoulder was observed. The same slow drop in emission occurred after quenching the second time. A similar afterglow from the initial portion of another peak was observed on quenching from -80° .

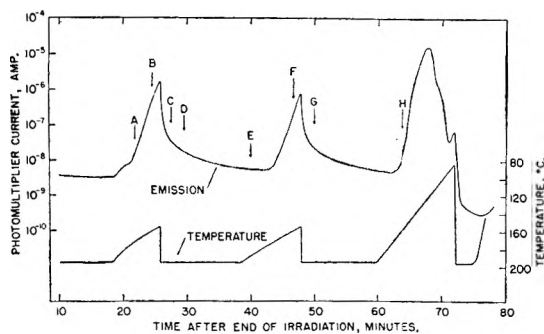


Fig. 11.—Thermoluminescence and temperature independent afterglow in lithium fluoride following 10^5 r. γ -irradiation in one hour at -196° .

Figure 12 shows spectra for thermoluminescence and temperature-independent afterglow of lithium fluoride. Within the limits of reproducibility determined by statistical fluctuations and response time, all of the spectra at times indicated by arrows in Fig. 11 are identical, and when corrected for photocathode sensitivity and spectrophotometer prism dispersion give the upper curve in Fig. 12. The emission process thus appears to be the same for the thermoluminescence and for the temperature-independent afterglow.

Similar temperature-independent afterglow was observed in sodium chloride and potassium bromide irradiated at -196° . Emission from silver-activated sodium chloride irradiated at 25° and quenched in the dark to -196° was independent of temperature between -196 and -100° but the emission spectrum was quite different from that for normal phosphorescence at 25° , indicating two different emission processes.

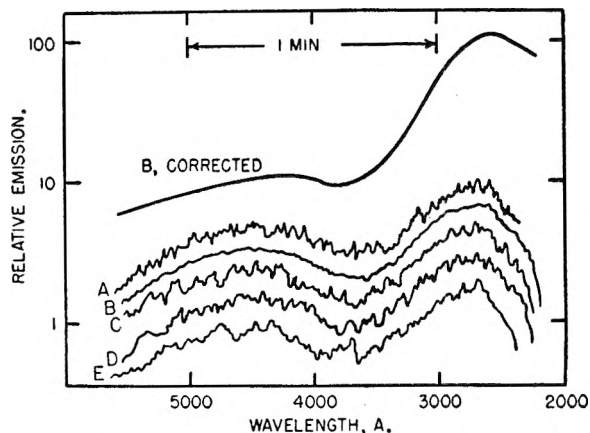


Fig. 12.—Emission spectra for temperature-independent afterglow and thermoluminescence in lithium fluoride at points indicated in Fig. 10. Upper curve is curve B corrected for cathode sensitivity and prism dispersion. Lower curves are traced directly from recorder chart and have been automatically corrected for changes in total light.

A phenomenon termed slow fluorescence¹⁸ has been reported for a number of materials. This temperature-independent emission is characterized by exponential decays with time constants of not more than a few seconds. The temperature-independent afterglow here reported showed decay times of many minutes and decay curves which were not exponential but which could be described as the sum of several exponentials.

Seitz² has suggested that when a high density of F-centers is reached the electrons in F-centers are able to combine with the positive holes by a quantum mechanical tunnelling process. Some tunnelling would be expected to occur at any concentration of trapped electrons and holes. The characteristics of temperature-independent afterglow in alkali halides appear explicable on the basis of tunnelling processes. There would exist a large number of possible mutual configurations for a trapped electron and trapped hole and each configuration will have a definite probability for reaction by tunnelling; therefore, the observed decay rate should represent a sum of exponential decays. Since no activation step is involved, the rate of the reaction should be temperature-independent.

REMARKS

Professor F. Daniels (University of Wisconsin): Is it not likely that in the experiments of Ghormley and Levy the crystal lattice was changed considerably by the radiation itself? As pointed out in the previous paper, the width of the peaks in the thermoluminescent glow curves and the absorption bands in the colored crystals broaden considerably with continued exposure to γ -radiation. It was pointed out that to obtain measurements characteristic of the original undamaged crystal lattice, the exposures should be quite short, perhaps of the order of 1,000 roentgens or less. Exposures described by Ghormley and Levy were of the order of many thousands of roentgens. It might be worthwhile to redetermine some of the measurements after very short exposures to γ -radiation in order to distinguish if possible the behavior of the original crystal from the behavior of the crystal which had been altered by the exposure to γ -radiation.

(18) P. Fringsheim, "Fluorescence and Phosphorescence," Interscience Publishers, Inc., New York, 1949, p. 290.

ELEMENTARY PROCESSES IN RADIATION CHEMISTRY. III. CHARGE TRANSFER MECHANISMS^{1,2,3}

BY JOHN L. MAGEE

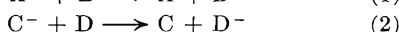
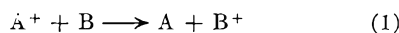
Department of Chemistry, University of Notre Dame, Notre Dame, Indiana

Received February 25, 1952

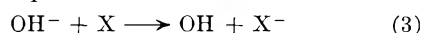
The mechanism of transfer of positive charge from an ion to a neutral molecule or atom is considered. The resonant process $A^+ + A \rightarrow A + A^+$ may have a large cross section since the momenta of the heavy pair (ion and molecule) do not have to change as the electron jump occurs and a close collision is thus not necessary. The non-resonant process $A^+ + B \rightarrow A + B^+$ is formally equivalent to a quenching reaction. For it to be possible, two potential curves of the system $(A + B)^+$ must cross. The potential curves contain the vibrational energy of the system and so the charge transfer will in general be accompanied by vibrational excitation. A special case of this excitation is dissociation of one of the molecules. The possibility for an adiabatic "charge transfer" exists when chemical reaction occurs.

Introduction

Singly charged ions occur in greater abundance than multiply charged ions in irradiated matter.^{4,5,6}

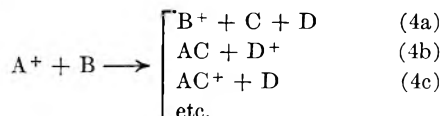


The charge transfer mechanisms will, therefore, cover most cases of interest for radiation chemistry. Of these two processes we believe that the first (*i.e.*, the transfer of positive charge) is of more general interest and it is with this process we shall be concerned here. In a formal sense, the two processes are equivalent because an electron jump occurs in each case. In aqueous systems, the charge transfer process



is sometimes of great importance, but we shall not consider it in this paper.

We recognize three mechanisms for the transfer of a single charge in gas phase collisions. (a) The resonant case, $A = B$. This case will usually be of no practical importance in radiation chemistry since no observable effect on chemical yields result from it. We consider it because of its theoretical interest. (b) The general transfer reaction, $A \neq B$. The two incident molecules or radicals A and B remain intact after the charge is transferred. This process is of great interest in radiation chemistry since the radiolysis products will in general depend upon the extent to which it occurs. (c) The transfer reaction accompanied by chemical change.



This process is not strictly a charge transfer in the same sense as the other two processes, since at least one of the incident pair undergoes chemical change. However, it is of great importance for radiation chemistry and so its mechanism will be considered briefly.

(1) A contribution from the Radiation Chemistry Project, operated under Atomic Energy Commission contract AT(11-1)-38.

(2) Paper presented before the Symposium on Radiation Chemistry, Division of Physical and Inorganic Chemistry, American Chemical Society, Cleveland, Ohio, April 11, 1951.

(3) Papers I and II of this series are given in references 7 and 8.

(4) M. Burton, *Ann. Rev. Chem.*, **1**, 113 (1950).

(5) M. Burton, *J. Chem. Ed.*, **28**, 404 (1951).

(6) D. E. Lea, "Action of Radiation on Living Cells," Cambridge University Press, Cambridge, England, 1947.

The ionization processes induced by energetic charged particles tend to be non-selective; *i.e.*, the fraction of positive ions produced in any given molecular component of a mixture is approximately proportional to the mass fraction of the component. It is, therefore, easy to prepare a mixture in which most of the positive ions will be of a type A^+ and also have a molecule B present which has a lower ionization potential than A. The transfer reaction 1 will frequently occur in such a system.

Previous work^{7,8} has indicated that electron capture takes place in a very selective way, and thus negative ions C^- are very special entities. There will usually be no molecule D in the medium which has a higher electron affinity than C. Thus we do not expect to find many systems in which reaction 2 is of great importance. As noted above, aqueous systems furnish a very important exception to this rule. The H_2O molecule is present in such high concentration in aqueous systems that it will capture all electrons even in the presence of a molecule (or radical) X which has good electron affinity.

The Ionization Process in Molecules

From spectroscopic and mass spectroscopic studies, ionization potentials of many molecules have been obtained.^{9,10} In Table I a collection of a few selected values of interest for radiation chemistry is given.

By "ionization potential" one frequently means the excitation energy of the lowest ionized state or the *least* amount of energy required to remove an electron. Any molecule will have many ionization potentials, since the resulting ion can have any one of many possible excited electronic states. The most important ionized states of the molecule can be reached by removal of an electron from any one of the various molecular orbitals without excitation of any of the other electrons. Thus the lowest ionized states are formed by removal of a valence (or possibly non-bonding) electron. There will be $n/2$ ionized states for a molecule with n valence electrons, and all of these should lie within a few electron volts of each other.

The equilibrium internuclear separations in the resulting ion will always be somewhat different

(7) J. L. Magee and M. Burton, *J. Am. Chem. Soc.*, **72**, 1965 (1950).

(8) J. L. Magee and M. Burton, *ibid.*, **73**, 523 (1951).

(9) R. E. Honig, *J. Chem. Phys.*, **16**, 105 (1948). References to earlier work are collected here.

(10) W. C. Price, *Chem. Revs.*, **41**, 257 (1947).

TABLE I

SOME IONIZATION POTENTIALS OF INTEREST IN RADIATION CHEMISTRY* (VALUES ARE GIVEN IN ELECTRON VOLTS)

Rare gases and atoms	Simple molecules	Unsatsd. hydrocarbons
He 24.581	H ₂ 15.422	Ethylene 10.50
Ne 21.559	N ₂ 15.576	Propylene 9.70
A 15.756	O ₂ 12.2	1-Butene 9.65
Kr 13.996	CO 14.1	Butadiene 9.07
Xe 12.127	CO ₂ 13.78	Acetylene 11.41
Rn 10.746	H ₂ O 12.61	Benzene 9.24
H 13.60	HBr 12.04	Toluene 8.92
C 11.217	HI 10.38	
N 14.48		
O 13.550		
Cl 12.952		
Br 11.80		
I 10.6		
Satsd. hydrocarbons	Substd. hydrocarbons	Radicals
Methane 13.1	Methyl alcohol 10.8	Methyl 10.07
Ethane 11.6	Acetone 10.1	Ethyl 8.67
Propane 11.3	Methyl bromide 11.17	n-Propyl 7.80
n-Butane 10.34	Methyl iodide 9.49	i-Propyl 7.77
		t-Butyl 7.19

* Values in table are to be found in references 9 and 20 or Herzberg, "Atomic Spectra and Atomic Structure," Prentice-Hall Publishers, Inc., New York, N. Y., 1937.

from the parent molecule, and so vibrational motion is excited along with ionization. This excitation can be so violent that dissociation will occur. It is known that a variety of dissociation products are formed when a molecule undergoes electron bombardment. In Table II the products formed from

TABLE II

APPEARANCE POTENTIALS OF THE POSITIVE ION PRODUCTS FROM BOMBARDMENT OF METHANE WITH 50-VOLT ELECTRONS

Ion	Appearance potential	Fraction energy used in process
CH ₄ ⁺	13.1 ± 0.4	50.7
CH ₃ ⁺	14.4 ± .4	39.5
CH ₂ ⁺	15.7 ± .5	4.2
CH ⁺	23.2 ± .6	1.7
C ⁺	26.7 ± .7	0.6
H ₃ ⁺	25.3 ± 1.0	.005
H ₂ ⁺	27.9 ± 0.5	.3
H ⁺	27.7 ± 0.5	3.0
	29.4 ± 0.6	

the bombardments of methane with 50-volt electrons in a mass spectrometer are given.¹¹ Each product has its characteristic appearance potential. A fast charged particle has, of course, sufficient energy to initiate all of these processes and so a distribution of them is expected. A theoretical prediction of this distribution has not been made in any case, although it is an important quantity for radiation chemistry.

Mass spectroscopic studies on hydrocarbons¹² indicate that the larger fragment usually retains the positive charge when dissociation occurs. There is a certain amount of resonance energy in positive ions which tends to increase with size of the ion, and this factor may determine the dissociation products. The low ionization potentials of the radicals (see Table I) is in agreement with great stability for the radical ions.

(11) W. Bleakney, E. U. Condon and L. G. Smith, *THIS JOURNAL*, **41**, 197 (1937).

(12) A. Langer, *THIS JOURNAL*, **54**, 618 (1950).

Interaction of Molecules with Ions

A positive ion interacts strongly with a neutral molecule. The three principal kinds of interactions which may be involved are:

(1) Dipole-ion attraction or repulsion. For neutral molecules which have permanent dipole moments this is the strongest force of a long range nature. The energy of the interaction is given by

$$V = - \frac{\mu e^2}{2R^2} \cos \theta \quad (5)$$

where θ is the angle the dipole makes with the line of centers of the approaching pair, R is their separation, e the electron charge, and μ the dipole moment. The energy is positive or negative depending upon the dipole orientation.

(2) Induced dipole-ion attraction. Any molecule has some polarizability and thus will form an induced dipole and interact in this manner. The energy is

$$V = - \alpha e^2 / 2R^2 \quad (6)$$

The polarizability α is really a tensor quantity and so this energy also depends in general upon orientation of the two molecules. The energy is always negative, however.

(3) Exchange attraction or repulsion. Exchange interaction decreases exponentially with distance and so is only effective at short range. At moderate distance this energy can be positive or negative depending upon the nature of the states involved. At sufficiently small distances, however, a repulsion always sets in.

The exchange interaction of a molecule in its lowest state, which has a closed shell of molecular orbitals, with a molecular ion, which has one vacant orbital is similar to the interaction of He with He⁺. It is known that the He₂⁺ molecule is stable from spectroscopic studies¹³ and the molecule has been investigated theoretically by Pauling¹⁴ who calculated an attractive potential. The interaction of excited states may be attractive or repulsive.

Between any molecule-positive-ion pair attractive forces will exist for separations of the order of kinetic theory diameters (this requires proper orientation of permanent dipoles) and so there will be a tendency to cluster. The early theory of S. C. Lind¹⁵ recognized this clustering tendency but overestimated its importance. Calculations of Eyring, Hirschfelder and Taylor¹⁶ for the case of H₂ indicate that relatively few ions, say 10% or so will be involved in AB⁺ pairs, and larger clusters are very unimportant. As we shall see later the pair formation tendency may be very important for the charge transfer mechanism.

The Resonant Charge Transfer Process

The most simple type of transfer process to dis-

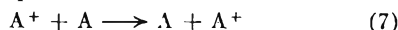
(13) G. Herzberg, "Molecular Spectra and Molecular Structure. I. Diatomic Molecules," 2nd edition, D. Van Nostrand Co., Inc., New York, N. Y., 1950.

(14) L. Pauling, *J. Chem. Phys.*, **1**, 56 (1933).

(15) S. C. Lind, "The Chemical Effects of Alpha Particles and Electrons," The Chemical Catalog Company (Reinhold Publ. Corp.) New York, N. Y., 2nd edition, 1928.

(16) H. Eyring, J. O. Hirschfelder and H. S. Taylor, *J. Chem. Phys.*, **4**, 479 (1936).

cuss theoretically is that which occurs between like atoms in the gas phase.



The initial and final states have exactly the same energy and so conservation of momentum is not violated for the electron jump at any separation of the pair. Quantum mechanical treatments of this problem have been given by several authors¹⁷ and a recent reconsideration has been made by Gurnee and Magee.¹⁸ Here we shall make a heuristic treatment which is expected to give the cross section only approximately.

Consider a collision between an ion and a molecule with relative velocity v and distance of closest approach b . If this distance b is moderately small, the resonance integral will be large and the electron has ample opportunity to jump from molecule to ion provided the velocity is *not* too great. The order of magnitude of the time required for the electron jump, at the separation b , is $h/\beta(b)$ where $\beta(b)$ is the resonant integral calculated for the distance b and h is Planck's constant. The time which the pair can be considered to be in collision is approximately b/v where v is the velocity. At some particular value of b , say $b'(v)$, for each velocity the ratio of these times is unity. If the collision takes place for $b \leq b'$ the electron certainly has time to jump, while if $b \geq b'$ the resonance integral β may be too small for the electron to jump in the allowed time. Thus we take as an approximation to the cross section

$$\sigma(v) = \pi(b'(v))^2 \quad (8)$$

In Fig. 1 values of $\sigma(v)$ for He^+ ions in He gas calculated from equation 8 are compared with experimental values¹⁹⁻²² and a more exact quantum mechanical treatment.¹⁵ For small values of the velocity the crude model described above gives cross sections which compare well with the more exact theoretical calculations, which are in satisfactory agreement with the experimental results.

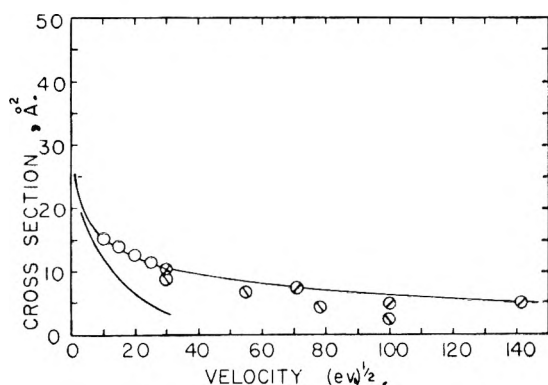


Fig. 1.—The cross section for the charge transfer process $\text{He}^+ + \text{He} \rightarrow \text{He} + \text{He}^+$ as a function of the velocity of the incident ion. Lower curve, equation 8; upper curve, Gurnee and Magee¹⁸; the various points are experimental values: O, Wolff²²; \diamond , Berry¹⁹; \square , Smith²¹; \odot , Dempster.²⁰

(17) W. Mott and H. S. W. Massey, "Theory of Atomic Collisions," Oxford University Press, 2nd edition, p. 1934, 1950. Other references are given here.

(18) E. F. Gurnee and J. L. Magee, forthcoming publication.

(19) W. H. Berry, *Phys. Rev.*, **74**, 848 (1948).

(20) A. J. Dempster, *Phil. Mag.*, **3**, 115 (1927).

(21) R. A. Smith, *Proc. Camb. Phil. Soc.*, **30**, 514 (1931).

(22) F. Wolf, *Ann. Physik*, **26**, 527, 737 (1936); **29**, 33 (1937).

If the ion is diatomic such as H_2^+ there is an additional factor involved. For the process $\text{H}_2^+ + \text{H}_2 \rightarrow \text{H}_2 + \text{H}_2^+$ the equilibrium separations of the protons in the ion and molecule are different and so, in agreement with the Franck-Condon principle, the electron jump can only take place for certain internuclear positions, *i.e.*, in a classical sense for certain phases of the oscillation of the pair of molecules. In quantum-mechanical language vibrational overlap integrals are involved in the transition probability. For the case of $\text{H}_2^+ + \text{H}_2$ the overlap integral is 0.1 and this factor reduces the resonance integral in the example given above as compared with the (fictitious) equivalent atomic case.

The $\text{H}_2^+ + \text{H}_2$ case has also been studied experimentally.^{21,23} In Fig. 2 calculated cross sections¹⁸ are compared with the available experimental results.

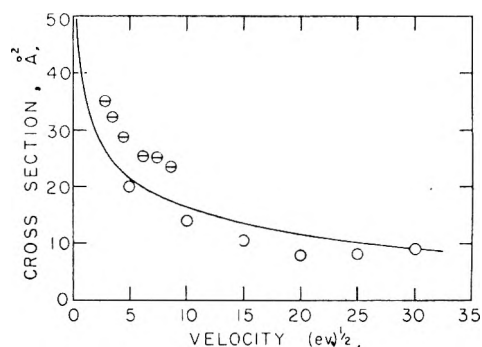
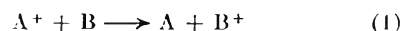


Fig. 2.—The cross section of the charge transfer process $\text{H}_2^+ + \text{H}_2 \rightarrow \text{H}_2 + \text{H}_2^+$ as a function of the velocity of the incident ion. The solid curve is calculated.¹⁸ The points are the experimental results: \odot , Simons²³; O, Wolf.²²

In more complicated molecules there is an overlap integral for every vibrational degree of freedom and their sizes depend upon the difference of internuclear separations in the molecule and ion. The overlap can be vanishingly small if there is a great disparity in these internuclear separations. Usually there are only small differences and so great restrictions are not placed by this factor on electron transfers.

The General Charge Transfer Process for Gases

For the general charge transfer process there is not equality of the energy of the initial and final states. The reaction



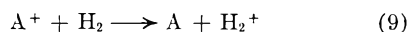
is exothermic, if it is expected to occur readily, since ions will usually have thermal energy only. The system $(A + B)^+$ passes from an excited electronic state to a lower state; the process is, therefore, formally equivalent to a quenching process of photochemistry. The general features of such processes are understood although the detailed mechanisms for very few cases have been examined.

Consider all the potential curves of $(A + B)^+$. Some of them will correspond, for large separations to $A^+ + B$ and excited states of this pair; others will correspond to $A + B^+$ and their excited states. (In this reaction we neglect the possibility for chemical change.) Since we start presumably

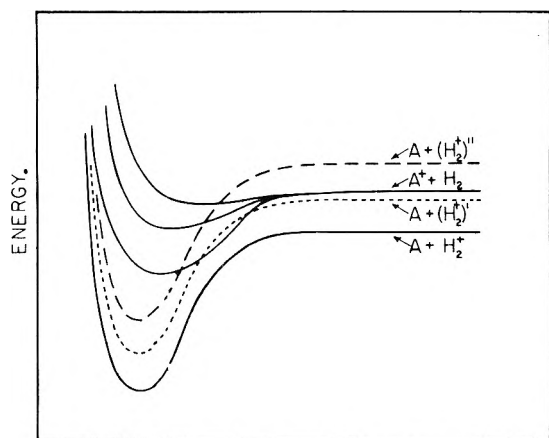
(23) J. H. Simons, *et al.*, *J. Chem. Phys.*, **11**, 312 (1943).

with the lowest state of $A^+ + B$, the excited states of this pair will not be important. The system can transfer exothermically to any state of $A + B^+$ which has lower energy. According to familiar arguments, the potential energy of the two states must cross in order for a radiationless transition to occur. The reaction coordinate will involve the motion of the unit A^+ with respect to B and the "potential curve" for the system must contain the vibrational energies of the two components. As A^+ changes to A and B changes to B^+ simultaneously at the crossing point in the potential curves, the various equilibrium internuclear separations and vibrational frequencies change too. The Franck-Condon principle applies to these simultaneous transitions, of course. Most internuclear separations and vibrational frequencies are only changed slightly, so that the most probable final state is the lowest, but there will be a definite probability for the excitation of one or more quanta of vibrational motion.

A "potential curve" must be drawn for every possible vibrational state of the products for each electronic state and at each crossing point a transition is possible. As an example a set of schematic curves are shown in Fig. 3. These curves apply to the charge transfer reactions between the rare gas argon and hydrogen



as regards asymptotic positions of states and vibration frequencies.²⁴ For $A^+ + H_2$ there are three curves since A^+ is in a P state. The solid curves apply to the two systems for H_2 and H_2^+ in their lowest vibrational states; the dashed curves indicate the H_2^+ ion in its first and second vibrationally excited states. If these curves are approximately correct in relative positions, there can be no transfer of charge from A^+ to H_2^+ in its ground state, but the transfer should occur readily to the first



SEPARATION OF MOLECULES.

Fig. 3.—Some potential curves for the system $(A + H_2)^+$. The solid curves give (schematic) behavior of the systems $A^+ + H_2$ and $A + H_2^+$ for the lowest vibrational state of H_2 and H_2^+ . The dotted and dashed curves are for the system $A + H_2^+$ for the first and second vibrational states of H_2^+ .

(24) In equations 9 and 10 only, A refers to the argon atom. Throughout the remainder of the paper it is used to represent an arbitrary molecule or radical.

vibrationally excited state of H_2^+ . A slight activation energy (~ 6.5 kcal./mole) is required for transfer to the second vibrationally excited state of H_2^+ . Higher states exist, of course, but they are not indicated in the figure to avoid complication.

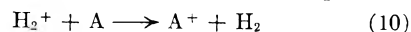
The mechanism described above for changes of vibrational excitation in radiationless transitions between pairs of electronic states is similar to the situation in ordinary electronic spectra where usually several vibrational levels of a final electronic state are obtained in a transition. The transition to a dissociated state is only a special case of this mechanism and it is to be expected if the potential curves of a molecule-ion pair have the necessary relative positions. Dissociation is possible also by an adiabatic mechanism which we shall consider in the next section.

In a molecule-ion collision there will frequently be several possibilities for charge transfer corresponding to several different vibrational levels of the products so that one would expect a rapid reaction. Furthermore, many of the collisions between any pair $A^+ + B$ will occur on attractive potential curves and thus will be "sticky," *i.e.*, the collision complex will not separate in the time of a vibration but will last for several or even many times this value. For such a complex the charge transfer will be an internal conversion and there will be more time for it to occur. Most exothermic processes should be possible with at least a small transition probability.

In certain cases in which potential curves do not cross, charge transfer with the emission of radiation is also a possibility. It is to be noted that the transition dipole moment for such a process could be very large since an electron jumps an ångström or more, and so the mean life could be quite small.

It has been emphasized here that the possibilities for charge transfer in low velocity collisions depends upon the potential curves. There is a definite possibility for certain exothermic processes to be forbidden or at least require large activation energy. As mentioned earlier, complicated molecular ions are expected to have low-lying excited states and these will frequently play an important role in the process. The transfer of charge may form electronically excited products.

There are no experimental measurements which give values directly for the process discussed above. Experimental values²³ for much higher energies, twenty-five to hundreds of electron volts, are available. At these high energies the transfer process

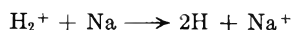


is found to occur with cross sections not much smaller than the kinetic theory value. These collisions certainly do not involve more than one oscillation of the complex and tend to confirm the belief expressed above that transition probabilities for this case should be high.

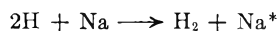
Adiabatic Charge Transfer

We have emphasized in this paper the mechanism in which an electron changes from one molecule to another without chemical transformation. This must be a "non-adiabatic" process, since the system changes from one state of excitation to

another. On the other hand, if there is a chemical transformation, the adiabatic connection of the initial to final state may involve an electron transfer which takes place with no restriction. There are many chemical reactions of ions which in this sense are "charge transfers." For example, the reaction



transfers the charge from the hydrogen molecule, although dissociation of the molecule results. This reaction is an "adiabatic" reaction in the ordinary meaning of the term; it is similar to the adiabatic chemiluminescent reaction



which has been discussed.²⁵

Another example of a reaction of this type has been discussed by Eyring, Hirschfelder and Taylor.¹⁶ It is the reaction



which is adiabatic and has a large rate constant.

Reactions of this type are important for radiation chemistry and will be the subject of a later paper.

Charge Transfer in Radiation Chemistry

While it is known from considerations such as we have been making above that positive charge transfer is certainly a very important elementary process in radiation chemistry, it is not known in any particular case just what the effect is in detail. Several types of experiments would seem to require charge transfer as an important step. The earliest example in the literature is the "catalysis" of the radiation induced polymerization of acetylene by various inert gases.²⁶ The most plausible explanations of the results requires that positive charge is readily transferred from many different kinds of ions to acetylene with high efficiency, since it is found that the reaction yield is almost completely independent of where the initial ionization occurs.²⁷ Dr. Lind²⁸ has recently pointed out that the efficiency seems to be related only to the total amount of ionization as compared among several unreacting gases which must receive considerably different amounts of electronic excitation. This

(25) J. L. Magee and T. Ri, *J. Chem. Phys.*, **9**, 638 (1941).

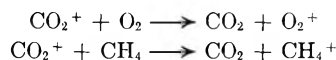
(26) He, Ne, A, Nz, Xe, Kr were used in the experiments.

(27) Reference 15, page 184.

(28) S. C. Lind, private communication.

seems to indicate greater importance for charge transfer than excitation transfer.

This series of experiments might suggest that charge transfer can take place with high efficiency between almost any pair $A^+ + B$ which has an exothermic reaction. It is also known, however, that large amounts of CO_2 present do not affect the rate of the radiation induced oxidation of methane.²⁷ It is possible that the charge transfer reactions which are also exothermic, have negligibly



small rates, and furnish examples of cases in which potential curves do not cross favorably.

It is almost certain that such phenomena as sensitization, protection, etc., are due in part to charge transfers. Manion and Burton²⁹ have used a charge transfer in their interpretations of the radiolysis of certain hydrocarbon mixtures.

REMARKS

Dr. J. NORTON WILSON (Shell Development Co., Emeryville, California): With regard to ionization potentials of hydrocarbons, it appears that the ionization potential of normal paraffins decreases monotonically with increasing chain length, whereas that of olefins more rapidly approaches a constant value with increasing chain length. The significance of this fact for charge-transfer processes is that it implies that the charge in $\text{C}_n\text{H}_{2n+2}^+$ is distributed over the whole molecule, whereas in $\text{C}_n\text{H}_{2n}^+$ it is concentrated in the vicinity of the double bond of the C_nH_{2n} , so the wave functions to be considered for computation of cross-sections for charge transfer differ considerably in spatial extent.

Dr. KURT E. SHULER (Applied Physics Laboratory, Silver Spring, Maryland): I should like to ask Dr. Magee about the meaning of the minima for the $A-A^+-\text{H}_2-\text{H}_2^+$ systems and how the potential curves for the vibrationally excited complexes were calculated.

REPLY: These curves are intended to be schematic only and have not actually been calculated. Qualitative arguments can be given, however, for the existence of large exchange interaction between H_2^+ and A. The electronic energy of the system $A^+ + \text{H}_2$ is almost identical with that of $\text{H}_2^+ + A$ and for small separations of the pair any method for calculating the resonant integral between the two states is sure to lead to a large value. This means exchange attraction exists for the system in its lowest state. There will be three other states of the system since A^+ is in a P state. One of these will be an antibonding state and higher than the others.

The vibrationally excited states have been obtained by adding the vibrational energy of H_2^+ , which is correct for large separations.

(29) J. P. Manion and M. Burton, *THIS JOURNAL*, **56**, 560 (1952).

RADIOLYSIS OF HYDROCARBON MIXTURES^{1,2}BY J. P. MANION³ AND MILTON BURTON*Department of Chemistry, University of Notre Dame, Notre Dame, Indiana**Received February 25, 1962*

Yields of hydrogen, methane, acetylene and ethylene resultant from action of 1.5 mev. electrons on pure liquid toluene, cyclohexene, benzene and cyclohexane as well as the liquid mixtures toluene-benzene, cyclohexene-benzene, cyclohexane-benzene and cyclohexane-cyclohexene are consistent with a mechanism in which both ionization transfer and excitation transfer play a significant role. Because of ionization transfer the primary chemical process occurring in a mixture tends to be characteristic of the component of lower ionization potential. Excitation transfer usually operates similarly. In cyclohexene-benzene radiolysis the two effects apparently act in opposition, with cyclohexene playing a sacrificial role in protection of benzene ions and benzene offering sponge-type protection to excited cyclohexene molecules.

Comparison of the C₂-gaseous products from liquid and vapor radiolyses of benzene and cyclohexene indicates fundamental differences in mechanism in the two phases. In the vapor mixture of these compounds, as well as in the pure vapors, violent attack by free atoms apparently occurs.

1. Introduction

According to Schoepfle and Fellows⁴ exposure of a solution of benzene and cyclohexane to 170 kv. cathode rays gives a yield of hydrogen much less than that predictable by application of the law of averages to the behavior of a mixture.⁵ The motivation of the work herein reported was the suggestion of Magee and Burton⁶ that in the radiation chemistry of mixtures ion-exchange processes may play an important role. In a mixture of two components, irrespective of the component primarily ionized, the ionization is quickly transferred to the species of lower ionization potential.⁷ Thereby, the resultant chemical processes may be greatly modified.

Protection in a binary mixture is, however, not so simple as might be expected merely from consideration of ionization potentials and reactivities of the molecules involved. Excited states of both components are produced in a primary process and the same, or other, excited states may be produced in neutralization processes. Energy may transfer from one component to the other so that it becomes difficult to predict *a priori* which excited species will predominate and control the nature of the primary chemical processes, although there is indication from studies of X-ray induced fluorescence by Kallmann and Furst⁸ that lower excited states will determine the end effects.

The various effects involved in ionization and excitation transfer and in reaction of intermediate free radicals in a mixture are important because most real situations in radiation chemistry, including especially those in radiobiology and radiology, pertain to multicomponent systems. Benzene, toluene, cyclohexane and cyclohexene have features both of similarity and dissimilarity. Consequently, comparisons of the radiation chemistry of

their mixtures promise some possibility of elucidation of the simpler aspects of the elementary processes involved. Four mixtures have been examined, namely, toluene-benzene, cyclohexene-benzene, cyclohexane-benzene, and cyclohexane-cyclohexene. Studies were confined to liquid systems, except for cyclohexane-benzene, and for the most part to determination of the gaseous products of radiolysis. The results obtained are consistent with an interpretation involving considerable emphasis on the ion and excitation-transfer mechanism.

2. Experimental

2.1 Chemicals.—One liter of Merck and Co., Inc., C.P. benzene, thiophene-free, was distilled at atmospheric pressure in a 50-theoretical-plate column. The middle one-third constant-boiling fraction was retained: n_D^{20} 1.4999; "International Critical Tables," n_D^{20} 1.5017.

A 500-ml. sample of Eimer and Amend C.P. toluene was distilled in a Todd column at atmospheric pressure and the middle constant-boiling 175 ml. fraction was retained: n_D^{20} 1.4954; "I.C.T.," n_D^{20} 1.4957.

Two liters of Dow Technical cyclohexane was distilled at atmospheric pressure in the 50-theoretical-plate column and the middle constant-boiling one-third fraction was retained: n_D^{20} 1.4253; "I.C.T.," n_D^{20} 1.4266.

A 500-g. sample of Eastman Kodak (1043) cyclohexene was distilled in the Todd column at atmospheric pressure and the middle one-third constant-boiling fraction was retained: n_D^{20} 1.4460; "I.C.T.," n_D^{20} 1.4451.

For prevention of accumulation of atmospheric water vapor the benzene, toluene and cyclohexane were stored over freshly prepared sodium wire in glass-stoppered bottles. The cyclohexene, which polymerizes in presence of sodium, was stored over finely powdered anhydrous magnesium sulfate which had been heated in an oven at 150° for two hours.

2.2 Cell Filling.—Two techniques were employed for filling of irradiation cells. In a "vacuum-filled" technique, liquid was stored and degassed on a vacuum line and transferred into the cells as described by Hentz and Burton.⁹ In a "pipet-filled" technique liquid stored over sodium wire was transferred by syringe-operated pipet into the irradiation cell which was then attached to a vacuum line by a ground glass joint, thoroughly degassed by conventional freezing and melting operations, and then sealed off under vacuum. The latter technique permits adventitious introduction of a small amount of atmospheric water vapor during pipet transfer. However, the two techniques were carefully compared in the case of cyclohexane without observable effect on the results. Consequently, for convenience in quantitative preparation of liquid mixtures, the "pipet-filled" technique was used for all mixtures, and most pure compound, irradiations.

2.3 Electron Bombardments.—Electron bombardments were made on the HVEC Van de Graaf generator of the Radiation Chemistry Project at the University of Notre Dame. Voltages were adjusted to 1.5 mev. \pm 1% by auto-

(1) Paper presented at Symposium on Radiation Chemistry, Division of Physical and Inorganic Chemistry, American Chemical Society, Cleveland, Ohio, April 11, 1951.

(2) Abstract of a thesis submitted by J. P. Manion to the Department of Chemistry of the University of Notre Dame in partial fulfillment of the requirements for the degree of Doctor of Philosophy.

(3) Sinclair Research Fellow; present address: Western Cartridge Co., East Alton, Illinois.

(4) C. S. Schoepfle and C. H. Fellows, *J. Ind. Eng. Chem.*, **23**, 1396 (1931).

(5) M. Burton, Proc. Conf. on Nuclear Chem., Chem. Inst. of Canada, 179 (1947).

(6) J. L. Magee and M. Burton, *J. Am. Chem. Soc.*, **73**, 523 (1951).

(7) H. D. Smyth, *Rev. Modern Phys.*, **3**, 347 (1931).

(8) H. Kallmann and M. Furst, *Phys. Rev.*, **79**, 857 (1950).

(9) R. R. Hentz and M. Burton, *J. Am. Chem. Soc.*, **73**, 532 (1951).

matic stabilization (before energy loss in the thin glass windows of the irradiation cell) and currents were adjusted either to 2.0 ± 0.1 or to 0.50 ± 0.05 microampere.

2.3.1. Liquid State.—Times of bombardment were varied over periods of 30 to 1200 sec. to permit accumulation of approximately the same amount of gaseous products in all cases. The type of irradiation cell used was similar to that described by Hentz and Burton.⁹ Thicknesses of the windows, measured with a micrometer to an accuracy of 0.001 in., varied from 0.018 in. to 0.030 in. A grounded aluminum shield of 4 mm. thickness, with a circular hole somewhat smaller in diameter than the cell window, located between the generator tube and the cell window, minimized the effect of secondary electrons originating in the thin aluminum window of the generator and permitted entry into the cell window only of electrons which entered at such angles as to ensure complete dissipation of their energy in the liquid. Accuracy of measurement of the number of coulombs entering the cell is estimated at $\pm 2\%$ except in the 30-second runs, in which the error may approach 10%.

Cells were cooled during exposure by a stream of water (temperature $\sim 20^\circ$) falling dropwise to ground. No water contacted the tungsten lead through which the current went from the cell *via* Leeds and Northrup Speedomax recording potentiometer to ground. The Speedomax recorder was standardized frequently with its internal standard cell and calibrated weekly externally with a Rubicon potentiometer. Earlier runs performed with a Brown recording potentiometer were corrected to the Speedomax base.⁹ Energy expenditure in the cell was calculated as described by Hentz and Burton.⁹

Conditions of irradiation (*e.g.*, location of cell in respect to generator window, method of water cooling, electrical contact to tungsten lead) were carefully reproduced. Periodic checks of a cyclohexane standard guarded against variation in technique during progress of the work.

Data on yield are reported in terms of G ; *i.e.*, number of molecules produced or converted per 100 e.v. of energy expended in the irradiated material.

2.3.2. Vapor State.—Benzene, cyclohexane and a 1:1 mixture of the two compounds were irradiated in the vapor state. Figure 1 shows the design of the Pyrex irradiation cell. Liquid was introduced from a pipet (cf. 2.3.1) at the standard-tapered joint C and thus into vessel G. Thereupon, the cell was connected at C to the vacuum apparatus and the liquid was degassed by conventional freezing and melting procedure prior to seal-off of the apparatus at B. Both compounds have the same vapor pressure of 100 mm. at 25° ; thus, the vapor in the irradiation compartment H was at a pressure of 100 mm. during irradiation of both compounds as well as the mixture. For removal of liquid film from the walls of compartment H, vessel G was submerged briefly in liquid nitrogen just before irradiation; in this way adventitious irradiation of liquid layers was avoided. The Pyrex window A was 0.080 inch thick and the cylindrical cell was about 2.7 cm. in diameter and 28.5 cm. long between window A and collector plate E. Current was collected on a nichrome disk E, just smaller than the internal diameter of the cell, spotwelded to a tungsten lead F which was in turn connected to ground through the Speedomax recorder. The cell was cooled during irradiation by an overhead sprinkling system which consisted of a length of copper tubing fitted with holes for exit of cooling water (temperature, 20°).

Each vapor-state irradiation lasted 6000 sec. with the generator preset to deliver 1.5 mev. electrons at 2μ amp. After exposure the cell was sealed at D to a vacuum apparatus for analysis and the break-off seal was broken.

The energy input was calculated as follows. According to the Feather formula a thickness of 0.101 in. Pyrex (density 2.5 g./cm.^3) will just stop a 1.5 mev. electron; 0.0175 in. stops a 0.5 mev. electron. Thus, in the energy range 0.5–1.5 mev. the average energy loss is 0.8% per mil of Pyrex. Since the window of the cell was 80 mil thick, a 1.5 mev. electron entering the window emerges into the vapor at an energy of 0.54 mev. Data on energy dissipation of high-energy electrons in biological tissue¹⁰ yielded a value of $0.200 \text{ kev. } \mu^{-1} \text{ g.}^{-1} \text{ cm.}^3$ for a 0.54 mev. electron. On the same basis, in cyclohexane vapor at 100 mm. and 25° (density $4.5 \times 10^{-4} \text{ g./cm.}^3$), a 0.54 mev. electron dissipates

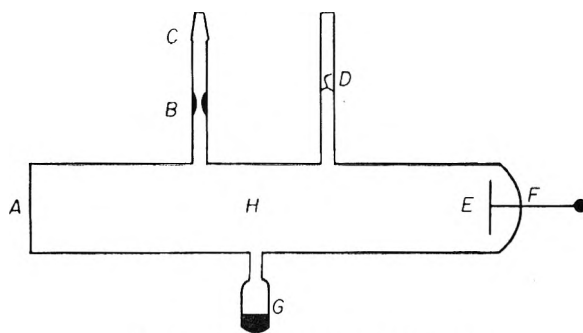


Fig. 1.—Vapor state irradiation cell.

4.75% of its energy in straight-line travel from the window to the collector plate (28.5 cm.).

Many electrons collected deviated considerably from straight-line travel. Furthermore, although the generator was preset to deliver 2μ amp. in all runs, the current collected at the plate ranged from 1.0 to 1.4μ amp.; *i.e.*, a sufficient number of electrons (up to 50%) were lost by back-scattering, by deviation to the wall, and by leakage to ground through ionized air so that they missed the collector entirely and were not recorded. The energy dissipation in the gas of such uncollected electrons was real but was probably less than 4.75%. Such factors result in a calculated energy input (based on 2μ amp. current) which is too high. Thus, G values so obtained represent a lower limit, not less than half of true values. Relative values, however, are felt to be reasonably accurate because of constancy of irradiation conditions throughout the vapor state studies.

2.4 Product Analyses.—After irradiation, each cell was attached to a vacuum line for analysis of product gases. Two gas fractions were examined, those non-condensable at -196° (*i.e.*, hydrogen and methane) and those non-condensable at -120° (*i.e.*, ethane, ethylene and acetylene). After determination of its pressure in a calibrated volume, the first fraction was analyzed for hydrogen by the Saunders-Taylor technique.¹¹ The residual gas, after treatment with moist potassium hydroxide to remove a small and reasonably constant amount of carbon dioxide evolved from hot copper oxide during hydrogen determination, was considered to be methane. Only in the case of toluene and its mixtures was the methane residue large enough for confirmation by mass spectrometry.

The second fraction, after measurement, was stored in a gas sample bulb for mass spectrometric analysis.

After gas analysis, the liquids were stored in contact with the atmosphere for various lengths of time. Polymer was determined by transfer of the liquids to tared weighing bottles and evaporation to constant weight. The value $G(p)$ is the estimated number of molecules converted to polymer per 100 e.v. input.

2.5 Reliability of Data.—Hydrogen values are accurate to better than 5%. Methane G values were usually too low for accurate determination. Only in the case of pure toluene and its mixtures was methane established by mass spectrometric analysis. The agreement obtained in repeated runs (*cf.* Table I) indicates that the technique employed leads to reproducible, if not absolutely correct, results. The interpretation requires comparison only between quantities of the same relative accuracy so that use of these data appears justifiable.

Analyses for C_2 -hydrocarbons were not so clean cut as for hydrogen, since some difficulty was encountered in deciding when all C_2 's had been collected. However, the reproducibility was good and, for this reason, significance can probably be attached to gross $G(C_2)$ values for both pure compounds and mixtures. On the other hand, mass spectrometric analyses of the C_2 -fractions can be in error by as much as 10%.

Polymer G values are not very accurate because of difficulty attendant on evaporation to constant weight. In cyclohexane and its mixtures, particularly, the polymer seemed to contain a component possessing rather high vapor pressure so that it was difficult to decide when solvent

(10) D. E. Lea, "Actions of Radiation on Living Cells," Cambridge University Press, Cambridge, 1947.

(11) K. W. Saunders and H. A. Taylor, *J. Chem. Phys.*, **9**, 616 (1941).

evaporation was complete. Since the polymer fraction is probably multicomponent, with some constituent possessing vapor pressure similar to that of the parent compound, this difficulty is expected. Thus, for $G(p)$ not even the relative accuracies are good and the data for the mixtures are not reported.

3. Results and Discussion: Liquids

3.1 Pure Liquids.—Tables I and II summarize results of irradiation of pure liquids. In all experiments included in those two tables total energy

TABLE I
DATA ON LIQUID STATE IRRADIATION OF PURE COMPOUNDS
WITH 1.5 MEV. ELECTRONS

Gas yield, ^a moles $\times 10^6$	Energy input, e.v. $\times 10^{-22}$	Cur- rent, μ amp.	H ₂ , %	CH ₄ , %	C ₂ , %	$G(g)^b$	$G(p)^c$
Cyclohexane							
5.13	0.0518	0.5	95.5	0.9	3.6	5.98	1.66
5.58	.057	.5	95.7	.8	3.5	5.92	
3.30	.0336	.5	97.0	.7	2.4	5.93 ^d	1.66
3.88	.045	2.0	96.6	.7	2.6	5.21 ^f	
12.70	.150	2.0	93.0	.6	6.5	5.12 ^f	
3.12	.0337	0.5	93.5	1.9	4.6	5.60 ^d	
4.00	.0405	2.0	91.5	1.5	7.2	5.96 ^d	
5.84	.049 ^e	0.5	95.8	0.6	3.6	5.98 ^d	
6.08	.052 ^e	0.5	96.0	0.4	3.7	5.88 ^d	
Benzene ^g							
1.85	1.90	2.0	62.0	1.0	37.0	0.0588	0.76
2.06	2.11	2.0	59.0	1.0	40.0	.0588	.77
1.97	1.67 ^h	2.0	58.1	0.8	41.1	.0581 ^d	
2.30	1.79 ^h	2.0	58.6	0.9	40.5	.0633 ^d	
1.96	1.52	2.0	59.5	1.8	38.9	.0614	
Toluene							
3.89	1.63	2.0	92.0	5.7	2.3	.144	
3.83	1.73	2.0	91.0	5.0	4.0	.133	.918
Cyclohexene							
3.60	0.157	0.5	88.3	1.4	10.3	1.38	12.4

^a Total gas volatile at -120° . ^b Total number of molecules of gas produced per 100 e.v. of energy dissipated in liquid. ^c Weight of polymer times Avogadro's number divided by molecular weight of parent compound and energy input in units of 100 e.v. ^d Cells filled by "vacuum technique." ^e Current recorded on Brown potentiometer; G corrected to Speedomax results. ^f Air was found in these samples after irradiation. ^g The $G(g)$ values for pure liquid benzene are confirmed by more accurate work of Mr. Sheffield Gordon; *cf.*, however, footnote 14.

TABLE II
100 e.v. YIELDS FOR PURE COMPOUNDS IN THE LIQUID
STATE¹⁴

	$G(H_2)$	$G(CH_4)$	$G(C_2)$	$G(p)$
Benzene	0.036	0.0012	0.022	0.76
Toluene	0.13	.0077	.0043	0.92
Cyclohexane	5.7	.09	.21	1.7
Cyclohexene	1.2	.019	.142	12.4

input varied over a rather small range (less than a factor of two except in one case) and intensity of irradiation was adjusted to one of two values varying by a factor of four. The data show rather well that the "vacuum-filling" technique gave results not significantly different from the "pipet-filling" technique gave results not significantly different from the "pipet-filling" technique.

The principal gas produced in all four pure liquids

studied is hydrogen. Methane comprises a significant portion of the total only in toluene irradiation and even in that case it is small, presumably because of protection of the methyl group by the ring.^{9,12,13} In the case of benzene the yield of C₂-gas comprises about 40% of the total.¹⁴ The relatively small amount of C₂-gas from cyclohexane is entirely ethylene, while in cyclohexene nearly all of of the C₂-gas is ethylene with only 2% acetylene present. Explanations of the low yield of acetylene from that compound and the high fraction of ethylene in the C₂-fraction of toluene are not obvious. An interesting point is the relatively low value of $G(C_2)$ for toluene compared with that for benzene. A possible explanation is that in toluene the more probable processes are at the side group, either primarily as a result of internal conversion of energy (*cf.* Hentz and Burton⁹) or secondarily in the reactions involving free radical disappearance.

3.2 Liquid Mixtures

3.2.1. General Examination of Data on Methane and Hydrogen Yields.—Since cyclohexane is saturated it may be presumed that product yields in the pure compound are determined principally by primary processes. In a mixture the fate of primarily produced radicals or atoms will depend in part on the other component present. However, the amount of primary chemical process in the cyclohexane should be linearly related to the amount of energy absorbed in the cyclohexane itself provided no other interfering process (*e.g.*, some special kind of deactivation) occurs in a mixture. This statement is equivalent to the proposition that the law of averages is obeyed in a mixture so far as the primary process is concerned. We assume as a reasonable approximation, lacking pertinent data, that the amount of energy absorbed in each compound in a mixture is proportional to the total number of electrons in each component; *i.e.*, to the combined atomic number (Z) of a compound times its mole fraction (n) in the mixture. For convenience, therefore, the figures show the yields as function of the fraction of electrons associated with one component—called electron fraction.

Figs. 2 and 3 give $G(H_2)$ as function of electron fraction for the four mixtures studied. The dotted lines represent the yields expected if the law of averages were to apply to the over-all processes. Figure 2 shows considerable departure from such behavior when benzene or cyclohexene is added to cyclohexane and a much smaller departure when benzene is added to cyclohexene. On the other hand, Figure 3 shows that in a mixture of benzene and toluene, compounds very much of the same type, the law of averages holds rather well.

Returning to Fig. 2 the ratio of the 100 e.v. yield of hydrogen which might have been expected on the law of averages and the 100 e.v. yield of hydrogen actually observed shows the extent of effect of the

(12) M. Burton, S. Gordon and R. R. Hentz, *J. chim. phys.*, **48**, 190 (1951).

(13) T. J. Sworski, R. R. Hentz and M. Burton, *J. Am. Chem. Soc.*, **73**, 1998 (1951).

(14) More accurate, as yet unpublished, work of Mr. Sheffield Gordon has now established that no methane is produced in the radiolysis of liquid benzene and that the product gases are exclusively hydrogen and acetylene.

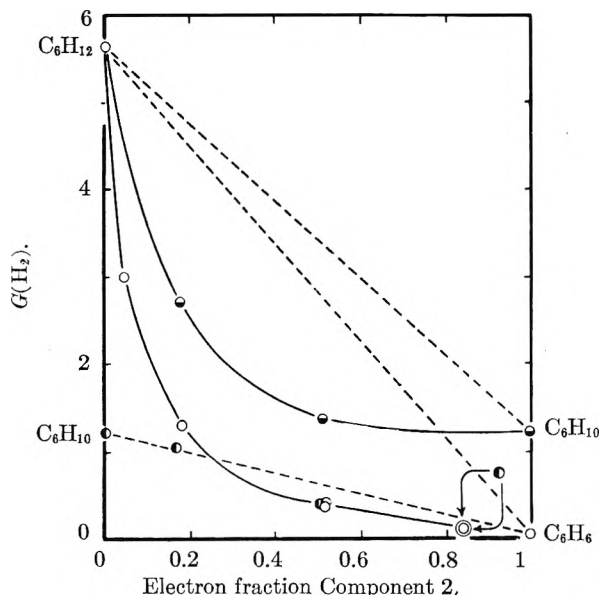


Fig. 2.—Variation of 100 e.v. yield of hydrogen with composition of mixtures: O, cyclohexane-benzene; ●, cyclohexene-benzene; ⊙, cyclohexane-cyclohexene.

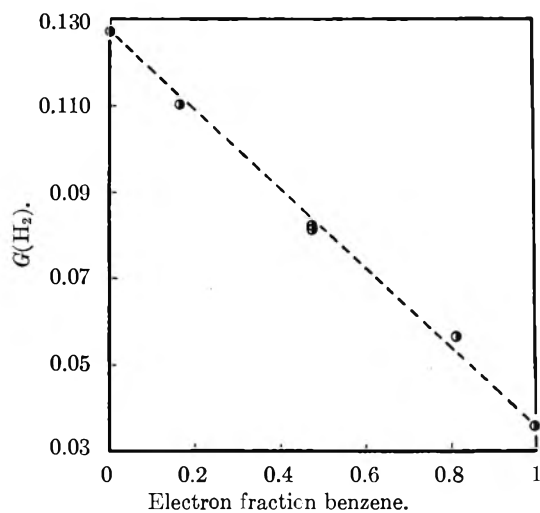


Fig. 3.—Variation of 100 e.v. yield of hydrogen with electron per cent. benzene for toluene-benzene liquid mixtures.

added component. However, it is more useful to calculate the law-of-averages 100 e.v. yield for the more sensitive component, $G(H_2, A)_{law}$, and to compare it with the portion of the observed yield calculated to come from that component, $G(H_2, A)_{obsd}$. The latter figure is obtained by subtraction from $G(H_2)$ of the contribution from the less sensitive component, on the assumption that the latter is a linear function of the electron per cent. of that component. We define a quantity

$$\rho = \frac{G(H_2, A)_{law}}{G(H_2, A)_{obsd}}$$

For a useful expression we require some additional definitions. We let A be the more sensitive component of the mixture, B the less sensitive. E_A and E_B are the respective electron numbers (*i.e.*, sums of atomic numbers in the molecules) and f is the ratio E_A/E_B . The values $1 - x$ and x are the respective mole fractions. The 100 e.v. yields

of hydrogen from pure A and pure B are, respectively, mc and m . From the definitions of $G(H_2, A)_{law}$ and $G(H_2, A)_{obsd}$, it follows that

$$\rho = \frac{f(1-x)mc}{f(1-x)+x} \div \left[G(H_2) - \frac{mx}{f(1-x)+x} \right]$$

or

$$\rho = \frac{f(1-x)mc}{G(H_2)[f(1-x)+x] - mx} \quad (I)$$

Figure 4 gives plots of ρ for the three mixtures shown in Fig. 2. In two of the cases (cyclohexane-benzene and cyclohexane-cyclohexene) ρ appears to be a simple linear function of the mole fraction of the less reactive component with a value equal to 1 when $x = 0$; *i.e.*

$$\rho = 1 + bx \quad (II)$$

It follows from equations I and II that

$$G(H_2) = \frac{f(1-x)mc}{(1+bx)[f(1-x)+x]} + \frac{mx}{f(1-x)+x} \quad (III)$$

where b is evaluated from Fig. 4 and is 11.9 for cyclohexane-benzene and 5.1 for cyclohexane-cyclohexene.

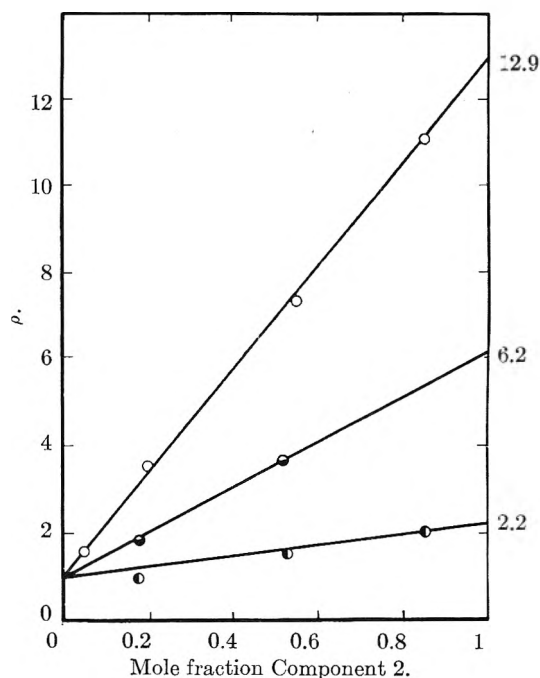
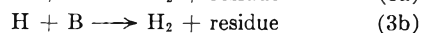
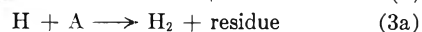
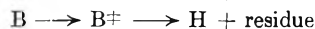
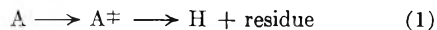
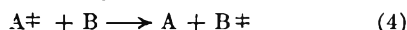


Fig. 4.—Variation of ratio "G(H₂) expected" to "G(H₂) observed" from Component 1 with mole fraction of Component 2: O, cyclohexane-benzene; ●, cyclohexene-benzene; ⊙, cyclohexane-cyclohexene.

A very simple interpretation of equation III may be made on a straightforward energy-transfer basis. Consider that energized molecules of A and B (*i.e.*, A^\ddagger and B^\ddagger) are the sole source of H atoms and that the latter readily give H₂ molecules by secondary reactions which involve either A or B in purely random fashion.

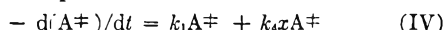


The descriptions A^\ddagger and B^\ddagger include both ions and excited molecules. Such entities are not all equally stable. While energized alkane molecules appear to decompose very readily, energized benzene molecules are very enduring.⁶ According to the Magee-Burton picture of the role of ionization transfer,⁶ ionization is transferred with high probability from a molecule of higher ionization potential to one of lower and the chemistry of the entity so-produced thereafter plays a dominant role. We write, quite formally



where both ions and excited molecules are indicated by reaction (4) and the excitation potential of A is likewise presumed to be higher than that of B.

The kinetics may be seen from the following scheme. For a particular concentration of A^\ddagger



The two terms on the right represent the respective rates of decomposition and of energy transfer to component B, the rate of the latter depending on its mole fraction x . Thus, the fraction of energized A decomposing and eventually yielding product H_2 molecules is $k_1/(k_1 + k_4 x)$; *i.e.*

$$\frac{1}{\rho} = \frac{G(H_2, A)_{\text{obsd}}}{G(H_2, A)_{\text{law}}} = \frac{k_1}{k_1 + k_4 x} = \frac{1}{1 + (k_4/k_1)x} \quad (V)$$

and from II

$$b = k_4/k_1 \quad (VI)$$

Now, according to the law of averages, the yield of H_2 which might have been expected from the component A in a mixture, had no other process intervened, would have been simply

$$G(H_2, A)_{\text{law}} = \frac{f(1-x)mc}{f(1-x) + x} \quad (VII)$$

but the "observed yield," $G(H_2, A)_{\text{obsd}}$ is less by the factor $1/(1 + bx)$ and the first term of equation III results.

The second term of equation III represents H_2 yield attributable to primarily energized B and makes a significant contribution only at very high values of x .

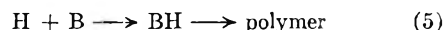
We might properly expect a third term in equation III to account for energy absorbed in A and transferred to B with resultant production of H_2 . This term would be

$$\frac{k_4 x}{k_1 + k_4 x} \times \frac{f(1-x)}{f(1-x) + x} \times m = \frac{bx}{1 + bx} \times \frac{f(1-x)}{f(1-x) + x} \times m$$

Such a term tends to be negligible at low values of x when m is small because mx will be small and approaches zero as x approaches unity. Thus, it has no usefulness in equation III for the two cases of interest.

Other explanations of the form of equation III have been suggested. One involves the idea that component B is the predominant absorbent of energy in a mixture and that its absorption is greater by a factor ρ . While this idea yields a formally satisfactory equation it is not in consonance with what we know of additivity of stopping power of atoms in a molecule; this additivity is the essential basis of the use of the parameter f in establishment

of the value of ρ . Another explanation (suggested by Dr. Eric J. Y. Scott) is that all the molecular hydrogen results from action of hydrogen atoms on component B and that two reactions compete, a reaction like (3b) and



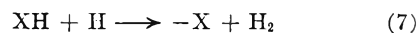
Such a treatment can be made to lead to a kinetic equation formally similar to that already discussed but involves considerations of the relative rates of (3b) and (5), no satisfactory data for which are presently available.

The deviation from linearity in Fig. 4 in the case of cyclohexane-benzene and, in particular, the failure of ρ to extrapolate to unity at zero mole fraction of the less reactive component are real and reflect a situation in which the $G(H_2)$ values of the pure separate components are not very greatly different and in which the defined term $G(H_2, A)_{\text{obsd}}$ is not approximately identical with any useful quantity.

At this point the mechanism of formation of observable hydrogen requires examination. Schematically the primary reaction involving C-H bond rupture may be written



In benzene, cyclohexane and cyclohexene the hydrogen atoms involved are, of course, connected directly to the ring but in toluene the hydrogen atom is in the methyl group.⁹ The ensuing reactions must depend on the energy with which the H atom is produced in reaction (6). The bond strength involved is roughly 4-5 e.v. while the energy involved in the decomposition process may be as low as 4.8 e.v. (as in excitation-induced decomposition of toluene⁹) or 5.9 e.v. (as in similar decomposition from the lowest excited state of cyclohexene¹⁵) or as high as 8 e.v. or more when an ionization process is involved.¹⁶ Thus, under certain conditions the H atom product of reaction (6) may carry with it 2 e.v., or more, excess energy; *i.e.*, the H atom may be "hot." The ensuing reactions are



or



Reaction (8) is ruled out only in the case of cyclohexane. Indeed, the evidence from the work of Melville and Robb¹⁷ is that it has zero activation energy for benzene and cyclohexene, at least in the gas phase, and presumably the same activation energy for toluene. On the other hand, reaction (7) has activation energy, E_7 , roughly near 10 kcal.; on the basis of bond strengths¹⁸ we may estimate that E_7 will be lowest for the vinyl C-H in cyclohexene, intermediate in toluene, and highest in benzene. For H-atoms of the same energy reaction (8) would thus be most favored, relatively to (7), in benzene, least in cyclohexene. Actually, the work of Melville and Robb¹⁷ indicates that the spe-

(15) L. W. Pickett, M. Munz and E. M. McPherson, *J. Am. Chem. Soc.*, **73**, 4862 (1951).

(16) Table V summarizes ionization potentials. Cf. M. Burton, *J. Chem. Ed.*, **28**, 404 (1951), for a general discussion of elementary processes in radiation chemistry.

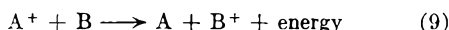
(17) H. W. Melville and J. C. Robb, *Proc. Roy. Soc. (London)*, **A202**, 181 (1950).

(18) M. Szwarc, *Chem. Revs.*, **47**, 75 (1950).

cific rates of reaction (8) (*i.e.*, with "cold" H) are 9.8×10^{13} and 9.6×10^{13} cc. mole⁻¹ sec.⁻¹ in benzene and cyclohexene, respectively. Greater yield of H₂ from cyclohexene, as compared with benzene may be attributed not only to greater probability of the primary reaction (6) but also to the lower activation energy of reaction (7).

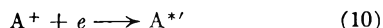
Returning now to the meaning of ρ , we see that $G(\text{H}_2, \text{A})_{\text{obsd}}$ is determined in a mixture by competition between both components for H atoms, which have an energy distribution determined by the relative amounts of the two components being simultaneously decomposed. Actually, observed yields of hydrogen are thus determined by relative probabilities of reaction (7) in the two components as well as by the extent to which the relative probabilities of reaction (6) in the two components affect each other. In particular, if the energy distribution of H atoms primarily produced varies considerably as the composition is changed, we must also consider the impact of this variation on the ratio of rates r_8/r_7 for each component and on the actual rate r_7 . In the interpretation of equation IV the explicit assumption was made that the primary H atoms yielded H₂ by purely random reaction with either of the components of a mixture. This assumption is consistent with the view that irrespective of the primary reaction the H atom is produced with sufficient excess energy to make the activation energy of reaction (7) a negligible consideration.

3.2.2 Ionization and Excitation Transfer.—In a mixture of two components A and B, both are primarily affected by ionizing radiation with production both of ions A⁺ and B⁺ and of excited molecules A* and B*. Both ions and excited molecules can be produced in states above the lowest but such states make a relatively small contribution and are neglected in the following discussion. Consider the situation $I_A > I_B$ where I_A and I_B are the respective ionization potentials. Then, according to Smyth⁷

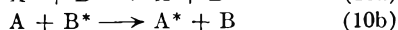
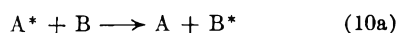


and it might appear, consequently, that the radiation chemistry of the mixture is really that of B, modified by the fact that secondary processes involving radicals may involve also component A. Such a conclusion is an over-simplification and neglects not only the processes intermediate between formation of B⁺ and the first chemical change but also the contribution of A* and B* to the chemistry of the whole system.

We consider first the contribution of primary excited molecules A* and B*. Let E_A and E_B represent respective excitation potentials. The relative values of E_A and E_B are not set by I_A and I_B . Indeed, E_A may be less than E_B and the situation is made even more complicated by consideration of higher excited states resulting from the general class of reactions

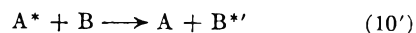


We note merely that either of the reactions

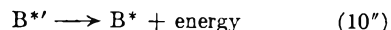


can occur dependent on the relative heights of the energy levels involved.

The condition for most probable excitation transfer is that $E_A = E_B$. Under such conditions excitation transfers in either direction. Our concern is with conditions which effectively favor energy flow in one direction, as in reaction (10a). Imagine that B has excitation levels lower than the lowest excited level of A. The reaction which occurs in the first instance may then be



where B* is an excited state of B above B*, which for simplicity we take as the lowest excited state of B. Thereafter, B* loses energy piecemeal in collisional processes and may be involved in internal conversion processes from one electronic state to another so that the terminal excited state may be B* or some other state of B lower than A*. We write to summarize this totality of processes



The over-all effect is as if reaction (10a) occurs. In this writing, as a sort of shorthand, we shall speak of reactions similar to (10a) as occurring when $E_B < E_A$, the reference being to lowest excited states, when actually the implication is the series of reactions epitomized in (10') and (10''). Similar remarks apply to the use of reaction (10b).

TABLE III

MASS SPECTROMETRIC ANALYSES OF C₂-HYDROCARBON PRODUCTS FROM IRRADIATION OF PURE LIQUID COMPOUNDS WITH 1.5 MEV. ELECTRONS

Compound	C ₂ H ₂ , %	C ₂ H ₄ , %
Benzene	100	Trace?
Cyclohexane	0	100
Cyclohexene	2	98
Toluene	42	58

The total effect of reactions (9), (10a) and (10b) in a mixture in which A has a higher ionization potential than B is that the effect of radiation on A is reduced but not eliminated. Processes possibly occurring are determined by relative excitation potentials, resistance of the various components to radiation, and secondary effects involving reaction between one component and free radicals produced from the second. Each case must be carefully examined separately.

Table IV gives ionization potentials of the gases of the compounds chosen for study. Spectral values are those calculated from extrapolation of the Rydberg Series. In the case of cyclohexene the character of the spectrum did not permit an unambiguous extrapolation but Price¹⁹ estimated from theoretical considerations that the extrapolated value was nearly the same as that for benzene. It should be emphasized that the values given in Table IV refer only to the gaseous state. We assume only that they remain in the same order in the liquid state.

3.2.3 Toluene-Benzene.—Toluene has the lower ionization potential and should therefore protect benzene and be itself sacrificed in the process (*cf.* remarks on reaction (9) and (10a) in the preceding section). However, free radicals are presumable intermediates in the reaction schemes by which

(19) W. C. Price, *Proc. Roy. Soc. (London)*, **A174**, 207 (1940).

TABLE IV

IONIZATION POTENTIALS OF COMPOUNDS STUDIED

Compound	Method	Potential, e.v.	Reference
Toluene	Spectral	8.77	20
Cyclohexene	Spectral	9.2 ^a	19
Benzene	Spectral	9.19	21
	Spectral	9.24	22
	Impact	9.43	23
Cyclohexane	Impact	9.8	24
	Impact	11.0	24

^a This value is selected by Price²³ as being approximately the same as that of benzene.

hydrogen and methane are produced. Toluene and benzene are approximately equally effective in removing such radicals by addition reactions. They are, however, different in their ability to yield hydrogen and methane. Work of Hentz and Burton⁹ suggests that in pure toluene the dominant primary chemical reaction in the liquid phase is



followed by

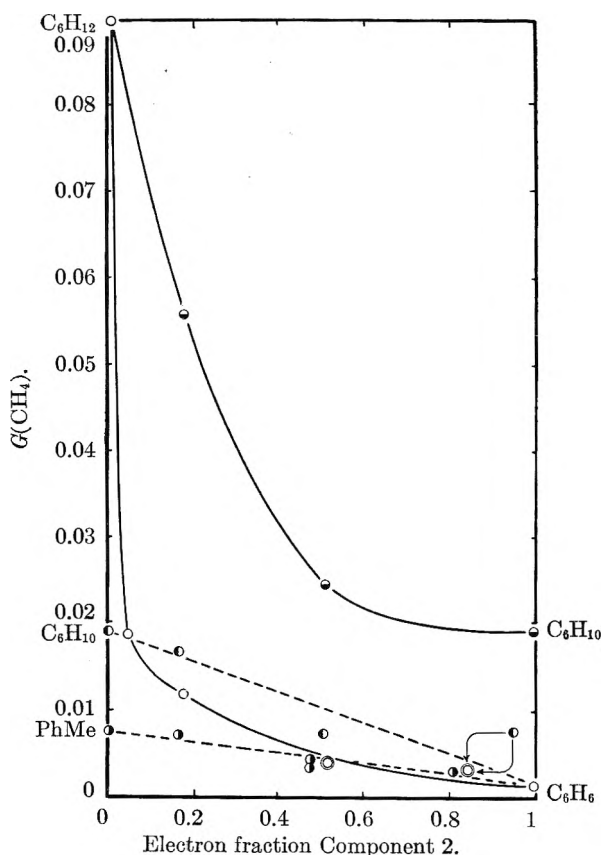


Fig. 5.—Variation of 100 e.v. yield of methane with composition of mixtures: ○, cyclohexane-benzene; ●, cyclohexene-benzene; ⊙, cyclohexane-cyclohexene; ⊚, toluene-benzene.

(20) W. C. Price and A. D. Walsh, *Proc. Roy. Soc. (London)*, **A191**, 22 (1947).

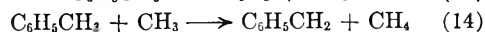
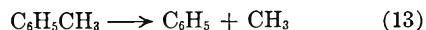
(21) W. C. Price and R. W. Wood, *J. Chem. Phys.*, **3**, 439 (1935).

(22) W. C. Price, *Chem. Revs.*, **41**, 257 (1947).

(23) R. E. Honig, *J. Chem. Phys.*, **16**, 105 (1948).

(24) A. Hustrulid, P. Kusch and J. T. Tate, *Phys. Rev.*, **54**, 1037 (1938).

Methane is produced by corresponding, but much less frequent, reactions involving methyl.



In a mixture of toluene and benzene, we may surmise, in terms of the ionization transfer mechanism, that the primary processes are essentially those peculiar to toluene. Secondary processes actually occur depend on the relative concentrations of toluene and benzene. Figures 3 and 5 are interpretable on the basis of such simple considerations.

When primary chemical processes involve production of ultimate molecules, the ionization transfer mechanism should be clearly revealed—if the excitation transfer mechanism does not confuse the situation. Photochemistry^{9,25,26} indicates that in the radiolysis of a mixture of toluene and benzene the contribution of the excitation transfer mechanism is unimportant, for the lower excited states make a negligible contribution to the total chemical effect. Differences in the character of the C₂-gaseous products from liquid and gaseous benzene (see Tables III and V) suggest that the former are produced by a rearrangement mechanism, while bond rupture and a free radical mechanism are the mechanism of production of the latter.²⁷ Consequently, we may expect that yields of acetylene and ethylene in radiolysis of this liquid mixture should be more clearly consistent with an ionization transfer mechanism. Tables II and III indicate that toluene makes an unimportant contribution to acetylene yield. Thus, if the primary chemical process involves principally toluene, as is required by the ionization transfer mechanism, the yield of acetylene in a mixture of toluene and benzene should be generally less than that in pure benzene, just as is shown in Fig. 6. On the other hand, the dominance of toluene in the primary chemical process should result in a yield of ethylene substantially the same as that found in pure toluene, just as is shown in Fig. 7.

TABLE V

APPROXIMATE 100 E.V. YIELDS IN VAPOR STATE BOMBARDMENT OF CYCLOHEXANE-BENZENE MIXTURES WITH 0.54 MEV. ELECTRONS^a

C ₆ H ₆ mole %	G(H ₂)	G(CH ₄)	G(C ₂)	G(C ₂ H ₂)	G(C ₂ H ₄)	G(C ₂ H ₆)
0	1.4	0.07	0.48	0	0.31	0.17
55	0.2	0.03	.39	0.06	.33	0
100	0.011 ^b		.16	.11	.05	0

^a For reasons stated in section 2.3.2 these values are minima and have only relative validity. ^b The combined hydrogen and methane fraction was too small for analysis in each of the two runs made.

The data as well as the hypothesis proposed, indicate that in a toluene-benzene mixture, toluene is a "sacrificial protector"¹² of the benzene.

3.2.4 Cyclohexene-Benzene.—Cyclohexene has about the same ionization potential as benzene.

(25) G. I. Krassina, *Acta Physicochimica (U. S. S. R.)*, **10**, 189 (1939).

(26) J. E. Wilson and W. A. Noyes, Jr., *J. Am. Chem. Soc.*, **63**, 3025 (1941).

(27) Cf. M. Burton, *THIS JOURNAL*, **52**, 810 (1948), for remarks on the increased importance of rearrangement processes in the radiation chemistry of liquid systems.

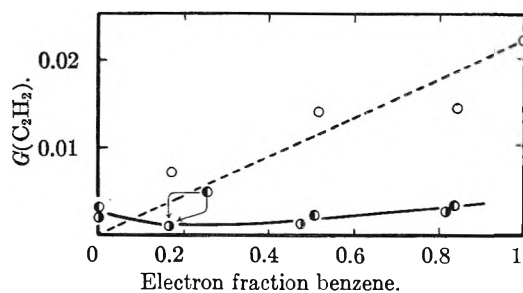
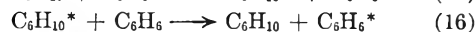
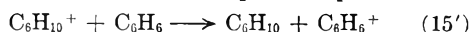


Fig. 6.—Variation of 100 e.v. yield of acetylene with composition of benzene mixtures: O, cyclohexane; ◐, cyclohexene; ●, toluene.

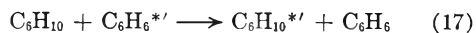
However, its lowest observed excitation potential in the vapor state is about 5.9 e.v.¹⁵ contrasted with about 4 e.v. for benzene. Photochemistry indicates that primarily excited states of benzene thus contribute practically nothing to the yield observed in radiolysis.^{5,25,26} Consequently, we may surmise, according to the mechanism under consideration, that the two secondary physical processes



play a dominant role.²⁸ The possible process



is not ruled out by the evidence at hand (*cf.* Table III and comments thereon). However, if (15) and (15') occur as reverse reactions, reaction (15) must have the dominant effect in determination of ultimate products. This conclusion follows from the resistance of benzene to high-energy radiation. The relative inertness of benzene is a reflection of the stability not only of the ion C_6H_6^+ but also of any excited molecule C_6H_6^* produced by its neutralization.⁵ Such a highly excited molecule will survive sufficiently long to transfer its energy to cyclohexene



On the other hand, a highly excited cyclohexene molecule will decompose with high probability before the reaction reverse to (17) occurs. The total effect is as if reaction (15') makes no important contribution to the over-all process. Indeed the results are the same as if cyclohexene has a slightly lower ionization potential than benzene, as may well be the case. According to this viewpoint the primary chemical process occurs mainly in the cyclohexene. However, to a significant extent the cyclohexene may be protected against decomposition by the benzene (*cf.* reaction (16)) without decomposition of the latter.

Consistency of the energy-transfer picture with the facts is clearly shown in Figs. 2, 5, 6 and 7. Yields of hydrogen, methane, acetylene and ethylene are all less in the mixture than would be expected on the law of averages. Cyclohexene itself yields practically no acetylene. The curve for yield of acetylene as a function of electron fraction of benzene is practically identical with the similar

(28) It is thought from mass spectrometric information that other ion fragments may also be involved. However, the parent ions are certainly the most important and lack of knowledge of any of the details of ionization in the liquid state precludes a more elaborate statement. Reactions (15) and (16) are illustrative of the main features of possible energy-transfer processes occurring.

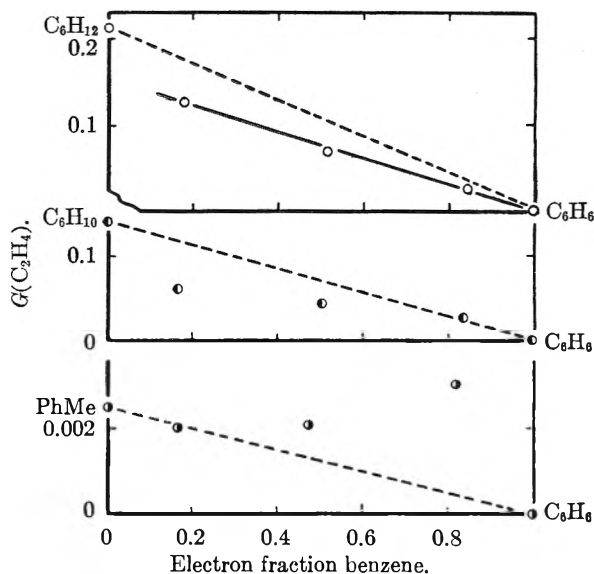


Fig. 7.—Variation of 100 e.v. yield of ethylene with composition of benzene mixtures: O, cyclohexane; ◐, cyclohexene; ●, toluene.

curve for the toluene-benzene mixture (*cf.* Fig. 6). According to the ionization transfer picture, this result means that toluene and cyclohexene both tap off ionization from the benzene to approximately the same degree and protect it against decomposition. To the extent that cyclohexene is itself decomposed as a result of this effect, its function is sacrificial.¹² However, the elementary physical processes result in production of a greater number of primarily excited molecules than of ions. The results are consistent with the interpretation that excited states of cyclohexene are depleted by reaction (16), for Figs. 2, 5 and 7 show hydrogen, methane and ethylene yields below the values predicted by the law of averages for the mixtures.

The data and theory here presented indicate that, because of ionization transfer, cyclohexene is a sacrificial protector for benzene and that benzene, because of excitation transfer, is a "sponge-type" protector¹² for cyclohexene.

3.2.5 Cyclohexane-Benzene.—Data on hydrogen, methane and ethylene yields shown in Figs. 2, 5 and 7 are all consistent with the interpretation that benzene protects cyclohexane because it has both lower ionization potential and lower excitation potential. Figure 6 indicates that in this process of protection benzene is itself sacrificed (to a relatively small extent), for the yield of acetylene appears generally (*i.e.*, within experimental error) to be above that predictable on the law of averages. However, because benzene itself is so resistant to reaction most of the ionization is transferred without any chemical effect.

3.2.6 Cyclohexane-Cyclohexene.—Cyclohexene has a lower ionization potential and should protect cyclohexane against decomposition. Figures 2, 5 and 8 show such an effect for yields of hydrogen, methane and total C_2 -gas, respectively. At the same time sacrifice of cyclohexene would be expected. The unfortunately limited evidence available indicates just such sacrificial protection. The C_2 -gas from the mixture containing 52 mole per

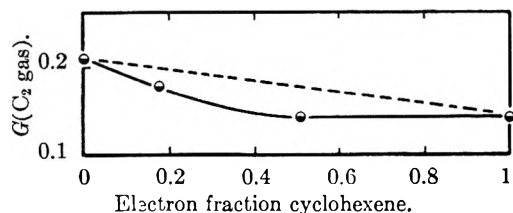


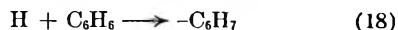
Fig. 8.—Variation of 100 e.v. yield of C₂-gas with composition of cyclohexane-cyclohexene mixtures.

cent. cyclohexene was lost but that from the 19% (0.174 electron fraction) cyclohexene mixture was saved and analyzed; it was 98% ethylene and 2% acetylene, the value found for pure cyclohexene (see Table IV). If this result can be accepted, it indicates that even at low mole fraction of cyclohexene the primary decomposition involves mainly the component of lower ionization potential.

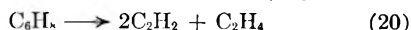
4. Results and Discussion: Vapors

4.1 Pure Vapors.—Table V summarizes information on 100 e.v. yields of gases from benzene and cyclohexene vapors irradiated with 0.54 mev. electrons as described. Although these values are uncertain and at best represent only minima, they are relatively correct for the same compound. Each value is the average of results of two experiments and, except for combined H₂ and CH₄ yield from benzene, is accurate to ±10%. The accuracy of G(H₂ + CH₄) in benzene is ±0.004.

Taken together with Tables II and III, Table V shows that the liquid state tends to deactivate excited molecules before they can decompose and thus to decrease the yield of product. In benzene, this fact is clearly evident for acetylene yield but is seemingly refuted for hydrogen and methane production. An explanation appears in the ethylene yield. Ethylene is not produced in radiolysis of liquid benzene although it is produced with a yield G(C₂H₄) = 0.05 from the vapor. Studies of the action of epithermal hydrogen atoms on benzene by Schiff and Steacie²⁹ (Wood-Bonhoeffer method) and by Scott and Steacie³⁰ (mercury sensitization at high temperatures) indicate cracking of the gaseous compound to yield mainly low molecular weight straight-chain hydrocarbons such as methane, ethane, acetylene, etc. (*cf.* also Bonhoeffer and Harteck³¹). The mechanism has not been established but may involve intermediate addition reactions; *e.g.*



which in the gaseous state is formed hot and decomposes before it can be deactivated, *e.g.*



Enthalpies of formation of benzene, cyclohexadiene, acetylene, and ethylene at 0°K. are 24.0, 20.5, 54.33 and 14.52 kcal., respectively.³² Taking the H-H bond strength as 103.2 kcal.,³³ it follows that ΔH

(29) H. I. Schiff and E. W. R. Steacie, *Can. J. Chem.*, **29**, 1 (1951).

(30) E. J. Y. Scott and E. W. R. Steacie, *ibid.*, **29**, 233 (1951).

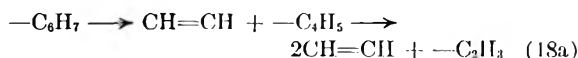
(31) K. F. Bonhoeffer and P. Harteck, *Z. physik. Chem.*, **139A**, 64 (1928).

(32) G. Glockler, *Discussions Faraday Soc.*, in press, 1951.

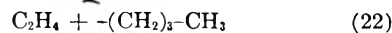
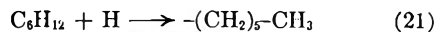
(33) A. G. Gaydon, "Dissociation Energies and Spectra of Diatomic Molecules," Chapman and Hall, London, 1947, p. 98.

for reactions (18) plus (19) is -97.7 kcal. It is not reasonable to assume that all of that energy remains available in the molecule at the end of reaction (19) as it would have to be were reaction (20) (with ΔH = 93.68 kcal.) to follow as an immediate consequence.

A simple interpretation of the results is that any acetylene and ethylene production in gaseous-state radiolysis of benzene involves action by a hot hydrogen atom produced in the primary step and that this hydrogen atom can act either in reaction (18) to open the chain and "unpeel," *e.g.* by the successive reactions



with C₂H₃ ultimately capturing a hydrogen atom, or by reactions (19) and (20). The relative yields of acetylene and ethylene are about what may be expected on the basis of predominance of reactions (18) to (20). On this same interpretation the decreased yield of hydrogen plus methane in benzene-vapor radiolysis is illusory and reflects merely increased probability of reaction (20), or perhaps of the whole sequence, in the vapor. This explanation is, however, wholly tentative and awaits completion of more detailed studies of the radiolysis of benzene. It accounts for substantial absence of ethylene in the C₂ product from liquid benzene only if we assume that in that case the small amount of acetylene produced comes from some mechanism other than the sequence (18) to (20); *e.g.*, decomposition of excited benzene directly into acetylene molecules. The ratio of G(C₂H₄) to G(C₂-H₆) in radiolysis of cyclohexane vapor suggests that a mechanism in which the ring opens in the first step and unpeeling occurs may be operative, *i.e.*



with the ethyl radical ultimately yielding C₂H₆ either by combination with a free H atom or by reaction with a hydrogen molecule. The evidence appears to be that large free radicals are stable at room temperature. However, the hydrogen atom involved in step (21) is probably hot so that the series (21) to (23) is reasonable. Since the G values have only relative significance, only conclusions based on relative values can be valid. The true G values for cyclohexane vapor are higher than those given. Nevertheless, it is clear that the ratio G(H₂)/G(CH₄) is higher in the liquid than in the vapor. Perhaps this fact is a reflection of the fact that a Franck-Rabinowitch cage³⁴ in a liquid is more effective for free methyl radicals than for free hydrogen atoms.^{9,13}

4.2 Vapor Mixtures.—Table V summarizes results on the radiolysis of the single cyclohexane-benzene mixture studied. As previously explained, the data have only relative accuracy and may be low by a factor approaching two. Benzene appar-

(34) J. Franck and E. Rabinowitch, *Trans. Faraday Soc.*, **30**, 120 (1934).

ently protects cyclohexane to some extent against primary decomposition as evidenced by effect on hydrogen yields. However, the picture is by no means simple for hot hydrogen atoms produced in a primary chemical act may react with either species present and produce changes not characteristic of the liquid state. In particular, it is difficult to understand absence of ethane from the products of the mixture. Thus, the ionization transfer picture is consistent with a portion of the results obtained in this case but, of itself, does not explain all of them. Much more extensive study of vapor mixtures would be required for unravelment of all possible effects.

5. Conclusion

Radiolysis of the hydrocarbon mixtures studied yields products not predictable on the basis of a simple law of averages. An ionization transfer mechanism is consistent with all the effects observed but if this hypothesis is adopted it is evident that excitation transfer also plays an important role in establishment of ultimate products in a liquid mixture. The latter effect is most clearly seen in the case of the cyclohexene-benzene mixture, in which the former component has the higher excitation potential and the ionization potentials are nearly the same.

Acknowledgment.—The authors are greatly indebted to Professor J. L. Magee and Doctors J. C. Devins and E. J. Y. Scott for suggestions and frequent discussion in regard to this work.

REMARKS

H. LINSHTZ (Syracuse University): Manion and Burton have shown that the presence of unsaturated molecules in irradiated hydrocarbon mixtures markedly decreases the yield of decomposition products. In this connection, I would like to point out that these unsaturated molecules are uniquely well suited for dissipation of the available energy, through the charge transfer process discussed by Magee.

According to this view, the degree of protection afforded by a given molecule should depend not only on the probability of a charge transfer reaction between it and the original ion but also on the nature of the excited states formed by combination of the new ion and an electron. In general, the reaction between odd ions and electrons may be expected to lead with high probability to triplet states which are not readily excited optically. In the particular case of unsaturated molecules the low-lying triplet states are stable, and the energy may thus readily be dissipated through normal quenching processes, without decomposition. On the other hand, formation of triplet states in saturated molecules should lead to considerable bond rupture, as is observed. The effectiveness of benzene as a protective agent compared with, say, cyclohexene may be due partly to its large cross-section for charge transfer (connected with the availability of charge over the whole molecule) and partly to the low energy of its deepest-lying triplet state. One may venture to predict that molecules like anthracene, with especially low-lying triplets and extensive charge distributions, would be even more effective than benzene.

DETECTION AND IDENTIFICATION OF FREE RADICALS IN THE RADIOLYSIS OF ALKANES AND ALKYL IODIDES¹⁻³

By LEWIS H. GEVANTMAN AND RUSSELL R. WILLIAMS, JR.

Department of Chemistry, University of Notre Dame, Notre Dame, Indiana

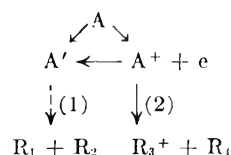
Received February 25, 1952

The use of iodine having a high specific activity in I^{131} has been applied to the detection and identification of free radicals formed in the radiolysis of alkyl iodides and alkanes. The fragmentation patterns observed were reliable to approximately $\pm 5\%$ and several tests of the identity of the fractions were successful. Fragmentation patterns have been obtained for the normal alkyl iodides methyl through butyl in both liquid and vapor states. In these cases the bond most frequently ruptured appeared to be the C-I bond. Radiolysis of the normal alkanes through pentane, plus neopentane, showed some complementary relationships to mass spectra of these compounds. Some possible reaction mechanisms are discussed.

Introduction

Free radicals undoubtedly occur as important intermediates in the decomposition of hydrocarbons and their derivatives produced by ionizing radiations. Recent discussions of the primary processes of radiation decomposition⁴⁻⁶ indicate a variety of ways in which they may be formed. The initial interaction of the ionizing radiation (electrons or X-radiation) produces both excitation and ionization. Dissociation into free radicals is a highly probable consequence of excitation and a similar dissociation

process may be expected of the ions. Subsequent ion neutralization also yields excited molecules and again dissociation into free radicals is a highly probable process. These possibilities may be summarized as



Fluorescence, ultimate molecule formation, collisional deactivation and other processes also occur but here we have mentioned only the main paths of free radical formation.

Process 1 may be considered a photochemical decomposition, although the fact that ionizing radiations are used in this work indicates that we shall be dealing with highly excited molecular energy states and probably a considerable variety of these.

(1) Taken from a thesis presented by L. H. G. in partial fulfillment of the requirements for the Ph.D. degree.

(2) Work supported in part by the Atomic Energy Commission under Contract At(11-1)-38.

(3) Presented at the Symposium on Radiation Chemistry, 119th ACS Meeting, Cleveland, Ohio, April 8-12, 1951.

(4) M. Burton, *THIS JOURNAL*, **51**, 611 (1947); **51**, 786 (1947).

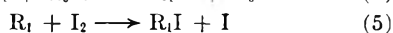
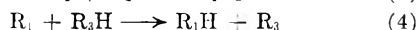
(5) H. Eyring, J. O. Hirschfelder and H. S. Taylor, *J. Chem. Phys.*, **4**, 479 (1936); **4**, 570 (1936).

(6) J. L. Magee and M. Burton, *J. Am. Chem. Soc.*, **72**, 1965 (1950); **73**, 523 (1951).

Process 2 can be studied by consideration of mass spectrographic data. It is well known that the mass spectra of alkanes and their derivatives show many mass peaks for molecule and radical ions of smaller mass than the parent ion.^{7,8} This attests to the importance of process 2 although the mass spectrometer detects the ion, whereas we shall be concerned with the complementary radical. Analogies between the results of this study and those of photochemistry and mass spectrometry may be expected.

The detection and identification of free radicals in photochemical processes has been a subject of much concern. Methods which may be regarded as precursors of the present one include: the use of metal mirrors by Paneth and Hofeditz⁹ and later by Rice, *et al.*¹⁰; the use of lead mirrors containing radioactive lead by Leighton and Mortenson¹¹; the use of carbon tetraiodide mirrors by Simons and Dull¹²; the use of molecular iodine mirrors by Belchetz and Rideal¹³; and the use of iodine vapor by Gorin.¹⁴ Hamill and Schuler¹⁵ used molecular iodine containing I^{131} (β^- , $t_{1/2} = 8$ days) to measure the rate of reaction of alkyl radicals with molecular iodine in the photolysis and radiolysis of alkyl iodides. This method was later extended by Williams and Hamill¹⁶ to systems in which complex mixtures of radicals were produced by radiolysis and photolysis. Durham, Martin and Sutton¹⁷ have applied the same technique to the detection of methyl and propyl radicals in the sodium flame reaction with propyl halide.

The present work continues the investigation of the nature and relative amounts of some free radicals formed by ionizing radiations from alkanes and alkyl iodides. The systems studied contain the alkane or alkyl iodide as liquids or gases plus a small concentration (mole fraction *ca.* 10^{-3}) of molecular iodine. As a first approximation the presence of iodine is neglected in the primary processes and radicals are presumed to form through reactions such as 1 and 2, above. Some secondary reactions of these radicals which might be considered are



At moderate reaction rates, the radical concentration will be so small as to make the rate of reaction 3 negligible in comparison to 4 or 5. Reaction 4 has an activation energy of 10–15 kcal., while reaction 5 has a very small activation energy, probably around 1 kcal. Therefore, at the temperatures (*ca.* 25°)

(7) G. C. Eltenton, *J. Chem. Phys.*, **10**, 403 (1942).

(8) A. Langer, *This Journal*, **54**, 618 (1950).

(9) F. Paneth and W. Hofeditz, *Ber.*, **62B**, 1335 (1929).

(10) F. O. Rice and K. K. Rice, "The Aliphatic Free Radicals," The Johns Hopkins Press, Baltimore, Md., 1935.

(11) P. A. Leighton and R. A. Mortenson, *J. Am. Chem. Soc.*, **58**, 448 (1936).

(12) J. H. Simons and M. F. Dull, *ibid.*, **55**, 2696 (1933).

(13) E. Belchetz and E. K. Rideal, *ibid.*, **57**, 1168 (1935); *ibid.*, **57**, 2466 (1935).

(14) E. Gorin, *J. Chem. Phys.*, **7**, 256 (1939).

(15) W. H. Hamill and R. H. Schuler, *J. Am. Chem. Soc.*, **73**, 3466 (1951).

(16) R. R. Williams and W. H. Hamill, *ibid.*, **72**, 1857 (1950).

(17) R. W. Durham, G. R. Martin and H. C. Sutton, *Nature*, **164**, 1052 (1949).

and relative concentrations used in this work, reaction 5 is taken to be the fate of substantially all thermal free radicals produced. Reactions such as 4 may yet play some part in the radiation decomposition, but if so they represent the reaction of excited or "hot" radicals, formed with excess internal or translational energy in reactions such as 1 and 2. The alkyl iodides, although formed in micromolar quantities, will contain a high specific activity of I^{131} . Addition of appropriate inactive alkyl iodide carriers to the reaction products, followed by fractional distillation and radioactivity determinations permits estimation of the relative free radical yields.

Experimental

Milligram quantities of iodine containing approximately ten microcuries of I^{131} ¹⁸ were prepared by oxidation of dry potassium iodide with dry potassium dichromate at elevated temperatures in vacuum. The iodine sample was distilled into a small break-off tube for later introduction into the reaction system.

The alkyl iodides used as target materials and as distillation carriers were purified by fractional distillation in a glass-packed Todd column 1.5×100 cm. at a reflux rate of 300 ml. per hour and a reflux ratio of 40:1. A middle cut from each distillation was retained, dried over phosphorus pentoxide and stored in a dark vessel. Samples for radiolysis were further subjected to bulb-to-bulb distillation in vacuum to ensure removal of dissolved gases. Alkanes used for radiolysis were of research grade and were further distilled in the vacuum line only to remove dissolved gases.

The radiolysis of liquid alkyl iodides was performed on 5-cc. samples containing approximately 1 mg. of dissolved iodine. Both components were introduced by vacuum distillation into an all-glass vessel 1.5×10 cm. This vessel was closed by a glass seal and opened after irradiation by a break-off. Radiolysis of alkyl iodide and alkane vapors was performed in a 500-cc. spherical flask having a thin "window" to reduce absorption of soft radiations. Again, the components were introduced by vacuum distillation, the vessel closed by a glass seal and re-entered through a break-off.

The radiations employed were of four classes: γ -radiations from a two curie Co^{60} source ($t_{1/2} = 5.3$ yr., $\gamma = 1.1, 1.3$ mev.); X-rays generated at 45–50 Kvp. and 17 ma. in a Machlett AEG-50 X-ray tube; X-rays generated at 2 mv. and 100 μ a. in a Van der Graaf generator; and electrons at 2 mv. and 2 μ a. from the same machine. In all cases the irradiation time was varied to produce about 50% reaction with iodine. The times of exposure varied from about 20 hours to 2 minutes for the various kinds and energies of radiations. No effects of such changes in rate of decomposition upon the fragmentation patterns were observed.

After irradiation, alkyl iodide carriers were introduced into the reaction vessel on top of the frozen products. The carrier mixture usually consisted of 5 cc. of methyl iodide, 3 cc. each of the normal alkyl iodides up to carbon chain length one unit greater than the target substance, and 3 cc. of methylene iodide. Isopropyl iodide was also used in some cases.

Excess iodine was extracted with aqueous sulfite solution, after which the carrier mixture was washed with water and dried over phosphorus pentoxide. In some cases a water extract was made before iodine removal, in order to estimate the amount of hydrogen iodide produced. Such activity is reported as per cent. of total organic activity.

The organic iodide mixture was distilled in a Podbielniak Miniature Hyper-Cal Fractionating Column 1×30 cm., packed with a heligrad fabricated from Hastelloy B, a halogen resistant alloy. The reflux rate was maintained at approximately 100 cc. per hour and the reflux ratio at approximately 40:1. The distillate flowed through a capillary grid in front of a mica window Geiger counter arranged so that approximately 0.1 ml. of distillate was retained in front of the counter (see Fig. 1). The count rate was observed with a linear count rate meter. A Brown two-point recording potentiometer continuously recorded the activity

(18) I^{131} obtained in millicurie amounts as carrier-free iodide solution from the Isotopes Division, Carbon and Carbide Chemicals Company, Oak Ridge, Tennessee.

of the distillate and the head temperature of the column. A pump and manostat were attached to the fractionation apparatus to permit distillation at reduced pressure in the case of higher iodides.

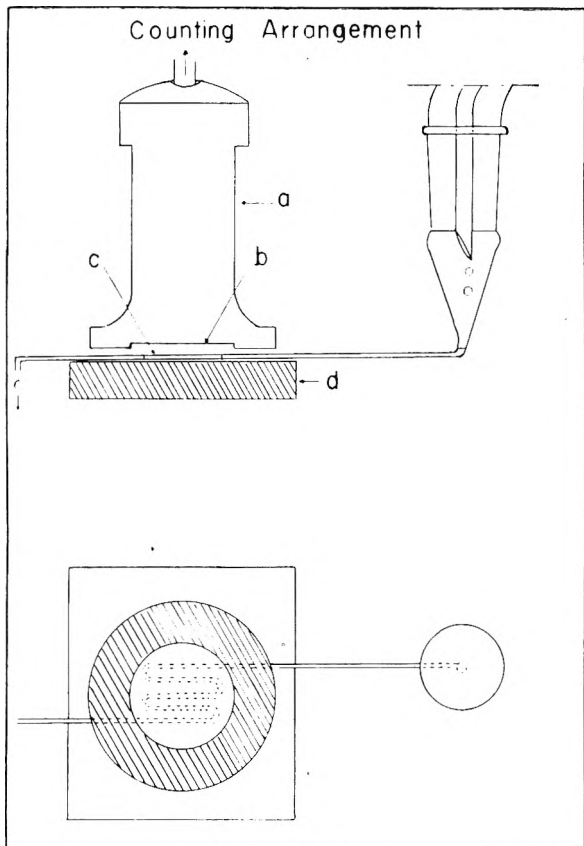
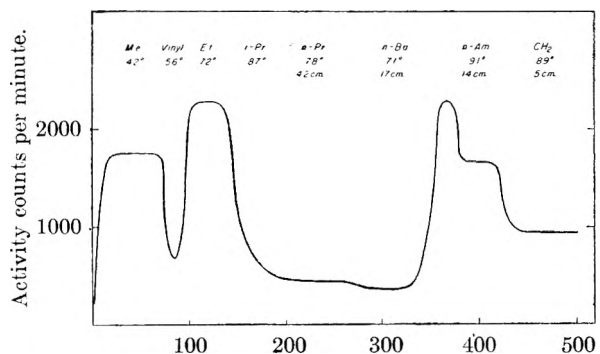


Fig. 1.—a, Geiger counter; b, mica window; c, capillary coil; d support.

For each fraction the head temperature and activity were expected to remain constant over a distillate volume of at least 0.5 cc. (approximately 30 min.) to be taken as a measure of the activity of that fraction. This activity was multiplied by the original carrier volume for comparison with other fractions on a percentage basis. Each fraction was collected separately for redetermination of activity or redistillation if desired.

Figure 2 depicts the values of pressure, temperature and activity encountered in the course of a typical distillation after irradiation of *n*-pentane. In this case, vinyl iodide carrier was also used. Clear values of activity associated with methyl iodide, ethyl iodide, *n*-propyl iodide, *n*-butyl iodide, *n*-amyl iodide and methylene iodide are observable. Little or no activity is associated with vinyl iodide, the *i*-propyl iodide fraction is obscured by carry-over of ethyl

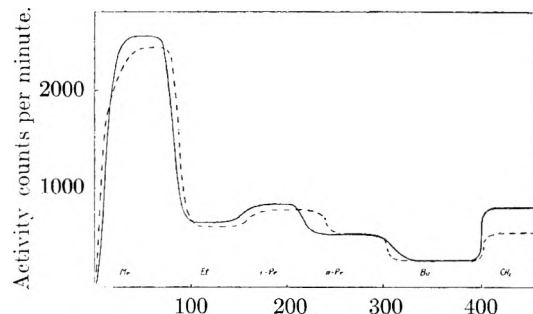


Distillation time (min.). Proportional to distillate volume.

Fig. 2.—Radiolysis of pentane.

iodide, and the peak between *n*-butyl and *n*-amyl can probably be attributed to uncarried active secondary amyl iodides.

Figure 3 shows the activity record from two irradiations of propane (with 45 kv. X-rays and with 2 mv. X-rays) normalized to the same scale. The correspondence of the yields in the various fractions illustrates the reproducibility of the method and demonstrates the lack of dependence on the maximum energy of the quanta used.



Distillation time (min.). Proportional to distillate volume.

Fig. 3.—Radiolysis of propane; duplicate experiments, normalized.

Relative yield data for the various substances studied are given in Tables I, II and III. The hydrogen iodide activity yield is given in terms of per cent. of total organic activity.

Special Tests.—Radiolysis of methane and ethane at an elevated temperature was performed by heating the reaction vessel with infrared lamps to a steady temperature of 80–100°, as indicated by a mercury thermometer in contact with the vessel. In this condition radiolysis with energetic electrons resulted in products experimentally indistinguishable from those obtained in experiments at room temperature (25°) (experiments 45 and 54).

Several experiments were performed to test the validity of the fractional distillation as an analytical technique. A sample of ethyl iodide containing dissolved iodine (with ¹³¹I) was irradiated with electrons and fractionated in the usual manner, using methyl iodide and *n*-propyl iodide carriers in addition to the ethyl iodide already present. From this distillation a constant boiling, constant activity sample, 9.5 ml. in volume, was collected. This fraction was hydrolyzed with 50 ml. of 10% potassium hydroxide at 80°. After 2.5 hours, 5.5 ml. of organic iodide remained. This sample was washed, dried and its specific activity was compared with that of the unhydrolyzed iodide. The two values were experimentally indistinguishable.

A second sample of active ethyl iodide prepared as above was distilled in mixture with 3 ml. each of inactive methyl, *n*-propyl, *n*-butyl and methylene iodides in the usual fashion. Only the ethyl iodide fraction was radioactive.

Discussion

The Analytical Method.—It is especially important to allow complete condensation of the reaction products before carriers are added. Failure to do this may result in disproportionate loss of the more volatile active iodides during the addition of carriers. However, after complete mixing of carrier and active iodides, minor losses are not objectionable, since it is the specific activity of each fraction which is determined. In the case of methane, its volatility at liquid air temperatures made the collection problem especially severe, and many early experiments were discarded on this basis.

Comparison of the results of experiments performed under substantially the same conditions (such as No. 28, 29 and 30 on butyl iodide or No. 19, 20, 42, 43 and 44 on methane) indicates that the relative yields is approximately $\pm 5\%$. The reality of fractions amounting to less than 5% of the total

TABLE I
 LIQUID ALKYL IODIDES

Expt. No.	Sample, iodides	Vol. of sample, ml.	Weight of I ₂ , mg.	Radiation	Products (% of total activity)					Methylene
					Me	Et	<i>i</i> -Pr	<i>n</i> -Pr ^a	<i>n</i> -Bu	
8	Methyl	3.0	1.0	γ	66	15	19
2	Ethyl	3.0	2.0	γ	9	88	1	1	0	1
7	Ethyl	3.0	1.0	γ	11	80	..	5	2	2
9	Ethyl	3.0	1.0	2 mv. X-ray	25	63	..	7	4	1
3	<i>n</i> -Propyl	3.0	1.0	γ	7	6	..	80	5	2
4	<i>n</i> -Butyl	3.0	1.0	γ	14	9	..	7	70	..

^a Wherever leaders occur the carrier was not present.

 TABLE II
 GASEOUS ALKYL IODIDES

Expt. No.	Sample, iodide ^a	Press. of sample, mm.	Radiation	Products (% of total activity)					Methylene
				Me	Et	<i>i</i> -Pr	<i>n</i> -Pr	<i>n</i> -Bu	
52	Methyl ^a	93	<i>e</i> ⁻	82	5	^b	13 ^c
10	Ethyl	140	2 mv. X-rays	27	55	..	6	3	9
12	Ethyl	140	50 kv. X-rays	34	66	..	0	0	0
13	<i>n</i> -Propyl	40	50 kv. X-rays	15	6	11	56	6	6
14	<i>n</i> -Propyl	40	50 kv. X-rays	17	5	5	61	5	7
28	<i>n</i> -Butyl	14	50 kv. X-rays	11	6	3	3	73	4
29	<i>n</i> -Butyl	10	50 kv. X-rays	9	7	2	2	74	6
30	<i>n</i> -Butyl	10	50 kv. X-rays	9	8	68	15

^a Pressure of iodine was 0.14 mm. in all cases. ^b Wherever leaders occur the carriers were not present. ^c Active HI 1% of total organic.

 TABLE III
 ALKANES

Run No.	Sample	Press. of sample, mm.	Press. of I ₂ , mm.	Radiation	Products (% of total activity)						Methylene	HI ^c
					Me	Et	<i>i</i> -Pr	<i>n</i> -Pr	<i>n</i> -Bu	<i>n</i> -Am		
19	Methane	120	0.14	2 mv. X-rays	74	5	^a	21	..
20	Methane	120	.14	2 mv. X-rays	74	5	21	..
42	Methane	120	.07	<i>e</i> ⁻	71	5	24	9.5
43	Methane	120	.14	<i>e</i> ⁻	77	5	18	15
44	Methane	120	.175	<i>e</i> ⁻	76	5	19	15
45 ^b	Methane	120	.14	<i>e</i> ⁻	74	4	22	13.5
46	Methane	22(CH ₄) 18(H ₂)	.14	<i>e</i> ⁻	77	6	17	5.4
47	Methane	20	.14	<i>e</i> ⁻	80	4	16	7.8
48	Methane	20	.14	<i>e</i> ⁻	77	4	19	4
50	Methane	334	.14	<i>e</i> ⁻	80	7	13	3.5
51	Methane	576	.14	<i>e</i> ⁻	77	5	18	7.8
21	Ethane	120	.14	2 mv. X-rays	30	40	..	10	10	..	10	..
22	Ethane	120	.14	2 mv. X-rays	41	43	16	..
38	Ethane	745	.14	<i>e</i> ⁻	28	55	..	5	3	..	9	21
54 ^b	Ethane	120	.14	<i>e</i> ⁻	30	46	..	4	4	..	16	9
23	Propane	120	.14	2 mv. X-rays	47	12	16	10	5	..	10	..
25	Propane	120	.14	50 kv. X-rays	45	11	14	10	5	..	15	..
32	Propane	140	.14	<i>e</i> ⁻	40	10	11	11	10	..	18	..
33	Propane	420	.14	<i>e</i> ⁻	27	9	9	13	13	..	29	..
34	Propane	745	.14	<i>e</i> ⁻	17	8.1	9	8	8	..	49	..
35	Propane	21	.14	<i>e</i> ⁻	52	11	9	9	5	..	14	..
57	Propane	470	.14	<i>e</i> ⁻	17	5	..	6	7	..	64	..
26	Butane	120	.14	50 kv. X-rays	20	14	29	13	10	..	14	..
27	Butane	120	.14	50 kv. X-rays	9	12	28	18	13	..	20	..
55	Pentane	120	.14	<i>e</i> ⁻	24	30	..	6	5	22	13	3
56	Neopentane	120	.14	<i>e</i> ⁻	80	4	..	2	6	2	6	4

^a Wherever leaders occur the carrier was not present. ^b Runs 45 and 54 irradiated between 80 to 100°. ^c HI reported as per cent. of total organic activity.

is questionable. Large changes in activity from one carrier fraction to the next tax the separation powers of the fractionating and counting systems, since the volumes of carriers used were small and some intermingling of fractions in the column head and counting chamber is unavoidable. This prob-

ably increases the uncertainty especially in cases of weakly active fractions which follow highly active fractions. Such considerations place considerable doubt on the reality of such activities as that in the ethyl iodide fraction of the experiments on methane, in spite of careful attention to constant

activity and constant boiling point in a given fraction.

The identification of a particular active fraction with the known carrier distilling at the same temperature seems quite clear, especially in the lower-boiling fractions. In addition to the constancy of boiling point and activity through an appreciable volume of distillate, the redistillation and hydrolysis experiments served to support this identification. With the higher-boiling iodides, the possibility of isomeric forms introduces some confusion, since not all possible carriers were introduced. Butyl iodide activity might well be a mixture of the isomers, all appearing with the carrier butyl iodide and, in the case of amyl iodide, clear indication of active secondary amyl iodides is present in Fig. 2.

For greater ease in correlation, the average values of the relative radical yields are shown in Figs. 4, 5 and 6 in the form of bar graphs.

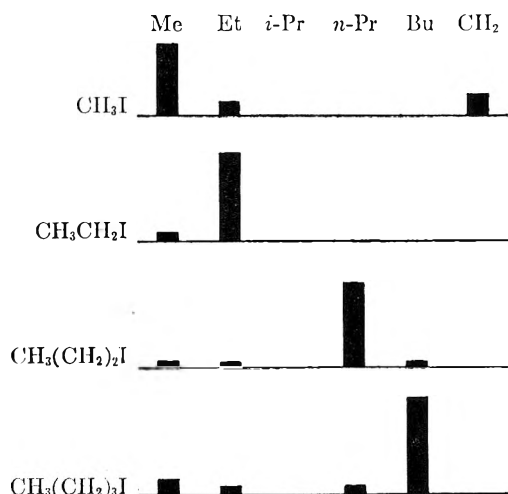


Fig. 4.—Radiolysis of liquid alkyl iodides.

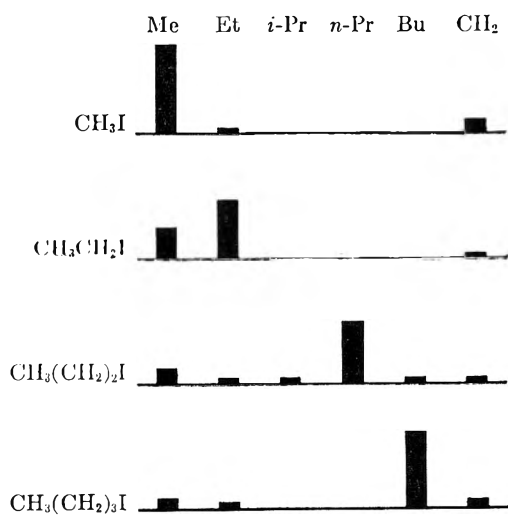


Fig. 5.—Radiolysis of alkyl iodide vapors.

Radiolysis of Alkyl Iodides.—In the radiolysis of the alkyl iodides, both liquids and vapors, the dominant characteristic of the radical yield values is the high yield of the parent substance. This may be taken as an indication that C-I bonds are broken more readily than C-C bonds. Since the only

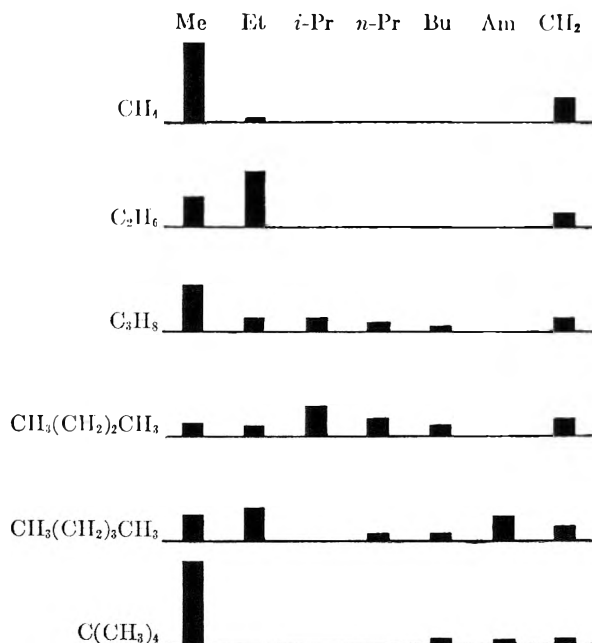


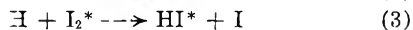
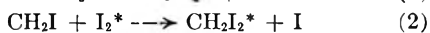
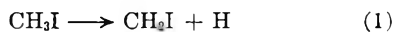
Fig. 6.—Radiolysis of hydrocarbons.

diiodide carrier used was methylene, only in the case of methyl iodide is direct support presented for the similar conclusion that C-I bonds are broken more readily than C-H bonds. However, this is certainly very likely with all of the alkyl iodides. These effects are to be expected on two grounds: First, the C-I bond is by far the weakest in these molecules and second, the iodine atom has far more electrons than any other atom of the molecule, and therefore, ionization or excitation at this point is most likely.

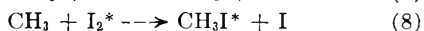
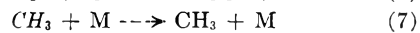
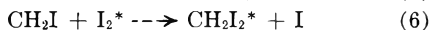
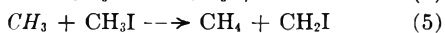
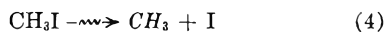
In comparison with the liquid halides, the halide vapors generally show a higher ratio of C-C to C-I bond rupture. Butyl iodide appears to be an exception to this rule, which may be explained as a greater tendency toward collisional deactivation of excited states in the vapor state.

In both liquid and vapor states it may also be noted that the relative yield of methyl iodide decreases as the carbon chain length increases. Liquid butyl iodide does not follow this trend again and one is inclined to suspect that the experimental data in this case are faulty, especially since the values are based in only one experiment in this case. Such a decrease in relative methyl yield might be explained as an increasing opportunity to rupture other C-C bonds, processes which ought not to have greatly different energy requirements. The production of methylene radicals from ethyl and higher iodides must represent the rupture of two bonds in the primary process or, perhaps more likely, the subsequent reaction of an energetic radical formed in the primary process. The yield of this product is very small except from methyl iodide.

To consider in more detail the radiolysis of methyl iodide vapor, note that the per cent. of methylene iodide formed is about 13. On the other hand, very little active hydrogen iodide (*ca.* 1%) was formed, which appears to rule out a mechanism involving C-H bond rupture



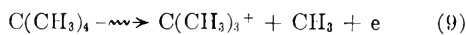
since an equivalent amount of active hydrogen iodide would be formed. The mechanism proposed by Hamill and Schuler¹⁵ and by Schultz and Taylor¹⁹ for the photolysis and radiolysis of such compounds



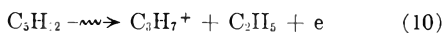
where CH_3 indicates a hot methyl radical, appears to satisfy those data also, and the ratio of methyl to methylene iodide may be taken as the ratio of the rates of the hot radical reaction 5 to the thermalization reaction 7.

Radiolysis of Alkanes.—The fragmentation patterns characteristic of the alkanes, as shown in Fig. 6, differ sharply from those found for the alkyl iodides. The radical corresponding to the parent substance is no longer dominant, except in the case of methane. Methyl radicals are frequently an important product although other small radicals, principally ethyl and propyl, are also formed in good yield. Methylene iodide is also a product of some importance. The contrast between normal pentane and neopentane is also noteworthy.

In some respects a complementary relation appears between these radical yield data and the mass spectral data as reported by Langer.⁸ The most important peak in the mass spectrum of neopentane is C_4H_9^+ , while the present method indicates a large yield of methyl radicals, suggesting that an important primary process is

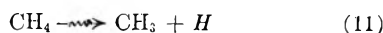


In contrast, the mass spectrum of normal pentane shows the C_3H_7^+ ion to be most important, and the present work indicates a large yield of ethyl radicals

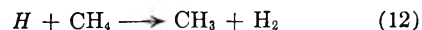


Butane does not obviously show such a complementary relationship, but with propane it again appears. C_2H_5^+ is the most important ion, while CH_3 is the most important radical.

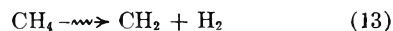
In the radiolysis of methane variation of the pressures of the reagents, the temperature of the system and the intensity of the radiation appeared to have no effect upon the relative amounts of products. Therefore, their ratio must be determined by the primary processes, or in subsequent hot radical reactions. The yield of active hydrogen iodide, although somewhat variable, is clearly much less than that of methyl iodide and nearly equal to the yield of methylene iodide (remembering that the chance of having I^{131} in CH_2I_2 is twice that in mono-halides). These facts suggest that a primary process



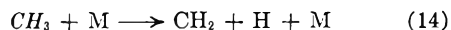
produces a hot hydrogen atom, which then reacts efficiently with methane



to produce hydrogen and another methyl radical. Thus only a fraction of the primary hydrogen atoms reach thermal energies, where they would efficiently react with iodine to yield active hydrogen iodide. Methylene radicals might be formed in a primary process such as

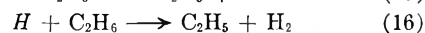
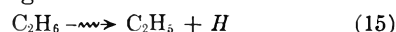


or in a subsequent reaction of hot methyl radicals formed by a reaction such as 11.

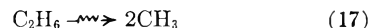


Since the ionization potential of methane is about 14 volts, neutralization of the ion would be a highly exothermic process. If all of this energy appeared as relative translational energy of the methyl radical and hydrogen atom, their energies would be about 0.6 volt (14 kcal.) and 9.5 volts (215 kcal.), respectively, indicating the feasibility of reaction 12 but not reaction 14.

Radiolysis of ethane again showed no dependence on pressure of reactants or temperature. The relative yield of active hydrogen iodide was larger than in the case of methane, but still much less than that of ethyl iodide. Therefore the postulate of hot hydrogen atoms is again made

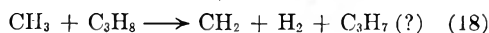


For the formation of methyl radicals in a concentration and temperature independent fashion one may write

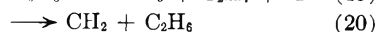


but the mechanism of formation of methylene radicals is not immediately evident.

Radiolysis of propane shows a distinct effect of the propane pressure, (Table III). With increasing pressure the relative yield of methyl decreases and the yield of methylene increases in such a fashion that the sum of these two yields is approximately constant. Since the yields of other radicals remain approximately constant, it is tempting to assume that some reaction of thermal methyl radicals with propane produces methylene radicals. Any such reaction written, for instance



must also produce another radical. Since none appears in the distillation analysis and indeed, such reactions must be highly endothermic, this is not a satisfactory proposal. Another proposal which appears more reasonable is to assume that methyl and methylene radicals are both primary products of the same excited or ionized molecular state, by reactions such as



and to assume a pressure effect on the relative efficiencies of these two processes. The rearrangement implied in reaction 20 may require collision with another molecule, the rate of such collisions increasing with increasing pressure. Unfortunately these proposals are far from satisfactory and must be further tested before serious adoption.

(19) R. D. Schultz and H. A. Taylor, *J. Chem. Phys.*, **18**, 194 (1950).

DECOMPOSITION OF WATER AND AQUEOUS SOLUTIONS UNDER MIXED FAST NEUTRON AND GAMMA RADIATION¹

BY A. O. ALLEN,² C. J. HOCHANADEL, J. A. GHORMLEY AND T. W. DAVIS³

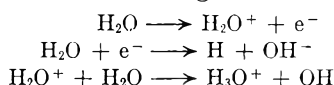
Oak Ridge National Laboratory, Oak Ridge, Tennessee

Received February 25, 1952

Purified water, irradiated in the Oak Ridge reactor, decomposes to a limited extent only. The products (hydrogen, hydrogen peroxide and oxygen) react with each other under radiation to re-form water, so that a steady state level of products is quickly reached, which in pure water at 25° lies at about 20 micromoles per liter of dissolved hydrogen. The steady state level is very sensitive to the presence of certain kinds of dissolved material or impurities, and is consequently poorly reproducible and tends to drift upward with time because of slow contamination with impurities from the vessel walls. Addition of hydrogen suppresses the decomposition, but added oxygen or peroxide, like many other solutes, greatly increase the decomposition. The kinetics of the reaction between dissolved hydrogen and hydrogen peroxide were found to be reproducible when the hydrogen was in excess, and were studied in detail. Results are explained quantitatively by consideration of reactions of H and OH radicals formed by combination of like radicals in regions of high ionization density (tracks of slow charged particles). Other radicals escape initial recombination, diffuse throughout the main body of water, and may react with the decomposition products or with other solutes.

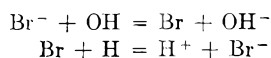
Introduction

The mechanism of reactions occurring in water in aqueous solutions under high radiations has been discussed in an earlier publication.⁴ According to the picture there presented, the primary chemical effect of radiation is probably to form the free radicals H and OH according to the mechanism



Direct dissociation of electronically excited water molecules may also contribute to the yield of free radicals. In heavily ionizing radiation, such as α -rays or the fast proton recoils formed by the passage of fast neutrons through water, the radicals are formed in high concentration along the track of the particle. In this small zone, the radicals will react with one another to form, to a certain extent, the molecules H₂ and H₂O₂. Some of the radicals will be able to escape from the zone and will react with dissolved H₂ and H₂O₂ molecules in the solution to lead to the re-formation of water. When fast electrons are the ionizing agents, the radicals are not so densely distributed and a much larger fraction of them will be able to react with dissolved product molecules before they disappear by reaction with one another.

When pure water is irradiated, the products H₂ and H₂O₂ will therefore build up to a steady state concentration at which the rate of back reaction of these products to re-form water is equal to the rate of their production from water. When the water contains dissolved material capable of oxidation and reduction, the radicals are expected to be destroyed by reacting with the solute. Thus with bromide ion, we may assume the reactions



Such reactions remove radicals so that they cannot react with dissolved hydrogen, hydrogen peroxide or oxygen. When reactive solute is present, the water

decomposition will proceed to relatively high product concentrations. The rate of hydrogen production should be the same in all such solutions and should furnish a measure of the rate at which the product molecules are formed in the radiation track. This rate should be greater the more densely ionizing the radiation.

In the earlier paper, experiments are referred to which were being performed in the nuclear reactor (or "pile") at Oak Ridge. The present paper describes these experiments in detail and presents additional data, which have allowed the subject to be treated in a more quantitative fashion than was possible at the time of the previous publication.

In all experiments described here, samples of water or solutions were exposed at a certain point inside the Oak Ridge nuclear reactor, and were cooled by a jacket of flowing water maintained at 25°. The radiation received in such a situation consists of a mixture of γ -radiation and of neutrons having all energies from thermal up to a few mev.

A great part of the work here described consisted of a protracted struggle with irreproducibility and poor material balances, caused by intervention in the reaction of material from the walls of the containing vessels. For this reason, results on pure water are of qualitative value only. Certain solutions, however, gave reproducible results, and allowed a quantitative treatment of the reaction mechanism.

Decomposition of Pure Water under Reactor Radiation

Samples of water, specially purified in various ways, were sealed in ampoules of fused silica and exposed in the reactor for various lengths of time. After exposure, the concentrations of H₂, O₂, H₂O₂ and CO₂ were determined by analysis. Some of the ampoules were practically full of water; others were about half-full. Results are reported in terms of concentration of products dissolved in the liquid phase. Experimental details are described in the last section of this paper.

The concentration of hydrogen produced by the radiation in pure water is plotted in Fig. 1 against time of exposure in the reactor. Since the solubility of hydrogen in water at the temperatures used (near room temperature) is close to 760 micromoles/liter, the concentration of dissolved hydrogen in μM , is very nearly equal to the pressure of hydrogen over the solution in mm.

Great irreproducibility is at once evident from this graph. The important factor, however, is that the concentration never becomes very high. For full ampoules, the concentra-

(1) This paper, describing work concluded in the summer of 1948, is based on report ORNL-130 (issued October 11, 1949).

(2) Department of Chemistry, Brookhaven National Laboratory, Upton, L. I., N. Y.

(3) Department of Chemistry, New York University, University Heights, New York, N. Y.

(4) A. O. Allen, *THIS JOURNAL*, **52**, 479 (1948).

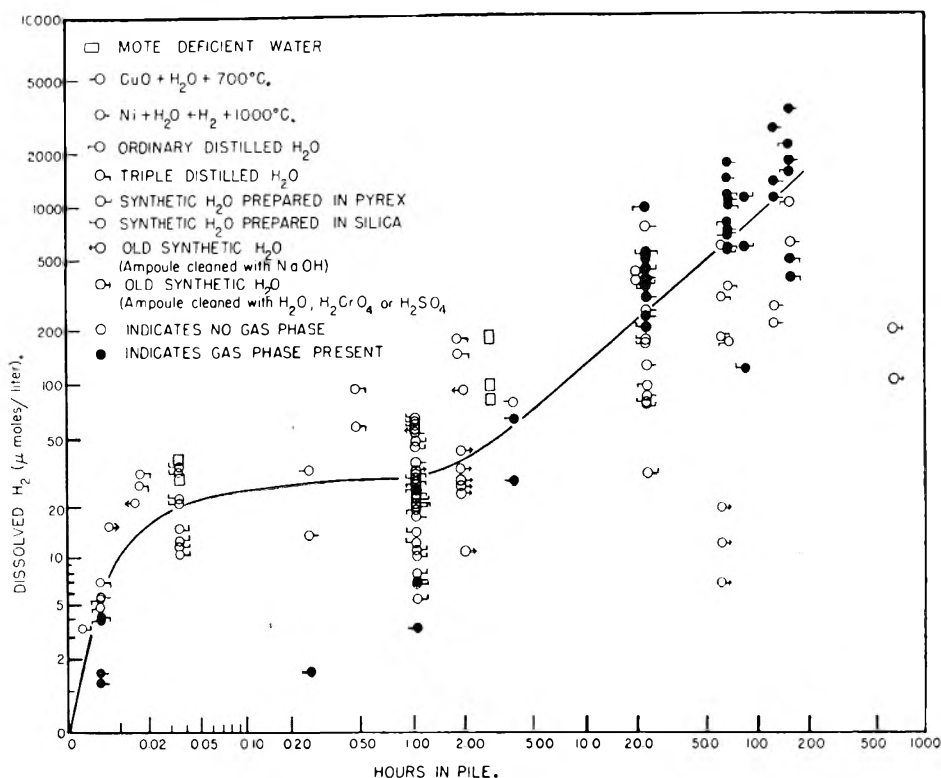


Fig. 1.—Decomposition of water in the pile.

tion of dissolved hydrogen within the first few minutes rises to values of the order of 20 μ M. and remains at this level without great change up to an hour. On exposure of many hours, the concentration tends to drift upwards. Thus the water decomposition reaches a steady state within two minutes, but this steady state rises slowly in the course of time presumably because of contamination of the water by impurities coming out of the vessel wall. For samples with gas phase (ampoules only partly full) the gas formed goes largely into the gas phase, so that the initial rate of rise of concentration of dissolved hydrogen with time is much less. In the course of a day in the reactor, however, the steady state is reached also in these ampoules, and the concentration of dissolved gas, as calculated from its solubility, not only reaches, but appears to exceed, the concentrations found in the filled ampoules. The tendency for greater hydrogen concentrations at large gas phases is ascribed to the higher H₂O₂/H₂ ratios present, and the effect will be discussed further in a later section.

The material balances as shown by the analysis were in some cases very poor. Theoretically, the number of moles of hydrogen formed should be equal to the number of moles of peroxide plus twice the number of moles of oxygen. In Fig. 2, the total equivalents of oxidant are plotted against the total equivalents of hydrogen (reductant). Deviation of the points from the 45° line indicates bad material balance. In most cases of poor balance, the hydrogen was in excess. The deviations in many cases were much too large to be explained by errors in the analytical procedure. It seems that either some reducing impurity was present in the water in unexpectedly large amounts, or that the vessel wall enters into the reaction in some way, possibly by the formation of some sort of persilicic acid complexes.

Carbon dioxide appeared in the products in variable amounts, ranging up to 15 or 20 μ M. Usually the CO₂ was present in considerably smaller quantities than the H₂, O₂ and H₂O₂, but in a few cases of small decomposition, it appeared to be an important product. In the material balances discussed above, CO₂ has been ignored; but including it among the oxygenated products did not greatly improve

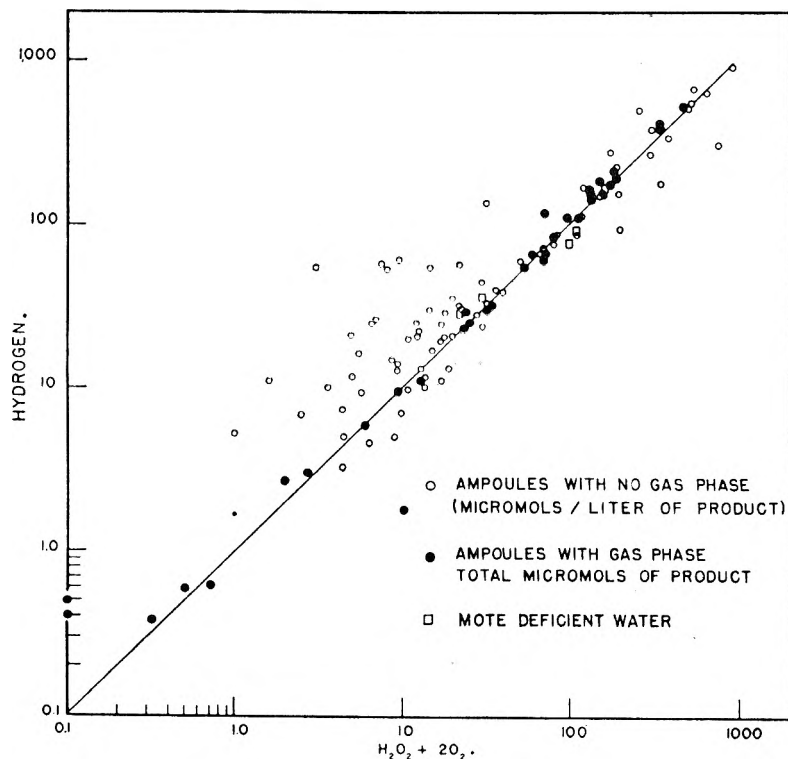


Fig. 2.—Balance between oxidant and reductant produced on irradiating water in the pile.

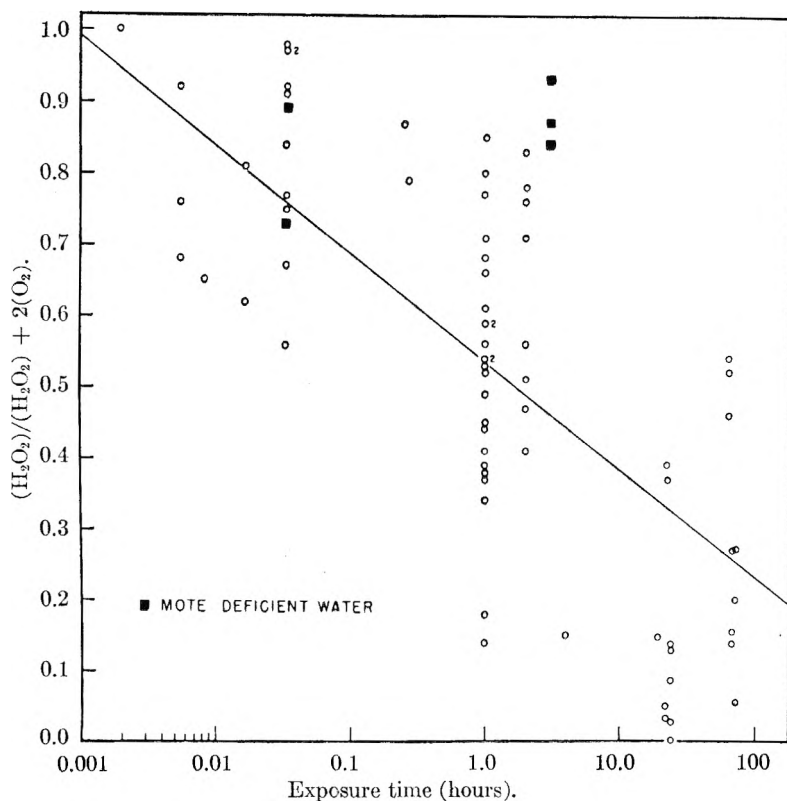
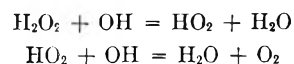


Fig. 3.—Ratio of peroxide to total oxidant produced in irradiation of water in the pile.

tion of hydrogen peroxide to oxygen in aqueous solutions shows that the determining factor in the quantum yield for the reaction is the number of dispersed particles or motes. It is believed that the radicals formed by photochemical action on the peroxide react on the surface of the motes with adsorbed peroxide or HO₂ radicals to give enhanced reaction. By special treatment of the container and water to eliminate motes or reduce their number, the quantum yield can be considerably reduced. The same factors might be thought to operate in the decomposition of water under high energy radiation. Samples of water sealed in silica were therefore prepared, following the directions given by investigators of peroxide photolysis for reducing motes to a minimum.

The yields of hydrogen, the oxidant-reductant balance and the peroxide-oxygen ratios given by five samples of mote-free water are among the results shown in Figs. 1, 2 and 3. The peroxide-oxygen ratio was higher in these samples than in most of the other water used, particularly in the case of the three-hour exposures. This is a good indication that with high energy radiation, as well as with ultraviolet light, the decomposition of peroxide to oxygen is hastened by the presence of dispersed glass particles. We believe that the decomposition of peroxide to oxygen is brought about by the reactions



the material balances. The CO₂ still appeared on irradiation of the most carefully purified synthetic water, and therefore probably did not arise entirely from organic impurities in the water. Perhaps some carbon-containing impurity was present in the fused silica containers, which passed into the water as CO₂ under the action of radiation.

A quantity of interest is the extent to which the oxygenated product appears as oxygen gas or as hydrogen peroxide. The ratio $\text{H}_2\text{O}_2/(\text{H}_2\text{O}_2 + 2\text{O}_2)$, which gives the fraction of total oxidant present as peroxide, is plotted in Fig. 3 against time. The points are seen to scatter very badly. It is clear, however, that at short exposures the oxidant is present mostly in the form of peroxide and that with increasing exposure time the oxygen tends to become more prominent. There is little doubt that the initial product of the reaction is hydrogen peroxide and that oxygen forms by subsequent decomposition of the peroxide. The photochemical decomposition of peroxide is known to be very sensitive to the presence of impurities, especially dissolved or suspended particles of glass. The rate of back reaction of the products will naturally be dependent upon whether the reacting material is oxygen or peroxide, and much of the irreproducibility in the amount of decomposition can be attributed to difference in the fraction of peroxide decomposing to oxygen.

Reference to the literature^{5,6} on photochemical decomposi-

(5) F. O. Rice and M. L. Kilpatrick, *This Journal*, **31**, 1507 (1927).

(6) R. Livingston, *ibid.*, **47**, 260 (1943).

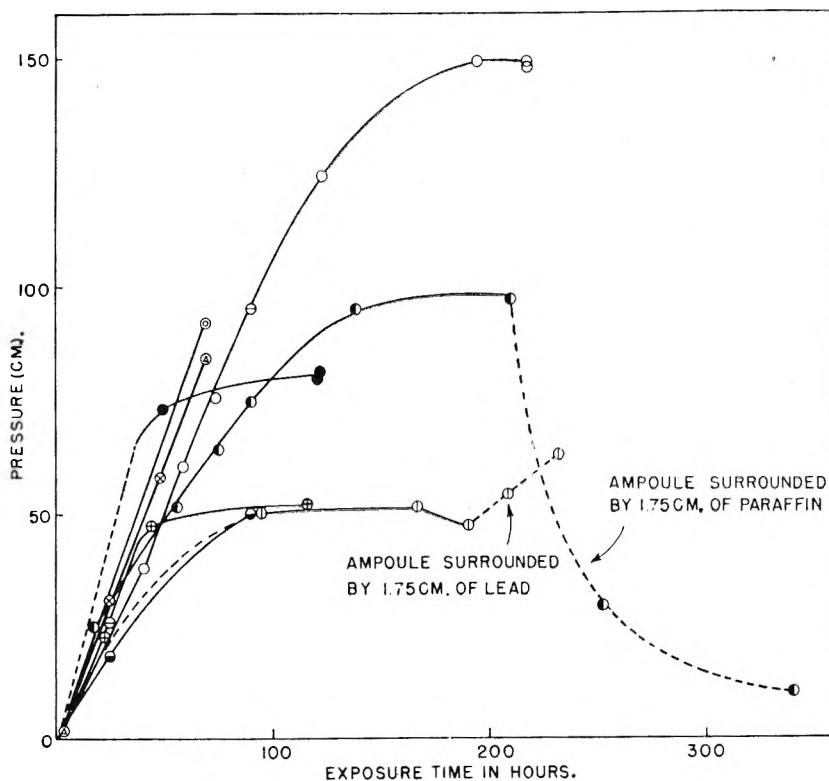


Fig. 4.—Water decomposition in pressure indicating ampoules.

One or both of these reactions occurs more readily on surfaces than in solution.

Containers of other materials than silica were tried—Pyrex, gold, tin and aluminum—but in metals, the reproducibility was even worse than in silica. Water-filled Pyrex am-

poules usually cracked in the reactor, probably because of heat generated by the nuclear reaction of neutrons with boron in the Pyrex.

Results obtained with different ampoules were so erratic that it became obviously desirable to measure the pressure of gas in an ampoule without opening it so that the development of gas could be followed as a function of exposure time in a single ampoule. This was accomplished by devising an arrangement for determining the boiling point of the water in the ampoule.

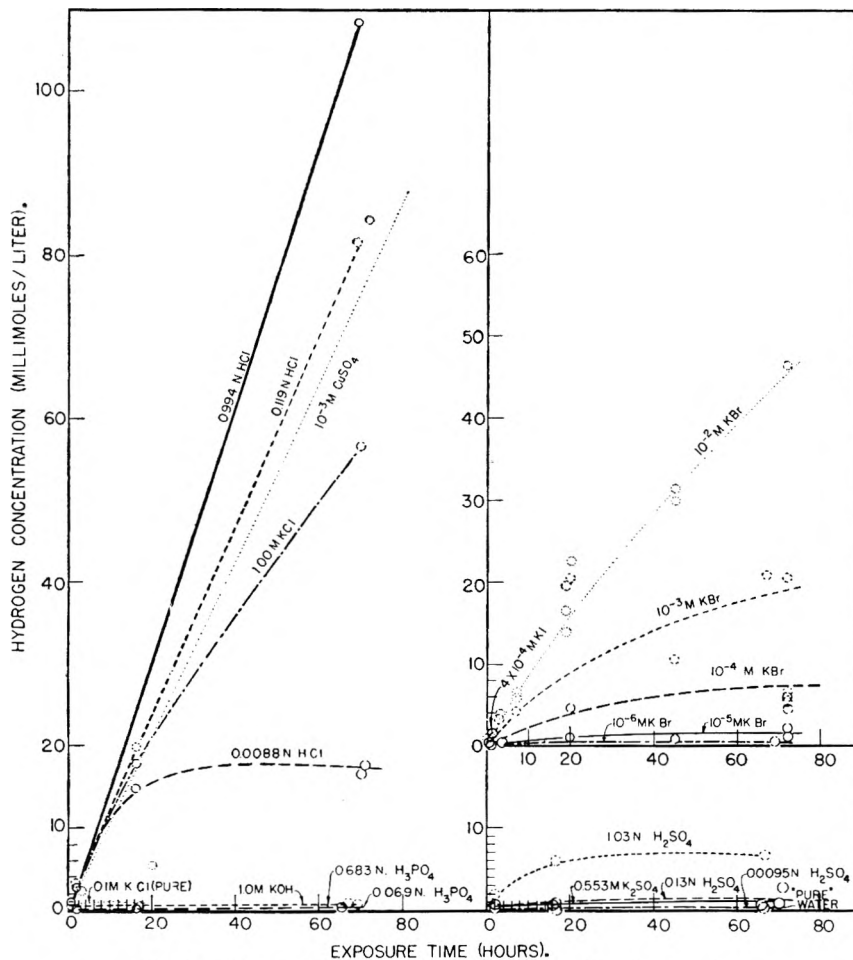


Fig. 5.—Effect of solutes on water decomposition in the pile.

A number of these ampoules were exposed in the reactor at about 25°, withdrawing at intervals for pressure measurement. The results are shown in Fig. 4. The rate of gas generation is initially about the same for the different ampoules, but sooner or later decreases and finally becomes zero (steady state). The final pressure attained varied for the different ampoules from 51 to 147 cm. The corresponding concentrations of H₂ dissolved in the water are of the order of a few hundred μ M.

Taking these data, together with those obtained with full ampoules, we get the following picture: In a full ampoule, a steady state is attained within a few minutes. The steady-state level of decomposition gradually drifts upward, however, because of aging of the ampoule which presumably involves dispersion in the water of material from the wall. In a half-filled ampoule, attainment of the steady-state concentration is necessarily much slower, and the aging process occurs concomitantly with the initial gas evolution, so that a smooth pressure-time curve results. After a few days, however, the aging process appears to reach an end, so that the pressure attains a true steady state. At this point, the dispersion of silica in the water may be balanced by reprecipitation on the wall. Different ampoules give different steady states because the nature of the foreign particles produced varies with different pieces of silica tubing. It is very doubtful that the steady-state pressure in these am-

poules would remain indefinitely constant. Further drifting would probably occur if the exposures were continued for many weeks.

We were able with these ampoules to confirm the theory that the steady state should be higher the greater the proportion of heavy-particle radiation impinging on the sample, *i.e.*, the greater the average density of radicals at the time of their formation. An ampoule was surrounded with $^{11}/_{16}$ " of lead. This cuts out much of the γ -rays absorbed by the sample, while reducing less the fast neutron flux in the water. The steady-state level of gas should, therefore, be increased. This actually happened; the pressure, which had been essentially constant for 95 hours without lead at 48-51 cm., rose in a further 44 hours exposure with lead to 61 cm. Another ampoule, which had leveled off at 95 cm. was put back surrounded with $^{11}/_{16}$ " paraffin. This reduces the fast neutron flux much more than it reduces the γ -ray flux. The pressure, as may be seen in Fig. 4, dropped precipitately, eventually reaching 10 cm. The initial rate of pressure drop when the paraffin was put on was actually greater than the initial rate of pressure rise obtained with fresh ampoules.

Decomposition of Water in Aqueous Solutions under Reactor Radiation

Solutions of KBr, KI, CuSO₄, KCl, HCl, KOH, H₂SO₄, K₂SO₄, and H₃PO₄ at various concentrations were exposed for different lengths of time in the reactor. All these experiments were made with full ampoules containing essentially no gas phase. Resulting yields of hydrogen gas are shown in Fig. 5. It is seen that in many cases hydrogen concentrations were obtained far exceeding anything found with pure water. In general, the pressure increases with time, then usually levels off to some steady-state value. With the more concentrated chloride solutions and with copper sulfate, the dissolved hydrogen pressure did not level off, even when values corresponding to hydrogen pressures of over 100 atmospheres

were attained. The initial rate, however, appeared to be the same in all cases. This is shown in Table I, which gives the hydrogen yields obtained in 1-minute exposures of the various solutions. The value is always about 27 micromoles/liter within experimental error, except for a few lower values obtained with pure water and solutions that gave low steady-state values; in these cases, the back reaction was apparently already important in the first minute.

TABLE I
YIELDS OBTAINED IN VARIOUS SOLUTIONS IN 1-MINUTE REACTOR EXPOSURES

Solution	H ₂ concentration (micromoles/liter)	Solution	H ₂ concentration (micromoles/liter)
1.0 N H ₂ SO ₄	33.7	1.0 M KCl	31.8
0.13 N H ₂ SO ₄	23.4	10 ⁻² M KBr	24.7
.0095 N H ₂ SO ₄	20.8	10 ⁻³ M KBr	23.8
.683 N H ₃ PO ₄	28.3	0.5 M K ₂ SO ₄	20.3
.069 N H ₃ PO ₄	25.8	10 ⁻³ M CuSO ₄	27.5
.994 N HCl	26.9	H ₂ O	17.1
.119 N HCl	29.7		30.8
.0088 N HCl	29.0		26.2

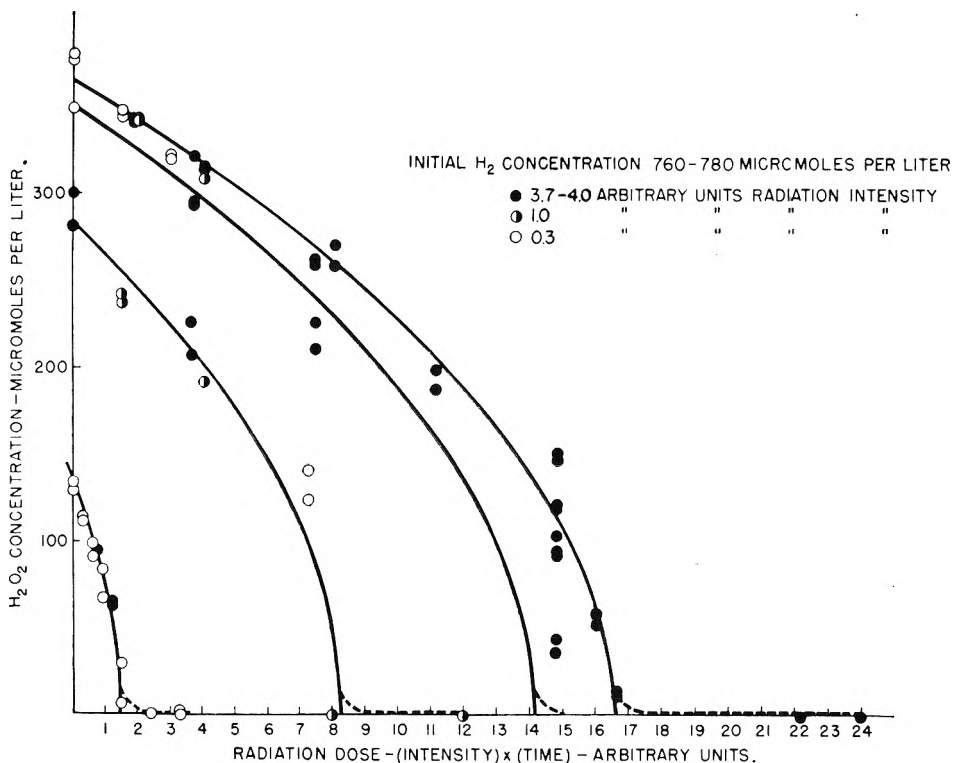


Fig. 6.—Combination of hydrogen peroxide and hydrogen in dilute aqueous solution under radiation from Oak Ridge pile. Curves are theoretical:

$$\frac{d(\text{H}_2\text{O}_2)}{d(\text{Dose})} = -7.5 + 9.42 \frac{(\text{H}_2)}{(\text{H}_2\text{O}_2)} = \frac{a + b(\text{H}_2\text{O}_2)}{(\text{H}_2\text{O}_2)}$$

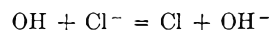
$$\text{DOSE} = \frac{(\text{H}_2\text{O}_2)_0 - (\text{H}_2\text{O}_2)}{b} - \frac{a}{b^2} / N \frac{a + b(\text{H}_2\text{O}_2)_0}{a + b(\text{H}_2\text{O}_2)}$$

$$\text{where } b = 9.42 - 7.5 = 1.92; \quad a = 9.42 [(\text{H}_2) - (\text{H}_2\text{O}_2)].$$

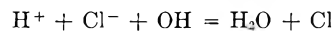
These results are readily explained in terms of our picture of the hydrogen-producing reaction, occurring in the densely ionized charged particle tracks, independently of the back reaction which comes about through the agency of free radicals escaping from the tracks. Those solutes which produce very high steady states react with radicals, and thereby prevent the radicals from reacting with dissolved hydrogen and hydrogen peroxide, so that the back reaction is inhibited. The forward reaction proceeds and the observed rate is that of the forward reaction until the dissolved hydrogen and peroxide reach a high enough concentration to compete with the dissolved materials for reaction with radicals. The observed rate then drops. This falling off occurs at a higher concentration of hydrogen the higher the concentration of any given dissolved material. The relative effectiveness of different materials in raising the steady state is a measure of the specific reaction rates of those ions with the radicals. Evidently bromide, iodide and copper ions react most rapidly with radicals, hydrochloric acid somewhat less rapidly, sulfuric acid still less rapidly, while phosphoric acid and hydroxide ions react little or not at all with the radicals. Reproducibility in these experiments was fairly good except for the more dilute solutions. With the more concentrated solutions the effect of the impurities was apparently swamped by that of the dissolved materials. With most of the solutions, the material balances were reasonably good. A few cases of poor material balance occurred, especially with sulfate solutions, suggesting that some oxidation or reduction of the solute may have occurred. The peroxide concentrations were very high in the case of sulfuric acid, suggesting that a persulfuric acid may have formed which is more stable to radiation than hydrogen peroxide. A complete elucidation of what occurs on irradiation of these solutions would require a more nearly complete analysis of the dissolved materials.

The high H_2 concentrations shown for 1 molar solutions of KCl (reagent grade) in Fig. 5 were shown to arise from bromide impurities. Some KCl, especially purified from bro-

midium by repeated chlorination and recrystallization, gave the low hydrogen yield shown in Fig. 5 under the heading 0.1 M KCl (pure). In a special series of experiments, the hydrogen yields from irradiated solutions of purified chloride, with pH adjusted by small additions of HCl, were shown to be small at pH greater than 4, with higher yields of hydrogen at lower pH. A possible explanation is that the reaction



is endothermic and does not occur in neutral solutions; but in acid solutions the exothermic termolecular reaction



becomes prominent.

The Reaction between Dissolved Hydrogen and Hydrogen Peroxide under Reactor Radiation

Since the back reaction between dissolved hydrogen and hydrogen peroxide plays such an important part in water decomposition, it was obviously desirable to study the rate of this reaction directly under various conditions. The kinetics of this reaction should also give us more detailed insight into the mechanism of the series of radical reactions occurring.

Solutions were made up in which the hydrogen was in excess of the peroxide and others in which the peroxide was in excess. The most interesting results were obtained from solutions in which hydrogen was in excess. Figure 6 shows the change of peroxide concentration with increasing exposure for solutions in which the initial concentration of peroxide was considerably less than that of dissolved hydrogen. In these cases no significant amount of oxygen appeared in the solution. The peroxide concentration decreased at a rate which became greater as the reaction proceeded. Then when the peroxide concentration approached zero, the rate fell abruptly, and a steady-state peroxide con-

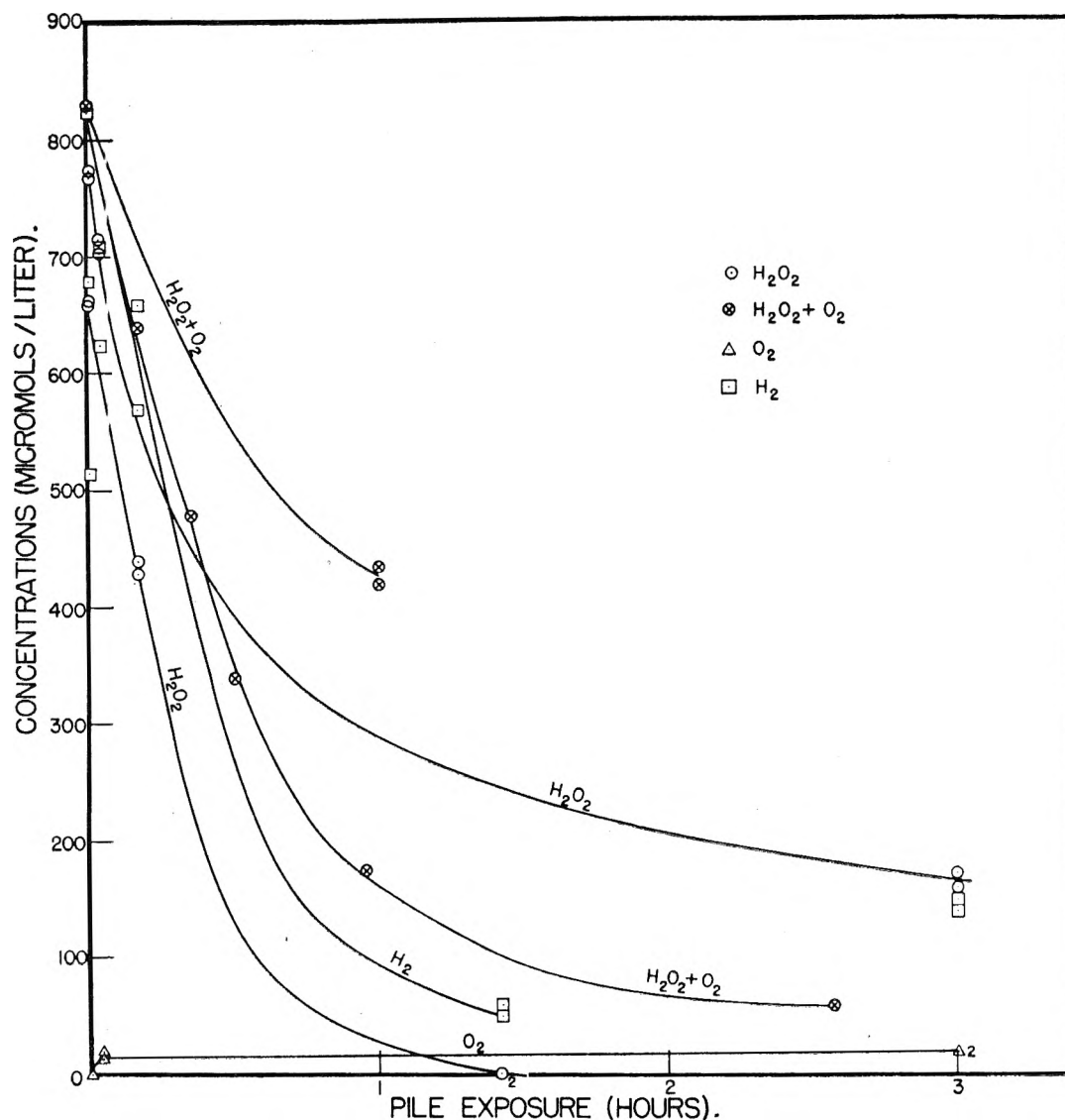


Fig. 7.—Decomposition of water in solutions containing comparable amounts of H_2 and H_2O_2 .

centration was reached at levels of the order of $1 \mu M$. Figure 7 shows results obtained from solutions where the initial hydrogen and peroxide concentrations were comparable; here steady states were found at levels comparable to those reached on exposures of pure water in the reactor for periods of 2 minutes to 1 hour. When considerable excess peroxide was present, concentration of hydrogen rapidly increased as shown by the curves in Fig. 8. Appreciable amounts of oxygen began to appear when the hydrogen and peroxide concentrations were equal, and much oxygen was formed when peroxide was in excess.

When only hydrogen was present initially, no appreciable peroxide or oxygen was formed in the solution, as shown in Fig. 9. A small drop in the dissolved hydrogen concentration on exposure must be ascribed to the absorption of hydrogen by the silica vessel walls. When only hydrogen peroxide or only oxygen was initially present, much water decomposition occurred (Fig. 9). In these cases, more hydrogen was formed than from water initially not containing any dissolved material.

In Fig. 10, the initial rate of peroxide disappearance is shown for the solutions, all of which contained the same concentration of dissolved hydrogen but different concentrations of peroxide.

The data all show definitely that the rate of back reaction—that is, the reaction of hydrogen with peroxide or oxygen to form water—increases with increasing hydrogen concentration but decreases with increasing concentrations of peroxide or oxygen. The oxygen or peroxide, although they

are reactants, also act as inhibitors for the reaction in the same way that other oxidizable and reducible solutes have been shown to behave. This is the explanation for the previously observed fact that, starting with pure water, a higher steady-state concentration of hydrogen is observed when a considerable space is available over the water than when the vessel is full. In the former case, most of the hydrogen formed escapes into the gas phase, leaving an excess of peroxide in the solution which inhibits back reaction and causes the hydrogen concentration and thereby its pressure to rise to high levels. Since excess peroxide inhibits the back reaction, a solution containing a large peroxide excess would presumably decompose under radiation indefinitely if it were not for the decomposition of peroxide to oxygen which occurs at the same time. The evolution of hydrogen stops when the peroxide level has been sufficiently reduced by its decomposition to oxygen.

For solutions containing excess hydrogen, the material balances were relatively good; since no appreciable amount of oxygen appeared, plots of the hydrogen and peroxide concentrations against time in any run would show parallel curves. The material balance in some of these runs is shown in Table II. In some of the later runs, only peroxide was determined, since it appeared superfluous to determine hydrogen.

In runs with excess peroxide, the material balances were not so satisfactory. The curves given in Figs. 8 and 9 for the amount of dissolved hydrogen are calculated from the oxygen and peroxide curves on the assumption of perfect

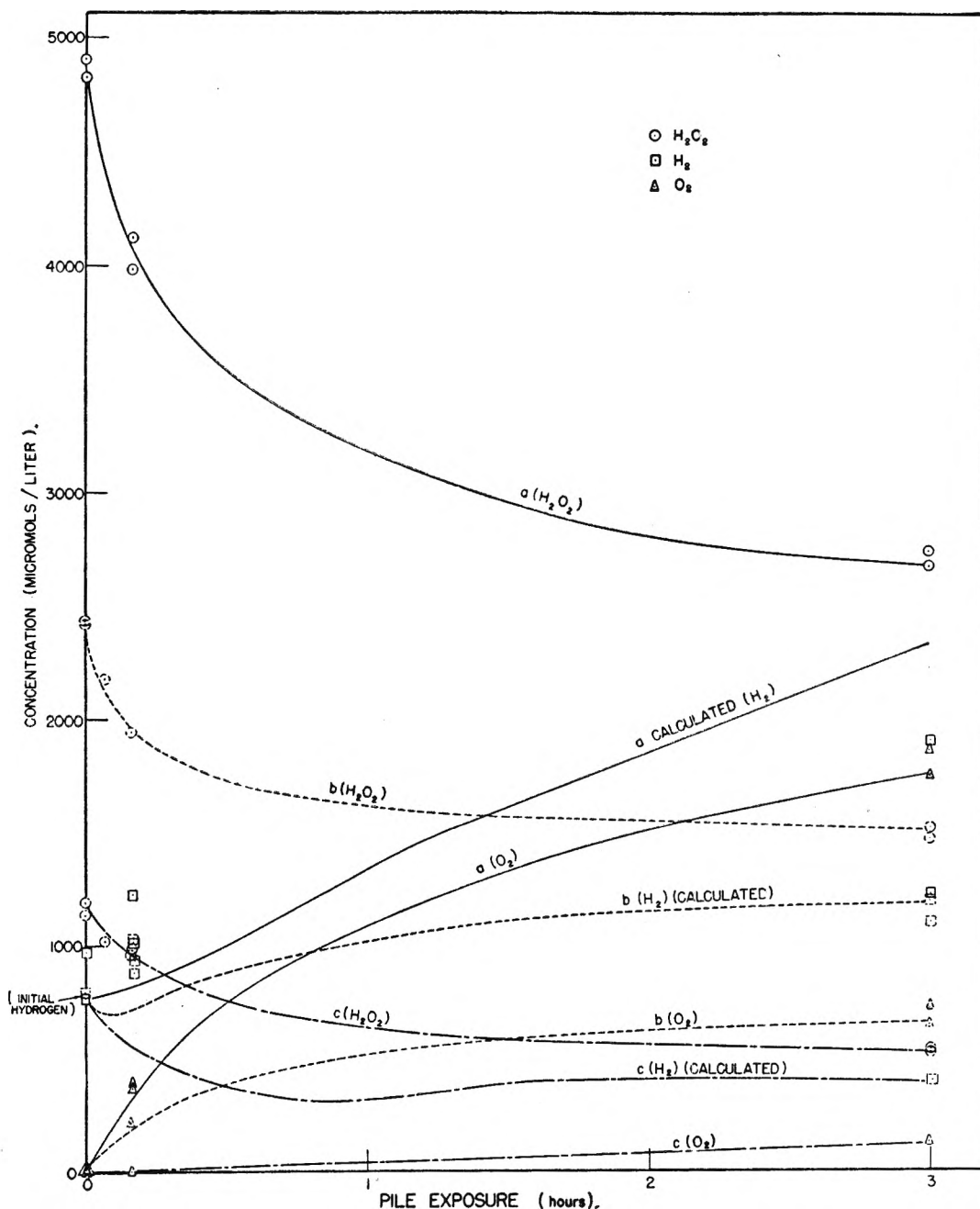


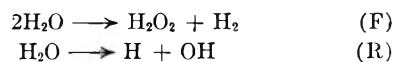
Fig. 8.—Decomposition of water in solutions containing hydrogen and peroxide when peroxide is in excess.

material balance, and the degree of experimental unbalance can be determined from the deviation of the observed hydrogen points on the graph from the calculated hydrogen curve. Bad material balances were likely to be found whenever oxygen appeared.

Discussion

The mechanism by which the decomposition of water is affected by various types of radiation was briefly discussed in the Introduction. Excitation or ionization of the water molecules leads ordinarily to bond breaking with the formation of the free radicals OH and H. In regions of high ionization density, such as the tracks of proton recoils or very slow electrons, radicals are formed in high concentrations. Many will react with one another to form the molecules H_2O_2 and H_2 before they have

time to separate by diffusion into the bulk of the water. In regions of lower ionization density, such as the tracks of fast electrons, most of the radicals will diffuse out into the water before they have a chance to react with one another. The system therefore behaves as though two different reactions were occurring simultaneously



The free radicals formed by reaction (R) disperse through the water by diffusion and are available to react with dissolved materials. Since H is a strong reducing agent and OH a strong oxidizing agent, oxidation-reduction reactions are common in irradiated solutions. Existence of the radiation-

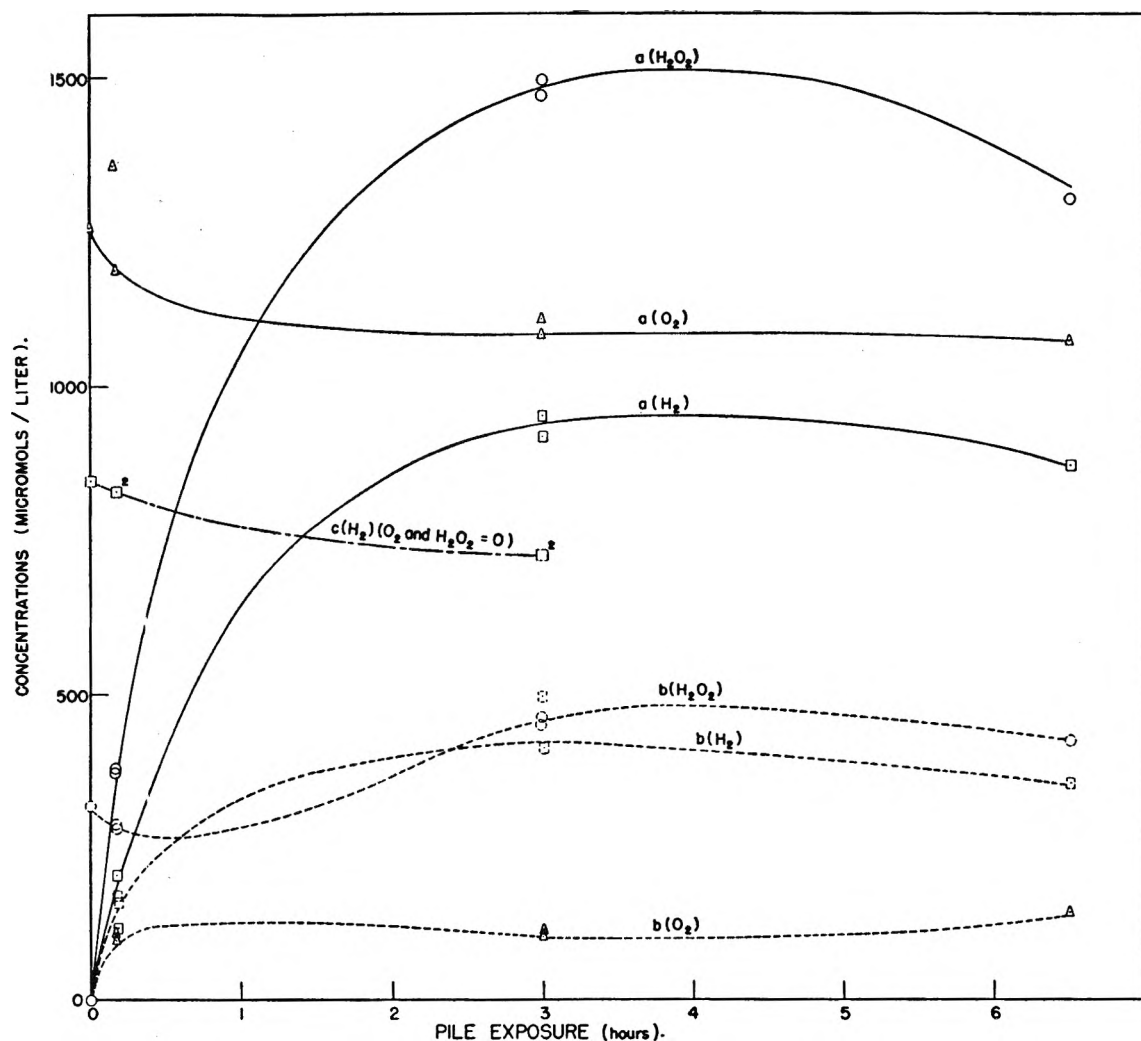
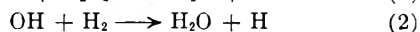
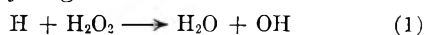


Fig. 9.—Decomposition of water in solutions containing initially only: (a) oxygen; (b) H_2O_2 ; (c) hydrogen.

TABLE II
MATERIAL BALANCE IN REACTOR IRRADIATED SOLUTIONS
CONTAINING HYDROGEN IN EXCESS OF HYDROGEN PEROXIDE

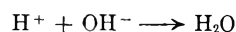
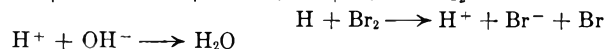
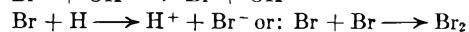
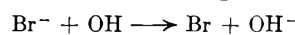
Exposure (reactor power \times time)	Product concentration (μM)			Excess H_2 (μM)
	H_2	O_2	H_2O_2	
0	773	6	350	411
3.7	687	6	296	379
7.4	635	10	220	395
14.8	412	15	41	341
0	742	11	301	419
2	736	9	240	476
3.6	694	5	218	466
4	667	5	192	465
7.2	715	4	134	573
8	518	6	0	506
12	451	14	0	433
16	450	7	0	436

induced back reaction between dissolved H_2 and H_2O_2 shows that the radicals can reduce peroxide and oxidize hydrogen

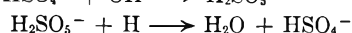


When both H_2 and H_2O_2 are present, a chain reaction will evidently be set up. This reaction is

completely analogous to the well-known gaseous chain reaction between hydrogen and chlorine; here the place of Cl is taken by OH , which has very similar chemical properties. The presence of readily oxidized material such as bromide ion will remove free radicals from the system and thereby interrupt the back reaction chain. The probable reactions occurring with bromide ion are



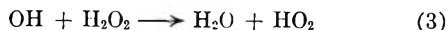
The bromide ions therefore act as catalysts for the recombination of radicals to water. We would expect most oxidation-reduction systems to behave in the same way. Anions containing oxygen probably interrupt the back reaction by a similar mechanism with peroxy radicals playing the role of the oxidized state.



While solutes interrupt the back reaction at high dilutions, they can have no effect on the forward reaction which takes place in the minute regions of high ionization density. The production of hy-

drogen and peroxide in the solution therefore proceeds uninterrupted until the concentration of these decomposition products becomes high enough for them to compete effectively with the foreign solutes for reaction with the radicals. The initial rate of hydrogen gas formation is therefore the same for all solutions in Table I.

Excess peroxide also inhibits the reaction by interrupting the chain. The reaction in this case is the same one by which peroxide is oxidized to oxygen



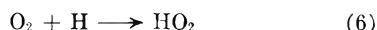
When many OH radicals are present, the resulting HO₂ radical can be oxidized further to oxygen.



However, the HO₂ can also be reduced back to hydrogen peroxide.



The sum of reactions (3) and (4) is again simply the combination of H and OH to water, so that excess peroxide acts in the same way that bromide ion does to inhibit the back reaction. When reaction (5) occurs the resulting oxygen can also be reduced back to HO₂.

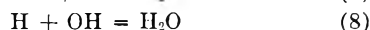


Reactions (5) and (6) are another oxidation-reduction pair, so that oxygen as well as H₂O₂ will act as a back reaction inhibitor.

When hydrogen is present in excess, reaction (5) apparently does not occur to any important extent since no appreciable quantity of oxygen is produced. The excess hydrogen keeps down the concentration of OH by reaction (2) so that most of the radicals are in the form of H and reaction (4) is favored over (5).

The relative rates of reactions of (F) and (R) are dependent on the ionization density characteristic of the particular radiation used. Since reaction (R) leads to disappearance of products produced in (F), the steady-state concentration levels of these products should be very sensitive to the ionization density. This was demonstrated by the experiments in which the proportion of the fast-neutron and γ -ray components of reactor radiation were changed (Fig. 4).

The only experiments which were sufficiently reproducible to permit quantitative treatment were those in which hydrogen and peroxide were initially present, with the hydrogen being in considerable excess. Here the reactions occurring were (F), (R), (1), (2), (3), (4) above together with the radical recombinations



Reaction of OH with OH may be neglected in these systems because with H₂ present in large amounts the OH concentration is much lower than that of H.

It is assumed in the following treatment that the free radicals are dispersed uniformly throughout the solution, so that the rates of their reactions are taken as proportional to their concentrations in the usual way. We assume, following the usual procedure, that the rate of change of radical concentra-

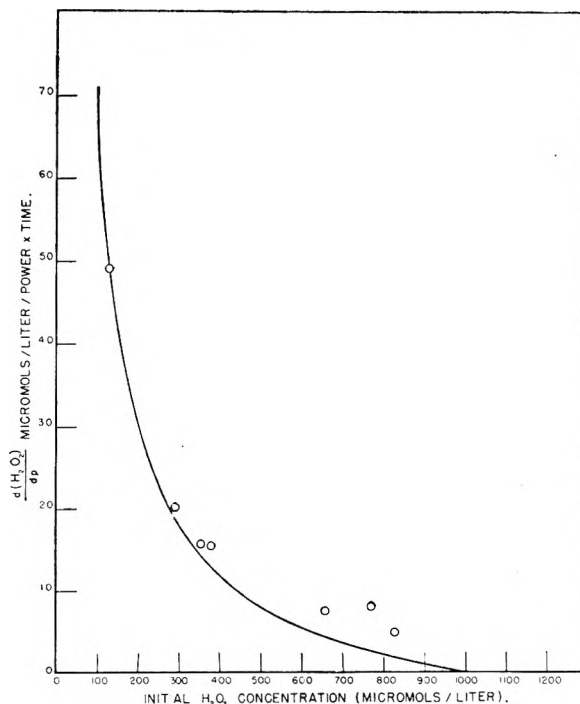


Fig. 10.—Initial rate of peroxide disappearance in hydrogen saturated solutions.

tions is small compared to the rates of the individual reactions involving radicals and may therefore be set equal to zero. At relatively high concentrations of H₂O₂ most of the radicals will disappear by reactions (3) and (4) so that reactions (7) and (8) may be neglected. We note that (3) followed by (4) does not change the H₂O₂ concentration. Then, if we let *I* be the radiation intensity, and *k* with an appropriate subscript the rate constant for any of the above reactions

$$-d(\text{H}_2\text{O}_2)/dt = k_1(\text{H})(\text{H}_2\text{O}_2) - k_{\text{F}}I \quad (\text{A})$$

$$-d(\text{H}_2)/dt = k_2(\text{OH})(\text{H}_2) - k_{\text{R}}I \quad (\text{B})$$

$$d(\text{H})/dt = 0 = k_{\text{R}}I - k_1(\text{H})(\text{H}_2\text{O}_2) + k_2(\text{OH})(\text{H}_2) - k_3(\text{H})(\text{H}_2\text{O}_2) \quad (\text{C})$$

$$d(\text{OH})/dt = 0 = k_{\text{R}}I + k_1(\text{H})(\text{H}_2\text{O}_2) - k_2(\text{OH})(\text{H}_2) - k_3(\text{OH})(\text{H}_2\text{O}_2) \quad (\text{D})$$

Since $k_4(\text{H})(\text{HO}_2) = k_3(\text{OH})(\text{H}_2\text{O}_2)$ (because HO₂ must be consumed as fast as it is formed) we have from (C) + (D)

$$0 = 2k_{\text{R}}I - 2k_3(\text{OH})(\text{H}_2\text{O}_2)$$

and setting (A) = (B), we obtain

$$(\text{OH}) = \frac{k_{\text{R}}I}{k_3(\text{H}_2\text{O}_2)} = \frac{k_1(\text{H})(\text{H}_2\text{O}_2)}{k_2(\text{H}_2)}$$

$$k_1(\text{H}) = \frac{k_2k_{\text{R}}I(\text{H}_2)}{k_3(\text{H}_2\text{O}_2)^2} \quad (\text{E})$$

Substituting in A

$$\frac{-d(\text{H}_2\text{O}_2)}{dt} = \frac{k_2k_{\text{R}}I(\text{H}_2)}{k_3(\text{H}_2\text{O}_2)} - k_{\text{F}}I \quad (\text{F})$$

Thus the mechanism gives the simple prediction that the back-reaction rate, after correcting for the forward reaction, should be directly proportional to the hydrogen concentration and inversely proportional to the peroxide concentration. The radiation yield, which is the rate of reaction divided

by the rate of radiation input I , is predicted to be independent of I .

To compare this expression with the data at hand, it must be integrated under the condition that the difference between the H_2 and H_2O_2 concentrations remains constant.

On integrating between the limits $(H_2O_2)_1$ at $t = t_1$ and (H_2O_2) at $t = t$, we obtain

$$\frac{(H_2O_2) - (H_2O_2)_1}{b} + \frac{a}{b^2} \ln \frac{a + b(H_2O_2)_1}{a + b(H_2O_2)} = t - t_1 \quad (G)$$

where

$$a = -Ck_2k_R I/k_3; \quad b = k_F I - (k_2k_R I/k_3) \\ C = (H_2) - (H_2O_2)$$

The quantity $k_F I$ appearing in the above equations is already known. This is the rate at which hydrogen is formed in solutions of active solutes such as HCl in which radicals are destroyed by the solute. We express the radiation intensity in arbitrary units of reactor power and set $k_F I = 30$ micromoles/liter-minute at a relative power of 4.0. (The experiments with solutions were performed with a relative power of about 3.6.) The experimental data shown in Fig. 6 include reaction-dose curves for four different starting concentrations of H_2O_2 , all having nearly the same initial concentration of H_2 . To fit these four curves, we have equations (F) and (G) which contain the single adjustable constant k_2k_R/k_3 . The curves drawn on Fig. 6 are the curves obtained from equation (G), with the above adjustable constant taken as 9.42. The curves fit the observed points within the experimental error except that the observed initial rate is somewhat greater than expected for the upper three curves. The initial rapid rates are probably due to presence of small quantities of organic impurities which accelerate the disappearance of H_2O_2 . The fit of the equation to the data is really much better than might be expected, and offers very good evidence for the assumptions made in deriving the equation.

Equation (3) predicts an infinite rate at zero peroxide concentration corresponding to an infinite concentration of hydrogen atoms. It is clear that when the peroxide concentration becomes sufficiently low, radicals will in actuality begin to disappear by reactions (7) and (8). When we include these reactions in the above scheme we obtain the following cubic equation for the concentration of hydrogen atoms

$$[k_1(H)]^3 + [k_1(H)]^2 \left[\left(\frac{k_1k_8}{k_8} + \frac{k_1^2}{k_7} \right) (H_2O_2) + \frac{k_1k_2(H_2)}{k_6} \right] + \\ k_1(H) \left[\frac{k_1^3k_2}{k_7k_8} (H_2O_2)^2 \right] - \frac{k_1^3k_2k_R I(H_2)}{k_7k_8} = 0 \quad (J)$$

The rate of disappearance of peroxide is still given by equation (A), with (H) now to be taken from equation (J). A qualitative examination of equation (J) shows that it predicts a curve that follows equation (F) down to peroxide concentrations of the order of $30 \mu M$, then rapidly bends over and levels out. This qualitative behavior is in complete agreement with the observations and is indicated by the dotted portions of the curves in Fig. 6. To attempt a quantitative fit of the cubic equation with the experimental data, and thereby obtain values for the various constants involved, would

have required much greater precision of experimental data than is possible to obtain.

The picture of radical behavior in irradiated water offered by the above mechanism differs in two important respects from that suggested by Lea.⁷ In the first place the change of radical concentration with time as the radicals diffuse away from the small volume in which they are formed is seen to be unimportant. Once a radical escapes by diffusion from the immediate neighborhood of others, the interaction of radicals becomes negligibly slow and the radicals spread out by diffusion until their concentration throughout the solution becomes essentially uniform. The interpenetration of expanding tracks, regarded by Lea as a meaningful quantity, is seen to have no significance. It appears that the rate of radical recombination must in actuality fall off much more sharply with time of diffusion than predicted by the Jaffe equation which Lea used. The second point of Lea's treatment which now appears unimportant is the alleged segregation of H and OH radicals in different parts of the track of the primary radiation. The formation of H_2 and H_2O_2 will occur in the track to some extent irrespective of the degree of segregation of the different kinds of radicals. The present results show that all observations can be explained without assuming this segregation; they neither prove nor disprove its occurrence.

Experimental

Preparation and Exposure of Silica Ampoules.—Water was exposed in the vertical water-cooled hole (No. 12) of the Oak Ridge reactor. The water samples were sealed in vessels made of fused silica tubing. Fused silica was used because it is more inert chemically toward water than most other materials and because it contains no great amount of any elements which become highly radioactive in the reactor. Most of the ampoules used for pure water were made from 15 mm. o. d. tubing, and held about 10 cc.; some ampoules were made from 6 mm. o. d. tubing and held about 2 cc. The tubes were sealed shut at one end and drawn down to small diameters at the other. After thorough cleaning with sulfuric-nitric acid mixture and rinsing and soaking with distilled water, the ampoules were sealed to a vacuum line and flamed to a red heat under vacuum. Degassed water was then distilled into the ampoules from a fused silica container and the ampoules sealed off. In some cases, the ampoules were practically full of water. In other cases they were only partially filled.

Hole 12 was maintained at 25° during the exposures. The water samples were probably about three or four degrees above this temperature, because of the heat resulting from absorption of radiation in the water.

After exposure for a predetermined time in Hole 12, the ampoules were withdrawn from the hole and allowed to stand for a time to allow the silicon activity to decay to a reasonably low level. The required "cooling" time varied from an hour to a day, depending on the length of the exposure.

Analysis of Decomposition Products.—The exposed ampoule was placed in a glass tube which was connected to a vacuum line. This tube was evacuated, and the ampoule was broken, either by warming the water in it with a heat lamp so that it expanded and broke the ampoule, by freezing the water so that the ampoule broke, or by breaking the ampoule under vacuum with a mechanical device. After the ampoule was broken, the water was warmed to reflux to assure expulsion of all gas, and the evolved gas passed through a trap maintained at -100° which collected all but traces of water vapor.

(7) D. E. Lea, "Effects of Radiations on Living Cells," The Macmillan Co., Inc., New York, N. Y., 1947, Chap. 2; *Brit. J. Radiol. Suppl.*, 1, 59 (1947).

The gas was collected in a gas analysis system which consisted of a McLeod gage connected to a platinum filament and a small liquid nitrogen trap. The gases present were assumed to consist of hydrogen, oxygen and carbon dioxide, with perhaps traces of nitrogen. The pressure of the gas was initially measured in the McLeod gage. Liquid nitrogen was then placed around the trap, and the reduction in pressure gave a measure of the carbon dioxide content. Considerations of vapor pressure and solubility allowed the conclusion that this component could not be any other substance which might conceivably form in the system, such as ozone, a silicon hydride or a nitrogen oxide. The hydrogen and oxygen were then determined by combustion on the heated platinum filament. Provision was made for the addition of small quantities of hydrogen and oxygen from the outside so that, by further combustion, a complete determination of hydrogen, oxygen and nitrogen in the gas was obtained. The diffusion of gas from the McLeod gage to the cold trap and the hot filament occurred rapidly and completely as long as the pressure was kept so low that the mean free path of the gas molecules was of the order of a centimeter. Quantities of gas as small as 1 cubic millimeter (S.T.P.) were analyzed with an accuracy of 1 or 2% in about 20 minutes. Table III shows the results of analyses on synthetic gas mixtures made to test the accuracy of the method. The accuracy of the analysis seems to be good and the chief error is probably incompleteness of removal of dissolved gas from the water sample. A test showed that the first outgassing of a typical sample removed 90% of the dissolved hydrogen, and it may be presumed that gas recovery was at least this good in all the work reported here when the dissolved gas concentration was as high as 300 micromoles/liter.

TABLE III
ANALYSIS OF SYNTHETIC GAS MIXTURES

Total gas, cc. std. $\times 10^2$	H ₂		O ₂		CO ₂		Total found, %
	Added, %	Found, %	Added, %	Found, %	Added, %	Found, %	
0.63	100	100					
0.60	39.2	40.8	34.4	33.4	26.4	25.8	100
0.38	37.5	38.5	49.9	42.9	12.6	13.0	94.4
1.17	63.7	65.6	26.3	25.9	10.4	8.8	100.3
0.68	47.3	47.3	47.9	47.1	3.88	4.76	99.2
0.7	56.0	56.6	38.5	38.5	5.7	5.09	100.2
0.95	17.9	18.2	32.1	32.1	50.2	50.9	101.2
1.0	44.9	46.6	21.5	20.8	33.7	32.7	100.1
2.02	24.1	24.1	21.8	21.7	54.4	54.0	99.8

The volumes of water and gas phase were determined by weighing the ampoule plus water sample, the ampoule full of water and the empty ampoule. For those ampoules which were practically full of water (~1% gas space in a small capillary) the concentrations of products in micromoles/liter were calculated assuming all of the products remained in solution. When a gas phase was present, the concentrations of products in solution were calculated on the basis of known solubilities and the measured amounts of products formed.

The water, after withdrawal of gas for analysis, was removed from the apparatus for colorimetric determination of dissolved hydrogen peroxide. Reagent for the determination was prepared by mixing equal volumes of (a) a solution containing 1 g. of NaOH, 33 g. of KI, 0.1 g. of (NH₄)₂MoO₄·4H₂O in 500 ml. of distilled water; (b) 10 g. of potassium acid phthalate in 500 ml. of distilled water. The alkaline iodide solution is stable, but iodide is slowly oxidized by dissolved oxygen at the pH of the mixed reagent, where peroxide reacts rapidly with iodide in the presence of molybdate catalyst. Samples of water ranging in volume from 0.1 to 2 ml., depending on the peroxide concentration, were mixed with 2.5 ml. of the reagent in a volumetric flask and distilled water was added to bring the volume to 5 ml. Samples were placed in a 1-cm. absorption cell and the optical densities were determined with a Beckman spectrophotometer at 350 m μ the wave length of maximum absorption for the triiodide ion. The concentration of peroxide in the original sample, in micromoles per liter, is given by $(D_a - D_b) \times 40.0 \times \text{diln.}$, where diln. is the ratio of the volume of the final mixture to the volume of the original sample, D_b is the optical density ($\log_{10} I_0/I$) of the reagent alone diluted

with distilled water, and D_a is the optical density of the sample. In most determinations the sample in one cell was compared with the reagent blank in another cell in the spectrophotometer, giving $D_a - D_b$ directly. The method was checked using a series of peroxide solutions prepared by diluting a standard peroxide solution analyzed by the ceric titration method. The determination is good to better than 3% at high peroxide concentrations. At low concentrations greater absolute accuracy was obtained by using the same cell for both the reagent blank and the sample, using for comparison each time the intensity with no cell in the optical path of the spectrophotometer. The probable error at low concentrations is believed to be ± 0.2 micromole per liter.

Preparation of Water.—Great efforts were made to purify the water used, in the belief that irreproducibility of results and poor material balances could be ascribed to traces of impurity introduced with the water. The persistence of carbon dioxide in the irradiated water suggested that organic impurities might be responsible for the lack of reproducibility. Distilled water was redistilled from acid permanganate, then from alkaline permanganate in a closed system allowing no contact with air. The triply-distilled water was sometimes distilled again, the steam passing through a tube containing copper oxide and kept at 700° to oxidize organic matter. Later the copper oxide was replaced with strips of pure nickel, the surface of which was purified by oxidation with oxygen at a high temperature followed by reduction with hydrogen. Steam was passed over the nickel at 1000°, in the hope that nickel would catalyze the reaction of organic impurities with steam to form oxides of carbon. None of these treatments suppressed the formation of carbon dioxide by irradiation. Water was then synthesized by combination of hydrogen and oxygen in a flame. The resulting water was distilled from potassium hydroxide which was found necessary to hold back traces of nitrous acid formed apparently by fixation in the flame of nitrogen present as an impurity in the oxygen used. All the water was thoroughly outgassed by refluxing under vacuum before the final distillation into the silica ampoules.

No essential differences were detected in the behavior of these various kinds of water under irradiation. In later work the water used was mostly laboratory distilled water which had been redistilled first from acid and then from alkaline permanganate in a Pyrex system and finally redistilled at atmospheric pressure in an all-silica system. The water, when air-saturated, had a conductivity of about 8×10^{-7} ohm⁻¹cm.⁻¹ which is close to the accepted value for pure air-equilibrated water. Redistillation of this water from KOH under vacuum in a silica system gave water with a conductivity of about 2×10^{-7} , which compares not unfavorably with the theoretical value of 0.5×10^{-7} for absolutely pure water containing only H⁺ and OH⁻ ions.

"Mote-free" Water.—The procedure used was that of Martin.⁸ Motes are formed by the action of water on a rough glass surface. To make a surface smooth, the glass (fused silica) was heated to the fusion point and cooled in the absence of moisture, since water vapor apparently invades the glass during cooling and causes surface roughening. Water was then distilled into the ampoule very slowly under vacuum. Some motes are said to be present, nevertheless, and these were removed by pouring the water carefully out of the ampoule back into the distilling bulb and redistilling. This process of distilling and pouring was repeated nine or ten times. Finally the ampoules were sealed off at the small capillary which connected them to the distillation tube. The amount of water in the ampoule was adjusted so that when it warmed up to room temperature no void was left in the ampoule.

Pressure Indicating Ampoules.—The method is illustrated diagrammatically in Fig. 11. The main part of the fused silica ampoule is drawn out into a capillary, a few cm. long, terminating in a small bulb into which is ring-sealed a further length of 1-mm. bore capillary, with the inner end ground to a tip. The ampoule was generally about half-filled with water; the method of filling was the same as for the regular ampoules. To measure the boiling point, the ampoule is placed vertically, with the capillary end down, immersed in a heated bath. The main upper part is immersed in an ice-bath. The lower capillary is heated to expel the gas from it. Bubbles of gas emerge from the capillary tip and pass through to the upper chamber. When

(8) W. H. Martin, *This Journal*, **24**, 478 (1920)

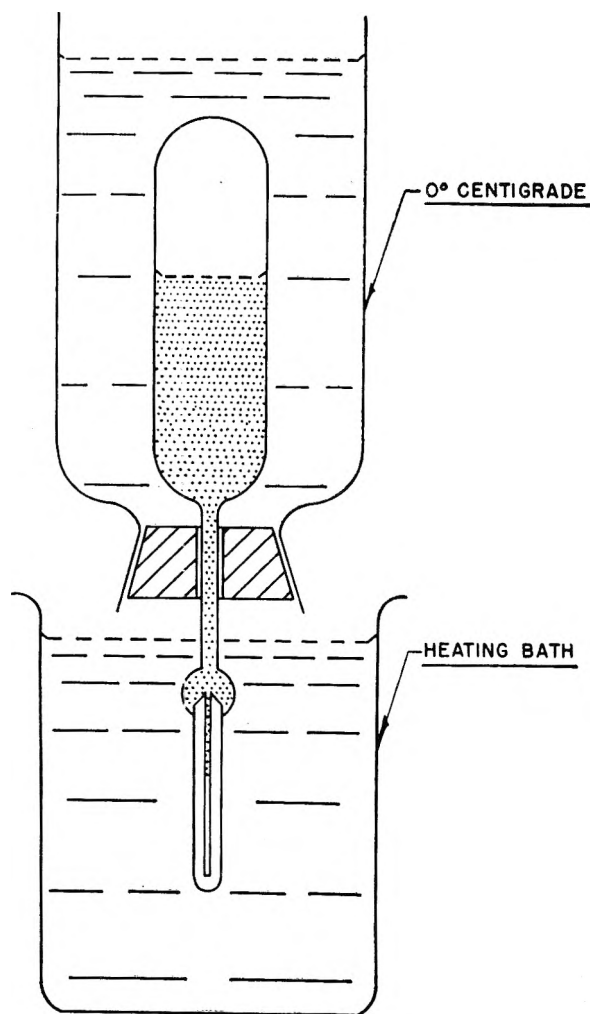


Fig. 11.—Determination of pressure in pressure-indicating ampoule.

bubbling stops, the end capillary should ideally contain water vapor only. The lower bath is then slowly cooled. When the temperature in the lower bath drops to the boiling point T_b of the water under the ambient pressure the vapor should suddenly condense and water rush in to fill the capillary. The pressure of gas P_0 in the main part of the ampoule would then be the vapor pressure of water at T_0 , T_{vb} , less the head of water h , less the vapor pressure of water at the ice point, P_{v0} . (The head h equals the actual distance between

the upper and lower water menisci, plus 3 cm. to take account of the capillary rise effect.) In practice, it is impossible to get rid of all the gas in the capillary, so that the water, instead of coming down suddenly into the capillary, comes down gradually over a range of 1–2° in the bath temperatures. The best procedure then is to note the temperature T_1 at which the volume of vapor phase remaining in the capillary is reduced to some value V_1 , and the lower temperature T_2 at which it reaches some smaller value V_2 , which is conveniently taken as one-half of V_1 . Then if P_{vT_1} and P_{vT_2} are the vapor pressure of water at T_1 and T_2 , P_{g1} is the unknown partial pressure of permanent gas in the capillary when the volume is V_1 , and P_1 and P_2 are the total pressures in the capillary when the volumes are V_1 and V_2 , we have, neglecting the Charles law contraction of the permanent gas in the capillary

$$P_1 = P_0 + h + P_{v0} = P_{g1} + P_{vT_1}$$

$$P_2 = P_0 + h + P_{v0} = P_{g1}(V_1/V_2) + P_{vT_2}$$

Since the change in h is negligible, we equate P_1 and P_2 . If $V_1/V_2 = 2$, we have $P_{g1} = P_{vT_1} - P_{vT_2}$, and finally by substitution

$$P_0 = 2P_{vT_1} - P_{vT_2} - h - P_{v0}$$

Successive pressure determinations are reproducible to about $\pm 2\%$.

Exposure of Solutions.—Solutions made up using triply-distilled water were placed in a fused silica bulb connected to a side arm to which the silica ampoules were sealed. The bulb was sealed on to the vacuum line and the solution was degassed. The bulb was then sealed off from the line under vacuum, the solution poured into the ampoules and the ampoules sealed off individually.

Preparation of Solutions Containing Hydrogen.—The water was triply distilled in all-silica apparatus. Hydrogen peroxide (Baker and Adamson, reagent grade, 30%) was vacuum distilled in silica apparatus before use. The silica ampoules used were sealed to a silica manifold connected to a silica bulb in which the water or peroxide solution to be used was placed. Hydrogen freed of higher-boiling impurities by passage through a liquid-air trap was bubbled through the solution in the bulb until air was expelled and the solution saturated with the gas at atmospheric pressure. The whole apparatus was then inverted, allowing the gas-saturated solution to flow into the ampoules, which were then sealed off. The ampoules were always completely full of solution at room temperature; care was taken to avoid the presence of any gas bubble.

Acknowledgments.—The above experiments were carried out at the Clinton Laboratories, later renamed Oak Ridge National Laboratory, under the auspices of the U. S. Atomic Energy Commission. The authors are happy to acknowledge the collaboration of G. V. Elmore and B. M. Haines in the experimental work.

EFFECTS OF COBALT γ -RADIATION ON WATER AND AQUEOUS SOLUTIONS¹

By C. J. HOCHANADEL

Chemistry Division, Oak Ridge National Laboratory, Oak Ridge, Tennessee

Received February 25, 1952

The radiation decomposition of water and the radiation-induced back reaction of the products H_2 and H_2O_2 have been studied using a cobalt gamma-ray source. Absolute yields were determined by comparison with an acid ferrous sulfate actinometer which had been calibrated calorimetrically. The measured yield for oxidation of Fe^{++} in air-saturated 0.4 M H_2SO_4 was $15.5 \pm 0.3 Fe^{++}$ oxidized per 100 ev. absorbed. The decomposition of water by any ionizing radiation is treated as occurring in two separate reactions.



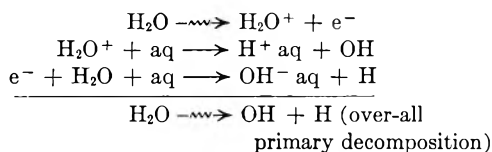
The value for $k_F = 0.46 H_2O_2$ and H_2 per 100 ev. was determined from H_2O_2 yield in oxygen-free acid bromide solutions. The value for $k_R = 2.74 H$ and OH per 100 ev. was determined from the H_2O_2 yield in solutions containing both H_2 and O_2 . The minimum yield for decomposition of water by γ -radiation is then 3.66 H_2O per 100 ev. or 1 H_2O per 27 ev. The radiation-induced reaction between dissolved product molecules H_2 and H_2O_2 was studied under a variety of conditions. The kinetics are discussed in terms of reactions with free radicals, H , OH and HO_2 .

Introduction

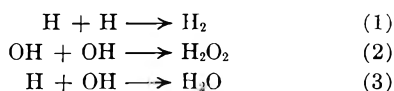
The present concepts involving the formation and reactions of free radicals in water and aqueous solutions exposed to ionizing radiations were developed by a number of people and have been summarized in several reviews.²⁻⁴

The effects of mixed fast neutron (through proton recoils) and γ -radiation (furnished by the Oak Ridge pile) on water and aqueous solutions were studied by Allen, *et al.*^{5,6} The results were explained in terms of reactions of the free H and OH radicals produced in water by the ionizing radiations. In this paper are presented results obtained on irradiating water and aqueous solutions with pure, essentially monoenergetic γ -radiation from radioactive cobalt⁶⁰.

The salient features of the mechanism proposed in the previous paper are listed for reference: (1) The primary chemical effect of the ionizing radiation is to produce H and OH radicals according to the mechanism.



(2) The spatial distribution of these radicals immediately after formation is characteristic of the ionizing radiation used and for α -particles, low energy protons or very low energy electrons the radicals are formed in high concentrations along the ionization tracks. Many will react with each other in these regions to form product molecules H_2 and H_2O_2 or reform water according to



(1) This work was performed for the Atomic Energy Commission.

(2) M. Burton, *THIS JOURNAL*, **51**, 611 (1947).

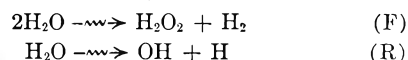
(3) (a) A. O. Allen, *ibid.*, **52**, 479 (1948); (b) F. S. Dainton, *ibid.*, **52**, 490 (1948).

(4) F. S. Dainton, *Chem. Soc. Annual Repts.*, **45**, 5 (1949).

(5) A. O. Allen, C. J. Hochanadel, J. A. Ghormley and T. W. Davis, *THIS JOURNAL*, **55**, 575 (1952).

(6) A. O. Allen, T. W. Davis, G. Elmore, J. A. Ghormley, B. M. Haines and C. J. Hochanadel, Oak Ridge National Laboratory Publication, ORNL 130, (1949).

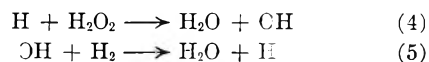
In regions of low ionization density such as tracks of fast electrons, most of the radicals will diffuse away from each other and are available to react with solutes. The system is therefore treated as though two separate reactions were occurring at the same time, namely



The first of these we refer to as the forward reaction and its rate is the rate at which product molecules H_2 and H_2O_2 are constantly formed in pure water or in dilute solutions. The relative rates of F and R depend on the specific ionization of the radiation considered.

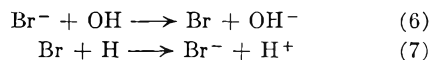
Although several workers⁷ report no decomposition of pure, air-free water by X-rays, in this picture some decomposition (forward reaction) is expected to occur in the regions of high specific ionization at the ends of recoil electron tracks. Values for k_F and k_R for cobalt γ -radiation will be reported in this paper. These values may be somewhat intensity-dependent.

(3) The radicals (R) are available to react with solutes, and in pure water two important reactions are



This back reaction chain is the chief method by which products of decomposition of water are removed. The steady state concentrations of products in pure irradiated water depend on the relative rates of (F) and (R) and therefore on the specific ionization of the radiation used. This dependency has been demonstrated.⁵ The steady state concentration of H_2O_2 for cobalt γ -rays was found to be $< 1.0 \times 10^{13}$ molecules, liter⁻¹, and to depend greatly on the presence of traces of impurities.

(4) Many added solutes in dilute solution inhibit the back reaction by causing recombination of radicals; *e.g.*, with bromide ion the reactions may be

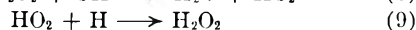
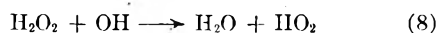


Many oxidation-reduction systems act in this way. Since in dilute solution these solutes are

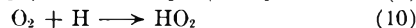
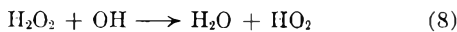
(7) H. Fricke, *Phys. Rev.*, **44**, 200 (1933).

expected to have little or no effect on the forward reaction, their addition allows a means for measuring k_F . This method was used to obtain a value for k_F using cobalt γ -rays.

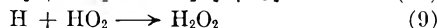
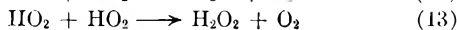
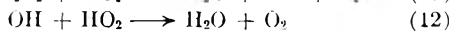
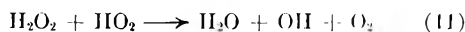
H_2O_2 itself inhibits the back reaction, probably through



(5) The presence of H_2O_2 or of O_2 in solution leads to formation of the free radical HO_2 through



Through reactions involving the HO_2 radical, H_2O_2 and O_2 are readily converted from one to the other as follows



(6) In solutions containing hydrogen and hydrogen peroxide with hydrogen in considerable excess, no O_2 is formed and the disappearance of H_2O_2 follows the simple rate equation

$$-\frac{d(H_2O_2)}{dt} = k_R I \frac{k_3 (H_2)}{k_3 (H_2O_2)} - k_F I$$

down to very low H_2O_2 concentration. Radiation intensity is represented by I .

The chief aim of this paper is to present constants k_F and k_R determined for cobalt gamma radiation and to show how the above rate equation fits the data obtained for the back reaction using cobalt γ -rays.

Experimental

Source of Radiation.—The source of γ -radiation used in this work was provided by approximately 300 curies of radioactive cobalt.⁶⁰ With its long half-life (5.3 yr.) and essentially monoenergetic radiation (1.17 and 1.34 mev. γ -rays in cascade), cobalt provides an excellent source of radiation for this type of study. The design of the shield for this source has been described elsewhere.⁹

Measurement of Energy Absorbed in Solutions.—Determination of the rate of energy absorption in solution was based on a calorimetric measurement⁹ of the rate of energy absorption in water at the position of maximum intensity. At the time of measurement this was 2.61×10^{20} ev., liter⁻¹ min.⁻¹. On the basis of this value, the yield for oxidation of ferrous ion in air saturated 0.4 M H_2SO_4 solution was found to be 15.5 ± 0.3 ferrous ions oxidized per 100 ev. absorbed in solution.

The rate of energy absorption in the solution contained in the irradiation cell was then determined using this ferrous sulfate actinometer. Results are plotted with concentrations given in units of 10^{18} molecules per liter and energy absorption (dose) in terms of 10^{20} ev. per liter. The slope of a curve then gives directly the yield G in terms of molecules per 100 ev. absorbed in solution.

(8) J. A. Ghormley and C. J. Hochanadel, *Rev. Sci. Instruments*, **22**, 473 (1951).

(9) J. A. Ghormley, C. J. Hochanadel, unpublished work, Oak Ridge National Laboratory.

Method for Saturating Solutions and Filling Irradiation Cells.—The arrangement for saturating solutions and filling the irradiation cells is shown in Fig. 1. The stopcocks and joints were lubricated with solution only, since the presence of organic material during irradiation would affect the results. The gas, after bubbling through the solution, flushed the irradiation cell and escaped out the 120° stopcock. The cell was filled by gravity through the 120° stopcock, with the stopcock above the bulb now providing the outlet for the gas. For the irradiation times used, no gas phase formed in the cell and it was assumed that no air diffused through the water sealed stopcocks and capillary tube into the main body of the cell. The opening at the top of the bulb allowed addition of solutes at any time.

The cells could be reproducibly placed for irradiations using the arrangement shown in Fig. 2. For most of the exposures the cobalt surrounded the irradiation cell. The solution could be thermostated by pumping water from a constant temperature bath through the outer jacket of the cell. For those samples on which a gas analysis was made, the cell was modified by replacing the stopcocks with capillary U-tubes in which the solution could be frozen and provide a vacuum tight seal for the gas analysis procedure.

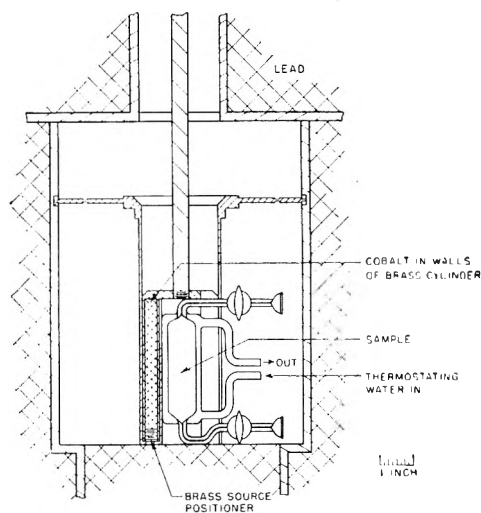


Fig. 2.—Arrangement for irradiating solutions with cobalt gamma rays.

Materials.—Water from a Barnstead still was redistilled from acid permanganate then alkaline permanganate. A further distillation was made in an all-silica system and the water was stored in silica vessels.

Several hydrogen peroxide preparations were used, each giving essentially the same results. These included 90% H_2O_2 kindly furnished by Buffalo Electrochemical Company, Inc., Baker C.P. 30% stabilizer-free H_2O_2 , Baker and Adamson 30% H_2O_2 containing a stabilizer, and also a solution prepared by irradiating with gamma rays oxygen saturated pure water with no gas phase present. An overnight exposure produced a solution containing 280 micromoles per liter.

Pure tank hydrogen and helium were passed over copper $\sim 500^\circ$ and then through a charcoal trap at -196° , primarily to assure removal of oxygen. Pure tank oxygen was used without further purification.

Baker and Adamson reagent grade sulfuric acid and KBr were used without further purification.

Analytical Methods.—Hydrogen peroxide concentration was measured using a colorimetric method developed by J. A. Ghormley.⁶ Iodide ion is oxidized by H_2O_2 in neutral or slightly acid solution and the absorption of I_3^- is measured at 3500 Å.

The iodide reagent was prepared immediately before using by mixing equal volumes of two solutions containing: (a) 66 g. KI, 2 g. NaOH, 0.2 g. $(NH_4)_2MoO_7 \cdot 4H_2O$ liter⁻¹; (b) 20 g. $KHC_8H_4O_4$ liter⁻¹. The alkaline iodide solution is stable but in the mixed reagent the iodide is slowly oxidized by dissolved oxygen. A measured volume of sample was diluted to a definite volume with distilled water and reagent with reagent making up one-half of the final volume. The optical densities for sample and blank were measured on a

Beckman Model DU spectrophotometer in the same 1-cm. cell using for comparison the intensity with no cell in the optical path. The concentration of peroxide in the original sample was calculated making use of the formula: Concentration (micromols liter⁻¹) = $(D_S - D_B) \times 38.7 \times$ dilution. The constant 38.7 was determined by diluting 0.1 *N* H₂O₂ which had been compared with ceric sulfate standardized against arsenious oxide. The accuracy is about 3% in the range of concentrations studied.

Gas was analyzed for H₂, O₂, CO₂ and N₂ using a low-pressure McLeod gage system. The gas was removed from solution by refluxing at about 50°, then after freezing the water with dry ice, was transferred by means of a Töppler pump into the McLeod gage. A trap at -100° removed the water vapor. The total amount of gas was determined from the measured pressure at known volume and a calibration for the fraction of gas measured. CO₂ was measured by the change in pressure on cooling a small tube with liquid nitrogen. Hydrogen and oxygen were determined by combustion on a platinum filament. The excess of one component was then determined by adding a measured amount of the other and burning a second time. The low pressure allowed rapid diffusion to the cold traps and filament.

Results and Discussion

Measurement of k_F : The Initial Yield for H₂O₂ Formation in Acid Bromide Solutions Irradiated with Cobalt γ -Rays.—It was pointed out in the introduction that some solutes such as Br⁻ react with the radicals H and OH formed in (R) thus preventing their carrying the back reaction chain. A measurement of the initial rate of H₂ or H₂O₂ formation in such solutions then gives a measure of k_F . The inhibition of the back reaction between H₂ and H₂O₂ by bromide ion is shown in a later section (see Fig. 10). Figures 3 and 4 show H₂O₂ formation in KBr solutions at various concentrations of Br⁻ and at various pH. The initial yield for H₂O₂ formation $G_F = k_F = 0.46$ molecule per 100 ev. is independent of Br⁻ concentration over a wide range.

In neutral or basic Br⁻ solution the H₂O₂ is converted rapidly to oxygen. The initial yield for decomposition of H₂O₂ in pure water saturated with helium was found to be approximately $G(-H_2O_2) = 3.7$ at concentrations of 10⁻⁴ *M* H₂O₂ and 4 × 10⁻³ *M* H₂O₂ and at intensities of 0.0054 × 10²⁰ ev. liter⁻¹ min.⁻¹ to 2.47 × 10²⁰ ev. liter⁻¹ min.⁻¹. Approximately this same yield was found for 10⁻⁴ *M* H₂O₂ containing 10⁻³ *M* or 10⁻² *M* KBr at pH 7 (pure water) or at pH 11.8 (NaOH). At pH 2.7 the yield was ~ 0. The yield of 3.7 probably represents the lower limit for H₂O₂ decomposition, found at high intensities and low H₂O₂ concentrations. In the photolysis in dilute aqueous solution, Lea¹⁰ had found a limiting quantum yield (1.39) at high intensity and low concentration. Under these conditions the chain reaction (sequence 8, 11) becomes unimportant and the kinetics become those of initiation and termination reactions only. The dependence on $I^{1/2}$ found at high concentration and low intensity no longer holds in this low concentration and high intensity range.

Fricke and Hart¹¹ showed that in bromide solutions irradiated with X-rays the hydrogen yield is the same at all pH's and that H₂O₂ is produced in acid solution and O₂ in basic solution in an amount equivalent to the hydrogen formed. They had found¹² an initial yield of hydrogen of 0.49 mole-

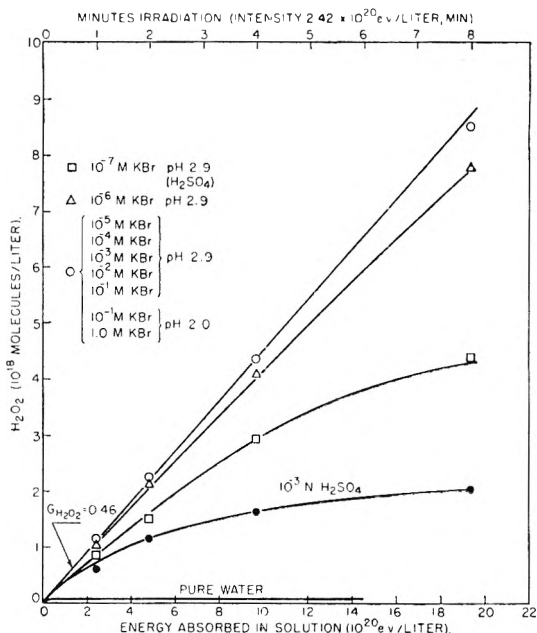


Fig. 3.—Effect of KBr concentration on initial H₂O₂ production in oxygen-free KBr solutions irradiated with cobalt gamma rays.

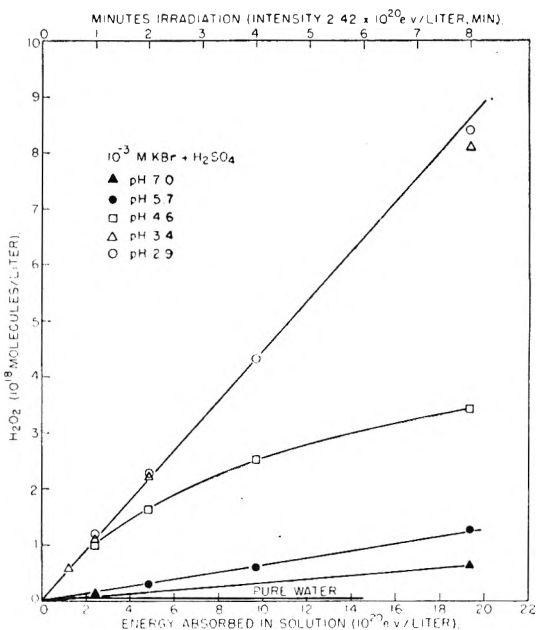


Fig. 4.—Effect of pH on initial H₂O₂ production in oxygen-free KBr solutions irradiated with cobalt gamma rays.

cule¹³ per 100 ev. for oxygen-free solutions of Br⁻, I⁻, NO₂⁻, SeO₃²⁻, AsO₃³⁻ and Fe(CN)₆⁴⁻ irradiated with X-rays. The Br⁻ and I⁻ acted catalytically but the other solutes were oxidized in an amount equivalent to the hydrogen produced. The interpretation according to our picture is that the radicals produced in (R) were catalytically recombined to form water, leaving either the hydrogen and H₂O₂ formed in (F) or the hydrogen and a net oxidation of solute equivalent to the H₂O₂ formed in (F).

(13) Calculated on the basis of $G = 15.5$ ferrous ions oxidized per 100 ev. in air saturated 0.4 *M* H₂SO₄ solution. H. Fricke and E. J. Brownscoble, *J. Am. Chem. Soc.*, **55**, 2358 (1933), had found $G = 18.2$ ferrous ions oxidized per 100 ev.

(10) D. E. Lea, *Trans. Faraday Soc.*, **45**, 81 (1949).

(11) H. Fricke and E. J. Hart, *J. Chem. Phys.*, **3**, 596 (1935).

(12) H. Fricke and E. J. Hart, *ibid.*, **3**, 365 (1935).

Measurement of k_F from H_2 Yield in Irradiated Oxygen-saturated Acid Ferrous Sulfate Solution.—In the mechanism proposed by Krenz and Dewhurst¹⁴ for oxidation of ferrous sulfate by gamma rays in aerated water, the forward reaction for water decomposition is neglected. In this mechanism ferrous ion is oxidized by OH and H (through HO_2) but would also be oxidized by the H_2O_2 , leaving the H_2 formed in the forward reaction (F). The production of hydrogen was measured on irradiating oxygen saturated $5 \times 10^{-3} M$ $FeSO_4$ in $0.4 M$ H_2SO_4 at an intensity of 2.65×10^{20} ev. liter⁻¹ min.⁻¹, giving the results:

Fe ⁺⁺ oxidized micromoles liter ⁻¹	H ₂ formed micromoles liter ⁻¹	GH ₂ , molecule per 100 ev.
2800	70.3	0.39
3540	84.0	.37
4150	102.5	.38

This yield is lower than that found for bromide solutions and owing to the type of analysis and complicated system is regarded with less confidence.

The fact that hydrogen is formed, along with other considerations, shows that the oxidation of ferrous sulfate is not so simple as the mechanism of Krenz and Dewhurst would indicate.

Measurement of k_R . The Initial Yield of H_2O_2 in Solutions Containing Oxygen and Hydrogen.—The initial yield for production of hydrogen peroxide in solutions containing both hydrogen and oxygen was used along with the value for k_F to calculate a value for k_R . Using X-rays Fricke¹⁵ had found the initial yield for conversion of O_2 to H_2O_2 to be independent of O_2 pressure from 4 to

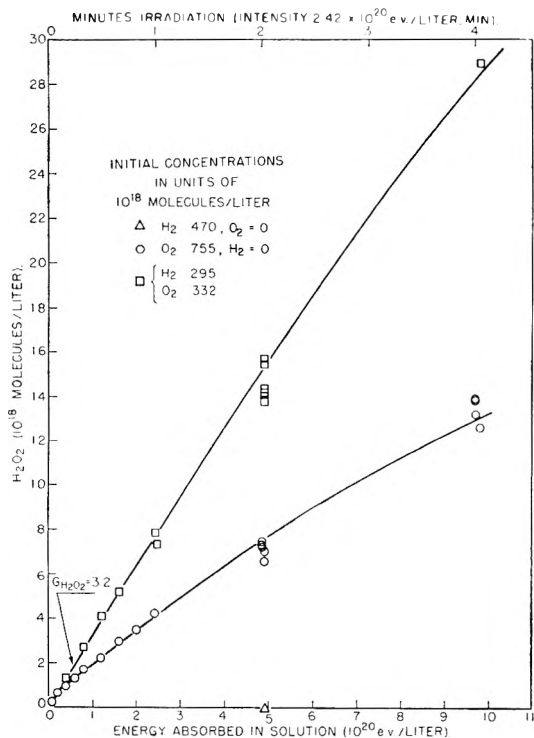


Fig. 5.—The initial production of H_2O_2 in solutions containing either oxygen, hydrogen or both gases.

(14) F. H. Krenz and H. A. Dewhurst, *J. Chem. Phys.*, **17**, 1337 (1949).

(15) H. Fricke, *ibid.*, **2**, 556 (1934).

70 cm. but varied¹⁶ from $iG_{H_2O_2} \sim 1.0$ in the pH range 3 to 8 to a value $iG_{H_2O_2} \sim 1.0$ in the pH range 11.5 to 13. Toulis¹⁷ showed that adding hydrogen to a solution containing oxygen enhances the initial rate of H_2O_2 formation, giving an estimated yield $iG_{H_2O_2} \sim 3.6$ at pH 7.

On irradiating solutions containing both hydrogen and oxygen in various proportions, the author found an initial yield $iG_{H_2O_2} = 3.2$ which was independent of pH from pH 2 (H_2SO_4) to pH 7 (pure water). The initial yield in oxygen-saturated solution was difficult to determine but is probably somewhat lower than this. The results are plotted in Figs. 5 and 6 showing the effects of varying the H_2/O_2 ratio and also of adding solutes.

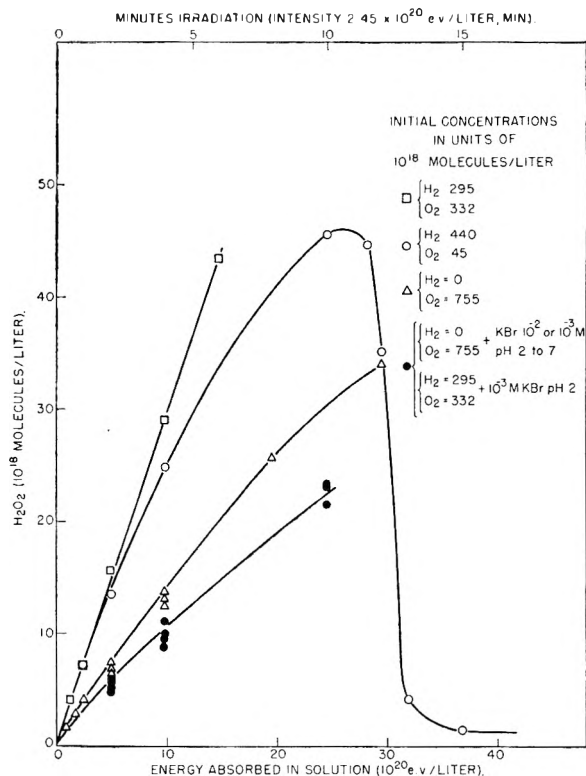
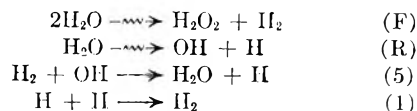
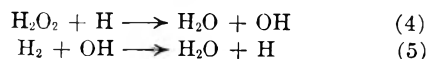


Fig. 6.—Effect of relative hydrogen and oxygen concentrations and of added solutes on H_2O_2 production.

With only hydrogen added to the water, no measurable amount of H_2O_2 or O_2 is formed and the H_2 concentration remains constant. This could be explained by the scheme



Some radicals would carry the back reaction chain



If oxygen alone is added to the water initially, H_2O_2 is formed at the rate shown in Figs. 5 and 6 and builds up to a steady state level. With both hydrogen and oxygen added to the water, H_2O_2 is formed at a rapid rate initially and its concen-

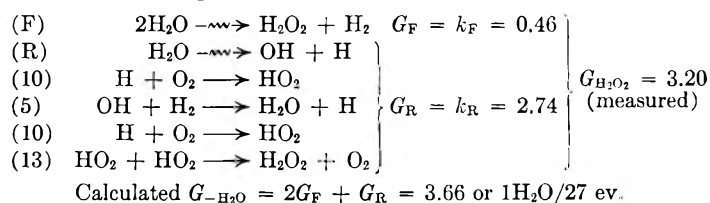
(16) Values based on G for ferrous oxidation of $15.5 Fe^{++}$ (100 ev.)⁻¹.

(17) W. J. Toulis, UCRL-583, February 10, 1950.

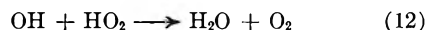
tration passes through a maximum if the initial H_2/O_2 ratio is sufficiently high. For the curve showing a maximum in Fig. 6, the O_2 is completely converted to H_2O_2 at which time the usual back reaction of H_2O_2 and H_2 sets in. The upper curve, for lower initial H_2/O_2 ratio, reaches a maximum H_2O_2 concentration at about 155×10^{18} molecules liter $^{-1}$ (not shown in the figure) after about one hour and then drops to a steady state concentration of about 47×10^{18} molecules liter $^{-1}$ in 10 hours.

With the addition of bromide ion in either neutral or acid solution, the initial yield is lowered and is approximately the same for all the solutions as shown in Fig. 6. This would indicate that in the presence of bromide ion, hydrogen has little chance to react with OH.

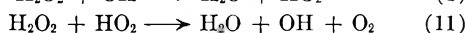
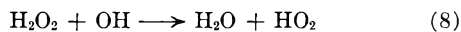
It is proposed that H_2O_2 formation in solutions containing both H_2 and O_2 occurs through reaction (F) and also through the conversion of each pair of radicals formed in reaction (R) into one H_2O_2 according to



Much evidence indicates that oxygen reacts readily with hydrogen atoms and would compete favorably for them. With no added hydrogen the initial H_2O_2 yield is lowered, probably by



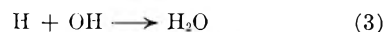
The curves also bend over more rapidly because of H_2O_2 decomposition to O_2 according to



Since hydrogen was shown to react readily with OH, it should compete favorably with HO_2 for the OH radicals at the concentrations used. It is assumed that reaction of H_2 with HO_2 does not occur to any great extent. This assumption is supported by studies on the back reaction between H_2 and H_2O_2 (next section). It was shown that H_2O_2 inhibits the back reaction whereas this would not be the case if reaction between H_2 and HO_2 occurred readily. Little or no effect of temperature from 25 to 65° was found on the initial yield for H_2O_2 production. This indicates that competing reactions which would lower the yield are not important or that the activation energies are small or approximately the same for the several reactions involved.

The measured yield $iG_{H_2O_2}$ is the sum of that formed in (F) and that from conversion of radicals (R) to H_2O_2 by H_2 and O_2 . These values show that of the measured number of water molecules decomposed by cobalt γ -rays, 25% of the radicals combine in the tracks to form stable products H_2 and H_2O_2 and 75% of the radicals diffuse into the bulk of the solution and are available to react with solutes. Assuming all water decomposition to occur through ionization, since the cage effect would probably render the contribution from ex-

cited molecules negligible, this $G_{H_2O} = 3.66$ corresponds to 27 ev./ion-pair for liquid water. This represents the maximum value for energy per ion pair since the yield 3.66 does not account for radicals produced by ionization and recombining through



The magnitude of this is difficult to assess but is at least as great as G_F . This correction would make the number ~ 22 ev./ion-pair.

Values for G_F and G_R for cobalt γ -rays were also deduced by Hart¹⁸ from the mechanism for oxidation of formic acid in solution containing H_2O_2 and O_2 . He found that of the total number of radicals produced in water by the γ -rays, 20% enter reaction (F) and 80% reaction (R). From a calculated value¹⁹ for $G_{-H_2O} = 3.48$, the corresponding values for G_F and G_R are 0.35 and 2.78, respectively. The value for G_F corresponds more nearly to that obtained in this work from the hydrogen yield in ferrous oxidation.

The relative values for G_F and G_R for pile radiation⁶ were calculated from the constants used in the rate equation

$$-\frac{d(H_2O_2)}{dt} = \frac{k_5}{k_8} k_R I \frac{(H_2)}{(H_2O_2)} - k_F I$$

where $k_F I = 7.5$ and $k_5/k_8 k_R I = 9.42$.

Taking for the ratio k_5/k_8 the value 0.94 used in this work (next section) the calculation shows that 60% of the radicals enter reaction (F) and 40% reaction (R). The values for both gamma and pile radiation are compared in Table I.

TABLE I

YIELDS FOR REACTIONS F AND R FOR GAMMA AND PILE RADIATIONS

	This work	Cobalt gamma		Mixed gamma and fast neutrons (Oak Ridge Pile)		
		Hart				
G_F	0.46	25%	0.35	20%	1.18 ^a	60%
G_R	2.74	75%	2.78	80%	1.57	40%
G_{H_2O}	3.66		3.48		3.93	

^a Calculated from experimental results reported previously.⁶

Mechanism of the Radiation-induced Back Reaction between H_2 and H_2O_2 in Aqueous Solutions.—The radiation-induced back reaction between hydrogen and hydrogen peroxide in solution was studied as a function of H_2O_2 concentration, radiation intensity, temperature, pH and added solutes. Plots of typical curves are shown in Figs. 7, 9 and 10. In the majority of solutions studied, the hydrogen was present in considerable excess over the peroxide. In these solutions, little or no oxygen is formed and the kinetics are simple enough to be dealt with. Figure 7 shows results for these solutions. Analyses are for H_2O_2 only, since with no O_2 formation the hydrogen curve parallels that for H_2O_2 . A curve for H_2O_2 decomposition in solution saturated with pure helium is shown for comparison. The rate of H_2O_2 disappearance in H_2 -saturated solution increases with dose until the concentration becomes low after

(18) E. J. Hart, THIS JOURNAL, 56, 594 (1952).

(19) Calculation based on G for ferrous oxidation of 15.5 Fe^{++} oxidized per 100 ev.

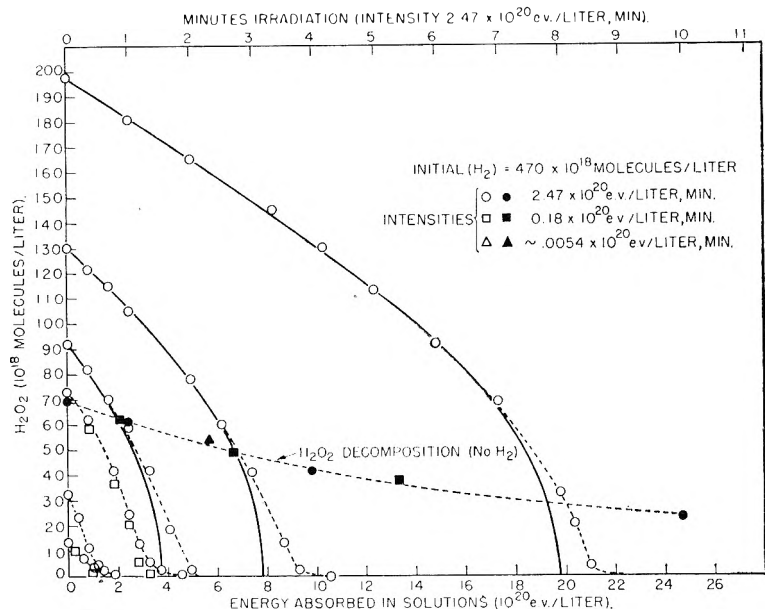


Fig. 7.—Gamma ray induced reaction between dissolved H_2O_2 and excess H_2 at 25° .

which the rate decreases and becomes zero at a very low steady state concentration ($< 0.1 \times 10^{18}$ molecules H_2O_2 liter $^{-1}$). These curves resemble those obtained for pile radiation⁵ where the rate law for peroxide disappearance

$$\frac{-d(\text{H}_2\text{O}_2)}{dE} = k_R \frac{k_3}{k_8} \frac{(\text{H}_2)}{(\text{H}_2\text{O}_2)} - k_F$$

derived by considering reactions F, R, 4, 5, 8 and 9 was found to hold at low H_2O_2 concentrations. This rate law was checked for data obtained with cobalt γ -rays using values presented earlier for k_F and k_R , namely, 0.46 and 2.74.

The ratio k_5/k_8 was obtained from the initial slope of the curves and was taken to be 0.94. This ratio was estimated by an independent method to be approximately one from the stoichiometry in mixing hydrogen saturated solutions of H_2O_2 and FeSO_4 .²⁰ Substituting these values, the rate law becomes

$$\frac{-d(\text{H}_2\text{O}_2)}{dE} = G_{-\text{H}_2\text{O}_2} = 0.94 \times 2.74 \frac{(\text{H}_2)}{(\text{H}_2\text{O}_2)} - 0.46$$

The integrated form of this equation gives the solid curves shown in Fig. 7. The initial rates of H_2O_2 disappearance as a function of initial H_2O_2 concentration in hydrogen saturated solution are shown in Fig. 8. The solid curve is that calculated from the simple rate law given above. The simple rate law is shown to hold in initially hydrogen saturated solution over a limited range of H_2O_2 concentration from $\sim 50 \times 10^{18}$ molecules liter $^{-1}$ to $\sim 250 \times 10^{18}$ molecules liter $^{-1}$. The maximum yield, observed at an initial H_2O_2 concentration $\sim 50 \times 10^{18}$ molecules liter $^{-1}$, corresponds to a chain length of about nine. At zero peroxide concentration this equation predicts an infinite rate corresponding to an infinite concentration of hydrogen atoms. In this low concentration range it becomes necessary to include reactions 1 and 3

(20) C. J. Huchanadel, unpublished work, Oak Ridge National Laboratory.

for removal of radicals, resulting in the complicated equation

$$[k_4(\text{H})]^3 + [k_4(\text{H})]^2 \left[\frac{(k_4 k_8 k_4^2)}{k_3 k_1} (\text{H}_2\text{O}_2) + \frac{k_4 k_8}{k_3} (\text{H}_2) \right] + [k_4(\text{H})] \left[\frac{k_4^3 k_8}{k_1 k_3} (\text{H}_2\text{O}_2)^2 - \frac{k_4^3 k_8 k_R (\text{H}_2)}{k_1 k_3} \right] = 0$$

where

$$k_4(\text{H}) = \left(\frac{-d(\text{H}_2\text{O}_2)}{dt} + k_F \right) / (\text{H}_2\text{O}_2)$$

Substituting values for $k_4(\text{H})$ obtained using measured slopes at the chosen H_2O_2 concentrations, one obtains an equation for which a set of constants can be found.

For solutions containing peroxide at an initial concentration comparable to the hydrogen concentration, the dose vs. concentration curves show a complicated behavior. The rate of disappearance first decreases with dose, then increases and finally becomes zero at a very low steady state concentration.

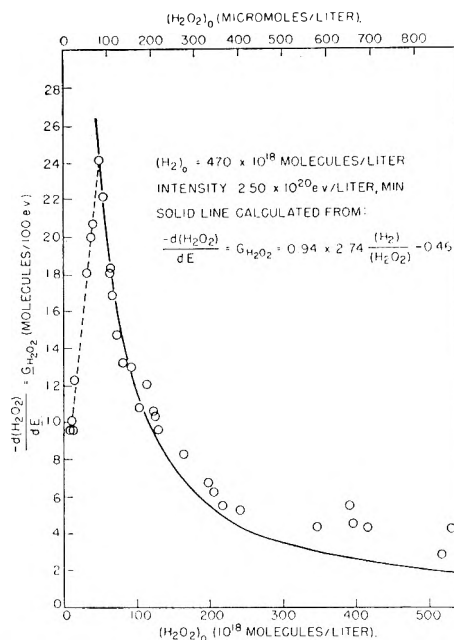


Fig. 8.—Initial yield for H_2O_2 disappearance versus H_2O_2 concentration in H_2 saturated solutions.

For initial H_2O_2 concentrations greater than the hydrogen concentration, the rate of H_2O_2 disappearance decreases continuously with dose as shown in Fig. 9. The curves resemble those for peroxide decomposition which is the predominantly occurring reaction. Oxygen is formed and along with H_2O_2 and H_2 reaches a steady state which becomes greater for higher initial peroxide concentration. The kinetics in these systems are very complicated.

The effects of various variables on the reaction in solutions containing H_2O_2 and excess H_2 are shown in Figs. 7 and 10. There was no intensity effect

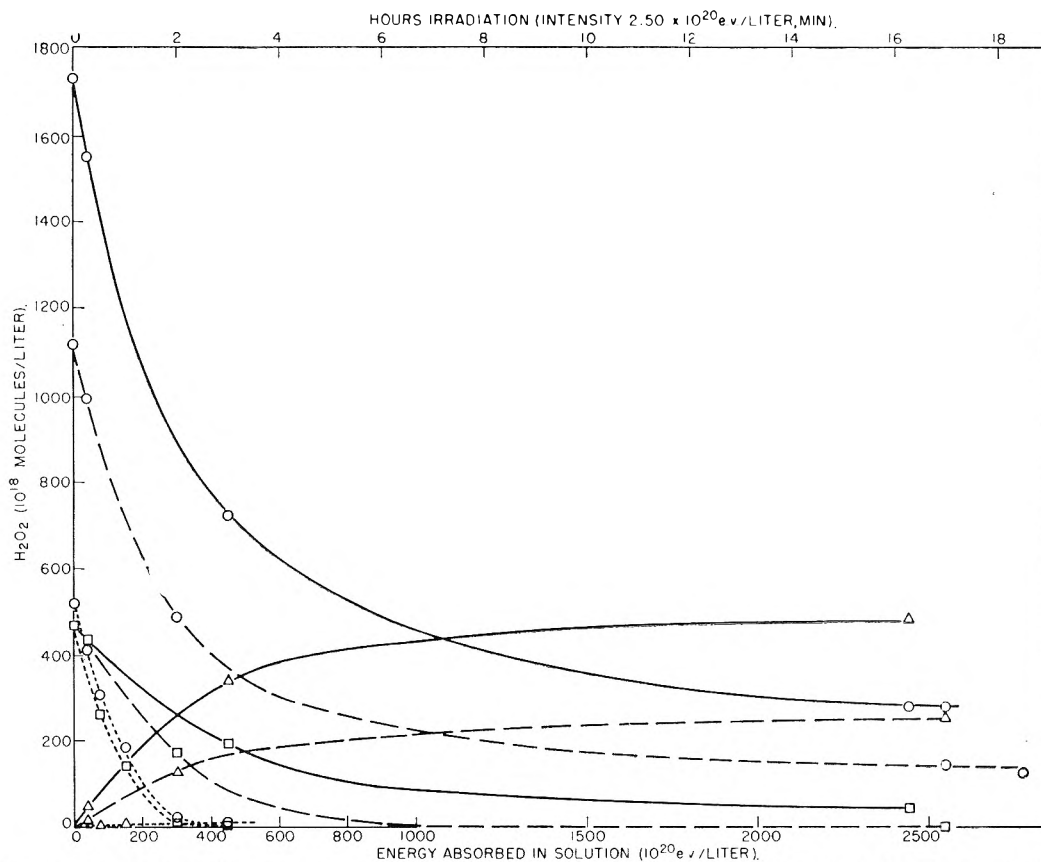


Fig. 9.—Effect of cobalt gamma rays on solutions containing H_2 and excess H_2O_2 : \circ , H_2O_2 ; \square , H_2 ; \triangle , O_2 .

over the range studied and also no pH effect from pH 2.5 to 7. Little effect was expected in either case. The forward reaction rate is expected to be independent of temperature but the reactions of stable molecules with radicals involved in the back reaction would be expected to have some activation energy. This would result in lower steady state concentrations with increased temperature. This was confirmed for pile radiation.⁴ The rate of back reaction was found to increase with temperature from 25 to 65° as shown in Fig. 10. From measured initial rates, values for k_5/k_8 were calculated assuming the simple rate law to hold. These values would indicate a difference in activation energies $E_5 - E_8 \sim 1.25$ kcal. mole⁻¹.

It was mentioned earlier that several H_2O_2 preparations gave the same H_2O_2 vs. dose curves. The effect of adding a commonly used stabilizer, acetanilide, is shown in Fig. 10. Little effect was found for low concentration of acetanilide corresponding to the concentration to be expected in a commercial stabilized preparation at the H_2O_2 dilutions used. At higher concentrations, the acetanilide definitely inhibits the back reaction, presumably through removal of OH radicals which

oxidized the organic material. This competition for radicals is the well-known protective

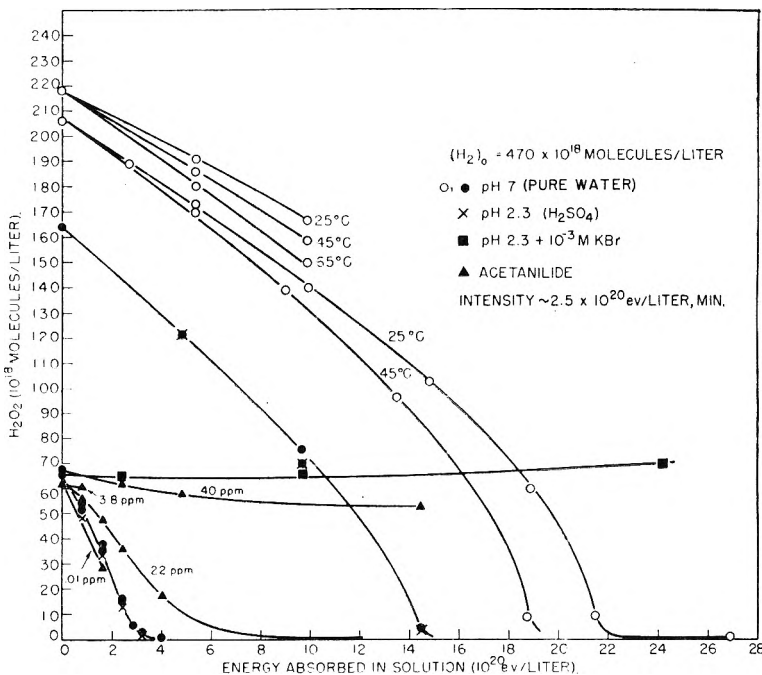


Fig. 10.—Effect of temperature, pH and added solutes on the gamma ray induced reaction of H_2O_2 with excess H_2 .

action.²¹

(21) D. E. Lea, "Actions of Radiations on Living Cells," The Macmillan Co., Inc., New York, N. Y., 1947.

The author wishes to thank J. A. Ghormley for many helpful discussions.

REMARKS

PROFESSOR BURTON (University of Notre Dame): It is interesting to note that we now have experimental information of an indirect sort on the ionization potential of water in the liquid state. The α -particle data indicate, if we assume about half the radicals to back-react to give water, that $G(\text{H}_2\text{O})$ primarily dissociated in ionization processes is ~ 6 .

If we further assume ions to be the sole source of radicals which can give products (this point has not been actually established, so far as I know), then the energy required per ion pair is ~ 17 ev. On the basis of the usual, reasonable approximation that approximately half the energy is consumed in excitation processes, it follows that the ionization potential in liquid water is ~ 8 ev. This figure agrees with one obtained by rough calculations involving the solvation energy of the H^+ ion. Dr. Hochanadel's data on G values in γ -irradiation of water lend additional support to the idea of such an ionization potential.

THE RADICAL PAIR YIELD OF IONIZING RADIATION IN AQUEOUS SOLUTIONS OF FORMIC ACID¹

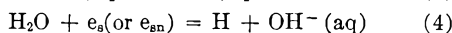
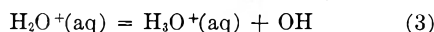
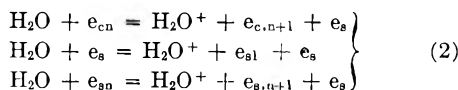
BY EDWIN J. HART

Chemistry Division, Argonne National Laboratory, Chicago, Illinois

Received February 25, 1952

The mechanism of formic acid oxidation by Co^{60} γ -rays and by β -rays from tritium disintegration has been studied in aqueous solution. In aqueous solutions subjected to ionizing radiation, hydrogen and hydroxyl radicals are produced. It is found that the formic acid-oxygen reaction may be employed to measure the relative amounts of those radicals that recombine to form hydrogen and hydrogen peroxide and of those capable of reacting with formic acid and oxygen. Twenty-one and thirty per cent. of these radicals undergo the above recombination in formic acid solutions irradiated by Co^{60} γ -rays and tritium β -rays, respectively. In aqueous solutions of formic acid subjected to β -ray irradiation from tritium 29.8 e.v. are expended per measurable radical pair.

The ionization processes which occur in water when a Compton recoil electron is formed by γ -ray interaction with water have been described by Lea,² Dainton,³ and Magee and Burton.⁴ The qualitative features of these reactions in aqueous solution are summarized by the equations



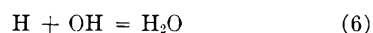
where e_c = Compton recoil electron, e_{cn} = Compton recoil electron after the n th ionization, e_s = secondary electron, and e_{sn} = secondary electron, after n th ionization.

The net reaction 5 is the formation of the hydrogen and hydroxyl radical pair. The individual radicals of the pair are separated by the distance the electron e_s travels from H_2O^+ before the capture process 4 takes place or before another ionization reaction 2 occurs.



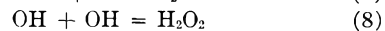
The distance between successive ionizations in the path of the primary recoil electron produced by Co^{60} γ -rays is great and of the order of 5000 Å.² On the other hand, the energy of the secondary electrons is low and substantially independent of the energy of the primary electron. Magee and Burton⁴ point out that only 8.2% of the secondary electrons resulting from the passage of a one mev. elec-

tron have energies exceeding 40.6 ev. Penetration of a 40.6 ev. electron in liquid water is estimated as 12 Å. from the data of Lea.⁵ This means that penetration of the solvent cage is assured but recombination becomes far more probable for radicals produced by secondary electrons than for radicals formed from the primary recoil electron. For secondary electrons of very low energy, the hydrogen atom and hydroxyl radical would be formed close together and radical recombination of type 6 becomes highly probable



The energy necessary for the escape of the secondary electron from the vicinity of the H_2O^+ so that the resulting free radical is not formed in the same solvent cage is unknown. However, some estimate of the energy required for the formation of a free radical pair will be made from results of the present work.

In the radiolysis of water solutions of formic acid it is possible to measure experimentally the free radicals capable of reacting with solute molecules and also those free radicals recombining in a pairwise manner such as



Radicals reacting to reform water as in reaction 6 cannot be measured by present experimental means. However, it is possible to measure the number of radicals produced in 5 that do not undergo reaction in 6, 7 and 8. The radicals so freed are available for reaction with solute molecules and are designated by 5'.



In light particle radiation work, the steady state concentration of hydrogen and hydrogen peroxide

(5) Lea, Table 10, p. 24, gives 30.1 Å. as the range of a 100 e.v. electron.

(1) Presented at the Symposium on Radiation Chemistry which was held at the April, 1951, Meeting of the American Chemical Society, Cleveland, Ohio.

(2) D. E. Lea, "Actions of Radiations on Living Cells," Cambridge University Press, London, 1946.

(3) F. S. Dainton, *THIS JOURNAL*, **52**, 490 (1948).

(4) J. L. Magee and M. Burton, *J. Am. Chem. Soc.*, **73**, 523 (1951).

is very low and incapable of precise measurement at low radiation intensities. This is due to a back reaction between hydrogen and hydrogen peroxide which is initiated by hydrogen and hydroxyl radicals that have escaped the primary recombination reactions 6, 7 and 8.⁶⁻⁸ Consequently it is difficult to carry out measurements on the extent of pairwise recombination in pure water. However, it is found that in the presence of an efficient free radical trap such as formic acid one may estimate the magnitude of reactions 7 and 8.

The number of free radicals formed is measured indirectly by determining the yield of the products in the radiolysis of dilute solutions of formic acid. For confidence in the result one must know the complete mechanism of the reaction so that the products associated with the reaction of the free radicals with formic acid can be identified. This is the standard kinetic approach to the measurement of transient species and the method in this case possesses the inherent disadvantage of giving only the number of radicals capable of reacting with formic acid. In general it is expected that the number of radicals counted is dependent on the reactivity of the solute molecules toward the free radicals. This is true since the competing radical recombination reactions $H + OH = H_2O$, $H + H = H_2$ and $OH + OH = H_2O_2$ are of considerable importance in the radiation chemistry of aqueous solutions.

Experimental

The methods employed for irradiation of solutions, purification of water, evacuation of samples, analyses for carbon dioxide, hydrogen, hydrogen peroxide and oxygen were identical with those previously described.⁹ Oxygen solutions of formic acid were prepared as follows. Air was removed from the aqueous solutions by evacuation through a carbon dioxide trap with a mechanical pump. Shaking and heating during evacuation assisted in the removal of air. Oxygen purified by liquefaction and partial evaporation was then introduced into the evacuation chamber by allowing the liquid oxygen to warm slowly to the desired pressure. By shaking for two minutes, the solution was equilibrated. For low concentrations of oxygen, the oxygen in the gas phase was removed by evacuation without too great a loss of the dissolved oxygen. The evacuation chamber was then inverted so that the solution could flow into the eight cells attached to the chamber by standard taper joints. Reintroducing oxygen over the solution helped in filling the cells. The small bubble of oxygen remaining in the cells was replaced by solution by a process of alternate pumping and reintroducing oxygen. The final concentration of oxygen in the cells was measured by means of a Van Slyke apparatus. A ground glass cap filled with the oxygen saturated solution was used to seal the 5/20 capillary joint at the end of the irradiation cell. At higher pressures (in the neighborhood of atmospheric), the evacuation and oxygen equilibration processes described above were repeated. The cells were partially filled with solution by introducing oxygen at slightly above atmospheric pressure to the solution. The thin-walled tips were then broken off and the solution forced into the cells. When the cell was filled, the thin capillary tube was resealed. In this manner the cells were filled one at a time. After filling, the ground glass caps containing the oxygenated solution were used to close the cells.

Two hundred and twenty-one curies of tritium water were prepared by reaction of tritium with oxygen at a palladium

surface. Tritium was passed through a palladium thimble heated electrically to about 600° with a platinum spiral. After passage through the thimble, the tritium came in contact with oxygen at 15 cm. pressure. Under these conditions reaction is rapid and the water formed is removed from the reaction zone by freezing at liquid nitrogen temperature. Two bulbs of tritium were treated in succession. The fraction of tritium passed through the thimble was 98.8% in one case and 99.7% in the other case. This was accomplished by the addition of normal hydrogen to the tritium bulb after the tritium pressure had been reduced to 3 to 4 mm. This blend was then treated as described above. The data appear below.

Sample bulb	15Z	17Z
Decay (N/N_0) ^a	0.9848	0.9863
Cc. T ₂ (NTP)	45.44	41.92
Fraction passed through Pd	0.988	0.997
Cc. T ₂ converted to water ^b	44.89	41.80

^a Calculation on basis of 12.46-year half-life. ^b T₂ + H₂ equivalent to 0.10 cc. of liquid water was formed.

After completion of the reaction, the water was transferred to a dilution bulb and exactly 20.00 ml. of triple distilled water added. This gives a concentration of 11.0 curies/ml. of water. (A factor of 2.56 curies/cc. T₂(NTP) calculated from the 12.46-year half-life for tritium was used for determining the activity of the water.) An assay of this water by K. Wilzbach using an ionization chamber previously calibrated with tritium gave an average value of 11.14 curies/g. water. In this latter method water is converted to hydrogen by passage over metallic zinc. The activity of the resulting hydrogen is measured in an ionization chamber filled to atmospheric pressure with hydrogen. At 225 volts 2.1×10^{-17} coulomb is collected per disintegration. This factor is used for obtaining the curie strength of the sample.

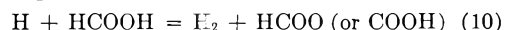
Reactions of Hydrogen and Hydroxyl Free Radicals with Formic Acid

Previous work⁹ has shown that hydroxyl radicals react with formic acid liberating carbon dioxide and water. From the mechanism deduced for the γ -ray induced reaction in dilute aqueous solution, hydrogen atoms are assumed to react directly with formic acid liberating hydrogen gas. The results of this work will be briefly reviewed and new work supporting this hydrogen atom reaction with formic acid presented. Further, the details of the method employed for measuring separately the amounts of reactions 5', 7 and 8 will be given.

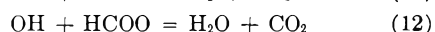
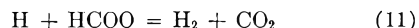
Oxygen-free Formic Acid.—Equimolar amounts of hydrogen and carbon dioxide are produced by irradiation of oxygen-free formic acid solutions at concentrations in the range from 0.01 to 0.0001 M.¹⁰ Hydrogen and hydroxyl radicals are known to react with formic acid or radicals derived from formic acid but the detailed mechanism is not settled. From the hydrogen peroxide-formic acid reaction to be described below, reaction 9 is known to occur



It is also postulated that



However, in the presence of the HCOO (or COOH) radical the following further reactions would be expected



(10) H. Fricke and E. J. Hart, *J. Chem. Phys.*, **6**, 229 (1938).

(6) A. O. Allen, *THIS JOURNAL*, **52**, 479 (1948).

(7) A. O. Allen, C. J. Hochanadel, J. A. Ghormley and T. W. Davis, presented at 119th American Chemical Society Meeting, Cleveland, Ohio, 1951.

(8) C. J. Hochanadel, presented at 119th American Chemical Society Meeting, Cleveland, Ohio, 1951.

(9) E. J. Hart, *J. Am. Chem. Soc.*, **73**, 68 (1951).

The main point here is that hydrogen gas is produced through reaction of hydrogen atoms with formic acid and not through recombination reaction 7. While the detailed mode of reactions of these radicals is important from the point of view of the mechanism, it has no direct bearing on the measurement of radical pair yields.

Hydrogen gas formed according to 7 would be produced from hydrogen atoms originating entirely in the water. While it is recognized that this reaction is very important when two hydrogen atoms are formed at close proximity, this is not the major source of hydrogen in the γ -ray induced oxidation of formic acid in dilute aqueous solution. This is demonstrated by the irradiation of deuterio-formic acid (DCOOH). In air-free solutions, 65% of hydrogen gas in the product is hydrogen deuteride and 35% is normal hydrogen. This experiment definitely demonstrates that part of the hydrogen originates in the formic acid. In line with the stoichiometry of 10 and 12 or of 9 and 11, it is assumed that half of the hydrogen atoms in the hydrogen gas liberated come from the water and the remaining half from the formic acid.

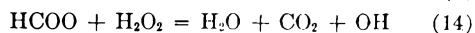
As an alternative to reactions 11 and 12 which consume hydrogen and hydroxyl radicals, reaction 13 would also account for the products formed if one assumed that the HCOO radicals are formed by reactions 9 and 10.



Further investigation is necessary in order to clear up these points.

While the formic acid reaction is able to measure the number of reacting hydrogen and hydroxyl radicals, the process is interfered with by the fact that hydrogen, a product of the hydrogen atom recombination reaction 7, is also a product of the formic acid reaction 10. Thus it is not possible by this means to distinguish what fraction of the radicals from 5' go into 7.

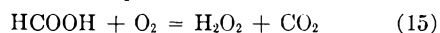
Formic Acid-Hydrogen Peroxide System.—The addition of hydrogen peroxide in small amounts to dilute aqueous solutions of oxygen-free formic acid results, on γ -ray irradiation, in a chain decomposition of both hydrogen peroxide and formic acid.⁹ Oxygen gas, the normal decomposition product of hydrogen peroxide radiolysis, is not formed. Carbon dioxide is the sole gaseous product of this chain reaction which has up to 55 links in 0.01 *M* formic acid. One molecule of carbon dioxide is produced per molecule of hydrogen peroxide consumed. The propagation steps consistent with this stoichiometry are



Hydroxyl and formate radicals alternate in these two steps and reaction 14 accounts for the absence of hydrogen peroxide in oxygen-free formic acid reactions. Hydrogen peroxide is expected from the hydroxyl radical recombination reaction 8 although the importance of this reaction in formic acid decomposition by γ -rays has heretofore not been estimated. Equal amounts of hydrogen and hydrogen peroxide are formed in reactions 7 and 8 and, since one molecule of carbon dioxide is produced per mol-

ecule of hydrogen peroxide by reaction 14, equimolar amounts of hydrogen and carbon dioxide always appear in oxygen-free formic acid radiolysis. Thus, since hydrogen peroxide disappears and hydrogen is formed, it is not possible to employ either the formic acid or the formic acid-hydrogen peroxide reactions in measuring the radical pair yields of reactions 5', 7 and 8.

Formic Acid-Oxygen Reaction.—Previously it was reported that oxygen served as a powerful inhibitor in the γ -ray induced chain decomposition of formic acid-hydrogen peroxide solutions.⁹ In studying the effect of oxygen concentration on this system it became apparent that this reaction could be used to measure separately the rates of reactions 5' and 7 (or 8). Under the influence of γ -rays, oxygen is converted quantitatively to hydrogen peroxide in solutions containing 0.01 *M* formic acid. In addition an equimolar amount of carbon dioxide is formed. The net equation is

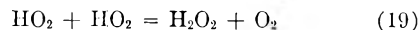
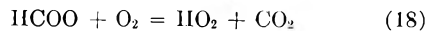
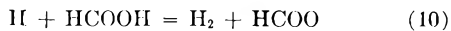
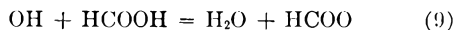
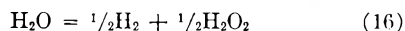
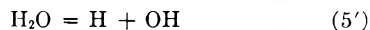


Owing to the inhibitory action of oxygen when present in excess, the hydrogen peroxide formed is not decomposed as is the case in the oxygen-free reaction. On the other hand, hydrogen production in the presence of oxygen is only a small fraction of that formed in formic acid solutions containing no oxygen. The results obtained using 0.01 *M* formic acid, 1 *mM* sulfuric acid, and 1.24 *mM* oxygen appear in Fig. 1. Under these conditions it is found experimentally that

$$\frac{d\text{H}_2\text{O}_2}{dt} = -\frac{d\text{O}_2}{dt} + \frac{d\text{H}_2}{dt} = \frac{d\text{CO}_2}{dt} + \frac{d\text{H}_2}{dt}$$

At these concentrations of reactants the condition is approximated that the hydrogen production is a measure of reaction 7 and oxygen consumption a measure of reaction 5'. Hydrogen peroxide formation is the sum of the recombination reaction 8 and the oxygen reaction 15.

In order to determine the degree of completeness of the oxygen inhibition reaction, the effect of oxygen concentration on hydrogen production was measured. Results appear in Fig. 2. Hydrogen production increases with lower oxygen in the manner expected from the equations



In the above mechanism, 5' gives the rate of formation of free radicals capable of reacting with formic acid and 16 is the net recombination reaction resulting from 7 and 8. Radicals recombining immediately to form hydrogen and hydrogen peroxide do not react with formic acid or oxygen. Therefore, from the point of view of the kinetics of the formic acid, reaction 16 may be treated as a primary one. Since many X-ray and γ -ray reactions in dilute aqueous solutions show an independence of yield on concentration of reactants over a wide range, a

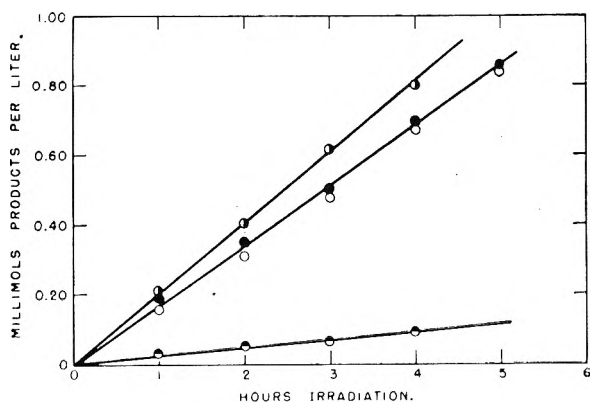


Fig. 1.—Oxidation of 0.01 *M* formic acid plus 1.24 *mM* oxygen by γ -rays at 50,000 r. per hour: \circ , CO_2 ; \bullet , H_2 ; \bullet , H_2O_2 .

constant fraction of the total radicals produced recombine to form hydrogen and hydrogen peroxide as illustrated by 16.

Hydrogen is produced through reactions 10 and 17. Under conditions where reaction 10 is entirely suppressed, hydrogen formation is a direct measure of reaction 16. Oxygen and formic acid compete with each other for the hydrogen atoms formed in reaction 5'. At 1.24 *mM* oxygen concentration, reaction 10 is suppressed and reaction 16 provides over 95% of the hydrogen. This was shown by measuring hydrogen deuteride formation in the deuterio-formic acid (DCOOH)–oxygen reaction. It is found that less than 5% of the hydrogen produced is hydrogen deuteride. In contrast, as reported above, the oxygen-free deuterio-formic acid radiolysis yields 65% hydrogen deuteride. Therefore, in the oxygen-formic acid reaction, 10 is small compared to 17. At infinite oxygen concentration, reaction 10 can be considered negligible and hydrogen production is due entirely to reaction 16.

Equations (20) to (23) are derived from the above mechanism by assuming that a steady state of intermediate free radicals is readily established.

$$\left(\frac{d\text{H}_2}{dt}\right)_0 = \frac{1}{2}k_{16} + \frac{k_5'}{1 + (k_{17}(\text{O}_2)_0/k_{10}(\text{HCOOH})_0)} \quad (20)$$

$$\frac{d\text{H}_2\text{O}_2}{dt} = \frac{k_{16}}{2} + k_5' \quad (21)$$

$$-d\text{O}_2/dt = k_6' \quad (22)$$

$$\frac{d\text{CO}_2}{dt} = k_6' \left(1 + \frac{1}{1 + (k_{17}(\text{O}_2)/k_{10}(\text{HCOOH}))}\right) \quad (23)$$

At high oxygen concentrations, the above equations reduce to

$$\frac{d\text{H}_2}{dt} - \frac{d\text{O}_2}{dt} = \frac{k_{16}}{2} + k_5' = \frac{d\text{H}_2\text{O}_2}{dt}$$

and

$$d\text{CO}_2/dt = k_5' = -d\text{O}_2/dt$$

which are identical with the stoichiometry experimentally established. Under conditions of high oxygen concentration, Equation 18 is believed to be the main source of carbon dioxide in this reaction, although it cannot be operative in the air-free formic acid radiolysis. Independent kinetic evidence for this reaction is also provided in the ferrous sulfate-formic acid–oxygen reaction.

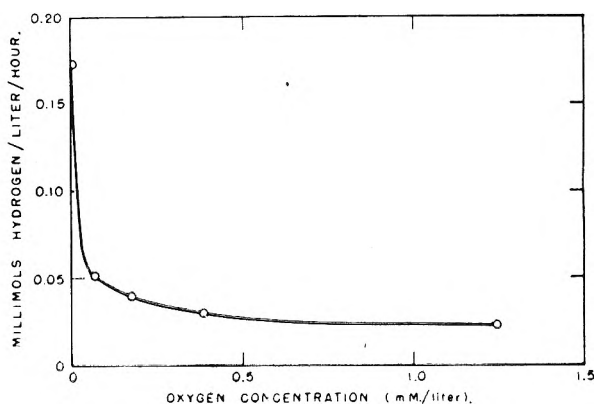


Fig. 2.—Effect of initial oxygen concentration on the γ -ray oxidation of 0.01 *M* formic acid.

A plot of the initial rates of hydrogen formation versus $1/(\text{O}_2)_0$ gives a suitably linear curve in the range of high initial oxygen concentrations (0.17–1.24 *mM*). An extrapolation to infinite $(\text{O}_2)_0$ concentration yields $\frac{1}{2}k_{16}$, the rate of the pairwise radical recombination reactions represented by Equation 16. At zero oxygen concentration the rate of hydrogen production equals $\frac{1}{2}k_{16} + k_5'$. k_5' , the rate of formation of hydrogen and hydroxyl radicals reacting with formic acid, may then be obtained. After evaluation of the remaining constant $k_{17}/k_{10}(\text{HCOOH})_0$ the equation for the initial rate of hydrogen production becomes

$$\left(\frac{d\text{H}_2}{dt}\right)_0 = 0.020 + \frac{0.153}{1 + 38.7(\text{O}_2)_0} \quad (24)$$

(Concentrations of formic acid, oxygen and hydrogen are in millimoles per liter and time is in equivalent hours at 3 cm. from an 80 curie Co^{60} source.)

Table I shows a comparison of experimental values for hydrogen production and values calculated from Equation 19.

TABLE I
EFFECT OF INITIAL OXYGEN CONCENTRATION ON HYDROGEN PRODUCTION IN THE γ -RAY OXIDATION OF 0.01 *M* FORMIC ACID^a

Initial O_2 concn., <i>mM</i> /liter	<i>mM</i> H_2 produced/liter/hr.	
	Exptl.	Calcd. from 24
1.24	0.0236	0.0231
0.384	.030	.0296
.172	.040	.040
.0635	.052	.064
.000	.173	.173
∞020

^a γ -Ray dose-rate is 35.3×10^{20} ev./l./hr. on the basis of 15.5 $\text{Fe}^{++}/100$ ev.⁸

By taking k_5' as 0.153 *mM* water dissociations per liter per hour and k_{16} as 0.040 *mM* water dissociations per liter per hour, it is found that 21% of the primary water dissociations result in recombination reaction 16. The remaining 79% are formed in water dissociation reaction 5' and are free to react with oxygen and formic acid, the solute molecules. Hochanadel's values⁸ of 25 and 75% for the recombination and dissociation reactions, respectively, are in agreement with the values obtained from the formic acid–oxygen reaction.

In view of the high energy (about 500,000 ev.)

of the recoil electron from a Co^{60} γ -ray, it is apparent that radical recombination occurs not only at the end of the primary electron track but far more prominently along the tracks of the low energy secondary electrons produced in reactions 1 and 2. Furthermore, from Table IV of Magee and Burton,⁴ one would expect that the energy of the primary electron would not be particularly important in altering the relative proportions of the radicals formed in reactions 5' and 16. This is found to be the case as is shown by formic acid oxidation induced by β -rays from tritium disintegration. The proportion of radicals undergoing the recombination reaction is increased only from 21 to 30% as the energy of the electron is reduced from 500,000 to 5690 ev.

Free Radical Pair Yield in Aqueous Solutions of Tritium Water.—In view of the present state of the dosimetry problem for aqueous solutions, it is not possible to calculate a reliable value for the energy expended in aqueous solutions irradiated by γ -rays. In order to circumvent this difficulty and also to measure relative proportions of 5' and 16 in the dissociation of water by low energy electrons, an irradiation was carried out using the 5690 ev. electron from tritium disintegration as the source of ionizing radiation. Tritium in the form of tritium water was used in these experiments at a level of 157 curies per liter.

Figure 3 shows a plot of the products formed as a function of time for 0.01 *M* formic acid containing 1.24 *mM* oxygen. At an activity of 157 curies per liter the oxidation of formic acid is rapid enough so that the thermal decomposition of hydrogen peroxide is not very pronounced. Consequently, Fig. 3 resembles Fig. 1 except that the relative proportion of hydrogen formed is greater for the tritium experiment.

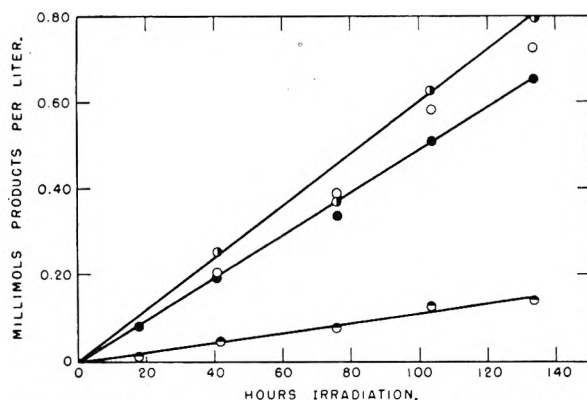


Fig. 3.—Oxidation of 0.01 *M* formic acid plus 1.24 *mM* oxygen by tritium disintegration at 157 curies per liter: ○, CO₂; ◐, H₂; ●, O₂; ◑, H₂O₂.

From the data of Fig. 3, the constants $k_{5'}$ and k_{16} may be calculated from Equation 18, since $k_{17}/[k_{16}(\text{HCOOH})_0]$ equals 38.7 mM^{-1} for these formic acid solutions. $k_{5'}$, obtained from the rate of oxygen consumption equals 4.64×10^{-3} $\text{mM}/\text{l.}/\text{hr.}$ Since the rate of hydrogen formation is 1.10×10^{-3} $\text{mM}/\text{l.}/\text{hr.}$, k_{16} is found to be 2.01×10^{-3} $\text{mM}/\text{l.}/\text{hr.}$ from Equation 18. The total rate of radical production ($k_{5'} + k_{16}$) equals 6.65×10^{-3} $\text{mM}/\text{l.}/\text{hr.}$ Therefore, 30% of the radical

pairs formed recombine in Equation 16 and 70% react with formic acid and oxygen. Thus, on reducing the energy of the electron from 500,000 to 5690 ev., the per cent. of radicals recombining without possibility of reacting with formic acid and oxygen is increased from 21 to 30% of the total formed.

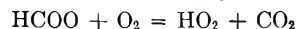
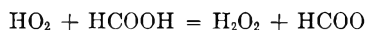
Tritium undergoes β -decay to form He^3 with a 12.46-year half-life and a mean energy of 5.69 ± 0.04 kev. At an activity level of 157 curies per liter the energy absorption amounts to 1.19×10^{20} ev./l./hr. Since 6.65×10^{-6} mole radical pairs/l./hr. are produced, an average energy of 29.8 ev./measurable radical pair are expended in aqueous solutions of formic acid. Using Hochanadel's value of 15.5 $\text{Fe}^{+++}/100$ ev. of Co^{60} γ -radiation, one calculates that 30.5 ev. are required per radical pair for γ -rays. By assuming that 13 ev. are required for ionization of water to H_2O^+ , an additional 17 ev. energy in the secondary electron is necessary on the average for the formation of a radical pair in aqueous formic acid solutions.

Acknowledgment.—The author acknowledges his indebtedness to S. Gordon for the preparation of deuterio-formic acid and mass spectrometer analysis of hydrogen products and to S. Gordon and M. Matheson for helpful discussions on this work.

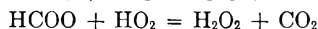
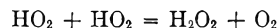
REMARKS

Dr. EVERETT R. JOHNSON (Brookhaven National Laboratory): During the decomposition of formic acid in the presence of oxygen why do you postulate that the HO_2 radical does not react with formic acid? Since this radical is given importance in other reactions it does not seem reasonable to neglect its oxidizing action in this system.

REPLY: Perhaps the HO_2 molecule does react with formic acid under certain conditions. However, in view of the non-chain character of the oxygen-inhibited formic acid reaction, the reaction of HO_2 with formic acid does not appear to play an important role in this mechanism. The following chain can be set up with HO_2 and formic acid



Since no chain is observed it appears reasonable that HO_2 reacts with more reactive species such as



Either of these two chain-breaking reactions accounts for the stoichiometry observed.

Dr. A. O. ALLEN (Brookhaven National Laboratory): Attempts to measure total yield of free H and OH (Hart's reaction (1), Hochanadel's reaction (R)) are likely to yield only lower limits, because whatever is done by one of these radicals may be reversed by the other. Thus, $\text{H} + \text{O}_2 = \text{HO}_2$ may frequently be followed by $\text{OH} + \text{HO}_2 = \text{H}_2\text{O} + \text{O}_2$, and the total number of H set free may be greater than the net O_2 consumption. It seems difficult or impossible to assess the contribution of such reversals. Actually, by analogy with other materials, we would expect much less energy than 27 or 30 ev. required per radical pair set free (since the number of radicals lost by initial recombination is relatively small).

REPLY: I agree that the energy required for formation of a radical pair represents an upper limit but not for the reason pointed out by Dr. Allen. The net dissociation reaction (5') gives the number of radicals not undergoing recombination reactions (6), (7), and (8). Formic acid reacts very efficiently with these H and OH radicals, otherwise the yield would not be independent of formic acid concentration over such a wide range. The concentration of OH radicals is reduced to a very low level by the large

excess of formic acid molecules. Therefore it appears that the reaction $\text{OH} + \text{HO}_2 = \text{H}_2\text{O} + \text{O}_2$ does not contribute significantly to a reduction in yield at least under the experimental conditions employed in this work. The number of

radicals lost in the recombination reaction $\text{H} + \text{OH} = \text{H}_2\text{O}$ is the principal unknown factor. For this reason the value of 30 ev./radical pair represents an upper limit to the energy required in the formic acid reaction.

RECOIL ATOMS FROM SLOW NEUTRON CAPTURE BY GOLD AND INDIUM SURFACES

BY SAMUEL YOSIM AND T. H. DAVIES

Argonne National Laboratory and the Institute for Nuclear Studies, University of Chicago, Chicago, Illinois

Received February 25, 1952

Au and In recoil atoms arising from slow neutron capture in Au and In films were caught on an opposed collector. The yields of radioactive recoils were determined with and without electric fields. The yields indicate recoil path lengths in the solid of no more than several lattice layers. Recoil atoms carrying a positive charge were observed with both Au and In and are attributed to internal conversion of the compound nucleus during transition to the ground state. The persistence of these charges in recoils emitted from a metal suggest that internal conversion is a late step in stabilization of the compound nucleus.

Introduction

Much of the disorder observed in solids after high energy particle bombardment is due to dislocated atoms which have recoiled from collisions with primary or secondary projectiles. From the discussion of Seitz¹ and others, we learn that most of these dislocated atoms left their original lattice positions with only a few hundred electron volts of "knocked on" atoms—their path lengths in the solid for instance—are of interest then in considering the over-all changes of irradiated solids.

We have, fortunately, a ready source of such projectiles with kinetic energies of the order of a hundred electron volts. These are the recoil atoms produced by any of several nuclear processes—for example, by β -decay, K-electron capture, and radiative neutron capture. Further, such recoiling species are frequently radioactive and this may permit the recoil atom to be traced without the need for substantial alterations in the macroscopic properties of the solid.

Very little is known by direct experiment concerning 100 electron volt recoil atoms. It is agreed that such particles will neither ionize themselves nor collision partners. A minor exception to this rule is that some recoil atoms may be initially ionized by the nuclear process itself. In illustration, the recoils from β -decay will usually begin as positive ions.

A second certainty is that the recoil path lengths will be extremely short and will be very dependent upon the chance direction of the recoil with respect to the positions of collision partners in the solid lattice. The evidence for very short paths comes through a variety of experiments with recoils from nuclear reactions—experiments usually performed with other aims. For example, in the hunt for neutrino recoil effects, Smith and Allen² and Sherwin³ have encountered sufficient difficulties with the surfaces of their solid sources to demonstrate that the penetration of 10–50 ev. recoil atoms is not more than a lattice layer or two. Frauenfelder⁴ studied recoil Ag¹⁰⁷ resulting from K

capture by Cd¹⁰⁷ on a silver surface. He found a yield of recoil atoms which declined as the silver surface aged. The declining yield was attributed to progressive diffusion of Cd¹⁰⁷ atoms into the silver and the inability of any but surface layer recoils to reach the collector. Magnusson⁵ has observed that when a gold plated surface is irradiated with slow neutrons, the recoil Au¹⁹⁸ atoms collected amount to only 3% of the recoils produced in an ideal gold layer.

The n, γ -reaction would seem at first glance to be an attractive experimental opportunity to study recoil atoms of about 100 ev. kinetic energy. The recoil energy from the reaction is given by the expression

$$E_R = \frac{5.36 \times 10^{-10} E^2 \gamma}{M}$$

where the kinetic energies are in ev. and M is the mass of the recoil atom in atomic mass units. Unfortunately for simplicity, the excitation of the compound nucleus is generally discharged in several γ -rays. Muehlhause⁶ has determined the average number of γ -rays above 50 kev. in energy emitted per neutron capture for some 25 different nuclei. His results show from 1.7 to 5.6 γ -rays per capture. The number tends to increase with mass number and there are certain correlations with odd-even characteristics which we need not discuss. The γ -ray energy spectrum has been studied by Kinsey and co-workers,⁷ by Hamermesh⁸ and by others. Kinsey has found several very simple spectra—for example, neutron capture of Pb²⁰⁷ yields a single energetic γ -ray, while the light nucleus N¹⁴ gives a spectrum which has been resolved into nine different transitions from seven different energy levels. Hamermesh has measured proton recoil tracks from the $\text{D}(\gamma, n)\text{H}$ reaction in deuterated photographic plates where the γ -rays were those following slow neutron capture by some 15 different nuclei. The resolution of the γ -ray energies is much less than with the coincidence pair spectrometer used by Kinsey and co-workers, but softer γ -rays can be seen,

(1) F. Seitz, *Discussions Faraday Soc.*, **5**, 274 (1949).

(2) P. B. Smith and J. S. Allen, *Phys. Rev.*, **81**, 381 (1951).

(3) C. W. Sherwin, *ibid.*, **75**, 1799 (1949).

(4) H. Frauenfelder, *Helv. Phys. Acta*, **23**, 373 (1950).

(5) L. B. Magnusson, *Phys. Rev.*, **81**, 285 (1951).

(6) C. O. Muehlhause, *ibid.*, **79**, 277 (1950).

(7) B. B. Kinsey, G. A. Bartholomew and W. H. Walker, *ibid.*, **77**, 723 (1950); **78**, 77 (1950); *Can. J. Phys.*, **29**, 1 (1951).

(8) B. Hamermesh, *Phys. Rev.*, **80**, 415 (1950); **81**, 487 (1951).

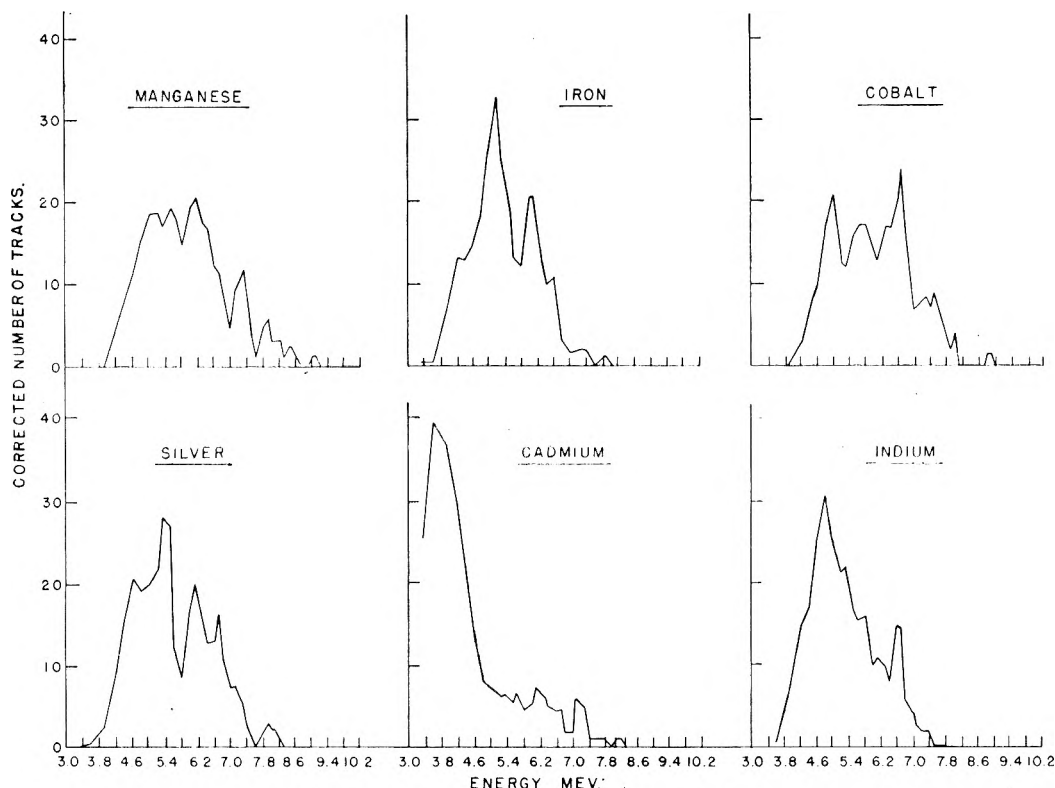


Fig. 1.—Neutron capture gamma ray spectra.

and an informative qualitative picture of the spectrum can be obtained.

Four of Hamermesh's⁸ results (Fig. 1) will illustrate the several types of spectra observed. The precision near the experimental cutoff of 3 mev. is poor, and the decline in the number of tracks in the case of Cd is not necessarily real. Reference to the spectra of Al, Cl and Fe reported by Hamermesh indicates no diminution of complexity with nuclear mass.

From the spectra and the data on multiplicity taken together, additional information on the γ -ray spectra may be obtained in favorable cases. Consider, for example, Hamermesh's γ -ray spectrum for In¹¹⁶ given in Fig. 1. The observed maximum energy of a 7.4 mev. is in sufficient accord with the value of 6.59 for the neutron binding energy obtained from the d,p-reaction threshold of In¹¹⁵.⁹ However, the intensity peak is at 4.8 mev. and the intensity is apparently zero below 4.0 mev. Given a γ -ray multiplicity of 3.3 (reported by Muehlhause⁶) for capture by In¹¹⁵, each γ -ray more energetic than 4.0 mev. must be accompanied in the same de-excitation process by 2.3 ($= 3.3 - 1$) γ -rays on the average and these must share 4.4 ($= 7.4 - 4.0$) mev. or less. Thus, the relative number of γ -rays emitted must rise again to a high peak at energies below the 3.0 mev. cutoff.

At least one further complication in the neutron capture process must be faced. Amaldi and Rasetti¹⁰ observed internal conversion in neutron capture by Gd. Goldhaber, Muehlhause and co-workers¹¹ have reported soft electrons emitted in neu-

tron capture by Cd, Gd, Sm, Eu, Dy and Hg. Hibdon and Muehlhause¹² have measured the energies of these radiations in the case of Gd and Sm¹⁴⁹ and found line spectra corresponding to internal conversion of 80 to 341 kev. γ -rays in the K, L and M shells of the target species. Wexler and Davies¹³ have found positively charged bromine recoil species from neutron capture by gaseous ethyl bromide at very low pressures. The observed charges are attributed to conversion of capture γ -rays of Br.

Turning from the γ -ray spectrum to the accompanying recoils, we shall expect a complementary complexity in the recoil spectrum. In illustration, the recoil energy of an unbonded atom of mass 100 from a single γ -ray of 10 mev. will be 536 ev., from a 1 mev. γ -ray, 5.36 ev. In addition, if we are concerned with the disruption of molecules by the recoil, we shall have to consider the time lapses between successive γ -rays of the cascade and the mutual orientation of these γ -rays. The usual estimate for this delay is 10^{-13} to 10^{-14} seconds. This figure makes it controversial whether the second of two successive opposed γ -rays will cancel the recoil of the first before the radiating atom shall have moved beyond bonding distance of a partner atom. Finally, the possibility that the recoiling species is a positive ion, particularly a highly charged ion as should result from internal conversion of inner orbital electrons, must be considered, since this may be a factor in determining the distances travelled in solids.

others at Argonne National Laboratory. O. Sala, P. Axel and M. Goldhaber, *Phys. Rev.*, **74**, 1249 (1948).

(12) Abstract, Washington Meeting, Am. Phys. Soc., April, 1951.

(13) S. Wexler and T. H. Davies, Brookhaven National Laboratory, Report C-7-AECU-50 (1948).

(9) J. A. Harvey, *Phys. Rev.*, **81**, 353 (1951).

(10) E. Amaldi and F. Rasetti, *Ricerca Sci.*, **10**, 115 (1939).

(11) Unpublished experiments by Muehlhause, Goldhaber and

While the lack of complete and precise information concerning the nuclear capture reaction and its general complexity make a detailed interpretation of the complementary recoil effects unlikely, some significant information should eventually emerge from experiments of the type which we shall now report.

Experiments and Results

We have studied indium and gold recoils from slow neutron capture. The sources were indium and gold metal films prepared by evaporating these metals upon glass or copper tubes, and gold foil prepared for test by careful cleaning. Figure 2 shows the evaporation chamber and the irradiation chamber used in our experiments. After evaporating metal onto the central tube of glass or copper during a half-hour period at a pressure of less than 5×10^{-5} mm., the cylinder carrying the metal film was lowered by means of the windlass to the bombardment chamber where the source is centered by an internal guide. Surrounding the source film at two different levels are two cylindrical copper collecting foils. One copper foil is made 1500 volts positive or negative to the central rod; the second foil is electrically connected to the central rod. The chamber is now sealed off and bombarded in the Argonne graphite pile for 20 minutes at a flux of 4×10^{10} neutrons per cm.² per second. A standard sample of In or Au solution, strapped to the chamber, is irradiated at the same time. The standard and the center section of each collecting cylinder are now analyzed for 54 min. In¹¹⁶ or 2.7d Au¹⁹⁸ to obtain the yield of recoil atoms. The metal source films are also analyzed to determine the average thickness. Finally, as a test for contamination, an unanalyzed aliquot strip of the collector is irradiated again after a proper decay period and analyzed for the appropriate activity. The second irradiation is made after the radioactivity from the first bombardment has decayed to stable Sn or Hg. Thus, the new yield of activity will be due to contamination of the collector with stable In or Au before or during the first bombardment.

The results of these measurements appear in Tables I, II, III and IV. The variation in the corrected counting rates of the In and Au standards reflects the variation in pile

from the number of neutron captures per $\mu\text{g.}$ disclosed in the standard sample. Evaporated Au films gave no higher yields than Au foil.

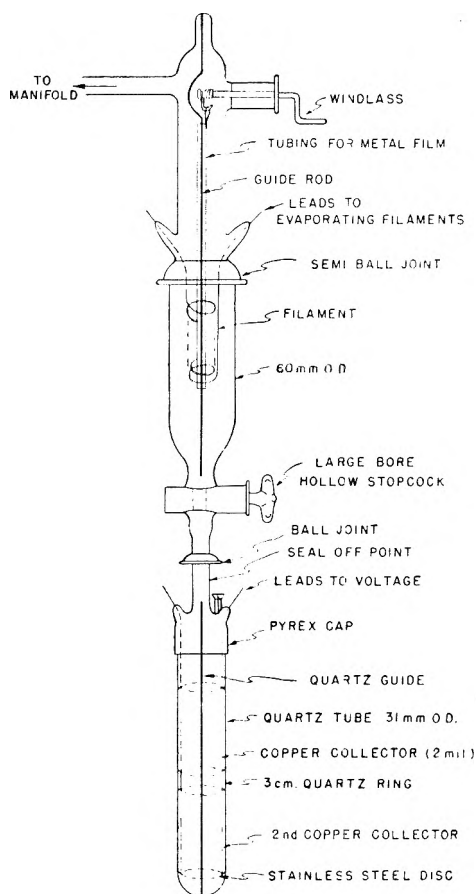


Fig. 2.—Evaporation (upper) and irradiation (lower) chamber.

TABLE I
INDIUM RECOIL YIELDS FROM INDIUM FILMS

Expt.	Backing	In ¹¹⁶ on collector, cts./min. ^a	In standard, cts./min./ $\mu\text{g.}$	$2 \times Y$ (%) ^b
25	Glass	147	2000	68
26	Glass	199	1910	95
28	Glass	158	1850	78
32	Glass	143	1890	70
34	Glass	107	1870	53
27	Cu	86	1900	42
30	Cu	130	1860	64
31	Cu	203	1870	100
36	Cu	115	1820	58
37	Cu	72	2050	32
38	Cu	74	2040	33
41	Cu	152	1850	75

^a The counting rate is corrected for yield of the radiochemical analysis, for contamination of the collector with stable indium, and to 4 half-lives after end of bombardment. The counting rate reported applies to 1 sq. cm. of the source surface and was made at about 10% geometry. ^b $Y =$ number of recoils collected divided by number of recoils created in top layer of source. 0.22 μg of In¹¹⁵/sq. cm. for the top layer was assumed.

neutron flux from run to run as well as errors in the over-all radiochemical analysis. Within the large scatter of results from one metal film to the next, no effect of backing on recoil yield is apparent. In only one of the experiments with Au and In (Table I, In #31) is the number of recoils collected equal to those which originate in an ideal first layer of the film and which are directed toward the collector. The estimate of the number of recoils originating in an ideal first layer was made from the bulk density of the pure metal and

The data of Tables II and IV show the presence of positive ions among both In and Au recoils. The fraction of positive ions is calculated in the following manner. The number of recoils emitted toward each of the two collectors is assumed to be the same in the absence of a field. When a repelling potential is imposed, however, it is assumed that all positive recoils directed toward the charged collector are driven back into the source films and are lost to analysis. Thus, the fraction of all recoils which must carry a positive charge equals $(N_i - N_c)/N_i$, where N_i is the number of recoils found on the

TABLE II
THE ELECTRIC CHARGE ON INDIUM RECOILS

Expt.	In ¹¹⁶ on field free collector, cts./min.	In ¹¹⁶ on collector at 1500 volts (+)	In ¹¹⁶ on collector at 1500 volts (-)	Positive ions, %
16	700	426		39
18	6,800	2850		58
20	3,900	3100		21
21	3,750		4000	
24	5,900	4200		29
27	3,040	2340		23
.....				
30	9,300	2680		72
31	14,400	5500		62
36	8,744		3396	
38	5,720		6580	
41	10,000	3380		66

^a In experiments below dotted line source films were protected from air throughout.

TABLE III
GOLD RECOIL YIELDS FROM GOLD SURFACES

Expt.	Au ¹⁹⁸ on collector cts./min. ^a	Au stand. ct./min./μg.	$2 \times Y$ (%) ^b	Backing
39	35.2	590	24	Au foil
40	38.8	620	25	Au foil
42	14.6	492	12	Au foil
44	38.4	573	27	Au foil
45	32.0	598	21	Evap. on glass
46	52.6	589	36	air exposed

^a The counting rate is corrected for yield of the radiochemical analysis for contamination of the collector with stable gold and to end of bombardment. The counting rate reported applies to 1 sq. cm. of the source and was made at about 25% geometry. ^b Y = number of recoils collected divided by number of recoils created in top layer of source. 0.50 μg. of Au/sq. cm. was assumed for the top layer.

TABLE IV
ELECTRIC CHARGE ON AU RECOILS

Expt.	Au ¹⁹⁸ on field free collector, cts./min.	Au ¹⁹⁸ on collector at 1500 volts (+)	Positive ions, %	Backing
39	440	136	69	Au foil
40	485	168	65	Au foil
42	182	209	?	Au foil
44	479	189	61	Au foil
46	657	326	51	Au film on glass

field free collector and N_0 is the number of recoils found on the charged collector. The small increase in recoils collected with a negative potential on the collector is not an indication of negative ions. Were negative ions present, a decline in yield for the charged collector should again be noted. The effect may be due to a slight penetration of the attractive electric field into the adjacent "field free" region with the result that some positive ions are diverted from the uncharged collector to the negative collector.

Discussion

The yield data suggest that the recoils are able to penetrate only a few lattice layers of the metal film at most. Accordingly, the character of the film surface is of decisive importance and until information on the surface used here is obtained, very little more concerning the path lengths can be said. The evaporated films are being examined by electron microscopy and electron diffraction and the results may prove informative.

The yields of recoil In and Au atoms are, however, not far from expectation. Earlier we have argued that in the case of In, only one energetic γ -ray appears in each deexcitation process and the others seen in the capture γ -ray multiplicity studies must each be less energetic than 3 mev. A similar argument may be made for Au. Since the recoil energy varies as the square of the γ -ray energy, the energies and mutual orientations of these softer γ -rays are relatively unimportant in determining the recoil energy. Thus, the recoil spectra for In and Au may be estimated directly from the γ -ray spectra reported. By this procedure, recoil energies of 70 to 280 ev. for In and 50 to 220 ev. for Au are found. One must remark, however, that the capture γ -rays reported by Kinsey, *et al.*,⁷ and by Hamermesh⁸ may be emitted in only a fraction of all capture processes, the remaining processes giving γ -rays all of which are too soft to be observed by their techniques. Should this prove to be the case,

then the lower limit for the recoil energy spectrum just estimated will be erroneously high.

This result can now be used in conjunction with Seitz¹¹ discussion of the fate of "knocked on" atoms. The rate of energy loss to the original recoil in displacing lattice atoms and in transferring kinetic energy to them is such, by Seitz' treatment, that a 100 ev. In or Au recoil originating in the third layer should, on the average, emerge from the top layer with very little residual energy. The calculation must not be taken seriously, of course, for with so few stopping events involved the deviation from the average will be very great. Nevertheless, all recoils from the surface layer directed toward the collector ought to reach it. We shall be interested to learn why the yields fall short of this value.

The charge which is observed on about half of the recoils must arise from internal conversion during the deexcitation of the compound nucleus. The work function of indium is probably less than its ionization potential and this relation is certainly true for gold. Thus, the recoils leaving the surface should not self ionize and internal conversion, already observed in neutron capture by several other nuclei,¹⁰⁻¹³ seems the only likely source for the production of ions.

The charges have an interesting connotation. They suggest that in a major fraction of the radiative captures, an internal conversion step must follow the emission of an energetic γ -ray. Were the order of events reversed, the Auger process and the neutralization of the charge by metal electrons should be completed before the recoil atom leaves the metal surface. Neutralization appears probable even if the energetic γ -ray is emitted and the recoil atom begins to move immediately after the internal conversion step.¹⁴

The chronology of events as diagrammed in Table V may make the argument clearer. The In¹¹⁶ is assigned an outward velocity of 10⁶ cm./sec. following the initial energetic γ -ray emission. If the delay until the internal conversion step is as short as 10⁻¹³ seconds (and it may be much longer), the recoil will be 10 Å. from the surface and safely beyond the reach of the metal electrons. Other studies support the argument that if internal conversion preceded the energetic γ -ray in radiative capture, then neutralization of even a surface atom would be accomplished before the recoil left the surface. Wright¹⁵ has studied the recoils from the neutrino accompanying K-capture by Cd¹⁰⁷. Here the nuclear process does not give a charged recoil atom directly as does internal conversion but, like the latter process, creates a vacancy in the K-shell of the atom. The vacancy is filled by the electrons from outer shells and in this process additional electrons may be lost. Nevertheless, when the Ag¹⁰⁷ recoils coming from a trace layer of Cd¹⁰⁷ on tungsten were examined for charge, none was found. Apparently the 10⁻¹² seconds required for the recoil to leave the surface was sufficient to neutralize the charge developed by the Auger process. Smith and Allen² found the lithium recoils from the neutrino in K capture by Be⁷ to be positively charged despite

(14) For ref. to Auger rates, see Wu and Ouram; *Can. J. Research*, **28A**, 542 (1950).

(15) B. T. Wright, *Phys. Rev.*, **71**, 839 (1947).

TABLE V
 CHRONOLOGY FOR In^{116} , Ag^{107} AND Li^{7} RECOILS FROM METAL SURFACES

	Time = 0	10^{-14} sec.	2×10^{-14} sec.	10^{-12} sec.	10^{-10} sec.	10^{-6} or 10^{-8} sec.
In^{116}	Hard γ ; accel. to 10^6 cm./sec.	Atom on surface, neutral	→	Atom 10 \AA . from surface ionized by int. conv.	→	Ion reaches collector
Ag^{107}	Neutrino, accel. to 3×10^6 cm/sec	Atom on surface, Auger proc- ess over	→	Atom on surface, neutralized by metal	→	Neutral atom reaches collector
Li^7	Neutrino, accel. to 4×10^6 cm./sec.	→	→	→	Atom $4 \times 10^4 \text{ A}$. from surface. Auger process over?	Ion reaches collector

the fact that lithium has an ionization potential higher than the work function of the tantalum backing employed. Here the velocity (4×10^6 cm./sec.) of the recoils is greater than in the Ag^{107} case and this allows less time for neutralization. The possibility that the Auger process is much slower with Be^7 than with Ag^{107} would seem more important, however. In very light elements the Auger process is reported to require about 10^{-10} seconds. Whether this estimate can apply to the Auger process following K-capture in a light element has not been discussed. In K-capture, not only is an orbital vacancy created, but the nuclear charge changes and this extra perturbation may enter into determining the time required to complete the Auger process.

In conformity with expectation, atoms recoiling

from neutron capture travel only a few interatomic layers from their original sites in a solid. Presumably this is also true for the atoms of a solid "knocked on" by high energy projectiles and is pertinent in discussing the healing processes by which "knocked on" atoms are restored to proper lattice sites. The frequency with which internal conversion accompanies the deexcitation after neutron capture in Au and In (as well as in other cases cited) and the implication of the Au and In results that internal conversion follows after, perhaps long after, an energetic γ -ray is emitted, may affect the chemical reactivity displayed by the hot atom. If the recoiling atom has been brought to rest by collisions before the internal conversion step occurs, the latter will provide a second opportunity for molecular disruption or synthesis.

THE REACTION BETWEEN TERTIARY AMINES AND ORGANIC ACIDS IN NON-POLAR SOLVENTS¹

BY SAMUEL KAUFMAN AND C. R. SINGLETERRY

Naval Research Laboratory, Washington, D. C.

Received February 26, 1961

Cryoscopic data indicate that tertiary aliphatic amines can react with carboxylic acids according to the equilibria $N + A_2 \rightleftharpoons NA_2$ and $NA_2 + A_2 \rightleftharpoons NA_4$ (N = monomeric amine; A = monomeric acid). It is probable that the dimeric acid molecule reacts directly with such amines. This mode of combination is consistent with compositions of solid phases isolated from non-aqueous solvents as well as with the cryoscopic data presented. A possible bonding mechanism and structure are suggested. The amine-carboxylic acid complexes are appreciably dissociated into free acid and free amine in dilute benzene solutions. The weakly basic aryl tertiary amines such as dimethylaniline do not react with carboxylic acids in benzene to a detectable extent. The heterocyclic conjugated pyridine reacts with these acids to only a slight extent. There is no evidence in the data presented to indicate micelle formation by the high molecular weight complexes formed between tertiary amines and carboxylic acids.

Introduction

Little information is available concerning the stability and the state of dispersion of the soluble compounds formed between amines and carboxylic acids in non-aqueous solvents. The amine picrates²⁻⁵ have been found to be stable 1-1 compounds, which in the case of primary and secondary amines are strongly associated to form dimers. With the exception of the tribenzylammonium salt the picrates do not dissociate appreciably into free acid and free amine. Certain primary amines have been reported to form 1-1 compounds with carboxylic acids^{6,7} in non-aqueous solvents. Studies in the absence of a solvent have been considered to give evidence of the existence of compounds containing from one to three molecules of acid per molecule of amine.⁸⁻¹¹

The present investigation was intended to establish the presence or absence of colloidal aggregates of amine-acid compounds in benzene solutions. Preliminary cryoscopic observations indicated that micelle formation did not occur to a detectable extent, and suggested further that the amine-acid compounds were dissociated into free amine and free acid to a degree that permitted detailed study of the reactions.

It was expected that the amine and acid might combine in equivalent proportions to form salts that could be recrystallized for cryoscopic study, but all of the crystalline compounds isolated contained more than one equivalent of acid per mole of amine. The variety of possible compositions deduced from studies of binary systems and from

analysis of the solid amine-acid compounds reported here do not prove the existence of the indicated compounds in dilute solutions in non-polar solvents. The combining ratios observed might be determined as a consequence of the relative solubilities of the possible compositions and the geometry of the crystal lattice. The equilibrium between acids and amines was therefore examined by adding amine and successive increments of acid to a quantity of benzene in which they would remain completely dissolved. Cryoscopic determinations were made with solutions of cetyldimethylamine, triisomyamine, pyridine, dimethylaniline, and acetic, myristic and picric acids, respectively. Further observations were made with additions of myristic acid to solutions of cetyldimethylamine, triisomyamine, pyridine and dimethylaniline, and with additions of picric and acetic acids to solutions of triisomyamine. Because of the pronounced association reported for primary and secondary amines and their salts,⁵ the scope of this investigation was limited to tertiary amines in order to simplify the interpretation of the data. The four amines studied were chosen to provide a wide range of basicity, structural type, and symmetry of substitution about the nitrogen atom.

Materials.—The myristic acid (Eastman Kodak No. 1116) was prepared for use by drying *in vacuo* to 60° (m.p. 52.3–53.0°). Ralston¹² considered 54.4° the best value for this acid. The neutral equivalent was 232.8 (theoretical 228.36).

The cetyldimethylamine was prepared by the method of Ralston, *et al.*,¹³ from hexadecylamine having a melting point of 45.6–46.6° (literature value 46.77°).¹⁴ The cetyldimethylamine was fractionally distilled *in vacuo*, and stored in sealed ampoules. Before use, it was dried by heating *in vacuo* to 80°. Its neutral equivalent was 278.7 (theoretical 269.5). Spot tests¹⁵ indicated that primary and/or secondary amines were present to the extent of less than 0.1%.

The triisomyamine (Eastman Kodak No. 1880) was dried over solid potassium hydroxide, and fractionally distilled *in vacuo*. Refractive index (n_D^{20}) 1.4330; neutral equivalent, 228.4 (theoretical 227.4).

The dimethylaniline (Eastman Kodak No. 97) was dried and fractionally distilled *in vacuo*. Its refractive index (n_D^{20}) was 1.5589 (I.C.T. value, n_D^{20} 1.5587).

The pyridine (Baker C.P. grade) was fractionally distilled

(1) The opinions or assertions contained in this communication are those of the authors and are not to be construed as official or reflecting the views of the Navy Department. This is a condensation of Naval Research Laboratory Report 3743 (October 9, 1950).

(2) F. M. Batson and C. A. Kraus, *J. Am. Chem. Soc.*, **56**, 2017 (1934).

(3) R. M. Fuoss and C. A. Kraus, *ibid.*, **57**, 1 (1935).

(4) C. A. Kraus and G. S. Hooper, *Proc. Natl. Acad. Sci.*, **19**, 939 (1933).

(5) A. A. Maryott, *J. Research Natl. Bur. Standards*, **41**, 1, 7 (1948).

(6) E. B. R. Pridaux and R. N. Coleman, *J. Chem. Soc.*, 462 (1937).

(7) B. A. Hunter, *Iowa State Coll. J. Sci.*, **15**, 223 (1941).

(8) W. W. Lucasse, R. P. Koob and J. G. Miller, *This Journal*, **48**, 85 (1944).

(9) P. Matavulj, *Bull. soc. chim. roy. Yougoslav*, **10**, 25, 35, 51 (1939).

(10) E. A. O'Connor, *J. Chem. Soc.*, **125**, 1422 (1924); **119**, 401 (1921).

(11) W. O. Pool, H. J. Harwood and A. W. Ralston, *J. Am. Chem. Soc.*, **67**, 775 (1945).

(12) A. W. Ralston, "Fatty Acids and their Derivatives," John Wiley and Sons, Inc., New York, N. Y., 1948, pp. 32–33.

(13) A. W. Ralston, D. N. Eggenberger, H. J. Harwood and P. L. DuBrow, *J. Am. Chem. Soc.*, **69**, 2095 (1947).

(14) A. W. Ralston, C. W. Hoerr, W. O. Pool and H. J. Harwood, *J. Org. Chem.*, **9**, 102 (1944).

(15) F. Feigl, "Qualitative Analysis by Spot Tests," 3rd edition, Elsevier Publishing Co., Inc., New York, N. Y., 1946, pp. 368ff.

with appropriate safeguards against the absorption of moisture. Its refractive index (n_D^{20}) was 1.5101 (I.C.T. value, n_D^{20} 1.509).

The picric acid (Eastman Kodak No. 210) was recrystallized from aqueous alcohol and from benzene, and desolvated *in vacuo* at 62° (m.p. 122.3–122.9°).

The acetic acid (Baker C.P. A.C.S.) was purified in a dry atmosphere by four partial freezings. The fraction reserved for cryoscopic work froze at 16.4°.

Thiophene-free benzene (A.C.S.) was percolated through activated silica gel to remove polar material and moisture, and was stored over sodium until used. Its freezing point was 5.37°.

The naphthalene (Eastman Kodak No. 168) was purified by double resublimation *in vacuo* and was heated to about 50° *in vacuo* just before use.

Special precautions were taken to protect chemicals and equipment from moisture.

Experimental Procedure.—A Beckmann cryoscopic apparatus was used for the freezing point measurements. The mean jacket temperature was held at 3.3° \pm ΔT within a tolerance of 0.1°. The contents of the inner tube were agitated by an externally driven glass stirring screw. Reciprocal vertical stirring was found to pump out solvent vapor at an appreciable rate. The losses with rotary stirring were about 0.05 g. per hour and corrections to observed data were made on this basis. The stirrer shaft entered the inner freezing tube through a glass T-tube. Dried nitrogen was forced past the shaft; omission of the nitrogen current allowed the entry of moisture, progressively depressing the freezing point. Before use, the inner tube was flushed with dried nitrogen for one hour or more to remove moisture. Omission of the flushing produced a variable and marked depression of the freezing point of the solvent.

The amount of supercooling was controlled at $0.2 \pm 0.05^\circ$ by seeding with minute dry crystals of benzene. Corrections¹⁶ were made for withdrawal of solvent by freezing. Within 1% equal quantities of benzene were used for all determinations. Observations were made in a constant-temperature room at 25° and 20 to 50% relative humidity. The temperature of the solution was read at half-minute intervals preceding freezing and after freezing began, until the temperature showed no detectable change during a minimum interval of four minutes. This constant temperature was taken as the observed freezing point. When all of the data for a given solute were combined in a single plot of ΔT , the freezing point depression vs. concentration, the average deviation of the experimental points from the best smooth curve was $\pm 0.002^\circ$.

Results

Although attempts to prepare solid compounds were not pursued far enough to produce materials of high purity, the results are reported briefly because of their relation to those obtained cryoscopically. (a) Cetyldimethylamine with molten stearic acid gave a solid which was recrystallized three times from acetone, m.p. 64.2–64.5°; N, 1.31 (calcd. for triacid complex 1.24%). (b) Cetyldimethylamine titrated with stearic acid in 95% ethanol to phenol red end-point gave a solid which was recrystallized from ethanol and from acetone, m.p. 77–79°, N, 1.62 (calcd. for diacid complex, 1.67%). (c) Cetyldimethylamine with equivalent proportions of lauric acid in ethyl acetate solution gave a solid which was recrystallized from acetone and from ethyl acetate, m.p. 56.8–57.5°; N, 2.13 (calcd. for diacid complex 2.09%). (d) Cetyldimethylamine with an equivalent amount of oleic acid gave a mush of crystals which were centrifugally filtered and washed with benzene, m.p. 36.2–37.3°; N, 1.80 (calcd. for diacid complex, 1.68).

Figure 1 presents the cryoscopic data for naphthalene and the amines. The average experimental

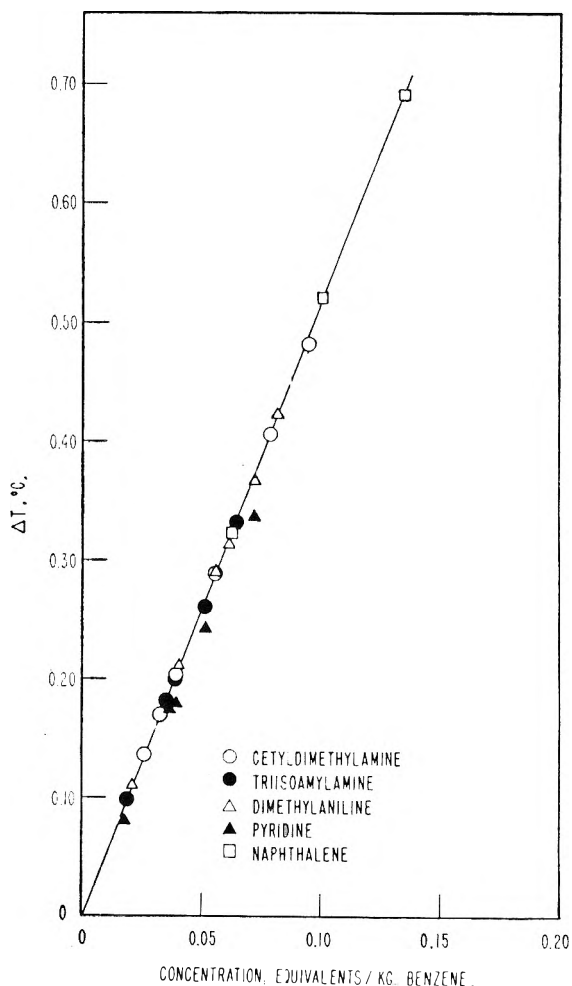


Fig. 1.—Depressions of the freezing point of benzene by amines and by naphthalene.

molal freezing point constant, K_f , of benzene found is 5.17°. The equation employed by the Bureau of Standards for the cryoscopic determination of the purity of benzene¹⁷ is consistent with a value of $K_f = 5.13$ at infinite dilution. The constant obtained in the present measurements is thought to differ from the accepted value because of small systematic errors arising from the materials and techniques employed; it was used for the treatment of other data obtained under the same conditions in order to minimize the effect of such errors.

The cryoscopic effect of the amines (Fig. 1) is very near that of the naphthalene, except for the case of pyridine, which is known to be abnormal in its cryoscopic behavior,¹⁸ probably because of the formation of solid solutions. Picric acid (Fig. 2) shows nearly ideal behavior. The dotted line, drawn for comparison purposes, represents one-half the freezing point depressions expected for naphthalene, and corresponds to the slope for a totally dimerized acid. Inspection of the graph suggests that appreciable quantities of the carboxylic acids are in the monomeric form, but that the dimeric form preponderates.¹⁹ There is little dif-

(17) A. R. Glasgow, A. J. Streiff and F. D. Rossini, *J. Research Natl. Bur. Standards*, **26**, 355 (1945).

(18) C. R. Burg and H. O. Jenkins, *J. Chem. Soc.*, 688 (1934).

(19) H. N. Brocklesby, *Can. J. Research*, **14B**, 222 (1936).

(16) K. Arndt, "Handbuch der Physikalisch-Chemischen Technik," 2nd edition, Ferdinand Enke, Stuttgart, 1923, p. 140.

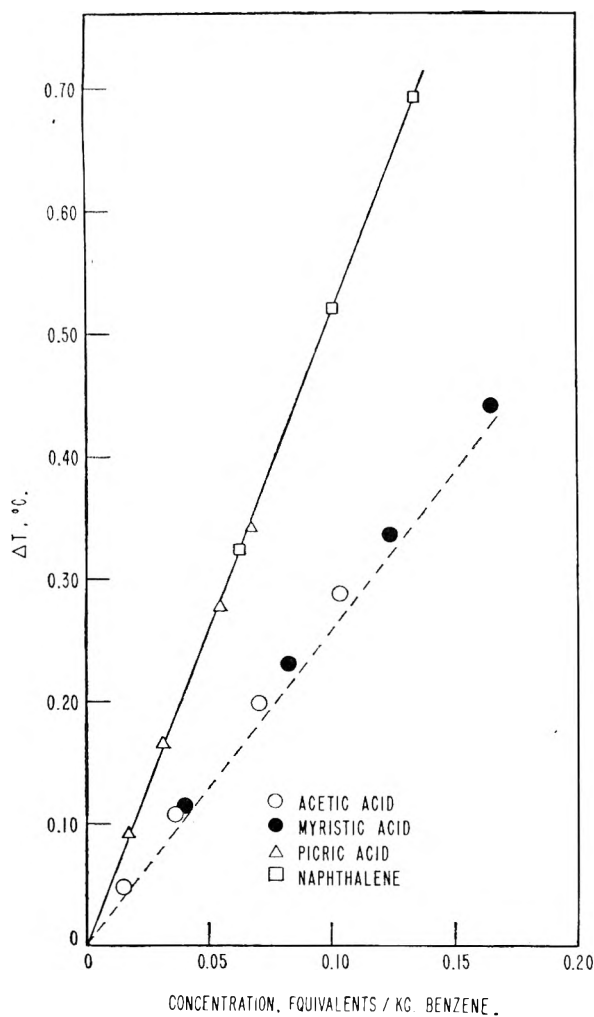


Fig. 2.—Depressions of the freezing point of benzene by acids and by naphthalene.

ference between the behaviors of myristic and acetic acids in this respect.

Concentrations recorded in the tables and figures were computed from measured neutral equivalent weights for cetyldimethylamine, triisoamylamine and myristic acid, and from formula weights for the remaining compounds.

TABLE I

DISSOCIATION OF ACID DIMER IN BENZENE FROM CRYOSCOPIC OBSERVATIONS

Myristic acid		Acetic acid	
Concn., (equiv./kg. solvent)	Dissn. constant $\times 10^4$ (K_{A_2})	Concn., (equiv./kg. solvent)	Dissn. constant $\times 10^3$ (K_{A_2})
0.0404	9.2	0.0153	1.8
.0826	12.0	.0363	2.0
.1240	7.2	.0703	1.4
.1649	4.7	.1037	1.2
Av.	8	Av.	1.6

The dissociation constants, K_{A_2} (Table I) of the dimeric acids were calculated from K_f and the cryoscopic data. The following reaction was assumed



where A represents the monomeric acid. Thus

$$K_{A_2} = [A]^2/[A_2]$$

The brackets signify concentrations expressed as moles per kilogram of solvent.

The values of K_{A_2} show a scatter which is not greater than is to be expected from the experimental uncertainty of the freezing point measurement. If the concentrations are expressed as mole fractions instead of molalities, k_{A_2} for myristic acid is 6.0×10^{-5} , and for acetic acid is 1.25×10^{-4} , where k_{A_2} is the dissociation constant on the mole fraction basis. The corresponding k_{A_2} derived from dielectric measurements²⁰ at 30° for stearic acid is 1.7×10^{-4} , and that for acetic acid is 2.4×10^{-4} . If it is assumed that the heats of dimerization in benzene solution of both stearic and acetic acids are equal to 8.6 kcal. per mole of dimer, the value reported for benzoic acid,²¹ then the constants at 5.4° for these acids may be computed from the Van't Hoff equation. At this temperature, approximately that of the cryoscopic observations, the computations lead to $k_{A_2} = 4.8 \times 10^{-5}$ for stearic acid and $k_{A_2} = 0.68 \times 10^{-4}$ for acetic acid. These estimated constants are in reasonable agreement with those obtained from the cryoscopic measurements.

TABLE II

CRYOSCOPIC EFFECTS RESULTING FROM THE ADDITION OF ACIDS TO AMINES IN BENZENE

Increment symbol	ΔT_{total} (°C.)	Solute added ^a (equiv./kg. solvent)	Increment symbol	ΔT_{total} (°C.)	Solute added ^a (equiv./kg. solvent)
Cetyldimethylamine + myristic acid			Pyridine + myristic acid		
Amine 1 _a	0.205	0.0393	Amine 1 _d	0.180	0.0393
Acid 1 _a	.217	.0337	Acid 1 _d	.270	.0437
Acid 2 _a	.243	.0723	Acid 2 _d	.370	.0843
Acid 3 _a	.293	.1127	Acid 3 _d	.475	.1243
Acid 4 _a	.363	.1514	Acid 4 _d	.572	.1629
Triisoamylamine + myristic acid			Triisoamylamine + acetic acid		
Amine 1 _b	0.182	0.0350	Amine 1 _e	0.200	0.0380
Acid 1 _b	.199	.0338	Acid 1 _e	.210	.0372
Acid 2 _b	.227	.0665	Acid 2 _e	.229	.0759
Acid 3 _b	.281	.1062	Acid 3 _e	.337	.1546
Acid 4 _b	.347	.1395	Acid 4 _e	.488	.2286
Dimethylaniline + myristic acid			Triisoamylamine + picric acid		
Amine 1 _c	0.212	0.0403	Amine 1 _f	0.200	0.0384
Acid 1 _c	.330	.0425	Acid 1 _f	.198	.0170
Acid 2 _c	.449	.0866	Acid 2 _f	.178	.0334
Acid 3 _c	.558	.1288	Acid 3 _f	.192	.0434
Acid 4 _c	.671	.1717	Acid 4 _f	.296	.0655
			Acid 5 _f	.438	.0959

^a Values for "Amine" increments are those for solutions of amine before additions of acid. Values for "Acid" increments represent total acid added.

The primary data of Table II were obtained by the addition of successive increments of various acids to benzene solutions containing fixed amounts of different amines. Plots of these data are not directly comparable since the initial concentrations of the pure amine solutions were not precisely equal.

(20) A. A. Maryott, M. E. Hobbs and P. M. Gross, *J. Am. Chem. Soc.*, **71**, 1671 (1949).

(21) L. Pauling, "The Nature of the Chemical Bond," 2nd edition, Cornell University Press, Ithaca, N. Y., 1940, Chap. IX.

For graphical purposes, the primary data have been reduced to direct comparability with respect to equivalence points, relative amounts of acid present, and slopes. The derived results are plotted (Figs. 3 and 4) with the relative cryoscopic effect, $\Delta T_{\text{total}}/\Delta T_{\text{amine } 1}$ as the ordinate, and the acid-amine ratio, equivalents acid/equivalents amine, as the abscissa. The depression ΔT_{total} is that of the observed solution, while $\Delta T_{\text{amine } 1}$ is that of the amine solution before acid additions. It is true that the relative cryoscopic effect for a given acid-amine ratio will vary somewhat with the level of absolute concentration. However, in the range studied, if the initial amine concentration differs by 10%, the maximum change in the relative cryoscopic effect is of the order of only 1%.

The dotted lines represent the hypothetical cases wherein the reaction of an amine with an acid attains irreversible completion at 0, 1, 2 or 3 equivalents of acid per equivalent of amine, following which additions of excess carboxylic acid exert an independent cryoscopic effect. The data for myristic acid were used for plotting the diagonal dotted lines in both figures. The difference between the cryoscopic behaviors of myristic and acetic acids is so slight as to be imperceptible in these graphs.

Because pyridine does not conform to the cryoscopic behavior of the other amines studied, the pyridine-myristic acid data in Fig. 3 were treated differently from the rest to permit convenient visual comparison. The ordinate in this case is

$$1 + (\Delta T_{\text{acid}}/[N_1] \times K_f)$$

where ΔT_{acid} is the total additional depression found after additions of acid to the amine solution,

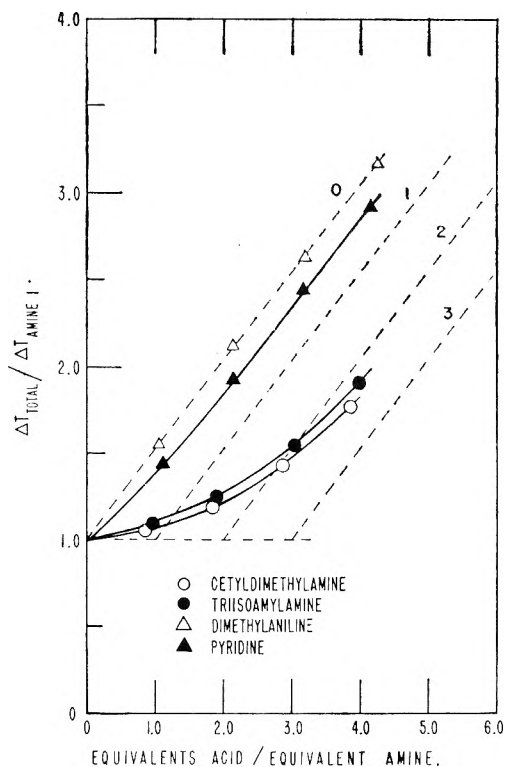


Fig. 3.—Relative cryoscopic effects resulting from additions of myristic acid to solutions of various amines.

and $[N_1]$ is the concentration of amine in the solution to which the acid was added.

Discussion of Results

The interpretation offered for these experimental results is based on the assumption that, in these dilute solutions, the individual kinetic units present have substantially ideal effects on the activity of benzene. The validity of the assumption is supported by the cryoscopic effects found for three of the four amines (Fig. 1), and by the satisfactory values calculated for the dimerization constants of myristic and acetic acids. The cryoscopic data of Kraus and co-workers^{2,3,22} for distinctly polar compounds such as triisoamylammonium picrate⁴ have been successfully explained on the basis of a similar assumption.

Accepting the validity of Raoult's law in the systems studied, it is clear that the compounds resulting from the reaction between amines and carboxylic acids in these solutions are in equilibrium with substantial amounts of free acid, even in the presence of excess amine. Dimethylaniline gives no indication of reaction with myristic acid; the points for the freezing point depression after the addition of acid lie quite precisely on the dotted line 0 (Fig. 3), which corresponds to the independent cryoscopic effect of the acid. This behavior is in accord with that observed by O'Connor¹⁰ for the same amine with acetic acid. There is evidently some interaction between pyridine and myristic acid, but the compound formed must be highly unstable. Even in the case of the two aliphatic amines the minimum amount of uncombined acid that must be assumed to explain the data is considerable.

The data for triisoamylamine plus picric acid (Fig. 4) indicate the formation of a stable amine picrate whose composition is one equivalent of acid to one of amine. No significant dissociation can

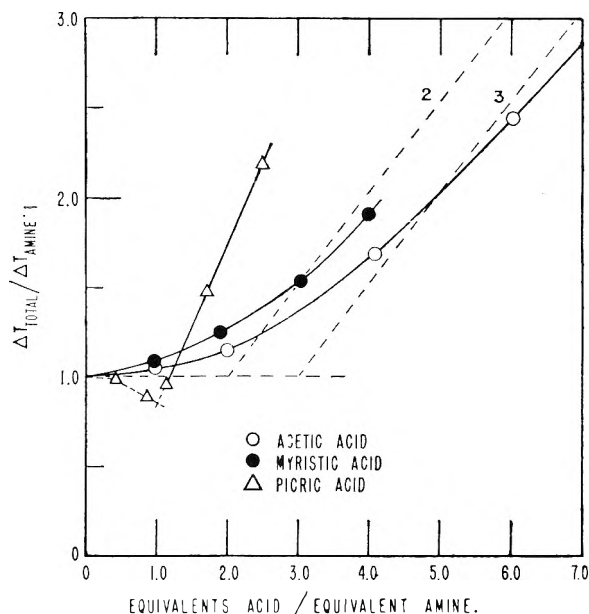
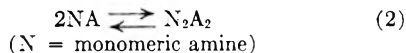


Fig. 4.—Relative cryoscopic effects produced by additions of various acids to solutions of triisoamylamine.

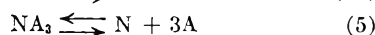
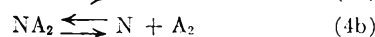
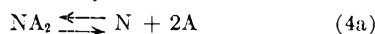
(22) D. A. Rothbrock, Jr., and C. A. Kraus, *J. Am. Chem. Soc.*, **59**, 1699 (1937).

be inferred from the data in this case. The abnormally small depressions produced by the compositions approximating stoichiometric proportions of the amine and acid indicate an appreciable interaction between the amine picrate molecules



which is not reflected in the dielectric measurements of Maryott,⁵ but which is supported by the data of Batson and Kraus.² The intersection of the extrapolated branches of a plot of ΔT vs. total picric acid added to triisoamylamine falls within 1% of the abscissa corresponding to a 1:1 ratio of acid to amine. The curve beyond the stoichiometric point is very nearly that to be expected from the independent action of the excess picric acid. It has a slope corresponding to $K_f = 4.7$ as compared with $K_f = 5.1$ for a benzene solution of picric acid alone. The difference exceeds the experimental error, and may indicate a slight tendency of the excess picric acid to associate with the amine picrate. Strong acids such as hydrogen chloride may be expected to react as completely with aliphatic tertiary amines as does picric acid.^{23,24}

A satisfactory explanation of the data for the reaction of triisoamylamine or cetyltrimethylamine with myristic acid requires that one equivalent of a tertiary aliphatic amine combine with two equivalents of myristic acid monomer (or directly with one unit of the acid dimer) to form a molecular complex that is considerably dissociated in dilute solutions. An attempt was made to compute equilibrium constants for some possible reactions between cetyltrimethylamine and myristic acid by a method that took account of the relative concentrations of the monomer and dimer forms of the acid required by the constants of Table I. No one of the equilibrium expressions corresponding to the reactions



was satisfactorily constant, although in the range between 0 and 1.5 formula weights of acid per formula weight amine, the expression

$$K_{\text{NA}_2} = [\text{N}][\text{A}_2]/[\text{NA}_2]$$

corresponding to equilibrium (4b) varied less rapidly with changing acid to amine ratio than did those for equilibria (3) and (5). Equilibrium (4a) could be used as an alternative for (4b) because $[\text{A}_2]$ and $[\text{A}]$ are mutually dependent upon K_{A_2} and equilibrium (1).

If the only equilibria to be considered were (1) and (4b), ΔT_{total} should approach the dotted line 2 (Fig. 3) asymptotically as the excess of the acid becomes sufficient to suppress the dissociation of the complex. The curves for both cetyltrimethylamine and triisoamylamine with myristic acid, however, cross this line. The same is true for the system triisoamylamine plus acetic acid (Fig. 4). The

fact that the cryoscopic effects are substantially less than can be accounted for by equilibria (1) and (4b) indicates some further interaction between the solutes present.

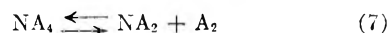
By analogy to the behavior of triisoamylammonium picrate, the equilibrium



was postulated, which should conform to the expression

$$K_{\text{N}_2\text{A}_4} = [\text{N}_2\text{A}_4]/[\text{NA}_2]^2$$

As an alternative, the equilibrium



was proposed, for which the expression

$$K_{\text{NA}_4} = [\text{A}_2][\text{NA}_2]/[\text{NA}_4]$$

would hold.

For the case in which an interaction represented by equilibrium (6) or (7) leads to a complex having a stability at least an order of magnitude less than that of NA_2 , it is possible to determine the approximate value of K_{NA_2} without reference to these interactions. This is done by computing apparent values of K_{NA_2} from the experimental data with the assumption that only equilibria (1) and (4b) apply, and extrapolating the resulting plot of K_{NA_2} vs. acid-amine ratio to zero acid-amine ratio. The extrapolation is improved in linearity but not altered in final value if, for a second approximation, a reasonable value of $K_{\text{N}_2\text{A}_4}$ or K_{NA_4} is introduced into the computations for K_{NA_2} .

By use of the value $K_{\text{NA}_2} = 3 \times 10^{-3}$ obtained by assuming equilibria (1) and (4b) only, an attempt was made to fit a value of $K_{\text{N}_2\text{A}_4}$ to the data for the system triisoamylamine plus myristic acid. No assignable value of $K_{\text{N}_2\text{A}_4}$ was consistent with a constant value of K_{NA_2} . On the other hand the similarly computed values of K_{NA_4} corresponding to increasing total acid content was respectively 0.71, 0.110, 0.0714 and 0.0855. The first of these was discarded as unreliable because of the large effect of experimental errors at this acid-amine ratio, and $K_{\text{NA}_4} = 0.0855$ was taken as the probable value.

To test the hypothesis that equilibria (1), (4b) and (7) are the controlling equilibria in this system, ΔT_{total} was computed for each of the experimental compositions, using the determined values of ΔT_{amine} , K_f and K_{A_2} , and the calculated values of K_{NA_2} and K_{NA_4} . For comparison a similar test was made, assuming equilibria (1), (4b) and (6). A value of $K_{\text{N}_2\text{A}_4} = 0.071$ was chosen, which would produce a fit most favorable to the two uppermost points in Fig. 5, since these two points are most sensitive to the variation of $K_{\text{N}_2\text{A}_4}$. The result of the computations demonstrates that equilibrium (7) is consistent, while equilibrium (6) is inconsistent, with the experimental data for the triisoamylamine-myristic acid system.

Examination of Fig. 4 shows that equilibrium (6) is not valid for the triisoamylamine-acetic acid system. The validity of this equilibrium requires that the curve approach the dotted line 3 asymptotically, whereas it very definitely crosses this line. Computations similar to those described above, assuming equilibria (1), (4b) and (7) were made for

(23) M. M. Davis, *J. Am. Chem. Soc.*, **71**, 3544 (1949); (b) M. M. Davis and E. A. McDonald, *J. Research Natl. Bur. Standards*, **42**, 595 (1949).

(24) J. A. Moede and C. Curran, *J. Am. Chem. Soc.*, **71**, 852 (1949).

the system triisomyamine-acetic acid. Results for this system were $K_{NA_2} = 1.02 \times 10^{-3}$ and $K_{NA_4} = 2.38 \times 10^{-2}$; these values were insensitive to further approximation cycles. A comparison (Table III) of the computed and measured freezing

TABLE III

TEST OF EQUILIBRIA IN SOLUTIONS OF TRIISOMYAMINE PLUS ACETIC ACID

Amine content = 0.0380 equiv./kg. benzene; $K_{A_2} = 1.6 \times 10^{-3}$; $K_{NA_2} = 1.02 \times 10^{-3}$; $K_{NA_4} = 2.38 \times 10^{-2}$

Total acid added, (equiv./kg. benzene)	ΔT_{total} , °C., exptl.	ΔT_{total} , °C., computed $NA_2 + A_2 \rightleftharpoons NA_4$
0.0372	0.210	0.210
.0759	.229	.229
.1546	.337	.335
.2286	.488	.489
.3026	.658	.665

point depressions shows that equally good agreement is obtained, except for the mixture of highest acid-amine ratio. It is concluded that equilibria (4b) and (7) are valid for dilute benzene solutions of tertiary aliphatic amines plus fatty acids.

The instability of the compounds formed between amines and carboxylic acids in benzene solution, and also the surprising amount of acid bound per equivalent of amine, indicate that the forces between the acid and amine are different in type from those operating in the amine picrates or the amine hydrohalides. The reaction appears to be the formation of a molecular complex between acid dimer and the amine rather than the formation of a true ion pair.

The successful description of the experimental results in terms of one or of a series of equilibrium constants does not, of course, furnish direct information concerning the type of bonds involved, nor as to whether the monomeric or dimeric form of the acid is the chemical unit actually reacting with the amine. It might have been postulated that the observed phenomena were the result of the stepwise reaction of the amine with four units of acid monomer. Thus the choice of the acid dimer as the reacting unit may appear arbitrary and justified only by the resulting convenience in the analysis of the data. However, the assumptions employed for calculating the concentrations of the various species involved in the equilibria impose a further restriction. The constants K_{NA_2} and K_{NA_4} were computed from concentrations of N, NA_2 and NA_4 that were derived from the freezing point data on the assumption that neither NA nor NA_3 were present in significant amounts. The fact that the values derived for these constants by ignoring the possible presence of NA or NA_3 lead to computed depressions of the freezing point in close agreement with experiment supports the idea that the acid dimer is the actual reacting unit.

It is difficult to construct a model for the association of a single amine molecule with four separate acid monomers that implies an energy of bonding sufficient to compete effectively for monomeric units with the dimerization equilibrium (1). On the other hand, a direct bonding of the dimeric acid unit to a tertiary amine might result if the nitrogen of the amine approached one side of the eight-mem-

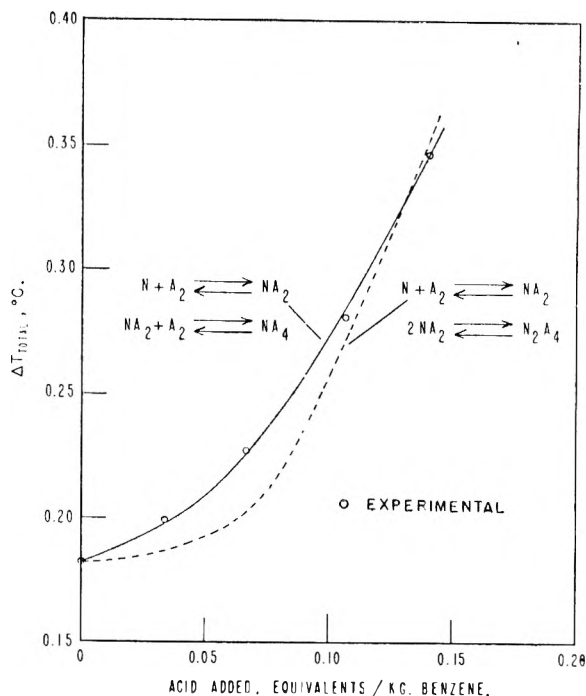
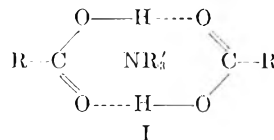


Fig. 5.—Test of alternative equilibria in solutions of triisomyamine plus myristic acid.

bered ring formed by the hydrogen bridges of the two carboxyl groups with such an orientation that the unshared electron pair of the nitrogen was equally available for dipolar interaction with either of the hydrogens of the dimeric acid, as represented in I.



Two six-membered chelate rings would result from the formation of I, and might lead to moderate stability of a type of hydrogen bridging that would otherwise be too weak to detect.

The bonding by a single hydrogen of more than two electronegative atoms at one time is unusual, although Pauling²¹ cites the "bifurcated hydrogen bond" $\text{N} \cdots \text{H} \cdots \text{O}$ inferred from the crystal structure of glycine.²⁵

The simultaneous direction of two hydrogen bridges toward a single oxygen atom has been postulated for the dimeric form of salicylic acid²¹ as well as in 1,8-dihydroxyanthraquinone and some similar compounds. Oxygen differs from nitrogen, it is true, in having two pairs of electrons not involved in covalent bonding, but hydrogen bonding is usually considered to be essentially an electrostatic or dipole effect and not electron sharing. The bonding of a second dimer by the NA_2 is difficult to explain. The first dimer unit may, however, be sufficiently polarized by the presence of the nitrogen atom so that the loose association of a second unit becomes possible.

The strength of bonding between the amine and

(25) G. Albrecht and R. B. Corey, *J. Am. Chem. Soc.*, **61**, 1087 (1939).

acid is not great; for triisooamylamine with myristic acid the degree of dissociation of NA_2 estimated for a concentration of 0.01 formula weight per kilogram of benzene is 46% as compared, for example, with 13% dissociation of the hydrogen-bonded dimer of myristic acid to monomer at the same concentration. (A smaller degree of dissociation in paraffinic than in aromatic solvents is suggested by the work of Pohl, Hobbs and Gross²⁶ who found that

(26) H. A. Pohl, M. E. Hobbs and P. M. Gross, *J. Chem. Phys.*, **9**, 408 (1941).

dimeric acetic acid was more readily dissociated in an aromatic than in a paraffinic solvent.) A bond of the type indicated in I implies a smaller heat of reaction and a smaller dipole moment than would be expected if a tertiary amine reacted with a fatty acid to produce an ionic compound.

Acknowledgment.—Acknowledgment is made to Kenneth L. Temple, formerly of the Naval Research Laboratory, for the preparation of two compounds of cetyldimethylamine with stearic (b) and lauric (c) acids.

SURFACE OXIDATION OF GALENA IN RELATION TO ITS FLOTATION AS REVEALED BY ELECTRON DIFFRACTION

BY HITOSI HAGIHARA¹

Taihei Mining and Metallurgical Laboratory,² Omiya City, Japan

Received February 26, 1951

The initial oxidation of galena surfaces was studied in air, in an enclosed atmosphere in galena powder, in a vacuum furnace, in water, and during dry and wet grinding. The electron diffraction examination of the oxidized faces revealed that the lowest oxidation product is in all cases lead sulfate (PbSO_4). Under dry conditions the sulfate crystallites were oriented in two ways on the cleavage face and no pseudomorphism was observed. In air the next higher oxidation product was the basic sulfate, Pb_2SO_5 . Considerations are given to the orientation relations of these oxidation products and their growth. In no instance were crystalline carbonate, hydroxide or the lower sulfoxides, PbS_mO_n (with n/m less than 4) observed.

Introduction

Electron diffraction investigation of the initial surface oxidation on galena is of interest from the theoretical as well as the practical viewpoint. The former interest is concerned with the mechanism of crystal growth of oxides on solid surfaces. With single-crystal substrates, particularly single crystal cleavage faces where the arrangement of atoms at the boundary surface is known, the above problem will be given the most detailed considerations. Interesting electron diffraction studies have already been reported with such sulfide minerals as zincblende, ZnS ,³⁻⁶ molybdenite, MoS_2 ,⁷ and stibnite, Sb_2S_3 .⁸ Galena⁹ is well suited for this purpose: its crystal structure is simple (NaCl-type cubic),¹⁰ its cleavage face is simple (cube face), and yet the detailed study of its initial oxidation is still lacking.

The practical viewpoint concerns itself with the separation of sulfide minerals by flotation. It is generally accepted that sulfide minerals undergo some degree of surface oxidation in the processes of crushing and grinding before entering into the

flotation cell. The reaction of the aqueous solutions of the collecting reagent with such oxidized surfaces has been of importance in the "chemical theory" of flotation advocated by Taggart, and accordingly a great deal of research has been devoted to its understanding.¹¹⁻¹⁶ It is now widely accepted that the surface of galena exposed to air either through dry or wet grinding is a complex mixture of sulfoxides, hydroxides and carbonates.¹⁷ This conclusion is based upon the chemical analyses of ions liberated into distilled water or into the aqueous solutions of the collecting reagent from galena. It is obvious that such deductions cannot be free from unavoidable ambiguities in interpreting which compounds actually exist on the mineral surfaces. The rate of oxidation is also controversial since reported studies range from "rapid"^{11, 16, 18, 19} to "slow."^{20, 21} It is, therefore, desirable that these conclusions be checked by an independent research technique such as is afforded by electron diffraction examination.

The present paper deals mainly with the initial

(1) Kobayasi Institute of Physical Research, Kokubunzi, Tokyo, Japan.

(2) Former Mitsubishi Mining and Metallurgical Laboratory.

(3) T. Yamaguti, *Proc. Phys.-Math. Soc. Japan*, **17**, 443 (1935).

(4) G. Aminoff and B. Broomé, *Kgl. Svenska Vetenskapsakad. Handl.*, **16**, 3 (1938).

(5) R. Uyeda, S. Takagi and H. Hagihara, *Proc. Phys.-Math. Soc. Japan*, **23**, 1049 (1941).

(6) D. M. Evans and H. Wilman, *Proc. Phys. Soc. (London)*, **A63**, 298 (1950).

(7) R. Uyeda, *Proc. Phys.-Math. Soc. Japan*, **20**, 656 (1938).

(8) S. Miyake, *Sci. Papers Inst. Phys. Chem. Research (Tokyo)*, **34**, 565 (1938).

(9) H. Hagihara, *Proc. Phys.-Math. Soc. Japan*, **24**, 762 (1942).

(10) R. W. G. Wyckoff, "The Structure of Crystals," The Chemical Catalog Co., Inc., (Reinhold Publ. Corp.), New York, N. Y., 1931. This monograph contains the structural data and references thereupon.

(11) A. F. Taggart, T. C. Taylor and A. F. Knoll, *Trans. Am. Inst. Mining Met. Engrs.*, **87**, 217 (1930).

(12) A. F. Taggart, T. C. Taylor and C. R. Ince, *ibid.*, **87**, 285 (1930).

(13) A. F. Taggart, G. R. M. del Giudice and O. A. Ziehl, *ibid.*, **112**, 348 (1935).

(14) A. Knoll and D. L. Baker, *Am. Inst. Mining Met. Engrs., Tech. Pub. No. 1313* (1941).

(15) A. F. Taggart and M. D. Hassialis, *Trans. Am. Inst. Mining Met. Engrs.*, **169**, 259 (1946).

(16) T. C. Taylor and A. F. Knoll, *ibid.*, **112**, 382 (1935).

(17) I. W. Wark, "Principles of Flotation," Australian Institute of Mining and Metallurgy, Inc., Melbourne, 1938, p. 134.

(18) P. A. Lintern and N. K. Adam, *Trans. Faraday Soc.*, **31**, 564 (1935).

(19) H. H. Herd and W. Ure, *This Journal*, **45**, 93 (1941).

(20) H. B. Bull, B. S. Ellefson and N. W. Taylor, *This Journal*, **38**, 401 (1934).

(21) P. Siedler, *Kolloid-Z.*, **68**, 89 (1934).

surface oxidation of fresh galena cleavage faces in air, along with short notes on its oxidation under conditions related to those prevailing in industrial ore crushing and grinding. Additional notes will also be presented which will reveal the anomalies often encountered on some fresh galena surfaces.

Initial Oxidation in Air.—Preliminary electron diffraction observations showed great variability in the patterns of the oxidized coatings, particularly in function of the temperature and duration of oxidation. This suggested that the outermost portion of the oxidized layer changes its structure or orientation as it grows. Accordingly, the following experimental procedure was selected.

A fresh cleavage face of galena, about $2 \times 2 \times 0.5$ mm. in size and free from visible surface irregularities, was placed upon the plane bottom surface of an ordinary nickel crucible maintained at a predetermined temperature. Oxidation was continued for the desired period of time. The temperature of the bottom surface of the crucible was estimated through the use of small particles of substances of known melting points. It is believed that the temperature is known to $\pm 10^\circ$.

The oxidized specimens were brought into the electron diffraction camera immediately upon preparation and the upper surfaces (not in direct contact with the crucible) were inspected. The camera length was 30 cm. and the accelerating voltage was 35 kv.

In the following descriptions of the experimental results the oxidation temperature and duration are, in a strict sense, the surface temperature of the crucible bottom and the total time the specimen remained in the crucible. Approximately they may, however, be regarded as the temperature of the crystal surface and the time during which the specimen was kept at a certain temperature.

Results.—The electron diffraction patterns thus obtained with these specimens were analyzed, identified and interpreted. Figure 1 shows the results of these identifications plotting temperature and duration as abscissa and ordinate, respectively. Figures 2-10 show the typical diffraction patterns obtained. With the oxidizing conditions as presented in Fig. 1 no visible change was observed on the specimen surface. The oxidized layer was too thin to produce interference colors.

The following is an analysis of each diffraction pattern for the various conditions of Fig. 1.

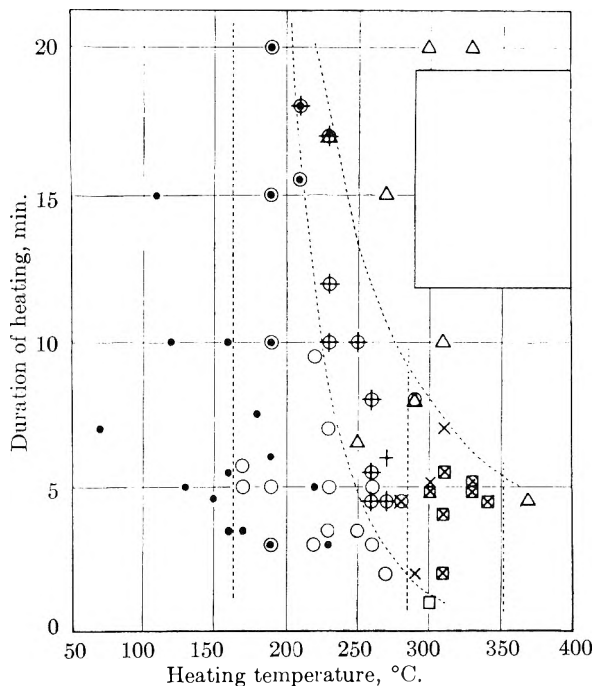


Fig. 1.—Identification of the initial oxidation products produced on galena cleavage face by its heat oxidation in open air: ● two-halo pattern; ○, $PbSO_4$; +, $PbSO_4 \cdot PbO$ I; ×, $PbSO_4 \cdot PbO$ II; □, elongated spots; Δ, complex patterns.

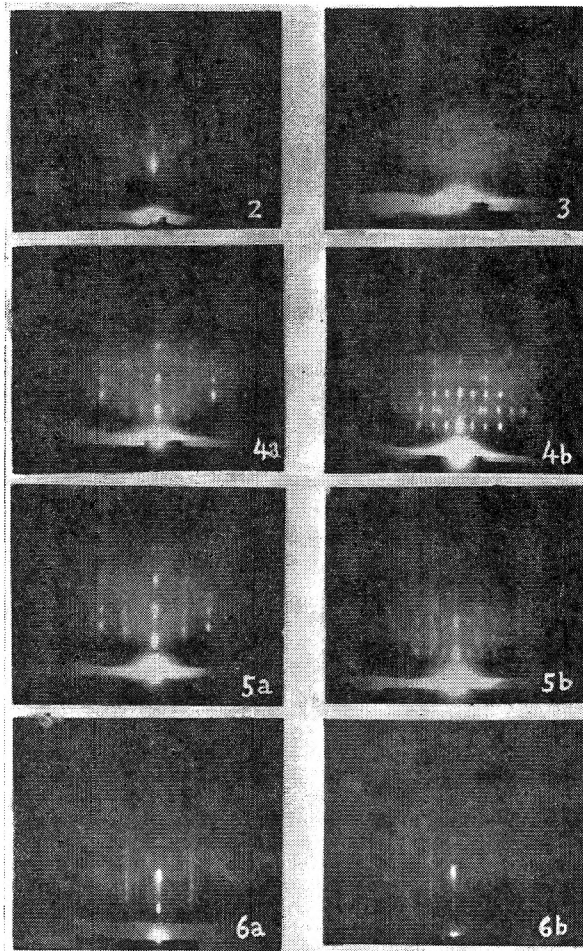


Fig. 2.—Fresh cleavage pattern of galena.

Fig. 3.—Two halo pattern obtained by a slightest oxidation of the galena cleavage face (black spots in Fig. 1).

Fig. 4.—Lead sulfate on galena cleavage face (plain circles in Fig. 1): a, beam parallel to cube edge; b, beam parallel to face diagonal.

Fig. 5.—Composite pattern due to lead sulfate and to basic sulfate, $PbSO_4 \cdot PbO$, on galena cleavage face (crosses on plain circles in Fig. 1): a, beam parallel to cube edge; b, beam parallel to face diagonal.

Fig. 6.—Basic sulfate of lead, $PbSO_4 \cdot PbO$, produced on galena cleavage face below about 280° (crosses in Fig. 1): a, beam parallel to cube edge; b, beam parallel to face diagonal.

Two-halo Pattern.—Below about 200° , the two-halo pattern shown in Fig. 3 was obtained. With slight oxidation, the cleavage pattern was predominant and a pattern like that of Fig. 2 was obtained. With increased oxidation the haloes increased in intensity, until the cleavage pattern almost disappeared. Above approximately 150° , a crystalline pattern appeared, intermingled with the halo pattern, and above, 230° the halo pattern was no longer observed.

By visual measurement the two haloes were found to correspond to spacings: $d_1 = 2.5 \text{ \AA}$. and $d_2 = 1.4 \text{ \AA}$. However, since the measurement of the radii of haloes was only approximate nothing definite was expected from the above two spacings except that something amorphous or of exceedingly minute crystalline grains was produced on the cleavage surface.^{22c}

Lead Sulfate Pattern.—As is seen in Fig. 1, a crystalline pattern was obtained between 170° and 280° . The diffraction pattern is shown in Figs. 4a and 4b. From the analysis of these and other patterns obtained at various azimuthal settings of the specimen to electron beams, this substance

(22) G. P. Thomson and W. Cochran, "Theory and Practice of Electron Diffraction," Macmillan Co., Ltd., London, 1939, (a) p. 153; (b) pp. 162-184; (c) p. 186; (d) p. 171.

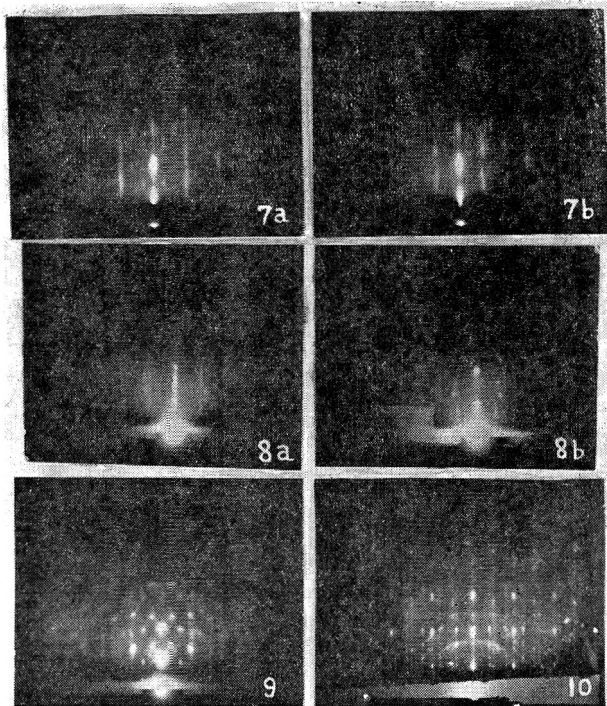


Fig. 7.—Basic sulfate of lead, $\text{PbSO}_4 \cdot \text{PbO}$, produced on galena cleavage face at temperatures between 280 and 350° (diagonal crosses in Fig. 1): a, beam parallel to cube edge; b, beam parallel to face diagonal.

Fig. 8.—Composite pattern due to the basic sulfate of lead and the unidentified elongated spot pattern (squares on diagonal crosses in Fig. 1): a, beam parallel to cube edge; b, beam parallel to face diagonal.

Fig. 9.—Complex pattern obtained by prolonged oxidation of galena cleavage face below 350°; beam parallel to cube edge.

Fig. 10.—Complex pattern obtained by oxidation of galena cleavage face at temperature above 350°; beam parallel to face diagonal.

was identified as lead sulfate, PbSO_4 .²³ Crystallites were oriented on the galena cleavage face in one of two ways as recorded in Table I.

TABLE I
ORIENTATION OF THE LEAD SULFATE CRYSTALLITES ON
GALENA CLEAVAGE FACE

Orientation	First direction	Second direction
I	$(001)_{\text{PbSO}_4} // (001)_{\text{PbS}}$	$[100]_{\text{PbSO}_4} // \langle 110 \rangle_{\text{PbS}}$
II	$(210)_{\text{PbSO}_4} // (001)_{\text{PbS}}$	$[001]_{\text{PbSO}_4} // \langle 100 \rangle_{\text{PbS}}$

In crystallite orientation I there is a virtual coincidence of the atomic distance along the $[100]_{\text{PbSO}_4}$ and $\langle 110 \rangle_{\text{PbS}}$ axes which lie in coincidence; and in orientation II the (210) section of the unit cell of lead sulfate lies parallel to the (100) face of galena. These two orientations were always induced simultaneously on the oxidized face so long as crystalline lead sulfate was produced. Their intensity ratio, however, was not a constant, but was affected largely by the rate of initial temperature rise in the oxidation and by other factors. A preliminary study of the relative abundance of the crystallites in the two orientations was made. For details the reader is referred to a microfilm record^{23a} of a detailed report of our work.

Basic Lead Sulfate Pattern.—In Fig. 1 it is seen that lead sulfate ceases to be the only oxidation product on the galena cleavage surface if oxidation is prolonged or if the temperature is raised above about 280°.

(23) R. W. James and W. A. Wood, *Proc. Roy. Soc. (London)*, **A109**, 598 (1925).

(23a) Microfilm record of "Surface Phenomena in Flotation," by Hitosi Hagihara, Massachusetts Institute of Technology Library, Cambridge, Mass.

A composite diffraction pattern due to lead sulfate and the basic sulfate produced on the galena cleavage surface is shown in Fig. 5. With additional oxidation the basic sulfate pattern increases in intensity until the patterns shown in Figs. 6a and 6b are obtained. From the analysis of these and other patterns obtained at various azimuthal settings of the specimen, this oxidation product was identified as "lanarkite," the basic lead sulfate Pb_2SO_5 .²⁴ This is orientated on galena in accord with orientation II of the neutral sulfate formed at lower temperature. For crystallographic details see microfilm record^{23a}. It is interesting to note that the diffraction pattern due to lanarkite becomes detectable only after the neutral sulfate layer has attained a thickness roughly estimated at 100 Å.^{22a}

Basic Sulfate Produced at Higher Temperatures.—Above approximately 280°, lead sulfate was no longer observed even under the shortest possible oxidation. Instead, two kinds of new patterns were observed between 280° and 350°. Of these one was determined to have the same unit cell as basic sulfate I with only a slight modification in its orientation. The other is intrinsically a new substance.

The basic sulfate pattern obtained at higher temperatures was often accompanied by a new type pattern consisting of diffuse, vertically elongated spots. An example is shown in Figs. 8a and 8b. The intensity ratio of these two intermingling patterns was not a constant, but varied even on the same specimen. This implies that the two substances are distinct from one another and are not distributed uniformly over the surface.

Higher Oxidation Products.—Upon prolonged oxidation, basic sulfate patterns are obliterated by other more complicated diffraction patterns. These are similar in appearance yet differ in that they are highly susceptible to slight changes in the conditions of sample preparation. An example of such patterns is shown in Fig. 9. Oxidizing temperatures above 350° resulted in varied types of diffraction patterns consisting of sharp spots. An example is shown in Fig. 10. The analysis and identification of such complicated patterns are beyond the scope of the present study.

Interpretation of the Results

Two-Halo Pattern.—Halo patterns on solid surfaces are either an amorphous substance, crystalline grains of a few atoms in diameter, or an adsorbed gaseous layer.^{22,25} A halo pattern obtained in any experiment should, therefore, be interpreted in the light of additional information concerning the nature of the surface substance.²⁶

In the present experiment the two-halo pattern was obtained by heating the galena cleavage face slightly in open air. To determine if this pattern was caused by thermal disturbances of the surface atoms, or by the oxidizing action of the surrounding atmosphere, fresh galena cleavage faces were heated in a vacuum furnace for one hour at a pressure of 10^{-2} – 10^{-4} mm. Electron diffraction results showed that thermal roughening of the cleavage face did not take place below 350°, and the two halo pattern was not observed at 100, 200, 250 or 300°. These facts indicate that the atomic aggregates responsible for the halo pattern were produced by the tarnishing action of air on the cleavage surface.

Additional observations which contributed to the identification of the halo pattern substance were: (1) a halo pattern was obtained simultaneously with the crystalline lead sulfate, (2) the halo pattern substance and the crystalline lead sulfate underwent the same chemical reactions with distilled water or with aqueous solutions of xanthate under various pH conditions (a detailed explanation is presented in Part II), and (3) the surface oxidation of galena became progressive above 150° with the formation of crystalline lead sulfate.

Orientation of Lead Sulfate Crystallites.—According to the theory of chemical kinetics on solid surfaces^{27,28} the

(24) W. E. Richmond and C. W. Wolfe, *Am. Mineralog.*, **23**, 799 (1938).

(25) H. Germer, *Phys. Rev.*, **49**, 163 (1936).

(26) G. I. Finch and H. Wilman, *Trans. Faraday Soc.*, **33**, 337 (1937).

(27) A. Smekal, "Strukturempfindliche Eigenschaften der Kristalle," *Handb. d. Phys.* 24/2, p. 807, Verlag von Julius Springer, Berlin, 1933.

(28) M. Volmer, "Kinetik der Phasenbildung," Verlag von Theodor Steinkopff, Dresden, 1939, p. 189.

tarnishing action of oxygen on a galena cleavage face commences at certain active sites. Such sites may be the corners and edges of cracks and steps inevitably present on cleavage surfaces or some points on its surface where atoms are loosely bound. At such sites the reaction, $PbS + 2O_2 = PbSO_4$, identical with activated adsorption may take place. Below approximately about 170° , however, the temperature may be too low to permit sufficient surface mobility for crystalline aggregation. Lead sulfate formed incoherently may yield the halo pattern. With additional oxidation the reaction is supposed to take place on less and less active points resulting in the intensification of the halo pattern. Above 170° these oxidation products become sufficiently mobile to order themselves into crystalline arrays.

The orientation of lead sulfate crystallites may be explained by the theory of crystal growth on solid substrates. It is generally accepted that the nucleus formation of the growing crystal is greatly facilitated at the edges of cracks or at the internal angle at the bottom of a step inevitably present on crystal surfaces.^{27,28} After Thomson and Cochran^{22b} the orientation of the growing crystal on a single crystal substrate is determined primarily by the law that one of the simple zone axes of the growing crystal lies in coincidence with the line of atoms along an irregularity of the substrate, which is also a simple zone axis. This is in accord with the observations recorded above with orientation II.

Formation of the Basic Lead Sulfate.—Formation of lanarkite, Pb_2SO_4 , in open air, by prolonged heating of the galena surface, may be interpreted as due to the dissociation, as it thickens, of the outermost portion of the sulfate layer. According to Schenck,²⁹ the first step in the decomposition of the lead sulfate in a roasting atmosphere containing sulfur dioxide and oxygen is represented by $2PbSO_4 = PbSO_4 \cdot PbO + SO_2$. The present study indicates a close orientation relationship between the basic sulfate in orientation I and the sulfate in orientation II.

At elevated oxidizing temperatures lead sulfate can no longer be in equilibrium with galena and the basic sulfate in orientation II is supposedly produced directly upon the cleavage face of galena. At still higher temperatures more basic sulfates such as $PbSO_4 \cdot 2PbO$, $PbSO_4 \cdot 3PbO$ or $PbSO_4 \cdot 4PbO$ are likely to be produced successively.^{29,30} Correlation of the complex electron diffraction patterns obtained at higher temperatures with the X-ray Debye-Scherrer ring data of the basic sulfates of lead reported by Clark, *et al.*,³¹ may be useful. As yet analysis of the patterns is incomplete.

Initial Oxidation under Environments Related to Flotation Studies

It is of interest, in connection with flotation to study the initial oxidation of galena under environments other than oxidation at elevated temperatures in a furnace atmosphere. Electron diffraction examination of ground powders does not give as definite a result as experimental work performed with single crystal cleavage faces. For ground powders this method is not expected to reveal surface states thinner than about 100 \AA . in thickness.^{22a}

Oxidation within Galena Powder.—Idealization of this dry-grinding oxidation condition was obtained by covering a fresh cleavage face of galena, about $2 \times 2 \times 1 \text{ mm.}$ in size, with powdered galena. The powder, approximately 200-mesh in size, was hand pressed from above, and another fresh cleavage face was placed upon the pressed powder. The boat containing the two specimens and the pressed galena powder was heated in a horizontal electric furnace with plugs on both ends to avoid the free circulation of open air within. Heating at a constant temperature was carried out for one hour, temperatures being measured with an alumel-chromel thermocouple inserted close to the buried specimen. After heating, the furnace was left to cool to room temperature, and the specimens were examined by electron diffraction. With the top specimen the exposed surface, not in direct contact with the powder, was inspected.

The results thus obtained below 350° are summarized in Table II. From this study it was confirmed that lead sul-

fate is again the lowest oxidation product on the galena cleavage surface oxidized in galena powder.

TABLE II

ELECTRON DIFFRACTION ANALYSIS OF THE SURFACE COATINGS PRODUCED ON GALENA CLEAVAGE FACE OXIDIZED UPON OR WITHIN GALENA POWDER FOR ONE HOUR

Temp., °C.	Above galena powder	Within galena powder
240	$PbSO_4$ only	$PbSO_4$ only
280	$PbSO_4$ + unidentified pattern	$PbSO_4$ only
300	$PbSO_4$ + unidentified pattern	$PbSO_4$ smeared with the other unidentified pattern
350	New pattern, no $PbSO_4$	New pattern, no $PbSO_4$

Oxidation in a Vacuum Furnace.—To study the surface oxidation of galena under extremely limited oxygen supply, an experiment on the oxidation of its cleavage face within a vacuum furnace was carried out at various temperatures. The time of oxidation for each temperature was one hour. The pressure within the furnace was maintained at about 10^{-3} mm. during the entire heating cycle. Moisture was removed from the furnace by phosphoric acid.

Electron diffraction results, directly connected with the present study, are summarized briefly in Table III. This study again shows that the lowest oxidation product on a galena cleavage face is lead sulfate even under limited oxygen supply.

TABLE III

ELECTRON DIFFRACTION ANALYSIS OF THE SURFACE COATINGS PRODUCED ON GALENA CLEAVAGE FACE OXIDIZED WITHIN A VACUUM FURNACE FOR ONE HOUR

Temp., °C.	Galena cleavage pattern	$PbSO_4$ pattern	Unidentified pattern	Pb_2O pattern
100	Very strong	Very faint		
200	Very strong	Very faint		
250	Weak	Weak	Weak	
300	Weak	Weak	Strong	
350				Strong

Oxidation in Water.—As a preliminary study of the surface changes of galena particles during wet grinding, changes of a fresh galena cleavage face in distilled water were studied. A fresh cleavage face $3 \times 3 \text{ mm.}$ size, was soaked in distilled water contained in a shallow glass dish. After the desired period, the specimen was removed from the water, dried in air, and examined by electron diffraction.

After a 20-minute soaking at 20° , the strong Kikuchi lines and bands peculiar to a fresh cleavage face were obscured. This implied that a slight disturbance had taken place on the ideally flat and regular cleavage surface.³²

Prolonged soaking for two days yielded a diffuse spot pattern of galena as shown in Fig. 11. Prolonged soaking for 4 to 7 days yielded similar, yet less diffuse spots. In all these cases, no visible change was observed on the soaked face; yet the surface remained hydrophilic.

Additional soaking up to 40 days at room temperature resulted in the formation of a visible layer on the surface. Its diffraction pattern consisted of rings formed by large numbers of sharp spots indicative of well grown crystallites oriented at random. Figure 12 shows this pattern. Upon analysis of the pattern it was concluded that this substance conforms best with the basic lead carbonate.³³

Oxidation in Wet Grinding.—Five grams of galena crystals, cleaned of tarnished surfaces, was hand ground in an agate mortar containing 10 cc. of water. The grinding was continued for 20 minutes. After grinding, one portion of the sediment was removed and dried. The remaining portion was left in the mortar until the water had evaporated slowly. These particles yielded electron diffraction patterns similar to those obtained with dry ground particles.

(29) R. Schenck, *Z. anorg. allgem. Chem.*, **148**, 351 (1925).

(30) R. Schenck and A. Albers, *Z. phys. allgem. Chem.*, **105**, 145 (1919).

(31) G. L. Clark, J. N. Mrgndich and N. C. Schieltz, *Z. anorg. allgem. Chem.*, **229**, 401 (1936).

(32) G. I. Finch and H. Wilman, *Erg. exakt. Naturwiss.*, **16**, 353 (1937); (a) p. 385.

(33) J. D. Hanawalt, H. H. Rinn and L. K. Fievel, *Ind. Eng. Chem., Anal. Ed.*, **10**, 457 (1938).

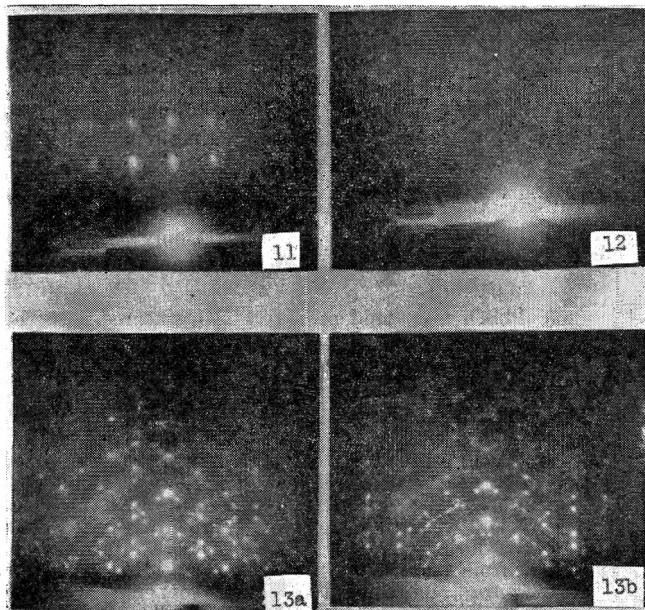


Fig. 11.—Galena cleavage face soaked in water for two days; beam parallel to cube edge.

Fig. 12.—Galena cleavage face soaked in water for 40 days.

Fig. 13.—Spot pattern due to the natural oxidation product on the cleaved surface of galena: a, beam parallel to cube edge; b, beam parallel to face diagonal.

The interpretation of these and the preceding results on the oxidation of galena under wet conditions may be that during wet grinding, the surface of each particle is oxidized to some degree, producing lead sulfate. This sulfate, however, is dissolved in water making the remaining surfaces slightly rough in molecular dimensions. Upon prolonged soaking, the dissolved sulfate reacts with carbon dioxide dissolved in water precipitating basic lead carbonate.

Some Anomalies on the Fresh Galena Cleavage Surface

During the course of the present electron diffraction study, certain anomalies of the fresh and apparently perfect cleavage surface of galena were observed.

Contamination of the Impurity Crystallites.—Fresh cleavage faces of galena cleaved from ideally shaped single crystals were often found contaminated with several kinds of impurity crystallites. These crystallites had complete orientations with respect to the galena lattice but were not distributed uniformly over the surface. In one instance the pattern was clear-cut enough to permit identification as aramayoite, $\text{Ag}(\text{Sb}, \text{Bi})\text{S}_2$, as analyzed by Yardley,³⁴ or as matildite, AgBiS_2 .³⁵ Several kinds of such diffraction patterns were obtained and are being compared with the X-ray structure data of various minerals.

Infiltrated Natural Oxidation Along the Cleavage Surfaces.—Another finding worthy of mention is the infiltrated natural surface oxidation along single crystal boundaries within a compact massive block of galena. An example shown in Figs. 13a and 13b is due to a surface film exposed by breaking the crystal along such surfaces. The film was thick enough to show interference colors. The pattern itself is of interest in that it shows a large number of twin and irrational spots.^{22d} Detailed explanations are beyond the scope of the present report; however, they will be presented in a separate paper. The possibility of such natural oxidation within mineral blocks should be considered in selecting massive galena for laboratory investigations of oxygen-free flotation, contact angles of air bubbles,³⁶ or for the study of its adsorptive property for the collecting reagents. The mere removal of the outer tarnished surface of the block may be unsatisfactory for the study of oxygen-free flotation.

(34) K. Yardley, *Mineralog. Mag.*, **21**, 163 (1926).

(35) P. Ramdor, *Sitzungsber. Preuss. Akad. Wiss. Nr.*, **6**, 71 (1938).

(36) I. W. Wark and A. B. Cox, *Trans. Am. Inst. Mining Met. Engrs.*, **112**, 189 (1935).

Discussions in Connection with Flotation Studies

Several flotation studies have been concerned with the chemical composition of the oxidized layers formed on galena. Taggart, Taylor and Ince¹² and Taggart, Taylor and Knoll,¹¹ have concluded that when galena is ground under oxidizing conditions, the surface changes to lead sulfate. Their conclusions are based upon the chemical analysis of Pb^{++} and SO_4^{--} ions in water when galena is placed in it. The newly formed sulfide surfaces are quickly changed into lead sulfate, PbSO_4 , basic lead sulfate, one of the more or less oxidized sulfur-oxygen compound of lead, PbS_mO_n (where the ratio of n/m is less than 4), and lead carbonate, PbCO_3 . Hydroxyl ions have also been found to be thrown into the solution. Gaudin, *et al.*,³⁷ have analyzed the sulfate, hydroxyl, carbonate and reducing ions in the aqueous filtrate from reaction between potassium *n*-amyl xanthate and galena. From these experimental studies it is now generally accepted that the surface of galena exposed to air in either dry or wet grinding, is a complex mixture of sulfoxides, hydroxides and carbonate of lead.¹⁷

The present electron diffraction study has confirmed the formation of lead sulfate as the lowest oxidation product on the galena cleavage face. In the dry grinding process the sulfate is evidently produced and anchored to each ground particle, as the close orientation relationship between the lead sulfate crystallites and the galena cleavage face indicates. In the wet grinding process, however, the sulfate is evidently produced and subsequently washed away into the solution without forming a surface layer thicker than a monoionic film. This is confirmed by the detection of very weak sulfate rings on dried wet ground powder and by the observation of surface roughening only on the cleavage face soaked in plain water. The sulfate layer produced on the cleavage face in a dry atmosphere is also easily washed away by soaking in water (detailed explanations will be given in Part II). Thus, Taggart, Taylor and Ince's view¹² of the *adherent* coating on galena exposed to water ($\text{galena} \cdot \text{PbSO}_4 \cdot \text{PbO} \cdot \text{H}_2\text{O}$) is not supported in the present research.

As to the lead-sulfur-oxygen compounds other than sulfate, only the basic sulfate, Pb_2SO_5 , has been confirmed to exist. In this instance the ratio of n/m in the formula, PbS_mO_n , will be greater than 4, which is contrary to the conclusion of Taggart, Taylor and Knoll.¹¹ There remains the possibility that the halo pattern substance may be a mixture of this PbS_mO_n with PbSO_4 and that it represents an incomplete monolayer. For, if the PbS_mO_n had formed a polymolecular coating, some crystalline pattern, *e.g.*, that due to PbS_2O_3 , already analyzed by X-rays³³ should have been observed when the oxidizing condition was slightly more intense than that corresponding to the formation of the halo pattern substance alone.

The formation of surface hydroxides and car-

(37) A. M. Gaudin, F. Dewey, W. E. Duncan, R. A. Johnson and O. F. Tangel, Jr., *ibid.*, **112**, 319 (1935).

bonate of lead, indicated from the chemical analyses, was not observed in the present study except on prolonged soaking when a visible film was obtained. The basic carbonate, however, is more likely to be produced from the sulfate dissolved in water, than directly upon the galena cleavage surface. Taylor and Knoll's observation¹⁶ that the carbonate ions do not increase by prolonged exposure of galena to air is in conformity with the present results.

Taylor and Knoll¹⁶ have presented a hypothesis that the compounds formed by the initial oxidation of galena are firmly anchored to the galena surface and differ in structure from compounds in their normal states. They have concluded that lead-sulfur-oxygen compounds (lead sulfate, etc.), first formed, are probably isomorphous with galena and that this "cubic" lead sulfate would have a solubility between lead sulfide and the ordinary orthorhombic lead sulfate. However, the above cubic modification of lead sulfate, etc., was never observed in this investigation where the thinnest possible layer detectable by electron diffraction was studied. Taylor and Knoll proposed this hypothesis because of their belief that the ordinary orthorhombic lead sulfate would not fit in register with the cubic lattice of galena. The present results show definitely that ordinary lead sulfate can orient itself in two manners, each having a close relationship in the arrangement of atoms at the interface between the substratum and the superstratum.

As to the speed of oxidation exact quantitative results cannot be expected from electron diffraction study alone. Qualitatively, it has been confirmed that the surface oxidation does take place in open air, even at room temperatures. The speed of oxidation, however, was found to be rather slow at room temperature, since after several days' exposure the cleavage pattern was still observed by electron diffraction although complete smearing of the cleavage pattern by diffuse haloes was observed on the cleavage face exposed to open air for over a month. These facts may be consistent with the experimental results and views reported by Siedler²¹ and Bull, Ellefson and Taylor²⁰ that the atmospheric oxidation of galena does not proceed rapidly at room temperatures. The result of Tag-

gart, Taylor and Knoll¹⁷ on the abstraction of xanthate by galena exposed to air for varied lengths of time also shows the slow progress of oxidation.

Oxidation of the cleavage face becomes markedly progressive with the formation of the crystalline lead sulfate upon it. This rapid progress commences at about 150° in open air.

During the wet grinding process the sulfate produced is evidently removed continuously from the surface to the solution, making the oxidation progressive. According to electron diffraction, the fresh galena cleavage face changes its surface state more rapidly in water than in open air; its surface change is detectable only after 20 minutes soaking in water at room temperature, and after a few days' soaking the characteristic feature of the ideally flat cleavage surface is completely lost. The rapid oxidation of galena as proposed by Taggart, Taylor and Knoll¹¹ and by Taylor and Knoll¹⁶ is in conformity with the present results on progressive oxidation in the grinding processes, since the oxidation they are concerned with is that involved in the grinding processes.

Thus, the present electron diffraction study has shown that there is no contradiction between the views of slow and rapid oxidation. The former is concerned with the slow progress of oxidation in air at room temperatures, while the latter is concerned with the rapid and progressive oxidation during wet grinding.

As to the rapid initial oxidation of a "cleaned and pure" galena surface reported by Lintern and Adam¹⁸ or by Herd and Ure,¹⁹ the electron diffraction method may be unable to detect the surface changes involved, since the surface phenomena in these cases are supposed to be the formation of a monomolecular or monatomic oxygen film on the surface.

The author wishes to express his sincere thanks to Professor S. Nishikawa for his encouragement and interest in this work. The author is also grateful to Professors A. M. Gaudin of M.I.T. and M. A. Cook, of the University of Utah, for their kind suggestions and help in the publication of the present paper. Finally, heartfelt thanks are expressed to Miss E. Matsudaira for her continuous assistance in the preparation of this manuscript.

MONO- AND MULTILAYER ADSORPTION OF AQUEOUS XANTHATE ON GALENA SURFACES

BY HITOSI HAGIHARA¹

Taihei Mining and Metallurgical Laboratory,² Omiya City, Japan

Received February 26, 1951

The action of aqueous xanthate on galena surfaces has been studied by electron diffraction. Its primary function on both fresh and slightly oxidized faces lies in the formation of minute monomolecular patches adsorbed on the galena lattice. It is suggested that the monolayer is composed of xanthic acid molecules adsorbed with their polar heads attached to the lead atoms of the galena lattice. The layer is unstable in air.

Introduction

Studies of the principles of flotation, particularly the mechanism of the formation of the water-repellent surface films on minerals by the action of the collecting reagents, are extensive. Despite this fact, it has not been possible to unify the field under any single definite and conclusive theory.^{3,4,5} One of the chief reasons for the discrepancies in the prevailing theories, most prominent of which is the ionic adsorption theory by Wark and Gaudin *vs.* the chemical theory by Taggart, seems to lie in the fact that accurate direct methods are lacking in analyzing the extremely thin surface coatings produced on the mineral surfaces. The experimental tools have consisted mainly of chemical analyses of ions withdrawn from or taken into the aqueous solutions of the collecting reagents as the result of their interactions with the mineral particles, of chemical analyses of the leached products from mineral surfaces, of surface potential measurement of the minerals involved in the reaction, and of contact angle measurement of air bubbles attached to them.³⁻⁶

The electron diffraction method, which has been shown capable of revealing coatings as thin as 10–12 Å. on an ideally flat cleavage surface of a single crystal^{7b} offers a new approach toward flotation theory.

In addition to the practical problem of flotation, it is of interest to study the structure of the surface films formed on crystal faces by adsorption of water-soluble heteropolar substances. The structures of surface films of water-insoluble substances formed on polished metal surfaces or on single crystal faces have already been studied by X-ray or electron diffraction,^{7c,8} or more recently by electron microscopy⁹; whereas, for the surface films of water-soluble heteropolar substances with short alkyl groups, no such structural studies have yet

been reported. Sodium alkyl xanthates are suitable since their aqueous solutions are known to affect the surface of sulfide minerals, *e.g.*, of galena. The alkyl group generally is ethyl, propyl, butyl or amyl.

In the following study, the mineral, galena, was selected because (1) it has well developed cleavage, which is well suited for electron diffraction study; (2) it does not require flotation activation; and (3) the current theories of flotation are based to a large extent upon experiments with this system.^{4b} It is the object of the present study to elucidate the molecular surface states found on xanthated galena. This should lead to a better correlation between the known principles of surface chemistry and the nature of water-repellent collector coatings in flotation.

Blank Experiments of the Action of Distilled Water on Galena Surfaces.—Before discussing the action of aqueous xanthate on galena surfaces, a brief explanation will be given of the action of distilled water itself. Three specimens typical of various oxidized states, each 2 × 2 × 0.5 mm. in size, were prepared by heating fresh cleaved faces in air. (See experimental results summarized in Fig. 1, Part I.) The first corresponded to the formation of a disorganized oxidized coating, perhaps lead sulfate (halo-substance), the second to crystalline lead sulfate, and the third to the basic sulfate. Each of these specimens was soaked in 20 cc. of distilled water for 20 minutes at 30°. Upon removing them from the water, they all were found to be covered with a thin water film which soon dried in open air. These specimens were examined by electron diffraction. The diffraction patterns showed similar features in every case as shown in Fig. 2. The pattern has been identified as due to the (100) face of galena, rich in uniform surface even in the ultra-microscopic sense, yet only slightly rougher than the fresh cleavage surface.^{7a,10a} The elongation of the diffraction spots toward the shadow edge is interpreted as being due to the refraction of the electron beam at the flat part of the surface. The sharpness of each elongated spot shows that such flat domains are fairly wide.

This experiment shows that the surface oxidation products on a galena cleavage surface (lead sulfate either in molecular or in crystalline form or basic sulfate) are washed away from the surface by distilled water making the exposed galena surface substantially uncoated by oxide and but slightly rough on a molecular scale.

Experimental Procedures with Aqueous Xanthate.—A fresh cleavage face of galena, free from visible surface flaws, was cut by cleaving to 2 × 2 × 0.5 mm. size and was oxidized dry to the desired extent (Fig. 1, Part I). The oxidation was carried out to various degrees as in the blank experiment. Each oxidized specimen was then immediately soaked in 10 cc. of aqueous xanthate for 20 minutes at 20°. The concentrations of the aqueous solutions were from 10 mg./l. to 500 mg./l. The xanthated specimens were placed in the electron diffraction camera immediately after completion of the reaction and the patterns obtained.

The xanthates used in the experiments were purified and kept in a desiccator until needed. The interval of preserva-

(1) Kobayasi Institute of Physical Research, Kokubunzi, Tokyo, Japan.

(2) Former Mitsubishi Mining and Metallurgical Laboratory.

(3) A. M. Gaudin, "Flotation," McGraw-Hill Book Co., Inc., New York, N. Y., 1932; A. M. Gaudin, "Principles of Mineral Dressing," McGraw-Hill Book Co., Inc., New York, N. Y., 1939.

(4) A. F. Taggart, "Handbook of Mineral Dressing," John Wiley & Sons, Inc., New York, N. Y., 1945; (a) p. 12-05, Fig. 1; (b) p. 12-04.

(5) I. W. Wark, "Principles of Flotation," Australian Institute of Mining and Metallurgy, Inc., Melbourne, 1938; (a) p. 122; (b) p. 130.

(6) W. Petersen, "Schwimmaufbereitung," Theodor Steinkopff, Dresden, 1936, Chap. 4.

(7) G. P. Thomson and W. Cochrane, "Theory and Practice of Electron Diffraction," Macmillan & Co., Ltd., London, 1939; (a) p. 146; (b) pp. 152–154; (c) pp. 197–209; (d) p. 205.

(8) G. L. Clark, "Applied X-Rays," McGraw-Hill Book Co., Inc., New York, N. Y., 1940, pp. 441–445.

(9) H. T. Epstein, *THIS JOURNAL*, **54**, 1053 (1950).

(10) G. I. Finch and H. Wilman, *Erg. exakt. Naturwiss.*, **16**, 353 (1937); (a) p. 385; (b) p. 394.

tion did not exceed one month at the longest, and in most cases they were used immediately after purification. For purification the xanthates were first washed with ether, then dissolved in acetone and recrystallized from the acetone solution by the addition of either ether or benzene. Vacuum drying was applied to the precipitated xanthates.

The pH of the aqueous solution was controlled by the addition of hydrochloric acid on the acidic side and by either potassium or sodium hydroxide on the alkaline side. pH measurements were made either with an electric pH meter using an antimony electrode or by the colorimetric method. In the study of the action of aqueous xanthate on fresh cleavage surfaces, the above oxidizing treatment was omitted, otherwise, the same procedures were used throughout.

Action of Aqueous Xanthate on Slightly Oxidized Faces.

I. Adsorbed Molecular Film.—Electron diffraction examination of these surfaces revealed three patterns, namely, the streak pattern, the built-up film pattern, and the ring pattern (Table I). Of these, the first two are more inclined to being associated and are taken as evidence of formation of an adsorbed molecular film. The other structure seems due to precipitation of crystallites, probably lead xanthate on the surface. The first type of film will be discussed first.

TABLE I

CLASSIFICATION OF THE ELECTRON DIFFRACTION PATTERNS OBTAINED ON GALENA SURFACES IN REACTION WITH NEUTRAL AQUEOUS XANTHATES

R, ring pattern; S, streak pattern; B, built-up film type pattern; +, a composite pattern

	Slightly oxidized faces				Cleavage faces	
	25 mg./l.	100 mg./l.	200 mg./l.	500 mg./l.	100 mg./l.	500 mg./l.
Na E X	R + S	S S	S S + B	S S B		S
Na P X		R + S		R + S		
Na B X	R	R + S		S S		S S
Na A X		S S S	S S S	S + B B	S S	S S S
Na h X ^a		S S	S S		S S	S
K E X	R + S	S S		S S + B	S S	S
K P X		R + S		S S?		S
K B X	R	B		R + S		
				S S S		S
K A X	S	S S B		S S?		
				S S S	S S S	S S S
K h X ^a				B B		
				S		

^a Higher xanthate; the mixture of propyl, butyl and amyl xanthates.

The most commonly encountered diffraction pattern obtained on slightly oxidized faces after reaction with neutral aqueous xanthate is the diffuse streak pattern shown in Figs. 3a and 3b. This pattern arises irrespective of the use of either potassium or sodium xanthate so long as the fresh solutions of the newly recrystallized xanthates are used. Changes in the degree of pre-oxidation of the cleavage face up to the formation of the basic sulfate exerts no influence on this diffraction pattern. With higher xanthates, the streaks are more intense.

The pattern consists of the cross-grating pattern of galena (the same as that obtained in the blank experiment, Fig. 1) plus the additional diffuse, almost continuous streaks just over the former sharp and elongated spots. (Compare Fig. 3a with Fig. 2.) On casual examination, the streaks might be identified with the Kirchner-Raether lines observed in the fresh cleavage pattern of galena, as shown in Fig. 1. However, those lines are sharp and not as wide as with the present diffuse streaks. Furthermore, the general features of the whole pattern are somewhat different: with a fresh cleavage face the Kikuchi lines and bands (diagonals) are more intense than the Kirchner-Raether lines, whereas, with the present pattern, the diffuse streaks situated at the positions of the K.-R. lines enhanced at the expense of the now Kikuchi bands. This may be seen by comparing Fig. 3a with Fig. 1.

On this evidence, it is concluded that surface changes due to xanthate are seen.

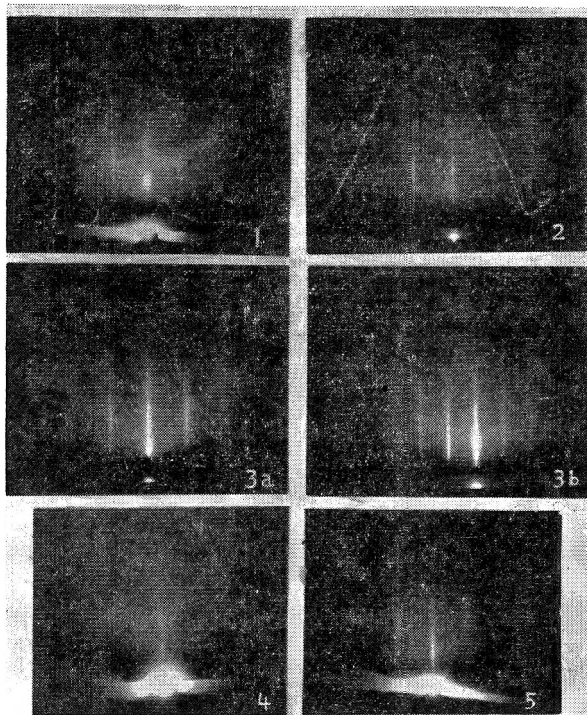


Fig. 1.—Fresh cleavage pattern of galena.

Fig. 2.—Slightly oxidized galena face soaked in distilled water; beam parallel to cube edge.

Fig. 3.—A diffuse streak pattern obtained on slightly oxidized galena face after reaction with aq. Na A X, 100 mg./l.: (a) beam parallel to cube edge; (b) beam parallel to face diagonal.

Fig. 4.—A multilayer pattern obtained on slightly oxidized galena face after reaction with aq. Na E X, 500 mg./l.; beam parallel to cube edge.

Fig. 5.—A built-up type pattern obtained on slightly oxidized galena face after reaction with aq. K A X, 500 mg./l.; beam parallel to cube edge.

Interpretation of the Diffraction Pattern.—In the preceding section, it was mentioned that the vertical diffuse streaks are situated just over the sharp lines of the galena pattern and that this is true at any azimuth of the crystal to the electron beam. This means that the scattering centers of the streak-producing substance are arrayed in the same way as the arrangement of one kind of atom, e.g., the lead atoms, on the (100) face of galena. That is, the lateral spacing of the coating substance is the same as that of the lead atoms in galena. In a direction normal to the crystal surface, the coherence is extremely poor, or else there is no periodicity at all, since if there were any coherence or periodicity in this direction, some spot pattern should have been observed instead of the streaks actually seen. The diffuseness in the breadth of the streaks means that the coherence in directions parallel to the crystal surface is somewhat imperfect. From the breadth of the streaks, it is estimated that the extent of the coherent areas is of the order of ten unit cells of the (100) face of galena, or of the order of 50 Å. in most cases.

Accordingly, the most probable geometrical interpretation of the present pattern seems to be that it is due to the scattering of electrons by minute patches of a two-dimensional lattice with its scattering centers arrayed in the same manner as

the arrangement of lead or sulfur atoms on the (100) face of galena, as illustrated schematically in Figure 6. The above expression of the "two-dimensional" lattice cannot be rigorous in the strict geometrical sense, since a flat surface layer a few scattering centers thick may also produce the streak pattern. It is impossible to determine from the electron diffraction experiment alone whether the surface layer is monomolecular or not, yet it is certain that it is extremely thin.

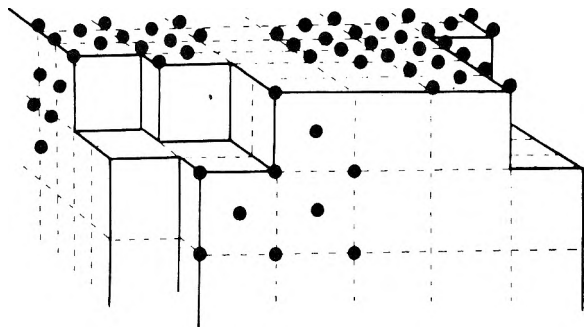


Fig. 6.—A schematic drawing of the interpretation of the diffuse streak pattern as obtained on galena faces by the action of aqueous xanthate.

As to the substance constituting the film, it is most likely to be connected with the xanthate group, since plain water did not produce the streak pattern, and since the nature of the alkyl group of xanthate has been found to influence the intensities of the streaks. The area occupied per molecule on the galena surface in the above arrays is $(5.97 \text{ \AA.})^2/2 = 17.8 \text{ \AA.}^2$, which is very near to the cross section of an alkyl group in solid paraffin, 18.5 \AA.^2 .¹¹ Thus, the above geometrical interpretation does not conflict with molecular volume considerations. Further detailed discussions on the nature of the present film will be given in a later section.

II. Built-up Film Type Multilayer.—With concentrated aqueous xanthate, *e.g.*, 500 mg./l., the reacted faces occasionally showed non-uniform patches of some visible film upon them. On such surfaces, crystalline patterns distinctly different from the preceding streak patterns were often obtained.

Diffraction Pattern.—Figures 4 and 5 show two examples obtained from oxidized faces conditioned in aq. Na E X and K A X, respectively. The treating solutions were 500 mg./l. in concentration in both cases. The characteristic features in these patterns are: (1) the equidistant array of spots on the center line; and (2) several very weak vertical streaks at some distances from it. Under certain circumstances, the side streaks consist of spot arrays. By comparing Fig. 4 with Fig. 5, it is apparent that the distance apart of the spots on the center line is directly affected by the length of the alkyl group of the xanthate used, the distance being smaller when the chain length is greater.

Interpretation of the Diffraction Pattern.—The result of the analyses of the present diffraction patterns is summarized in Table II. The equidistant spots on the center line are interpreted as some layer built up parallel to the substrate surface with the periodicity of the above tabulated long spacing. The second intense region observed with butyl or amyl xanthate corresponds to spacing 1.2–1.3 Å., in an approximate coincidence with the C—C

TABLE II
RESULTS OF THE ANALYSIS OF THE BUILT-UP FILM TYPE
MULTILAYER

	Number of specimens	Long spacing, Å.	Second intense region, Å.	Side spacings
Na E X	2	11–12		13.5?; 5.9; 4.4; 4.2; 3.6; 2.1
Na B X (iso-)	1	16.5	1.2–1.4	6.0; 4.3; 4.0; 3.0; 2.0
K E X	1	12		?
K B X	4	17	1.2–1.3	?; 4.7; ?
(<i>n</i> - and iso-)				
K A X	3	17–18	1.2–1.4	5.5; 4.5; 3.4; 2.3
(<i>n</i> - and iso-)				

spacing of an alkyl group, 1.27 Å. The observation of this region on the center line suggests that the alkyl group is oriented upright. The difference of the long spacings in the films due to *n*-butyl and ethyl xanthates is 5 Å. (Table II) whereas the difference in the lengths of a *n*-butyl and an ethyl group should be 2.54 Å., since the addition of each carbon atom increases the length of an alkyl group by 1.27 Å. Thus, the long spacing of the film may be explained by postulating that the periodic layer contains two upright alkyl groups. This would occur if the film were of the Y-type in which heteropolar molecules form alternate layers as shown schematically in Fig. 7.

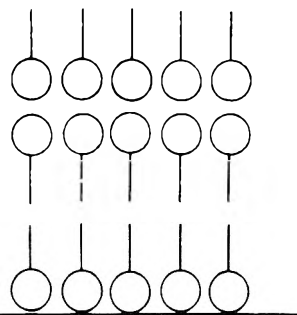


Fig. 7.—A schematic drawing of the built-up Y film.

The next problem to be considered is what kind of molecules constitute this Y-film. Because of the lack of data on the structure of xanthate molecules, their probable shapes have been constructed from the data on atomic distances, bond angles and ionic radii of the constituents.¹² The shaded area in Fig. 8 represents such a drawing of the K *n*-butyl xanthate molecule. With this model the length of an isolated K *n*-B X molecule is estimated to be between 11 and 12 Å. If these molecules are built into a Y-film, stretched to their full lengths, the long spacing observable in a diffraction experiment should lie between 22 and 24 Å. This is too large to explain the long spacing of the actual film obtained. The discrepancy is too large to be explained either by the error in the measurement of the separations of the spots on the center line or by the possible modifications in the probable shape of the —C—S— group.



This discrepancy, however, is removed most reasonably by assuming a configuration of the two

(11) A. Müller, *Proc. Roy. Soc. (London)*, **A120**, 437 (1928).

(12) L. Pauling, "The Nature of the Chemical Bond," Cornell University Press, Ithaca, N. Y., 1940.

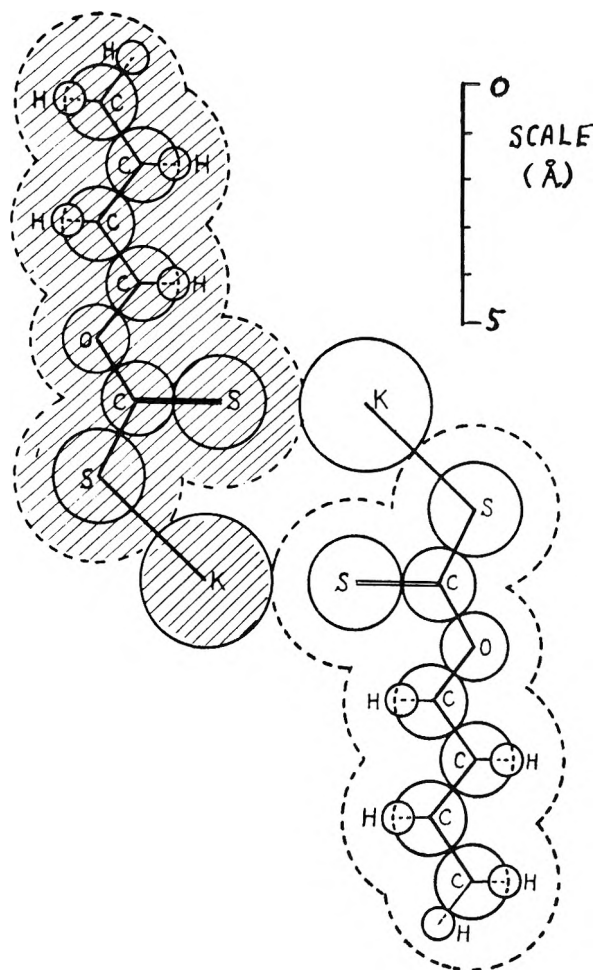


Fig. 8.—The probable shape of a K *n*-B X molecule (shaded) and the coupled state of two K *n*-B X molecules (total).

oppositely faced polar heads of the molecules as in the supposed arrangement of the two oppositely faced COONa groups in sodium stearate or palmitate crystals in their β -forms.¹³ In order to make the long spacing near 17 Å. for K *n*-B X with this configuration, an arrangement of molecules as shown in Fig. 8 is required. The long spacing of 12 Å. for ethyl xanthates is also explained with this configuration. The value 17 Å. for K A X is also explained consistently by assuming that the alkyl group in this case is of the isoamyl type.

As to the lateral configuration of the molecules in the film, the side spot rows or streaks have not been observed so distinctly in the present electron diffraction experiment that their measured and calculated spacings in Table II are inevitably inaccurate. Qualitatively, the observation means that there exists some regularity in the lateral arrangement of the molecules in the present Y-film.^{7c} The determination of the geometrical configuration in terms of the above spacings, however, may be too speculative with the present diffraction patterns.

Effect of the pH of the Solution on the Adsorbed Film.—Figure 9 represents a diffraction pattern obtained with a slightly oxidized face conditioned in aq. K A X, 100 mg./l.

at pH 3. It consists of the elongated diffuse galena spots resembling those obtained with a fresh cleavage face soaked in plain water for a few days. The interpretation may be the same, *i.e.*, a surface roughening on the molecular scale has taken place on the crystal face.

At pH 4.5 or 4.8, the adsorbed film patterns were observed clearly, yet the elongated galena pattern was also fairly strong suggesting that the reaction in these solutions were intermediate between the strongly acidic and the neutral cases. At pH 6, the reaction was the same as with the neutral solution.

At pH 11, a diffuse pattern was obtained, similar to the "curved lines and short arcs of circles" reported by Murison¹⁴ on the surface films of alcohols or fatty acids spread on metal blocks. Figure 10 represents a pattern obtained with aq. K A X, 100 mg./l. at pH 11.

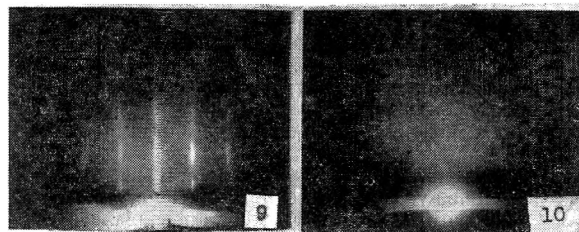


Fig. 9.—Slightly oxidized galena face after reaction with aq. K A X, 100 mg./l. at pH 3. Beam parallel to cube edge.

Fig. 10.—Slightly oxidized galena face after reaction with aq. K A X, 100 mg./l. at pH 11. Beam parallel to cube edge.

Since at pH 11, our aqueous solutions became opaque from suspended white precipitates, a deposit of non-crystalline character may have formed on the surface examined by electron diffraction.

Stability of the Adsorbed Films.—The diffuse streak pattern obtained by conditioning either fresh or slightly oxidized galena cleavage faces in xanthate solutions changes rapidly into a halo pattern on exposure of the specimen to air. The change is marked even after several hours exposure and within a few days the pattern changes completely into the mixture of the haloes and the elongated galena spots regardless of the kind of xanthate used.

The built-up film type pattern is also changed into haloes by the exposure of the specimen to air. With Na E X or with Na B X, this change was as rapid as with the streak pattern, whereas with K B X the change was rather slow. In one instance the built-up film type pattern obtained with K B X persisted after 10 days exposure to air.

Prolonged exposure of the specimens to air for a few weeks resulted in very diffuse rings in every case. This is believed to be due mainly to the oxidation of the galena surface and not to further decomposition of the already collapsed layer. The same diffuse rings have been obtained from galena surfaces exposed to air for over a month after reaction with water.

Transition of the Fresh Cleavage Surface to the Oxidized State.—The multilayer pattern has never been obtained on fresh cleavage faces even under conditions corresponding to slightly oxidized surfaces. Accordingly, with the progress of the oxidation of the fresh cleavage face, there is expected to be observed an intermediate surface state between the above two in its adsorptive property for the aqueous xanthate. This intermediate state was observed with the fresh cleavage face exposed to air for five days at room temperature before reaction with aqueous xanthate. After the reaction, the specimen showed the composite pattern due to the mono- and multilayers. The multilayer may well be produced with less oxidation, yet for the present purpose it is sufficient to know that the transition is gradual and without any particular intermediate state of adsorption, and that the fresh galena cleavage face is changed to an oxidized state in a few days exposure to air at room temperature.

Additional Experiments on the Structure of the Multilayer.—In order to obtain further experimental data as to

(13) P. A. Thiessen and J. Stauff, *Z. phys. Chem.*, **A176**, 397 (1936).

(14) C. A. Murison, *Phil. Mag.*, **17**, 201 (1934).

the nature of the built-up film type multilayer formed on dry-oxidized galena surfaces by aqueous xanthates, an analogous experiment has been carried out using the natural surface of pyrite. A well developed (210) face of pyrite, on which an extremely thin $\gamma\text{-Fe}_2\text{O}_3$ (or Fe_3O_4)¹⁵ film was observed by electron diffraction, was conditioned in a 100 mg./l. K E X solution at 20°. At pH 7.3 the treated surface was still hydrophilic. The electron diffraction examination of the reacted surface showed the unchanged oxide layer. At pH 4.4, the surface was hydrophobic and yielded the equidistant spot array on the center line. The long spacing of the pattern was calculated to be 12 Å., the same value as that obtained on slightly oxidized galena surface with the same aq. K E X.

Recently Sato¹⁶ obtained the built-up film type multilayer on the cleavage face of zinc blende, activated by copper sulfate, and conditioned in aqueous xanthates. He reported that the long spacing of the layer is 12.3 Å. with ethyl xanthates and 17.2 Å. with K n-B X. These results on galena, pyrite and activated zinc blende suggest that the structure of the built-up film type multilayer is unaffected by the chemical composition of the adsorbing crystal surface, but is dependent on the type of xanthate used in the reaction.

The most natural supposition, therefore, is that the multilayer present may be formed simply by the crystallization of xanthate with a certain crystallographic plane parallel to the underlying galena surface, and is not to be taken as a built-up film type layer. In order to decide whether this is due to simple crystallization or if any difference in the array of molecules exists between this layer and the solid xanthate, a preliminary X-ray structure analysis was carried out with a single crystal of K n-B X. The single crystal was prepared by the slow precipitation of the purified xanthate from its acetone solution. The symmetry and the dimensions of its unit cell were determined by the Laue, crystal rotation and the Sauter methods. The results of the analysis, though provisional as yet, indicates a monoclinic unit cell with $a = 9.6$ Å., $b = 19.6$ Å. and $c = 4.4$ Å. with $\beta = 93^\circ$. The longest spacing in the structure which gives rise to strong reflection was approximately 10 Å. quite different from 17 Å. obtained as the long spacing in the multilayer formed on crystal surfaces by conditioning in an aqueous solution of the same xanthate.

An example of the simple crystallization of K n-B X on solid surface from its aqueous solution was observed on a polished nickel plate conditioned in a 500 mg./l. solution of K n-B X for 20 min. at 20°. In this case the attachment of a comparatively thick, yellow hydrophobic surface coating was obtained. The electron diffraction examination yielded a crystalline pattern with fiber orientation. The periodicity along the fiber axis normal to the substrate surface was about 10.3 Å. This may well be interpreted as resulting from the crystallization of the xanthate with its b -axis normal to the substrate surface with otherwise random orientation.

Thus, the multilayer formed on crystal surfaces from aqueous xanthate was confirmed to have a configuration of molecules quite different from that of the reagent salt in its crystalline state. However, in order to carry out a more detailed consideration of the structural relationships between the multilayer and solid xanthate further studies in the structural analyses both of the multilayers by electron diffraction and xanthate single crystals by X-rays are desired.

Discussion

In the foregoing sections a description of the observed results and their interpretations have been given in detail. In the present section these results are summarized and compared with the existing theories of flotation.

The first problem to be considered is what type of adsorbates constitute these surface films. Tag-

gart and his collaborators^{17,18,19} have proposed the theory that the lead xanthate is precipitated by the double decomposition of lead sulfate (PbSO_4), lower sulfoxides (PbS_mO_n with n/m less than 4), lead carbonate (PbCO_3) or hydroxide (Pb(OH)_2). Recently Taggart has modified the earlier view by showing xanthate ions sorbed on a galena surface, the ratio of xanthate to lead being 1:1 rather than 2:1.^{4a} With this latter array of chemisorbed molecules on a galena surface as well, electron diffraction would be expected to yield the same streak pattern as that obtained in the present experiment, but this configuration would appear impossible from the standpoint of molecular volumes.²⁰ The surface area occupied per pair of lead and sulfur atoms on the (100) face of galena is $(5.97 \text{ \AA.})^2/2 = 17.8 \text{ \AA.}^2$, whereas the cross section of an alkyl group is about 18.5 \AA.^2 ¹¹ even in its most densely packed state, *e.g.*, solid paraffin. The above array requires the packing of two alkyl groups on each 17.8 \AA.^2 , so that the hydrocarbon chains would crowd each other.

Gaudin and Preller²⁰ recently suggested that chemisorbed xanthate ions at galena surface may be disposed in register. They suggested that this disposition of the adsorbate on the adsorbent is one reason why galena is so well floated by xanthate. If this array were really the case, there should have been observed additional streaks situated just in between those observed in Fig. 3a, where the incidence of electron beam is parallel to the $\langle 100 \rangle_{\text{PbS}}$ direction. With all the electron diffraction patterns obtained in the present experiment, no indication of such additional streaks has ever been encountered, and accordingly it is again improbable that the Gaudin-Preller array is realized.

The result of the present experiments shows that if xanthate ions are chemisorbed on galena to form a surface film, the chemical formula of the surface compound should be represented as PbX , since the adsorption has been found to take place regularly on one type of lattice atom of the (100) face of galena. This type of chemisorption has been proposed earlier by Gaudin.²¹ However, for the chemisorption of xanthate ions to take place on the crystal face, the negative charges added to the crystal surface by the chemisorbed anions should be compensated either by the adsorption of an equal number of cations or by the release into solution of a comparable quantity of anions composing or already attached to the crystal lattice. Otherwise, the electrostatic repulsion may prevent the successive adsorption of the xanthate ions completely. An increase in alkalinity stoichiometrically equal to the xanthate adsorbed, implying either the release of hydroxyl or adsorption of hydrogen ions, has already been demonstrated.^{17,22}

(17) A. F. Taggart, T. C. Taylor and A. F. Knoll, *Trans. Am. Inst. Mining Met. Engrs.*, **87**, 217 (1930).

(18) A. F. Taggart, G. R. M. del Guidice and O. A. Ziehl, *ibid.*, **112**, 348 (1935).

(19) A. F. Taggart and M. D. Hassialis, *ibid.*, **169**, 259 (1946).

(20) A. M. Gaudin and G. S. Preller, *Am. Inst. Mining Met. Engrs., Tech. Pub. No. 2002* (1946).

(21) A. M. Gaudin, *ibid.*, No. 4 (1927).

(22) A. M. Gaudin, F. Dewey, W. E. Duncan, R. A. Johnson and O. F. Tangel, Jr., *Trans. Am. Inst. Mining Met. Engrs.*, **112**, 319 (1935).

(15) R. W. G. Wyckoff, "The Structure of Crystals," The Chemical Catalog Co., Inc., (Reinhold Publ. Corp.), New York, N. Y., 1931.

(16) R. Sato, Research Report Taihei Mining Met. Lab. No. 1200 (1950) (in Japanese).

The compensating adsorption of cations on sites adjacent to the chemisorbed xanthate ions (*i.e.*, either potassium or sodium ions with the ionic radii of 1.33 Å. and 0.97 Å., respectively), is quite improbable, since there is no room to accommodate them in the required close packed array of xanthate ions. Furthermore, it has already been proved by chemical tests¹⁷ that the alkali-metal ions are not involved in the xanthating of minerals.

Thus, the remaining possibilities are: (1) the compensating adsorption of small hydrogen ions (H^+) adjacent to the chemisorbed xanthate ions (X^-); and (2) the adsorption of the neutral xanthic acid (HX) molecules on the galena lattice. This subject has already been discussed ably by Cook and Nixon.²³ Since no direct evidence can be obtained from the diffraction experiment to determine at once which of the types of adsorption is responsible for the monolayer, this new evidence is to be weighed in conjunction with evidence obtained by other methods. The fact that the collector film is unstable in air suggests that it is a xanthic acid film, and the conclusions of this study are therefore depicted schematically in Fig. 11 on the basis of this evidence.

Acknowledgments.—The author wishes to express his sincere thanks to Professor S. Nishikawa for his encouragement and interest in the work of this and the previous paper. The author is also grateful to Professors A. M. Gaudin of MIT and M. A. Cook, of the University of Utah, for their kind suggestions and help in the publication of these

(23) M. A. Cook and J. C. Nixon, *THIS JOURNAL*, **54**, 445 (1950).

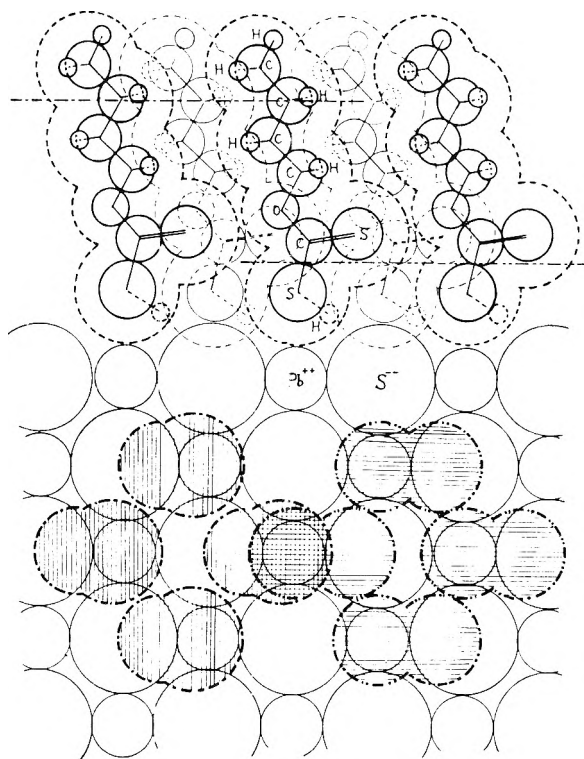


Fig. 11.—Representation of proposed xanthic acid collector film on galena.

papers. Finally, heartfelt thanks are expressed to Miss E. Matsudaira for her continuous assistance in the preparation of the manuscripts.

OXIDE FILM FORMATION ON THE SURFACE OF METALLIC MERCURY IN AQUEOUS SOLUTIONS AND THE ANOMALY BETWEEN ITS POTENTIAL AND THAT OF THE MERCURY-MERCURIC OXIDE ELECTRODE

BY S. E. S. EL WAKKAD AND T. M. SALEM (MRS. S. E. S. EL WAKKAD)

Department of Inorganic and Physical Chemistry, University of Liverpool

Received March 16, 1951

The reason for the previously reported anomaly between the potential of the mercury electrode in aerated solutions and that of the Hg-HgO electrode is clarified by studying: (A) The anodic behavior of mercury utilizing both the cathode ray oscillographic method and the direct potentiometric method. (B) The effect of bubbling oxygen through the solution on the potential of the electrode as well as on the pH value of the solution. It is shown that the discrepancy is mainly due to the increase of the pH of the solution by the increased amount of HgO which must go into solution in order to satisfy the Hg_2^{++}/Hg^{++} equilibrium and the probable consequent formation of a basic salt.

In a previous study carried out by the present authors¹ it was shown that the mercury electrode in aerated solutions gave a potential which varied linearly with the pH value of the solution from the extreme acid to the extreme alkaline pH range with a small break at $\sim pH$ 5. This behavior was attributed to the formation of an oxide over the surface of the metal, however, when such behavior was compared with that of the Hg-HgO electrode it was found that the two were in agreement only in extremely alkaline solutions. At lower pH values the potential of the mercury electrode devi-

ated to less positive values than the corresponding values of the Hg-HgO electrode. Many suggestions have been advanced for the reason of this discrepancy, each view has its advantages and its defects and it was inferred that further experimental work was needed before arriving at a certain conclusion.

In this paper this point is clarified by studying: (A) The anodic behavior of mercury utilizing both the cathode ray oscillographic method and the direct potentiometric method. No previous work has been published from the present standpoint, but a little information on the anodic dissolution

(1) El Wakkad and Salem, *THIS JOURNAL*, **54**, 1371 (1950).

of mercury can be obtained from the work of Shukov² and Jirsa and Loris.³ (B) The effect of bubbling oxygen through the solution on the potential of the electrodes as well as on the *pH* value of the solution.

By means of these two procedures it was possible to ascertain that the cause of the discrepancy is neither due to mercurous oxide nor to the formation of a form of HgO which is less soluble than the ordinary form of HgO as suggested by Gatty and Spooner.⁴ Also the idea of the slow saturation of the solution with HgO is rejected and it is shown that the discrepancy is mainly due to the increase of the *pH* of the solution by the increased amount of HgO which must go into solution in order to satisfy the Hg₂⁺⁺/Hg⁺⁺ equilibrium and the probable consequent formation of a basic salt.

Experimental

(A) **The Anodic Behavior of Mercury.**—In this study the following procedure was adopted: (1) The investigation of the anodic polarization of mercury by the cathode ray oscillograph method, should serve to detect any oxides formed on the surface before oxygen evolution. (2) The anodic polarization of a large mercury electrode at very low current densities using an ordinary potentiometric method was also studied. Here the rate of formation of mercuric oxide was controllable and variable at will, thus serving to show under what conditions the anomalous static potential changes to the normal Hg-HgO potential.

In the oscillographic method, the apparatus used was essentially the same as that previously utilized by Hickling, *et al.*,⁵⁻¹⁰ which records the variation of potential with quantity of electricity passed prior to oxygen evolution. The electrode used was prepared by electrodeposition from an acidified mercury nitrate solution on platinum electrodes of 0.05 sq. cm. apparent area. The platinum electrode was cleaned in hot concd. HNO₃ and plated for 45 minutes at a current density of 0.04 amp./sq. cm. The resulting mercury electrode was washed with running distilled water and then with solution in which it would be examined. A fresh electrode was prepared for each experiment. Observations have been made in *N* NaOH, 0.1 *N* NaOH, *M* CH₃COOH + *M* CH₃COONa and 0.1 *N* HClO₄ solutions. Except where otherwise stated all experiments were made at 18°.

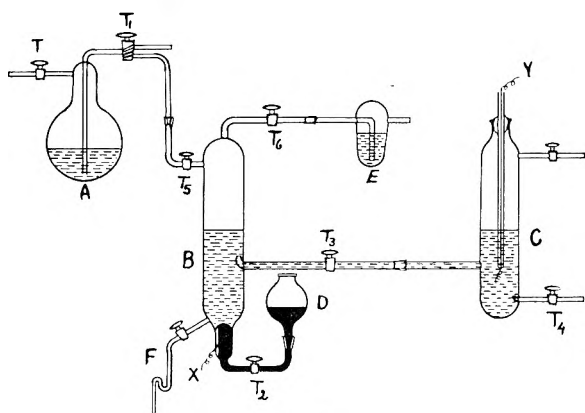


Fig. 1.

(2) Shukov, *J. Russ. Phys. Chem. Soc.*, **38**, 1253 (1907); *C.A.*, **1**, 1224 (1907).

(3) Jirsa and Loris, *Z. physik. Chem.*, **113**, 235 (1924).

(4) Gatty and Spooner, "The Electrode Potential Behavior of Corroding Metals in Aqueous Solutions," Oxford, 1938, p. 122.

(5) El Wakkad and Hickling, *Trans. Faraday Soc.*, **46**, 820 (1950).

(6) Hickling, *ibid.*, **41**, 333 (1945).

(7) Hickling, *ibid.*, **42**, 518 (1946).

(8) Hickling and Spice, *ibid.*, **43**, 762 (1947).

(9) Hickling and Taylor, *Faraday Soc. Discussion*, 277 (1947).

(10) Hickling and Taylor, *Trans. Faraday Soc.*, **44**, 262 (1948).

The results are shown as photographed oscillograms in which the ordinates represent potentials and the abscissas are proportional to quantities of electricity passed. Suitable horizontal reference lines at intervals of 0.25 v. were photographed immediately after the polarization tracks, so that significant potentials can be read directly from the oscillograms. All potentials quoted are on the hydrogen scale. The quantity of electricity passed at any stage in the polarization is obtained from the known capacity of the condenser in series with the electrolytic cell and the horizontal displacement which is governed by the voltage to which the condenser is charged (on the original photographs 1 v. on the condenser corresponds to an average horizontal displacement of 1.0 mm.). Except where otherwise stated, a 50.4 μ F. condenser was used in series with the cell as this was found to be a convenient value for the exhibition of the full polarization track.

In the study of the anodic behavior of mercury using the direct potentiometer method, a constant current unit employing a pentode valve was used. The potential of the electrode under study was measured against a saturated calomel reference electrode with a valve potentiometer. The mercury electrode used in this case was the pure metal of surface area 33 sq. cm. and which was contained in a Pyrex beaker provided with a platinum contact for electrical connection. The platinum cathode was contained in a glass plugged tube. The measurements were carried out at room temperature ($18 \pm 0.5^\circ$) in *M* acetic acid + *M* sodium acetate, 0.1 *M* disodium hydrogen citrate, 0.1 *M* borax, *N* sodium carbonate and in 0.1 *N* sodium hydroxide. In each case the solution was added to the mercury electrode and potential measurements were recorded till equilibrium was attained after which the polarizing current was allowed to pass. Polarizing currents between 10 and 100 μ a. were employed.

(B) When examining the effect of oxygen on the potential of the mercury electrode as well as on the *pH* value of the solution, the gas was simply bubbled into the system for a long period of time and the potential followed using a saturated calomel reference electrode. The *pH* values were measured with a Marconi *pH* meter.

The basic salt probably formed in acetate solutions was prepared either by shaking the appropriate amount of metallic mercury with red HgO in acetate buffer of *pH* 3.6 until all the red color of HgO disappeared and only the white basic salt remained or by shaking metallic mercury alone for a long time with the buffer through which oxygen was bubbled.

For measurements in the complete absence of oxide film on the mercury surface and in absence of atmospheric oxygen, the cell shown in Fig. 1 was constructed from Pyrex glass using ungreased taps. Flask A contained the solution in which the electrode was to be examined. Pure nitrogen passing through tap T₁ was allowed to bubble into this solution for about 1/4 of an hour to remove dissolved oxygen; then by applying a pressure of pure nitrogen at T the solution was blown over into B which contains 3 times distilled mercury and was connected to the mercury reservoir D by tap T₂. Electrical connection was made to the mercury by the tungsten contact X. Pure nitrogen was again bubbled into the solution, this time entering through tap T₃ and leaving through the bubbler E so that the solution as well as the atmosphere above it was free from oxygen. The part B was then connected to C and the solution in B allowed to run into the latter which was provided with the platinum electrode Y. Pure nitrogen could be also bubbled through the solution in C through tap T₄.

The measurements in this case were carried out in 1 *N* CH₃COOH of *pH* 2.5. Before each measurement the system was subjected for two periods of electrolysis of 20 hours, each at a current density of $\sim 10^{-3}$ amp./cm.² while pure nitrogen was bubbled slowly through T₄. In these electrolyses the mercury in B acted as the cathode and the Pt electrode in C as the anode. The first period of electrolysis was to remove possible impurities from the solution and after which tap T₂ was opened thus allowing the mercury surface to run off the side tube F and exposing a fresh surface. The second period of electrolysis was carried out to reduce any oxide film which might be present on the surface. When the purifying electrolysis was complete, taps T₃, T₅ and T₆ were closed, the part B was separated from the rest of the apparatus and the mercury electrode was connected through F to a saturated calomel reference electrode.

Results and Discussion

The Anodic Behavior of Mercury.—In Plate IA is shown the characteristic oscillogram in N NaOH for the anodic polarization of mercury at 18° with a polarizing c.d. of 0.04 amp./sq. cm. The spot on the extreme left of the photograph indicates the steady oxygen evolution potential at the same c.d. The corresponding point for steady hydrogen evolution was too negative a potential to be recorded on the same plate. Plate IB shows the cathodic track and the potential of steady hydrogen evolution. It may be noted from the anodic oscillogram that we have a very rapid initial build up of potential which is followed by one main well defined arrest prior to oxygen evolution. The step appears to start at a potential of 0.08 v. The oscillogram was very reproducible and did not vary with time over a period of 10 minutes pulsating electrolysis.

Current density had marked effect and Plate IC shows the anodic tracks obtained in N NaOH at c.d.'s of 0.02 and 0.06 amp./sq. cm. (tracks I and II, respectively). It may be noticed that by decreasing the current density the length of the arrest increases. Both tracks rise, however, to the oxygen evolution value.

The effect of temperature on the oscillogram is shown in Plate ID, which represents the anodic tracks at 18 and 60° .

Decreasing the pH has no appreciable influence on the track other than the normal shift of the whole track to more positive potential. In Plate IE is shown the anodic track in $0.1 N$ NaOH, while Plate IF is the same track in M sodium acetate + M acetic acid buffer solution of pH 4.6. Plate IIG represents the anodic and cathodic tracks in $0.1 M$ HClO₄ of pH 0.96; these show that the sole anodic process in perchloric acid is the dissolution of mercury and the corresponding cathodic process is the discharge of mercury ions.

From the above experimental results it can be concluded that mercury gives a characteristic anodic polarization track which is reproducible and not dependent on either temperature or time but depends on the c.d.

In the standard anodic track we can distinguish: (1) A very rapid rise of potential barely recorded by the plates and which by analogy with the previous metals studied corresponds to the charging of a double layer. (2) A comparatively long arrest which is clearly defined in the oscillograms. This step begins at about 0.08 v. in N NaOH, 0.18 v. in $0.1 N$ NaOH and at 0.63 v. in the acetate buffer. The previously determined values¹ of the reversible Hg-HgO electrode in solutions of the same pH values are 0.08, 0.18 and 0.62 v., respectively. The close agreement between these results shows that this stage corresponds to the formation of mercuric oxide.

Under the standard conditions in N NaOH the length of the arrest was fairly constant and measurements of several oscillograms showed that the quantity of electricity passed was 37,800 microcoulombs per sq. cm. of mercury which is sufficient to liberate 141×10^{15} atoms of oxygen. By taking the density of mercury at 18° as 13.55

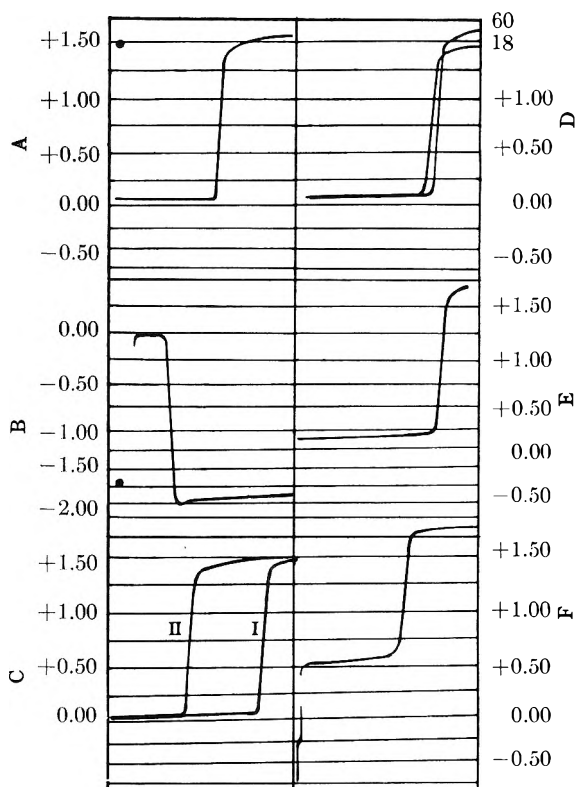


Plate I.

g./cc., the volume of one gram atom will be $200.61/13.55$ and by dividing by Avogadro's number this gives the volume of one atom of mercury as 2.44×10^{-23} . Assuming that the atom occupies a space approx. cubic in shape, then taking the cube root gives us the diameter of the mercury atom as 2.90×10^{-8} cm. and the space occupied on the surface of a mercury electrode by one atom will be in the ideal case the square of this, i.e., 8.41×10^{-16} sq. cm. The number of mercury atoms/sq. cm. will be, therefore, 1.19×10^{15} . Since the film consists of HgO then the above figures show that the oxide formed must be approximately 12 molecules thick. It must be inferred here that this thickness of HgO film is at a c.d. of 0.04 amp./sq. cm. and it varies as was shown before by changing the c.d.

From the above oscillographic results it can be seen that no oxide other than mercuric oxide is formed on the surface of the metal and that the latter oxide is always formed at the reversible potential of the Hg-HgO electrode at the corresponding pH .

The Anodic Behavior of Mercury at Very Low c.d.—Figure 2 shows the current-potential curves obtained for the mercury electrode in solutions of different pH values. From these curves it can be seen that in all cases the potential of the mercury electrode increases gradually with the increase of the polarizing current but without any definite break. The potential in each case tends toward the Hg-HgO value at the corresponding pH . The behavior at very low c.d. was also studied oscillographically using the single sweep technique. Thus in the oscillographic apparatus it was possible to run the

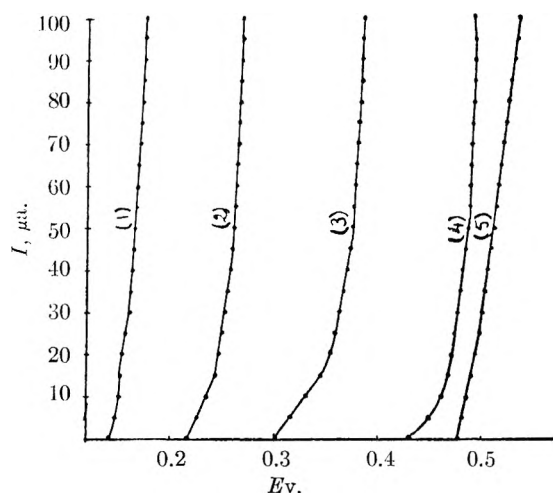


Fig. 2.—(1) 0.1 *N* sodium hydroxide (*pH* 12); (2) *N* sodium carbonate (*pH* 11.2); (3) 0.1 *M* borax (*pH* 9.2); (4) 0.1 *M* disodium hydrogen citrate (*pH* 6.4); (5) *M* sodium acetate + *M* acetic acid, (*pH* 4.6).

polarizing current and the time base independently and so produce single sweep tracks covering the polarization from hydrogen evolution to oxygen evolution without repetition. By adopting this procedure to the large mercury electrode (33 sq. cm. of surface area), using a 50.4 μ F. condenser the results shown in Plates II H, I, J, K and L were obtained in 0.1 *N* NaOH, *N* sodium carbonate, 0.1 *M* borax, 0.1 *M* disodium hydrogen citrate and *M* acetic acid + *M* sodium acetate solutions, respectively, using c.d.'s of 0.03, 0.14 and 0.3 ma./electrode in each case.

These results show that in all cases the track

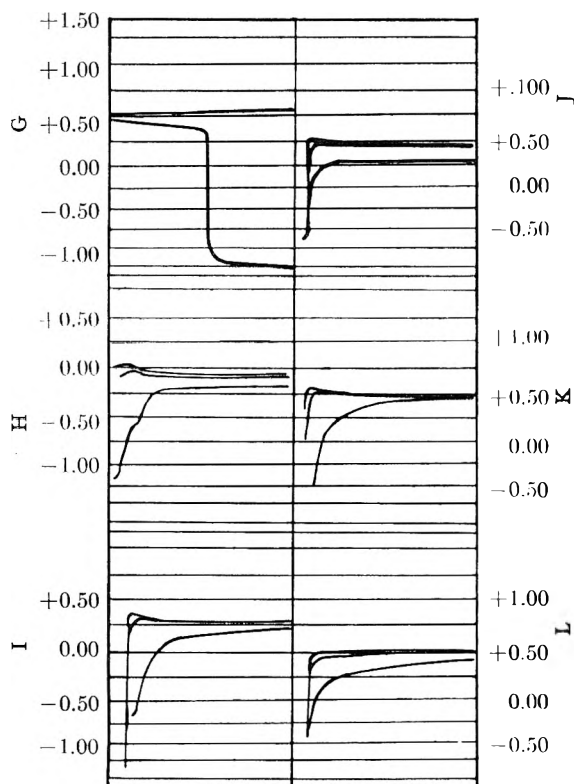


Plate II.

obtained is dependent on the polarizing c.d. the lower the c.d. the less positive the potential reached. It can be seen also that the potential increases gradually with the increase of the quantity of electricity passed and that at lower c.d. the quantity passed was not enough to raise the potential of the electrode to the Hg-HgO value; this latter value was only reached at higher c.d. These results are summarized in Table I in which are given the highest potential reached with each polarizing current and the corresponding Hg-HgO potential.

TABLE I

Solution	Hg potential using polarizing currents, v. of			Hg-HgO potential, v.
	0.03	0.14	0.3 ma.	
0.1 <i>N</i> sodium hydroxide	0.08	0.16	0.19	0.18
<i>N</i> sodium carbonate	.19	.26	.27	.23
0.1 <i>M</i> borax	.26	.32	.35	.38
0.1 <i>M</i> disodium hydrogen citrate	.40	.48	.50	.51
<i>M</i> acetic acid + <i>M</i> sodium acetate	.48	.52	.55	.62

From all the above results it is quite clear that there is no sign of a definite break corresponding to a lower oxide which may be considered to be responsible for the lower equilibrium potential obtained with the mercury electrode. The fact that a considerable quantity of electricity must be passed before the electrode potential reaches the Hg-HgO value suggests that the lower potential obtained may be due to the very slow saturation of the solution with HgO; however, as stated previously,¹ the reproducibility of the results of static measurements as well as the fact that the mercury ions present at any lower *pH* value as determined from the measured potentials are enough to exceed saturation at higher *pH* values as expected from the solubility product of HgO are against this view. Further it was found that by bubbling oxygen through the systems

Hg-CH₃COOH *M* + CH₃COONa *M* and Hg-0.1 *M* borax the constant potential reached after 10 days was 0.56 v. in the former and 0.31 v. in the latter as compared with 0.66 v. and 0.38 v. for the Hg-HgO electrode in the same solutions, respectively.

By using the apparatus shown in Fig. 1 the potential of the mercury electrode in complete absence of an oxide film over its surface was found in *N* CH₃COOH of *pH* 2.5 to be equal to 0.52 v. at 20° which agrees quite satisfactorily with the previously reported value within this region of *pH* in the absence of an oxide film over the surface.¹ When the basic salt, prepared by continuously shaking the mercury with the solution through which oxygen was continuously bubbled, was added the potential changed to 0.68 v. On the other hand, when metallic mercury was shaken with the acetate buffer solution of *pH* 3.6 for 10 days while oxygen was continuously bubbled through the system, the final *pH* value of the solution was found to be 5.9 as measured with the glass electrode. This final result indicates quite clearly that the most important factor affecting the potential of the mercury electrode was not mainly the basic salt formation but the *pH* value of the solution in the

interphase between the electrode and solution. The discrepancy between the behavior of the mercury electrode in solutions of different pH values as compared with the behavior of the Hg-HgO electrode can, therefore, be explained quite satisfactorily according to the previous experimental results as follows: In case of metallic mercury exposed to air an oxide film is already present on the surface of the metal as mercuric oxide (this was proved experimentally by the present authors as will be published elsewhere by studying the adsorption of oxygen over the surface of mercury when it was found that oxygen at low pressure is chemisorbed over the surface of mercury forming a unimolecular layer of HgO). Owing to the liquid nature of the metal one would not expect such an oxide film to be completely protective, but there are always patches of the bare metal. When this is dipped in aqueous solutions, the metallic surface exposed allows the mercurous-mercuric equilibrium to be reached which necessitates that the $[Hg_2^{++}]$ must be about 81 times that of the $[Hg^{++}]$. This great increase in the amount of the oxide dissolved decreases the hydrogen ion activity

of the solution at least within the interphase between the electrode and solution with the result that the potential recorded will be that corresponding to the newly prevailing pH . This view can be further substantiated by the fact, although when we take the potential of the mercury electrode in acetate buffer of original pH 3.6 we find that it is equal to 0.55 v. as compared with 0.66 for the Hg-HgO electrode at the same pH , yet if we calculate the Hg-HgO potential for the final pH of 5.9 we obtain a value of 0.54 v. which agrees quite satisfactorily with the potential obtained with the mercury electrode. It must be stated here, however, that this increase in the pH value owing to the increase in the amount of HgO dissolved may precipitate a basic salt, but, as was shown before, the formation of such basic compounds does not affect the potential greatly as most of the discrepancy lies actually in the change in the pH which is taking place between the electrode and solution.

The authors wish to acknowledge their gratitude to Dr. A. Hickling for the facilities he provided during the course of this work and kindly reading through this paper.

ON THE DISTRIBUTION OF LIQUID ASCENDING IN A FILTER PAPER

BY HIROSHI FUJITA

Department of Fisheries, Faculty of Agriculture, Kyoto University, Mazuru, Japan

Received April 26, 1951

The present-day theory for paper chromatography due originally to Martin and Synge⁵ is based on the assumption that the distribution of liquid ascending, or descending, in a filter paper is uniform at every instance. Recently, this assumption was examined experimentally by Takahashi^{6,10} and it was revealed that this was not so in actual case. Although he attempted to interpret his experimental data by using the diffusion theory, he could not obtain a successful result. In the present paper, the author presents a different treatment of this problem from that used by Takahashi in the hope of obtaining a mathematical explanation of the experimental data. It will be seen that the present analysis leads us to a result which agrees well with the experimental data.

I. Introduction

1. Chromatography is a special case of the so-called percolation problem in which material or heat transfer between a moving fluid and a fixed bed of granular solid is considered. A rather complete review of the theoretical articles on this problem was given by Thiele.¹ Along with the remarkable progress in the general theory of percolation, theoretical investigations of chromatography have been presented in this decade by many authors,²⁻⁴ and many important contributions to chemical assay have been made. Particularly, paper partition chromatography due originally to Martin and Synge⁵ is certainly a most important one because of its great applicability.

In all theoretical work on chromatography hitherto, it has been assumed that the distribution of liquid flowing through the bed is uniform. However, it can easily be observed that this is not the case in paper chromatography. In fact, Taka-

hashi⁶ has recently confirmed this by making a detailed experiment, obtaining an interesting family of curves for the distribution of liquid ascending a filter paper of unit width. One of his results is reproduced in Fig. 1, in which a_L denotes the amount of liquid contained in a unit area of filter paper, x the distance measured in the direction of ascending flow from the free surface of the liquid in a vessel, and the number attached to the curves implies the time elapsed until the liquid front reaches the height $x = X$ starting from the free surface of liquid. This graph reveals clearly that a_L is never uniform everywhere throughout the bed as is presumed in the usual theory of paper chromatography. Thus, as was pointed out by Takahashi, the present theory of paper chromatography requires reexamination in the light of this experimental fact.

In an attempt to obtain a theoretical explanation of this fact as shown in Fig. 1, Takahashi applied the theory of diffusion to the movement of liquid in the filter paper, but unfortunately only a partial description of the experimental fact can be expected from his treatment. In this paper, the

(1) E. W. Thiele, *Ind. Eng. Chem.*, **38**, 646 (1946).

(2) J. N. Wilson, *J. Am. Chem. Soc.*, **62**, 1583 (1940).

(3) D. DeVault, *ibid.*, **65**, 532 (1943).

(4) J. E. Walter, *J. Chem. Phys.*, **13**, 229 (1945).

(5) A. J. P. Martin and R. L. M. Synge, *Biochem. J.*, **35**, 1358 (1941).

(6) A. Takahashi, *Kagaku*, **20**, 41 (1950) (in Japanese).

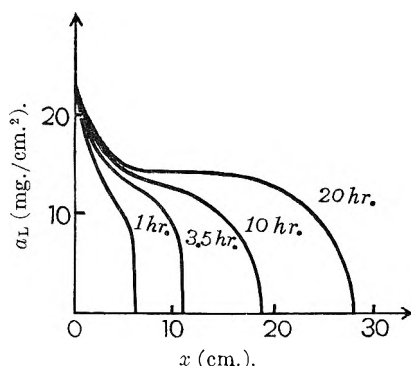


Fig. 1.—A typical family of curves representing the amount of liquid per unit area of filter paper as a function of time and position.

present author proposes a different mechanism from that assumed by Takahashi in the hope of obtaining a mathematical explanation of the experimental data.

II. Theoretical Considerations

2. We shall consider the problem of liquid distribution in a strip of uniform filter paper of unit width which is kept in a vertical position and whose bottom end is immersed in the free surface of a liquid (Fig. 2).

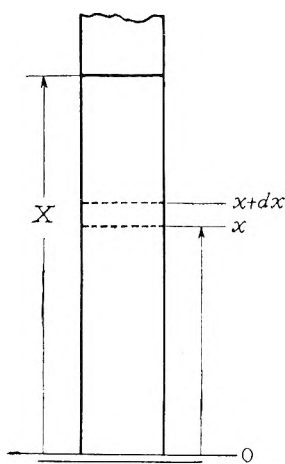


Fig. 2.—Reference system used in the analysis.

When the bottom end of such a strip of filter paper touches the liquid surface it is observed that the liquid impulsively invades the paper from the bottom and moves first rapidly but later rather slowly upward, making an exactly one-dimensional flow. We shall first deal with this one-dimensional flow from hydrodynamical points of view. Filter paper is considered to be a porous material whose pores are very small in size and are connected with each other in a complicated manner, thus giving rise to complicated microscopic or submicroscopic channels, *i.e.*, zigzag capillaries. Because of the strong capillary forces exerted by these capillaries, the liquid which has entered the bottom of filter paper can diffuse to dry parts through these capillaries and thus moves as a whole in an upward direction. This process is rather similar to that

of liquid rise in a capillary tube which has recently been investigated by Brittin⁷ and Ikeda,⁸ but a significant difference between these should be noticed. In the latter case the liquid amount per unit length of the liquid column is, of course, the same at every instant, while in the former case this is not obtained for the following reasons. As the liquid ascends through capillaries, which are distributed uniformly in filter paper, it seems to be sorbed on or in the wall of these capillaries, or to be absorbed into microscopic pores opening to the capillaries. In addition, such a sorbed or absorbed liquid probably remains fixed there and thus the general flow through capillaries is diminished in amount as it continues upwards. If we denote by W the amount of liquid per unit area of filter paper which is contained as the capillary flow and by w the one corresponding to the fixed liquid mentioned just above, this relation between W and w is mathematically described by the equation of continuity such that

$$\frac{\partial W}{\partial t} + \frac{\partial}{\partial x}(vW) + \frac{\partial w}{\partial t} = 0 \quad (2.1)$$

where t is the time, x the distance measured to the direction of capillary flow from the free surface of liquid and v the velocity of capillary flow at any point. Except for very small values of t the velocity of capillary flow is observed to be very small, so that the partial transfer of W to w may be supposed to be completed instantaneously, namely, the equilibrium between W and w can be presumed. Therefore, we may put

$$w = kW \quad (2.2)$$

where k is a certain constant depending chiefly on the porosity of filter paper. Substitution of (2.2) in (2.1) gives

$$(1+k)\frac{\partial W}{\partial t} + \frac{\partial}{\partial x}(vW) = 0 \quad (2.3)$$

We shall next establish the equation of motion for the capillary flow in filter paper. Take an infinitesimal length dx at $x = x$ and consider the x -components of all the forces acting on the capillary liquid streaming in this infinitesimal domain. They are: K at $x = x$, $K + dK$ at $x = x + dx$, and viscous force exerted from the capillary wall.⁹ The third of these is taken to be $cWvdx$ (referring to this point, see references (7) or (8)), c being a certain constant mainly dependent upon the viscosity of the liquid and the average roughness of capillary walls. As said before, the motion of capillary flow is generally so slow that we may neglect its acceleration Dv/Dt . In this way the form of the equation of motion becomes

$$-\frac{\partial K}{\partial x} = cWv \quad (2.4)$$

Since K is considered to be proportional to both p and W we have

$$K = apW \quad (2.5)$$

where p is the pressure acting at x in the direction of

(7) W. E. Brittin, *J. Appl. Phys.*, **17**, 37 (1946).

(8) Y. Ikeda and T. Soeya, *J. Phys. Soc. Japan*, **4**, 306 (1949).

(9) Because of the smallness of capillary radii the gravitational effect may be neglected.

capillary flow and a is a proportionality constant. Eq. (2.4) then becomes

$$-\frac{\partial}{\partial x}(pW) = bW^n \tag{2.6}$$

with $b = c/a$.

Next, denoting by p_0 the value of p at $x = X$, X being the height of the front of liquid column, and by P the atmospheric pressure acting on the free surface of liquid, then to the first approximation p is represented by the equation

$$p = P - \frac{P - p_0}{X} x \tag{2.7}$$

Since the radius of capillary is generally small enough to neglect p_0 against P , the above relation may be replaced by

$$p = P \left(1 - \frac{x}{X}\right) \tag{2.8}$$

Putting both (2.6) and (2.8) in (2.3) we get

$$(1 + k) \frac{\partial W}{\partial t} = \frac{P}{p} \frac{\partial^2}{\partial x^2} \left\{ \left(1 - \frac{x}{X}\right) W \right\} \tag{2.9}$$

On the other hand, inserting (2.8) in (2.6) and then putting $x = X$, it follows

$$X \frac{dX}{dt} = \frac{P}{b} \tag{2.10}$$

from which we get immediately the relation

$$X^2 = \beta^2 t \tag{2.11}$$

where $\beta^2 = 2P/b$. This relation was checked experimentally by Takahashi,⁶ an example of the agreement between the theory and the experiment being shown in Fig. 3. Using this relation Eq. (2.9) can be transformed to

$$(1 + k) \frac{\partial W}{\partial X} = X \frac{\partial^2}{\partial x^2} \left\{ \left(1 - \frac{x}{X}\right) W \right\} \tag{2.12}$$

which is the fundamental equation for determining W as a function of position and time.

3. Because of the finite capacity of porous spaces in the filter paper there exists a certain limit to the amount of liquid which can be contained as capillary liquid in a unit area of filter paper. If we denote by W_0 the saturation value of W which will be attained after a long run, such a limiting amount of liquid is given by $(1 + k)W_0$. Since, however, the filter paper can keep further a considerable amount of liquid on its surface by virtue of the cohesive force, the maximum amount of liquid that the filter paper can possess should be rather larger than $(1 + k)W_0$.

Now, in the present problem the bottom part of filter paper is in contact with the liquid at its surface, while the other upper parts are not. Accordingly, the bottom part contains the larger amount of liquid compared with the other upper parts by the amount due to the surface contribution mentioned above. However, in the actual case this non-uniform state in the surface distribution of liquid cannot be maintained stationary and the excess amount of surface liquid at the bottom part will diffuse to the surface of portions adjacent to it. Thus, we can predict the occurrence of a certain type of flow along the surface of filter paper. In fact, the existence of such a surface flow has also been observed by Takahashi, though he has not

developed a detailed discussion on this. In this place the author assumes that this surface flow obeys the well-known Fick's law usually fitted to diffusion phenomena. Then, if we denote by V the amount of this surface liquid per unit area of filter paper, V is governed by the equation

$$\frac{\partial V}{\partial t} = D \frac{\partial^2 V}{\partial x^2} \tag{3.1}$$

where D is the diffusivity.

Thus, if we obtain the expressions for W and V in terms of position and time by solving both the equations (2.12) and (3.1) with suitable auxiliary conditions given physically, the required expression for a_L is given at once by

$$a_L = (1 + k)W + V \tag{3.2}$$

4. Before proceeding to solve Eq. (2.12) we must consider the auxiliary conditions for determining uniquely the required solution. Since it might be assumed that there is no resistance to liquid transfer from the surface to the inner capillary pores, all the capillary pores at the lowest part will be saturated with liquid soon after the bottom end touches the free surface of liquid, and such a saturated state will remain all through the run. This condition can be expressed as

$$W = W_0 \quad \text{at } x = 0 \tag{4.1}$$

Also, it is obvious that for $x > X$, $W = 0$. Hence, if we assume the continuity of W over the whole range of x the following condition must be given

$$W = 0 \quad \text{at } x = X \tag{4.2}$$

As will be seen below these two conditions suffice to determine the solution of Eq. (2.12) uniquely.

First, on making the change of variables

$$\frac{1}{X} = y, \quad \frac{x}{X} = z \tag{4.3}$$

Eq. (2.12) is transformed to

$$(1 + k) \left\{ z \frac{\partial W}{\partial z} + \frac{\partial W}{\partial y} \right\} + \frac{\partial^2}{\partial z^2} \{ (1 - z)W \} = 0 \tag{4.4}$$

Substitution of $W = Y(y) \cdot Z(z)$ in (4.4) gives immediately the following equations for $Y(y)$ and $Z(z)$

$$\frac{1}{Y} \frac{dY}{dy} = - \frac{\alpha}{1 + k} \tag{4.5}$$

$$(1 - z) \frac{d^2 Z}{dz^2} - [2 - (1 + k)z] \frac{dZ}{dz} - \alpha Z = 0 \tag{4.6}$$

where α is a separation constant. Equation (4.5) can be readily integrated, giving

$$Y(y) = C \exp \left[- \frac{\alpha}{1 + k} y \right] \tag{4.7}$$

where C is an integration constant. Next, we write Eq. (4.6) in the form

$$\xi \frac{d^2 Z}{d\xi^2} + (\gamma - \xi) \frac{dZ}{d\xi} + \alpha' Z = 0 \tag{4.8}$$

by the substitutions

$$\xi = -(1 + k)(1 - z), \quad \gamma = 1 - k, \quad \text{and } \alpha' = \frac{\alpha}{1 + k} \tag{4.9}$$

It is found that Eq. (4.8) is a confluent hypergeometric equation and, therefore, the general solution can be written directly. Since, however, from

(4.2) Z must vanish at $\xi = 0$ the required solution of Eq. (4.8) takes the form

$$Z(z) = C'(1-z)^{1-\gamma} F(1-\gamma-\alpha', 2-\gamma; -(2-\gamma) \times (1-z)) \quad (4.10)$$

in which $F(\alpha, \beta; x)$ is a usual notation of the confluent hypergeometric function whose elements are α and β , and C' an arbitrary constant. Thus, we get

$$W = C''(1-z)^{1-\gamma} e^{-\alpha'z} F(1-\gamma-\alpha', 2-\gamma; -(2-\gamma) \times (1-z)) \quad (4.11)$$

C'' being a new constant. In order that the solution (4.11) may furthermore satisfy the condition (4.1) the parameter α' must be chosen to be zero and C'' to be such that

$$C'' = W_0/F(1-\gamma, 2-\gamma; -(2-\gamma))$$

The final expression for W is then obtained as

$$W = W_0(1-z)^{1-\gamma} \frac{F(1-\gamma, 2-\gamma; -(2-\gamma)(1-z))}{F(1-\gamma, 2-\gamma; -(2-\gamma))} \quad (4.12)$$

which is written in terms of z and k as

$$\frac{W}{W_0} = (1-z)^k \frac{F(k, 1+k; -(1+k)(1-z))}{F(k, 1+k; -(1+k))} \quad (4.13)$$

It should be noted here that the expression for W thus obtained is a function of z only.

5. The next problem is to determine the solution of Eq. (3.1) with appropriate auxiliary conditions imposed physically on V . The consideration of such conditions is rather involved and open to more objection than in the case of W because of the fact that the kinetic process of liquid coherence on the interface between the liquid and the filter paper has not yet been elucidated. So, we shall here confine our analysis to the simplest case when the rate at which the liquid in the vessel coheres on the interface at the bottom part is infinitely large. In this case, we may put

$$V = V_0 \quad \text{at } x = 0 \quad (5.1)$$

where V_0 is a saturation capacity of V . This condition is, as will be seen later, realized almost exactly in actual cases investigated by Takahashi.^{6,10} Further, it is plausible to suppose that any dry part of the filter paper can possess no surface liquid, since any drop of liquid placed on the surface of such a dry part will immediately be absorbed into the inner pores and not remain cohered there. Thus, it follows that

$$V = 0 \quad \text{at } x = X \quad (5.2)$$

Then, as before, transforming Eq. (3.1) in y, z -system and solving after a similar manner, there results

$$\frac{V}{V_0} = 1 - \frac{F\left(\frac{1}{2}, \frac{3}{2}; -rz^2\right)}{F\left(\frac{1}{2}, \frac{3}{2}; -r\right)} \quad (5.3)$$

where r means

$$r = \frac{\beta^2}{2D} \quad (5.4)$$

This result can also be written in terms of the error function ϕ in the form

(10) A. Takahashi, private communication.

$$\frac{V}{V_0} = 1 - \frac{\phi(\sqrt{rz})}{\phi(\sqrt{r})} \quad (5.5)$$

and, accordingly, the evaluation of V as function of z can be performed in a straightforward manner by using a table of the error function.

6. We now substitute the results (4.13) and (5.3) thus obtained in Eq. (3.2) and the required expression for a_L is readily obtained in the form

$$a_L = W_0(1+k)(1-z)^k \frac{F(k, 1+k; -(1+k)(1-z))}{F(k, 1+k; -(1+k))} + V_0 \left\{ 1 - \frac{F\left(\frac{1}{2}, \frac{3}{2}; -\frac{\beta^2}{2D} z^2\right)}{F\left(\frac{1}{2}, \frac{3}{2}; -\frac{\beta^2}{2D}\right)} \right\} \quad (6.1)$$

which shows that a_L is also a function of z only. An experimental check of this relation becomes a rather interesting problem in what follows.

III. Comparison of the Theory and the Experiment

7. We now come to compare the theoretical result of the present analysis with the experimental data obtained by Takahashi. The plot of a_L against x in Takahashi's paper cited before⁶ is rather too small in size to make a detailed comparison of the theory and the experiment, and so the author here uses the more detailed and larger scaled plots which have been sent to him from Takahashi.¹⁰ These plots involve the following three cases of liquid used: phenol saturated with water, butanol saturated with water and water. Among these plots only the one for phenol satisfies rather exactly the conditions (4.1) and (5.1) adopted in the foregoing analysis, while the other two do so merely in approximate degrees. That is to say, in these cases the constancy of $(a_L)_{x=0}$ is not realized so strictly as requested in the foregoing analysis, but $(a_L)_{x=0}$ approaches asymptotically, but fairly quickly, a certain final saturation value. Due to this situation we must restrict the comparison between the theory and the experiment only to the case of phenol, the original plot for this case being shown in Fig. 4. The comparisons for the other two cases will be made in future work.

First, on making the plot of a_L against z from Fig. 4, the result shown in Fig. 5 is obtained, in which various points correspond to the observed values. This plot shows clearly that a_L can be considered to be a function of z only, independent of the values of X as was expected theoretically from the foregoing analysis. Then, to examine how the observed plot of a_L against z is fitted by the theoretical formula (6.1) we assign the following numerical values to the parameters in Eq. (6.1)

$$W_0 = 15 \frac{\text{mg.}}{\text{cm.}^2}, \quad V_0 = 6 \frac{\text{mg.}}{\text{cm.}^2}$$

$$k = 0.3, \quad D = 0.0125 \frac{\text{cm.}^2}{\text{min.}}$$

and determine the value of β^2 from the experimental plot between X^2 and t . The calculated curve is shown in Fig. 5 with a solid line and it will be found that the agreement of the theoretical and the observed value is fairly satisfactory.

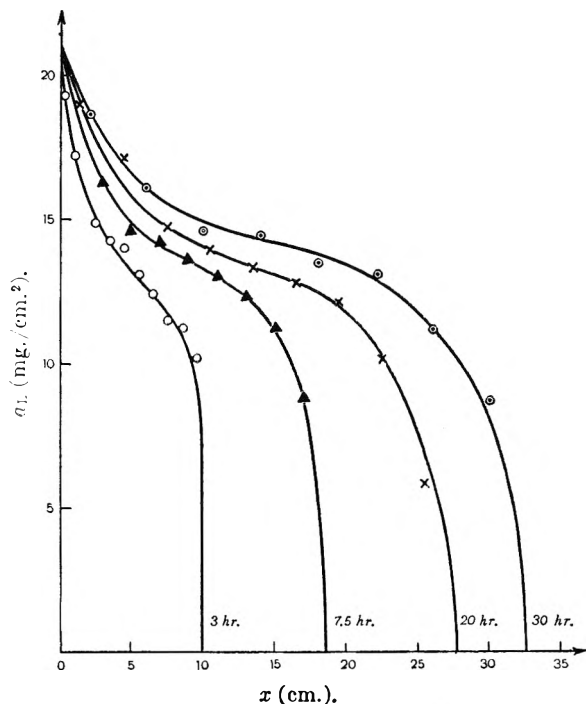


Fig. 4.—Experimental results obtained by Takahashi for the case of phenol saturated with distilled water.

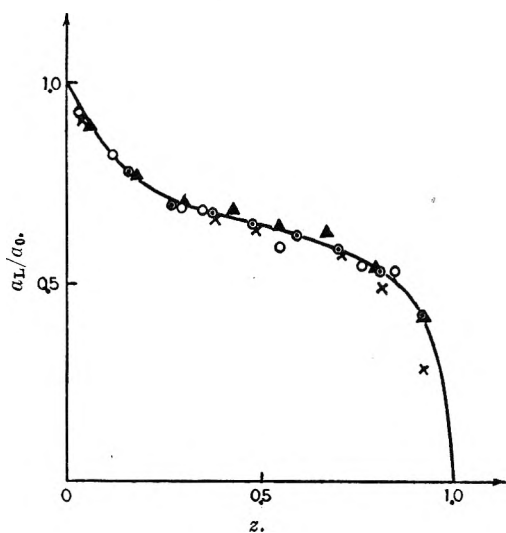


Fig. 5.—Comparison between theory and experiment for the case of phenol saturated with distilled water; points: experimental; \circ , $X = 10$ cm.; \blacktriangle , $X = 18.6$ cm.; \times , $X = 27.7$ cm.; \odot , $X = 32.6$ cm.; line: calculated.

8. Finally, we call attention to an interesting feature of the plot of a_L against x shown in Figs. 1 and 4. All these plots have the so-called S-shaped form and reveal such an interesting property that if the area U enclosed by them with the x -axis, namely

$$\int_0^X a_L dx$$

is represented by Xa_L^* , a_L^* takes almost a constant value independent of the values of X under considerations. Accordingly, we have the relation that $U \sim X$. The establishment of this relationship is indicated graphically in Fig. 6. The present day theory of paper chromatography due to Martin and Synge is based upon the assumption: $U = a_L X$ with a uniform distribution of a_L , and according to the above discussion the proportionality relationship: $U \sim X$ proves to be still valid though the distribution of a_L is never uniform but varies considerably from place to place. Consequently, the well-known formulae for computing the R_f -value in the present day theory of paper chromatography is still applicable correctly for practical purposes in chemical assay.

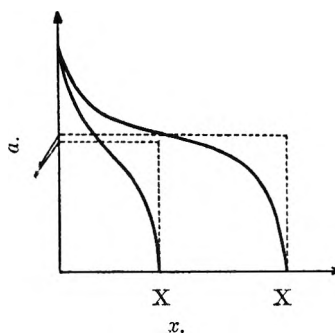


Fig. 6.—Diagram showing the approximate relation as $\int_0^X a_L dx = X a_L^*$.

Acknowledgment.—In concluding this paper the author wishes to express his cordial thanks to Mr. A. Takahashi of Tokyo University for his kind permission of utilizing his valuable experimental data, and to Associate Professor T. Kawakami for his helpful discussions and suggestions given throughout the course of this work. The author is also indebted to Professor Neal R. Amundson of the University of Minnesota who gave him much encouragement and who read the manuscript of this paper.

MEASUREMENT OF SURFACE PHOSPHATE ON HYDROXYLAPATITE AND PHOSPHATE ROCK WITH RADIOPHOSPHORUS¹

BY STERLING R. OLSEN

U. S. Department of Agriculture, Fort Collins, Colorado

Received May 28, 1951

Radioactive tracers have been used to measure the specific surface of various salts and the fractions of the salt components which are on the surface of the crystals.²⁻⁸ The principle of the method is based upon the isotope exchange of the radioactive tracer element with the element on the solid surface. The reaction for radioactive P³² on minerals containing phosphorus would be: surface P³¹ + solution P³² ⇌ surface P³² + solution P³¹.

In general the method followed is to (1) shake a portion of the solid in water until equilibrium is established, (2) introduce a small aliquot containing P³² and continue shaking until equilibrium is reached, and (3) determine the amounts of P₃₁ and P³² in the solution and the amount of P₃₂ on the solid phase. Since the ratio of the two isotopes on the solid surface can be taken equal to that in the solution, the equilibrium constant for the reaction is unity, and the extent of surface reaction at equilibrium can be determined with the aid of the equation

$$P^{31} \text{ surface}/P^{31} \text{ solution} = P^{32} \text{ surface}/P^{32} \text{ solution}$$

These conditions hold provided the surface-solution equilibrium can be attained and distinguished from other possible processes, such as penetration of the isotope into crystal layers beyond the surface layer.

This isotope-exchange method is applied to the measurement of surface P³¹ in hydroxylapatite and phosphate rock in the work reported here. The results provide a basis for studies on the nature of

surface phosphate reactions between native and applied phosphate in calcareous soils.

Description of Samples

Two samples of hydroxylapatite, No. 1540-a and 2453, and a sample of ground, raw rock phosphate, No. 913, from Florida, were used. The hydroxylapatites were precipitated materials having a P₂O₅/CaO ratio of 0.795 (pure hydroxylapatite has a P₂O₅/CaO ratio of 0.76 from the formula Ca₁₀(PO₄)₆(OH)₂), and they differed in particle size due to differences in the manner of preparation. The raw rock phosphate, No. 913, had been ground to pass a 200 mesh screen. The major constituents present are given in Table I.

Experimental

Initial Method for Sorption of P³².—To study the distribution of P³² between solution P³¹ and surface P³¹, the following general method was employed in the first series of experiments: a 50-mg. sample of the solid was shaken 3-4 days with 25 ml. of water to attain equilibrium of the solid with the solution. Then a one- or two-ml. aliquot of P³² solution (this solution was saturated with the ions dissolving from the solid) was introduced and the mixture shaken continuously for one hour. The flasks were placed in a constant-temperature bath at 25° and shaken several times a day by hand for the longer reaction periods. At the end of each reaction period the mixture was centrifuged and samples of the solution taken for the determination of P³¹ and P³² concentration. The P³¹ was determined by the isobutyl alcohol method¹⁰ and P³² after precipitation as MgNH₄PO₄·6H₂O¹¹ by an end-window counter tube.

The P³¹ solution concentration was varied by using K₂HPO₄ solutions adjusted to the same pH as the saturated solution of hydroxylapatite.

Modified Method for Sorption of P³².—In the second series of experiments, the technique for sorption of P³² was modified as follows: the volume of solution was increased to 500 ml. and the weight of solid decreased to 10-15 mg. The P³² solution was saturated with ions dissolving from the solid and added directly to the sample in a 500-ml. flask. The mixture was stirred continuously in a constant temperature room at 24°. A 2-ml. aliquot was removed for sampling, centrifuged and two 0.4-ml. aliquots taken for P³² determination. The excess solution and solid were returned to the 500-ml. flask. The solution P³¹ concentration was determined at the last sampling. The reaction flasks and centrifuge tubes were coated with "Dri-film," (#9987, General Electric Company), to make them water repellent and to decrease the adsorption of phosphorus on the glass surface. The P³² counts were made with a proportional counter from 0.4-ml. aliquots evaporated on a thin aluminum planchet. Each sample was counted long enough (usually 2-4 minutes) to give a total count greater than 10,000.

The P³² for these experiments (Item S-3 from the Atomic Energy Commission, Oak Ridge) was a dilute solution of H₃PO₄ containing 0.025 mg. of P³¹ per millicurie of P³². The P³² was free from radioactive impurities as indicated by checking the activity for a 14.3 day half-life.

Desorption of P³².—The desorbing solution was 0.05 M K₂HPO₄ adjusted to the same pH as the saturated solution of hydroxylapatite. To desorb the P³², 25 ml. of the 0.05 M K₂HPO₄ was added to the solid, which had been separated from the P³² in solution by centrifugation, shaken for one hour or longer, centrifuged and the process repeated.

TABLE I

COMPOSITION OF SAMPLE 913, A RAW, ROCK PHOSPHATE FROM FLORIDA

Constituent	Composition, %
P ₂ O ₅	35.4
CaO	49.0
SiO ₂	7.5
F	4.0
HOH	1.7
CO ₂	1.5
Al ₂ O ₃	1.1

(1) Contribution from the Soil Phosphorus Research Project for the Western Region, the Bureau of Plant Industry, Soils and Agricultural Engineering, the Colorado Agricultural Experiment Station, and the Western Soil Research Committee cooperating. Authorized by the Director of the Colorado Agricultural Experiment Station for publication as Scientific Journal Series Article No. 361.

(2) Marlene Falkenhein, W. F. Neuman and H. C. Hodges, *J. Biol. Chem.*, **169**, 713 (1947).

(3) I. M. Kolthoff, *This Journal*, **40**, 1027 (1936).

(4) I. M. Kolthoff and W. M. MacNevin, *J. Am. Chem. Soc.*, **58**, 499 (1936).

(5) I. M. Kolthoff and A. S. O'Brien, *ibid.*, **61**, 3409 (1939).

(6) I. M. Kolthoff and C. Rosenblum, *ibid.*, **55**, 2656 (1933).

(7) C. D. McAuliffe, N. S. Hall, L. A. Dean and S. B. Hendricks, *Proc. Soil Sci. Soc. Am.*, **12**, 119 (1948).

(8) F. Paneth and W. Vorwerk, *Pulver. Sci. Phys. Chem.*, **101**, 445 (1922).

(9) The P³² was obtained from the Atomic Energy Commission.

(10) W. A. Pons, Jr., and J. D. Guthrie, *Ind. Eng. Chem., Anal. Ed.*, **18**, 184 (1946).

(11) A. J. MacKenzie and L. A. Dean, *Anal. Chem.*, **20**, 559 (1948).

Results

Sorption of P^{32} Using Initial Method.—In the first series of experiments where the solution to solid ratio was low, about 85% of the P^{32} was sorbed by the solid within ten minutes, followed by a very slow sorption period. A true equilibrium was not reached in 400 hours, but very little change occurred after 24 hours. For reaction periods longer than 24 hours, the sorption curve followed the relationship indicated in either of the experimental equations (1) $A = A_i - Kt^{-1/2}$ or (2) $\ln A/A_i = Kt^{-1/2}$ where A = amount of P^{32} sorbed or exchanged in time, t ; A_i = amount taken up in infinite time, and K = a constant representing the slope of the straight line.¹²

The effect of time and solution P^{31} concentration on the rate of sorption of P^{32} are shown in Table II, and the amount of P^{32} sorbed at infinite time as found by extrapolation. From these data the surface P^{31} was calculated as shown in Table III. The amount of surface P^{31} remained constant over a wide range of solution P^{31} concentration. Falkenheim, *et al.*,² obtained similar results on a precipitated hydroxylapatite for the effect of solution P^{31} concentration on the surface P^{31} measured by P^{32} exchange. The added P^{31} as K_2HPO_4 was not sorbed in detectable amounts by the hydroxylapatite as indicated by determining the solution P^{31} concentration before and after addition of the solid.

TABLE II

SORPTION OF P^{32} ON HYDROXYLAPATITE (#2453) IN RELATION TO TIME AND SOLUTION P^{31} CONCENTRATION

Sorption time, hours	P^{32} sorbed in cts. per second		
	1.6	31.6	316
0 ^a	396.2	467.0	488.4
24	359.0	157.0	23.4
70	...	181.4	28.0
94	367.6
168	...	192.0	31.2
212	368.6
378	369.2
∞ ^b	375	220	39

^a P^{32} initially present. ^b Values calculated by extrapolating curves plotted from equation (2) to infinite time.

TABLE III

THE AMOUNT OF P^{31} IN THE HYDROXYLAPATITE (#2453) EQUILIBRATING WITH P^{31} AT INFINITE TIME

Solution P^{31} p.p.m.	Surface P^{31} exchanging mg. per gram
1.6	14.1
31.6	14.1
316	13.8

It was assumed in the above calculations that the P^{32} on the surface remained exchangeable with P^{31} in solution. The P^{32} on the surface is exchangeable with P^{31} in solution under these experimental conditions as shown by the data in Table IV. A similar set of data was obtained for another sample of hydroxylapatite (#1540-a). The P^{32} sorbed during short reaction periods (less than 24 hours) was

(12) Equation (1) was suggested by V. R. Dietz, National Bureau of Standards, and equation (2) by N. S. Hall, North Carolina State College.

readily desorbed with 3–4 extractions, but as the sorption period increased, the P^{32} was less readily desorbed. The six extractions used in this experiment covered a 6–8 day interval for the longer sorption periods. Evidence for entrapped or inner surfaces on similar materials have been shown.¹³ The P^{32} penetrating to these areas on long sorption periods would be less readily desorbed than the P^{32} on surfaces readily accessible to the solution.

TABLE IV

AMOUNT OF SORBED P^{32} ON #2453 WHICH WAS DESORBED BY SIX EXTRACTIONS WITH 0.05 M K_2HPO_4

Adsorption time, hr.	P^{32} adsorbed, cts./sec.	P^{32} desorbed by P^{31} cts./sec.
1	32.7	33.0
122	35.3	34.3
287	35.2	33.8
478	34.8	34.0

Sorption of P^{32} Using the Modified Method.

The experimental conditions for sorption of P^{32} by the initial method are not entirely satisfactory because of the long time involved. The concentration of P^{32} in the solution was rapidly decreased to about 10% of its initial value. By modifying the technique, however, as described for the second series of experiments, the concentration of P^{32} in the solution decreased to only 80–90% of its initial value. Under these conditions a true equilibrium was reached within 24 hours, and near equilibrium in 5 hours. Thus, the surface P^{31} of a sample can be calculated from the data obtained at equilibrium without the use of a plot that must be extrapolated to infinite time. The data in Table V were obtained by this procedure.

TABLE V

AMOUNT OF PHOSPHORUS PER UNIT OF SURFACE AREA EQUILIBRATING WITH P^{32} IN VARIOUS CALCIUM PHOSPHATE

Sample no.	P_2O_5/CaO	MATERIALS		
		Specific ^b surface, m. ² /g.	Surface P^{31} , mg./g.	Surface $P^{31}/m.^2$ surface area, mg.
2453	0.795	57.7	14.3	0.246 ± 0.010
1540-a	0.795	36.3	8.54	0.236 ± .006
913	0.723	13.9	3.23	0.233 ± .013
Apatite ^a		51.1	12.2	0.238

^a Calculated from equation (1) from published data.² ^b Measured by the BET method.¹¹ Samples 2453 and 913 were measured by V. R. Dietz of the National Bureau of Standards, sample 1540-a was measured by the BPIS & AE Beltsville Laboratory, and the apatite sample by N. V. Wood.²

The amount of surface P^{31} per unit of surface area was found to be essentially constant for the various samples and equal to 0.238 mg. per square meter of surface area (average value for four samples), or the average surface area occupied by one phosphate group equaled 21.6 Å.² The values for surface P^{31} shown in Table III for #2453 checked the value given in Table V. Thus, it appears that either experimental method may be used, but the modified method is more rapid and convenient.

(13) S. B. Hendricks and W. L. Hill, *Proc. Natl. Acad. Sci.*, **36**, 731 (1950).

(14) S. Brunauer, P. H. Emmett and E. Teller, *J. Am. Chem. Soc.*, **60**, 309 (1938).

Application of Data for Determining Surface Areas.—The results shown in Table V indicate that these data may be used to calculate the surface area of calcium phosphates such as apatite and hydroxylapatite, *i.e.*, the surface P^{31} in mg. per gram obtained by isotopic exchange on a sample to be measured, divided by the average value 0.238, should give a fairly accurate measure of the specific surface in square meters per gram. This method would be much more rapid than the usual BET method for measuring surfaces on these calcium phosphates. The general isotopic exchange method should be applicable to other materials, provided a suitable isotope can be obtained, by determining the area occupied by the isotope and the amount of the isotope exchanging with the non-active isotope on the surface.

The rock phosphate sample (913) contains some impurities (notably silica) not present in the other materials, which might be expected to cause a lower value for surface P^{31} per $m.^2$ surface area compared to a pure hydroxylapatite. Quartz is commonly found associated with rock phosphate, however, and the portion of the total surface area contributed by this relatively coarser material probably would be small.

Comparison of Experimental Values with Crystallographic Data.—It is of interest to compare the experimental value of $21.6 \text{ \AA}.^2$ per phosphate group with values calculated from the unit of structure for apatite. According to X-ray crystallographic data, the dimensions of a unit cell for apatite are, $a = 9.37 \text{ \AA}.$ and $c = 6.88 \text{ \AA}.$ Thus, one of the possible faces of the crystal would have an area of 9.37×6.88 or $64.5 \text{ \AA}.^2$ within which there would be three phosphate groups or $21.5 \text{ \AA}.^2$ per phosphate group. Other faces at the surface with different areas and number of phosphate groups are possible

also, and it is probable that there would be a random orientation of the various faces at the surface, some having a larger area than the unit cell dimensions. The fact that the experimental value of $21.6 \text{ \AA}.^2$ happens to be one-third of the surface area of a unit cell, indicating three phosphate groups available for exchange, does not constitute valid proof that this particular face is the one always exposed at the surface, but more likely it represents an average value of the various faces.

Another estimate of the area occupied by a phosphate group in apatite can be calculated from the molecular volume, *i.e.*, molecular weight divided by the density. Using a density of $3.16 \text{ g./cm}.^3$ for apatite, the molecular volume per phosphate group is $88.1 \text{ \AA}.^3$. Assuming a cube, one edge is $4.45 \text{ \AA}.$ in length, so the surface area of a side is $19.8 \text{ \AA}.^2$, which is the same order of magnitude as the experimental value obtained by isotopic exchange.

Application of Surface Phosphate Measurements to Soil Phosphorus Fertility Problems.—The phosphate fertility level and the supplying power of the soil for the phosphorus removed by plants from the soil solution may be related in part to the amount of surface phosphate.⁷ A measurement of the surface phosphate in soils may help also to explain some of the reactions taking place between the soil and a phosphate fertilizer and possibly aid in evaluating the residual effect of the applied phosphorus to plants.

Acknowledgment.—The author wishes to acknowledge the helpful suggestions of Dr. L. A. Dean, Mr. W. L. Hill, Mr. Robert Gardner, and Dr. S. B. Hendricks and the analytical assistance of Mr. Frank S. Watanabe. The author also wishes to acknowledge the assistance of Dr. V. R. Dietz of the National Bureau of Standards for the surface area measurements.

TITRATION CURVES OF THE CLAY MINERALS ATTAPULGITE AND NONTRONITE

BY R. P. MITRA AND H. B. MATHUR

Department of Chemistry, University of Delhi, Delhi, India

Received June 4, 1951

Hydrogen attapulgite and hydrogen nontronite show three inflections in their potentiometric and conductometric titration curves, indicating three stages of neutralization with the base. Both of them give a weak first inflection. Hydrogen attapulgite shows a sharp second inflection but with hydrogen nontronite, this inflection is also not so prominent. Hydrogen nontronite, however, gives a pronounced third inflection; only a prolonged interaction with the base reveals this inflection in the case of hydrogen attapulgite.

On continued treatment with a *N* BaCl₂ solution of pH 9.0, hydrogen attapulgite takes up an amount of Ba⁺⁺ ions which is equal to its base combining capacity given by the third or final inflection in its titration curve; the Ba⁺⁺ ions, under these conditions, replace all the H⁺ ions on the surface, including those dissociated from the available OH groups. If the pH of the BaCl₂ solution is only 5.0 or 7.0, only the H⁺ ions balancing the "isomorphous charge" are replaced. In the case of hydrogen nontronite, a complete replacement of H⁺ ions indicated by the final inflection in the titration curve takes place even when the solution of BaCl₂ has as low a pH as 5.0.

The titration curves of hydrogen clays, *i.e.*, acid forms of soil colloids, have been studied by several investigators.¹⁻⁵ More recently, pure specimens of clay minerals have also been used for such studies.⁶⁻⁸ Mukherjee, Mitra and their co-workers⁷⁻¹⁰ observed characteristic differences between the titration curves of montmorillonite and kaolinite, and they used these differences as criteria for identifying the two minerals in soil colloids. Mitra and Rajagopalan¹¹ have reported the titration curve of hydrogen mica obtained by replacing the exposed K⁺ ions of ground muscovite by H⁺ ions. Their titration curve has a different form compared with that of hydrogen montmorillonite and hydrogen kaolinite but hydrogen illite, as is to be expected, gives an almost similar titration curve.¹² Not much work, however, appears to have been done on the important series of clay minerals represented by nontronite and attapulgite although Caldwell and Marshall¹³ have published some interesting observations on them. However, as Marshall and Caldwell¹⁴ themselves point out, further work on these minerals is desirable. The present investigation was undertaken with this object in view. Aqueous suspensions of hydrogen forms of the minerals¹⁵ obtained on repeatedly treating their 2.0-micron fractions with 0.03 *N* HCl, were titrated potentiometrically and conductometrically with KOH and Ba(OH)₂. Titrations were done in the presence and absence of neutral salts. The features

of the titration curves have been discussed in relation to the lattice structures of the minerals and factors which are known to play a part^{9,16} in ionic reactions on surfaces.

The titration technique of Mukherjee and Mitra¹⁷ was followed. "Continuous" as well as "bottle" titrations as explained below were done. In a continuous titration, changes of the pH were measured following additions of increasing amounts of the base to a given volume of the sol kept in an atmosphere of pure hydrogen or nitrogen gas. A fresh addition of the base was not made till the e.m.f. after the previous addition remained constant to within 1.0 millivolt for a period of at least 15 minutes. In bottle titrations, increasing amounts of the base were added to a fixed volume of the sol contained in each of several Jena glass bottles, the mixtures kept overnight, and their pH's separately determined on the following day. The "bottle" titrations, by allowing a long time of interaction between the hydrogen mineral and the titrant base, made it certain that the resulting titration curve truly depicted equilibrium conditions. Both the continuous and bottle titration techniques gave titration curves showing similar features.

Inflection Points and Breaks in the Titration Curves

Figure 1 shows the titration curves of a 0.83% sol of hydrogen attapulgite, obtained using the continuous titration technique. Each potentiometric curve shows two inflections and each conductometric curve, two breaks. The run of the curve and the pH at the inflection depend, to some extent, on the base used for the titration, and it illustrates the part played by the adsorption of the cation of the base in its interaction with H⁺ ions on the surface.^{9,16} The pH's at the inflections and the base exchange capacities (b.e.c.) calculated from them as also from the breaks of the conductometric curves are given in Table I.

Caldwell and Marshall¹³ did not use the conductometric method of titration. They did not notice the first inflection in the potentiometric curves. An inspection of their curves shows that the first inflec-

(1) M. S. Anderson and H. G. Byers, *U.S.D.A. Tech. Bull.*, **542** (1936).

(2) L. D. Baver, *Soil Sci.*, **29**, 291 (1930).

(3) R. Bradfield, *Proc. 1st Internatl. Cong. Soil Sci.*, **4**, 858 (1927).

(4) I. A. Denison, *Bur. Standards J. Res.*, **10**, 413 (1933).

(5) R. P. Mitra, *Indian J. Agric. Sci.*, **6**, 555 (1936).

(6) C. E. Marshall, *Z. Krist.*, **91**, 433 (1935).

(7) R. P. Mitra, S. N. Bagchi and S. P. Roy, *THIS JOURNAL*, **47**, 549 (1943).

(8) J. N. Mukherjee, R. P. Mitra and D. K. Mitra, *ibid.*, **47**, 543 (1943).

(9) R. P. Mitra, *Indian Soc. Soil Sci. Bul.*, **4**, 41 (1941-1942).

(10) J. N. Mukherjee and R. P. Mitra, *J. Colloid Sci.*, **1**, 141 (1946).

(11) R. P. Mitra and K. S. Rajagopalan, *Nature*, **162**, 105 (1948).

(12) R. P. Mitra and K. S. Rajagopalan, Abstracts of Proc. 36th Indian Sci. Congress.

(13) O. G. Caldwell and C. E. Marshall, *Missouri Agric. Exp. Sta. Res. Bul.*, **354** (1942).

(14) C. E. Marshall and O. G. Caldwell, *THIS JOURNAL*, **51**, 311 (1947).

(15) The minerals were obtained from Dr. S. B. Hendricks through Dr. S. P. Raichandhuri of the Indian Agricultural Research Institute.

(16) J. N. Mukherjee, R. P. Mitra and S. Mukherjee, *Trans. National Inst. of Sciences India*, **1**, 227 (1937).

(17) J. N. Mukherjee and R. P. Mitra, *Indian J. Agric. Sci.*, **12**, 433 (1942).

TABLE I

Base used	B.e.c. (in meq. per 100.0 g.)		Conductometric curve	
	Potentiometric titration curve at first inflection	Potentiometric titration curve at second inflection	at first break	at second break
KOH	3.0 (4.7) ^a	20.0 (7.6)	5.0	18.0
Ba(OH) ₂	4.0 (4.7)	20.0 (7.6)	5.5	18.0

^a The figures within brackets indicate the pH's at the inflection points.

tion was missed by them because of too large an addition of the base at the very first installment. That this inflection is real and indicates H⁺ ions on the surface, will be seen from the fact that it is not indicated by the titration curve of the ultrafiltrate of the sol given in Fig. 1. Caldwell and Marshall¹³ also did not notice the inflection at about 20.0 meq. of the added base when the titration was done with KOH. Our titration curves with this base, potentiometric and conductometric, clearly bring out this inflection.

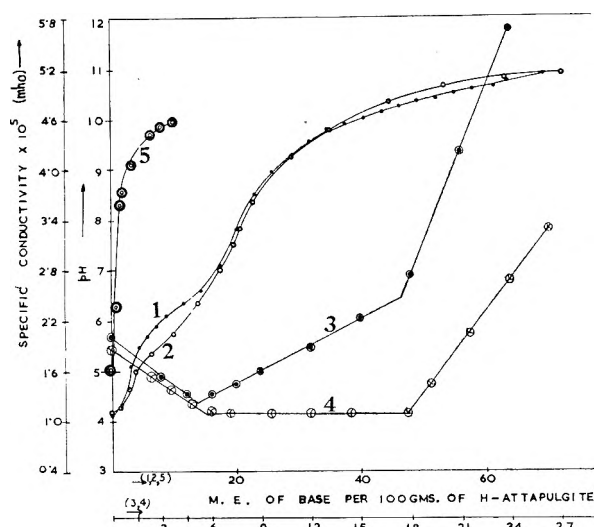


Fig. 1.—Curve 1, KOH potentiometric; curve 2, Ba(OH)₂ potentiometric; curve 3, KOH conductometric; curve 4, Ba(OH)₂ conductometric; curve 5, ultrafiltrate.

Caldwell and Marshall,¹³ in effect, used the “bottle titration” technique. It is our experience—and the case in point further confirms it—that the continuous titration technique can be used with much greater effect for studying the fine features of the titration curves and, if the titration is not intended to be extended beyond a pH of about 7.0, it is certainly to be preferred to the bottle titration technique. In a continuous titration, the electrode maintains a constant solution tension all the time. The absolute value of the pH at each stage of the titration may be slightly in error, but this error being constant throughout the titration, one gets a very smooth titration curve whose form and run are easily reproduced and are very dependable. Each point in the bottle titration curve, however, is the result of an independent determination of the pH on a separate quantity of the sol and is, therefore, subject to the uncertainties of a variable solution tension of the electrode¹⁸ in the separate determinations. The titration curve is, therefore, difficult to reproduce and unless confirmed by repli-

cations, its features cannot be depended upon. However, above a pH of about 7.0, the reaction with the base becomes extremely slow, and one is left with no other alternative but to take recourse to the bottle titration technique.

The inflection point at pH 7.6 in the titration curves (see Fig. 1) of the hydrogen attapulgit, does not indicate all the H⁺ ions on the surface. As stated above, a very slow reaction with base takes place above this pH. The course of the reaction in this range is revealed by the bottle titration curves given in Fig. 2. Each of these curves shows an inflection at about pH 10.0 which marks the completion of the slow reaction. A b.e.c. of about 55 m.e. per 100 g. is obtained at this inflection as also observed by Caldwell and Marshall.¹³ The bottle titration curves do not show the first inflection due, apparently, to too large an addition of the base at the very first installment. They give a somewhat higher b.e.c. at the second inflection than the “continuous” titration curves.

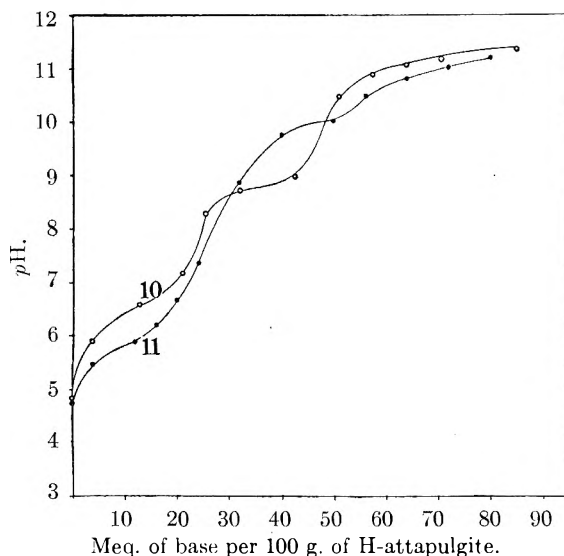


Fig. 2.—Curve 10, KOH potentiometric; curve 11, Ba(OH)₂ potentiometric.

The titration curves of the hydrogen nontronite are shown in Fig. 3. Each curve, potentiometric and conductometric, shows three inflections, the first two of them, rather weak. The bottle titration curves, not shown here, also present similar features. Some of Caldwell and Marshall's curves—they carried out only potentiometric titrations—show similar inflections but the curves are not very smooth and not much notice of the inflections, especially, the two earlier ones, appears to have been taken by these authors. We find that both the hydrogen attapulgit and the hydrogen nontronite behave as a tribasic acid. However, differences between the two minerals certainly exist. Their b.e.c.'s calculated at the final (*i.e.*, third) inflection are materially different. Another point of dissimilarity which seems to be of more than passing interest is the fact that the reaction with the base beyond the second inflection is much faster in the case of the hydrogen nontronite compared with hydrogen attapulgit, which explains why even a continuous titration shows the third inflection of hydrogen

nontronite quite clearly, though only a bottle titration brings out this inflection in the case of hydrogen attapulgite.

Inflection Points and Breaks in the Titration Curves in Relation to the Lattice Structures of the Minerals

Inflection points in the titration curves of dissolved acids indicate, as is well known, neutralization of H^+ ions having markedly different energies of dissociation. The three inflections in the titration curves of hydrogen nontronite and hydrogen attapulgite, therefore, appear to indicate the presence of H^+ ions in three distinct affinity levels on the surface. Mitra and Rajagopalan¹⁹ have discussed the structural factors which might be expected to give rise to different bonding energies of the H^+ ions on the surface. As emphasized by them and also by Marshall,²⁰ isomorphous replacements of cations within the lattice for others having smaller positive charges constitute an important source of the negative charge which could hold the H^+ ions and other exchangeable cations on the surface. In the case of attapulgite, Caldwell and Marshall¹³ believe that the b.e.c. of about 20 m.e. per 100 g. indicated by the second²¹ inflection in the titration curves is due to this "isomorphous charge." If this is really the case, a different type of isomorphous replacement might have to be assumed to explain the first inflection. Actually, replacements may occur in the tetrahedral as well as octahedral layers of the lattice. The separation of the negative charge from the surface will be greater in the latter case. The bonding energies of the H^+ ions on the surface will, therefore, be weaker and consequently the H^+ ions will be neutralized at a lower pH. The first inflection may then indicate H^+ ions balancing the part of the isomorphous charge which resides in the octahedral layer, the second inflection giving a measure of the total "isomorphous charge" located in both the octahedral and tetrahedral layers. The fact that the b.e.c. at the first inflection is small shows, in the light of the above assumption, that only a limited replacement has taken place in the octahedral layer.

One can think of yet another explanation of the first inflection, assuming that all the isomorphous charge resides in the tetrahedral layer. It is possible that this inflection indicates only such of the H^+ ions balancing the total charge as occur at the edges and corners of the crystals.¹¹ Attapulgite, however, does not have a platy habit, which makes this explanation less plausible than in the case of the other clay minerals.

Caldwell and Marshall¹³ believe that the portion of the titration curve beyond the inflection point found at about 20 m.e. of the added base, indicates neutralization of H^+ ions dissociated from the available OH groups of the crystals. An acid character of OH groups in clay minerals has often been assumed²² without bringing any conclusive experi-

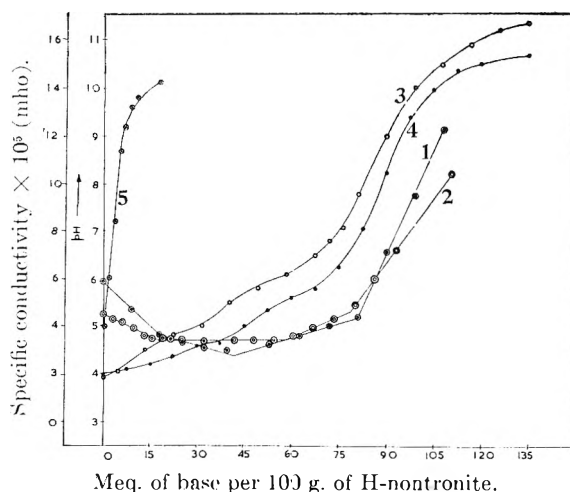


Fig. 3.—Curve 1, KOH conductometric; curve 2, $Ba(OH)_2$ conductometric; curve 3, KOH potentiometric; curve 4, $Ba(OH)_2$ potentiometric; curve 5, ultrafiltrate, KOH.

mental evidence to bear on such an assumption. Very strong evidence appears to have been obtained for the first time from Mitra and Rajagopalan's work on hydrogen mica.¹¹ They have shown that the theoretically calculated amount of OH groups of the mica crystals reacts with the base after the H^+ ions balancing the isomorphous charge of the surface have been neutralized. In the light of this observation, there seems to be little doubt that the portion of the titration curve of the hydrogen attapulgite between the second and third inflection indicates the neutralization of the available OH groups of the lattice.

One would be inclined, on a first thought, to interpret the three inflections in the titration curve of the hydrogen nontronite on the above lines. However, unlike hydrogen attapulgite, the second inflection in the case of hydrogen nontronite is not sharp and the titration curve, during its entire course, slowly changes its curvature till the final inflection is reached. No sharp distinction appears to exist between H^+ ions balancing isomorphous and hydroxylic charges so far as their energies of dissociation and neutralization by the base are concerned.

Titration Curves in the Presence of Salts

Figure 4 shows the titration curves²³ of the hydrogen attapulgite (HA) to which enough solid $BaCl_2$ and KCl were added so as to have normal concentrations of the salts in the sol + salt mixture. The titration curve of the clear supernatant liquid above the coagulum of the sol + KCl mixture is also shown in the figure. An interpretation of such curves obtained with hydrogen clays and of the reactions they depict has been given by Mukherjee, Mitra and their co-workers.^{9,16} It will be sufficient for our purpose to recall their main conclusion, *viz.*, that the quantity of H^+ ions on the surface which is neutralized by the base is rather ill-defined and it depends, firstly, on the prevailing pH and, secondly, on the valency, radius (including water of hydration) and concentration of the cations present in the system. The higher the

(23) Obtained using the continuous titration technique.

(19) R. P. Mitra and K. S. Rajagopalan, *Indian J. Phys.*, **22**, 129 (1948).

(20) C. E. Marshall and W. E. Bergman, *This Journal*, **46**, 52, 325, 327 (1942).

(21) It is the first inflection in Caldwell and Marshall's curves.

(22) R. K. Schofield, *Soils and Fertilisers, Imp. Bur. Soil Sci.*, **2**, 1 (1939).

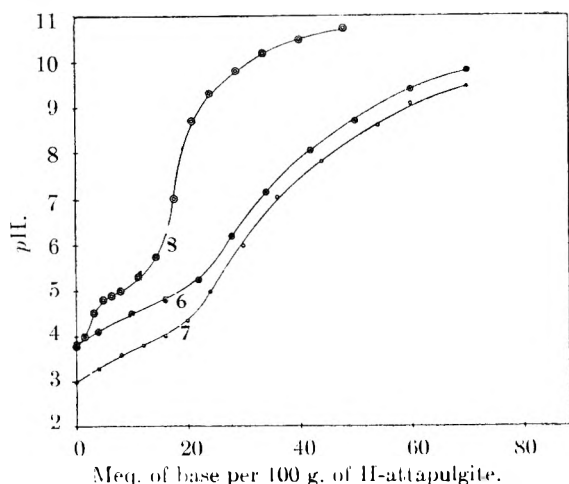


Fig. 4. —Curve 6, HA + *N* KCl-KOH; curve 7, HA + *N* BaCl₂-Ba(OH)₂; curve 8, HA + *N* KCl (supernatant liquid)-KOH.

pH and/or the greater the valency as well as concentration of the cations added to the sol, the larger will be the amount of H⁺ ions which will be neutralized, such "pH—, and cation effects" being a characteristic feature of heterogeneous acid systems.

The titration curve of the H-attapulgit + *N* KCl mixture gives an inflection at about pH 6.0 and the b.e.c. (about 25 meq.) calculated from this inflection is greater than that (20 meq.) at the second inflection of the "continuous" titration curve of the hydrogen attapulgit itself, though the latter inflection occurs at a higher pH, viz., 7.6. The "cation effect" here more than counterbalances the "pH effect."

The sol + salt mixture contains free H⁺ ions²⁴ exchanged for the cations of the salt and H⁺ ions still adhering to the surface. Because of their lesser binding energies compared with the hydroxylic hydrogens, the H⁺ ions balancing the isomorphous charge will be more easily exchanged than the other category of H⁺ ions. On the addition of the base to the mixture, the free H⁺ ions will be the first to become neutralized and that is why the titration curve of the mixture shows a more or less strong acid character. After these free H⁺ ions have been neutralized, H⁺ ions still adhering to the surface react with the base, and this reaction is facilitated by the exchange adsorption of the cations of the salt present in large numbers.

The titration curve of the clear supernatant liquid above the sol + *N* KCl mixture shows a pronounced inflection at about pH 7.0 and the b.e.c. calculated from this inflection is only slightly less than that given by the second inflection in the titration curve of the hydrogen attapulgit alone. This further shows that most of the H⁺ ions balancing the isomorphous charge were exchanged for the K⁺ ions of the added KCl. The titration curve of the supernatant liquid, however, does not resemble that of free HCl as would have been the case if only H⁺ ions had been exchanged for K⁺ ions. Actually, Al⁺⁺⁺ ions were also found in the supernatant liquid. The titration curve of the latter does show

(24) Al⁺⁺⁺ ions are also present.

features which would be expected if it contained Al⁺⁺⁺ ions in addition to free H⁺ ions, the first inflection in the titration curve indicating the free H⁺ ions. The Al⁺⁺⁺ ions, in all probability, were obtained by a secondary dissolution process, being the result of the action of the free acid created by the exchange of the H⁺ ions, on the hydrogen attapulgit.²⁵

Titration of the hydrogen nontronite in the presence of salts and of the clear supernatant liquid of the sol + salt mixture revealed features similar to those found in the case of the hydrogen attapulgit and they admit of a similar interpretation.

Adsorption of Ba⁺⁺ Ions from Solutions of Salts

Amounts of Ba taken up by the hydrogen attapulgit on repeated treatment with solutions of *N* BaCl₂ of pH 5.0, 7.0 and 9.0, respectively, are given in Table II which also shows, for the sake of comparison, the b.e.c.'s at the second and third inflections as given by the bottle titration curve (see Fig. 2) of the hydrogen attapulgit with Ba(OH)₂.

Ba adsorbed at pH			B.e.c. from bottle titration curve at	
5.0	7.0	9.0	Second ^a inflection	Third inflection
24.5	25.4	54.6	25.0	54.0

^a It is to be remembered that the first inflection in the bottle titration curve is really the second inflection.

The amount of Ba taken up at pH's 5.0 and 7.0 agrees with the b.e.c. calculated at the second inflection of the titration curve and, in the light of what has been said before, it indicates Ba⁺⁺ ions acquired by the surface in exchange for H⁺ ions balancing the isomorphous charge. The fact that a complete exchange of such H⁺ ions takes place even when the pH is as low as 5.0, shows that the "cation effect," in this case, is particularly strong and more than counterbalances the weak "pH effect." However, this strong cation effect, by itself, is ineffective in bringing about an exchange of the hydroxylic hydrogens. For this purpose, the leaching solution must have a pH as high as 9.0 as it is only then that the amount of Ba taken up from the solution agrees with the b.e.c. calculated at the third inflection in the titration curve. It appears, therefore, that the pH plays a more important part in the exchange of hydroxylic hydrogens compared with the H⁺ ions belonging to the other category.

Using 0.1 *N* calcium acetate as the leaching solution, Marshall and Caldwell¹³ found that even when the pH of this solution was as high as 9.0, the amount of Ca taken up from it did not exceed the value which would be expected from the isomorphous charge alone. Our experiments with 1.0 *N* BaCl₂ solution of pH 9.0, however, lead to a different conclusion. The larger concentration of the salt used by us and the stronger adsorption of Ba⁺⁺ ions compared with Ca⁺⁺ ions may account for the different results obtained. Caldwell and Marshall's titration curve with Ca(OH)₂ shows the final inflection at about pH 8.2 where all the available H⁺ ions, including the hydroxylic hydrogens, were neutralized. If this pH could be sufficiently high for a complete neutralization by the base alone, it is difficult

(25) H. Paver and C. E. Marshall, *J. Soc. Chem. Ind.*, **53**, 750 (1934).

to see why at the higher pH, 9.0, no hydroxylic hydrogen should have been replaced by Ca^{++} ions when the salt was also present. One would rather expect a reinforcing effect of the salt on the effect of the pH only.

The hydrogen nontronite behaves differently from hydrogen attapulgite in respect of Ba^{++} ions taken up from 1.0 *N* BaCl_2 solutions. Bottle titration of a fine fraction (<0.7 micron) of hydrogen nontronite gave a b.e.c. of 105.0 meq. at the final inflection of its titration curve. This amount of Ba was also taken up from 1.0 *N* BaCl_2 solutions having pH's 5.0, 7.0 and 9.0. In the case of hydrogen nontronite, therefore, the cation effect plays a dominating role in the matter of an exchange of H^+ ions on the surface. Assuming that the final inflection in the titration curve of the hydrogen nontronite indicates hydroxylic hydrogens in addition

to H^+ ions balancing the isomorphous charge, comparison of the above results with those obtained with hydrogen attapulgite shows that the hydroxylic hydrogens in hydrogen nontronite are less strongly attached to the surface than in hydrogen attapulgite. The fact that the pH (about 8.0) at the final inflection in the titration curve of the hydrogen nontronite is much lower than in the case of the hydrogen attapulgite, also points to the same conclusion. Hydrogen montmorillonite also gives the final inflection at a pH of about 8.0⁷ and, like hydrogen nontronite, it shows this inflection in a continuous titration. Taking all these aspects into consideration, hydrogen nontronite appears to have a close resemblance with hydrogen montmorillonite; hydrogen attapulgite, on the other hand, shows significant differences insofar as electrochemical properties are concerned.

COLLECTOR-DEPRESSANT EQUILIBRIA IN FLOTATION. I. INORGANIC DEPRESSANTS FOR METAL SULFIDES

BY GEORGE A. LAST¹ AND MELVIN A. COOK

University of Utah, Salt Lake City, Utah

Received June 12, 1951

The "bubble pick up" method of Cooke and Digre was employed to obtain comprehensive equilibrium data for the system potassium *n*-amylxanthate-sodium sulfite-galena at 25°. A free acid collector-free acid depressant single site mechanism was developed, based on the Cook hydrolytic adsorption theory and found to give a complete and self consistent correlation of the experimental results of this study together with results of investigation of sixteen other similar systems studied by Wark.

The term "depressant" is generally applied in flotation technology to any substance which will prevent or limit flotation of a mineral. While this generally occurs by means of a competitive adsorption with the collector, in some instances this interference may act in other ways, for example some colloidal depressants may function by adsorbing and thereby buffering the collector. Depressants may be classed into: (1) the "ionic" depressants which are vastly important in metal sulfide flotation, and (2) the colloidal depressants. Class (1) depressants are those obtained from aqueous solutions of such salts as sodium sulfide and sodium cyanide. Examples of class (2) are glue, gelatin, casein, tannin, quebracho, starch and dextrine. This paper deals with certain of the class (1) depressants.

Recently there was introduced² a new theory of so-called "anionic" and "cationic" collectors in which collector properties were attributed to "hydrolytic" adsorption, that is, free acid (or free base) adsorption in the case of anionic (or cationic) collectors. The mechanism was applied in metal sulfide flotation with xanthates and related collectors by Cook and Nixon, and was employed by

Wadsworth, Conrady and Cook³ in obtaining an equation relating contact angle and surface coverage for ethylxanthic acid on galena. It was also applied in interpreting the behavior of oleic acid as a collector for fluorite⁴ both at low temperatures where, with oleic acid, non-selective (physical) adsorption occurs and at high temperatures where selective chemisorption occurs. The experimental data interpreted in this paper include data measured in the present study for the system potassium *n*-amylxanthate sodium sulfide-galena together with extensive data obtained by Wark and co-workers^{5,6} for some sixteen different collector-depressant-mineral systems involved in metal sulfide flotation.

The earlier work by Wark⁵ indicated that the collector-depressant equilibria in metal sulfide systems were governed by a competitive adsorption of collector "ions" (designated here X^-) and depressant "ions" (D^-). Depressant species considered by Wark included HS^- , CN^- and OH^- . Wark also showed that D^- and the ratio X^-/D^- were constant along an m_{D} (depressant salt) vs. pH curve, and thus concluded that the effective collector and depressant were the corresponding anions.

This paper discusses the limitations of Wark's

(1) This paper comprises part of a thesis presented by G.A.L. in partial fulfillment of the requirements for the degree of Doctor of Philosophy, June, 1951, Department of Metallurgy, University of Utah, Salt Lake City, Utah. This work was supported by the Atomic Energy Commission.

(2) M. A. Cook, "Mechanism of Collector-Mineral Attachment in Flotation" (unpublished); summarized in *Eng. Min. Jnl.*, **160**, (2) 110 (1949); *Chem. Eng. News*, **27**, 489 (1949).

(3) M. E. Wadsworth, R. G. Conrady and M. A. Cook, *This Journal*, **55**, 1219 (1951).

(4) M. A. Cook and A. W. Last, *Bulletin #47*, **40**, (14) May, 1950.

(5) I. W. Wark, "Principles of Flotation," Australasian Institute of Min. and Met., Melbourne, 1938.

(6) I. W. Wark and A. B. Cox, *AIMME*, TP 659 (1936).

explanation and provides unification of the experimental data by postulating not only hydrolytic (free acid) collector adsorption but also hydrolytic (free acid) depressant adsorption.

Experimental

The "bubble pick up" method of Cooke and Digre⁷ was employed to obtain equilibrium data for the potassium *n*-amylxanthate-sodium sulfide-galena system. The "bubble pick up" tubes consisted of 3.7 dm. (round bottom) tubes 20 cm. in length. These were fitted with a one holed 7 rubber stopper through which a 25 cm. length of 1.0 cm. glass tubing was passed to within 1 or 2 mm. of the bottom. A short length of rubber tubing, closed at one end, was attached to the central tube in such a manner that it could be mechanically collapsed to force an air bubble down the tube.

All reagents used were of analytical grade. The potassium *n*-amylxanthate was prepared and purified according to the method described by Foster.⁸ The final product (after three purifications) was believed to be of high purity.

The mineral used was a high purity -35/+48 mesh galena. This was cleaned by carrying it through the cycle of (1) boiling with dilute NaOH solution, (2) washing with distilled water, (3) boiling with nearly saturated NaCl solution, and (4) washing with distilled water until no chloride ion could be detected in the decanted solution. The galena was considered to be clean when no more than 4 or 5 particles were picked up when tested in a pick up tube containing distilled water. The galena was stored under distilled water and recleaned immediately before using by steps (3) and (4).

The temperature in all tests was maintained at $25 \pm 0.1^\circ$. A Coleman model 3-D pH meter was used to determine the pH of all solutions having a pH < 10.0. The indicated accuracy of this instrument was ± 0.05 pH unit. For solutions with a pH > 10.0, the pH was calculated from the concentrations of the components present in the solution. Buffered stock solutions were prepared using pure KCl to bring the ionic strength to 0.2. The buffers used were $\text{HCO}_3^-/\text{CO}_3^{2-}$ for pH values between 8.0 and 11.0, and $\text{H}_2\text{PO}_4^-/\text{HPO}_4^{2-}$ for pH values below 8.0. KOH was used to control pH above 11.0.

Each test was run by pipetting given volumes of the collector, depressant and buffer solutions into the "bubble pick up" tube (original solution being in the non "pick up" range) and adding approximately 0.5 g. of galena powder. After allowing 10 minutes or more for equilibrium to be established, the sample was tested by pressing an air bubble against the powder for 15 seconds, raising the bubble, and visually noting the "pick up." Successive additions of collector were made (allowing at least 10 minutes between each) until "pick up" was established. Some difficulty is experienced in a test such as this in deciding what constitutes a "critical bubble pick-up." For example, at least one or two small particles will generally adhere to an air

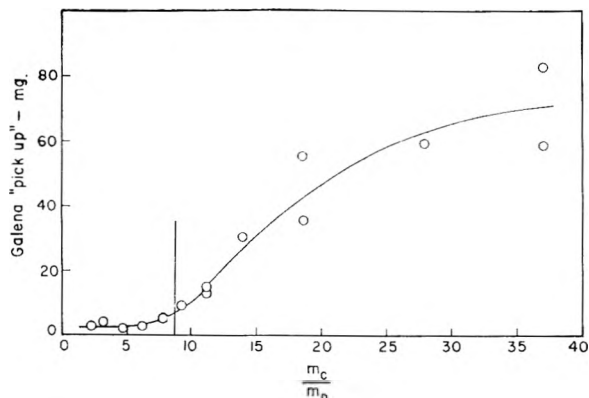


Fig. 1.—Sensitivity and standardization of "bubble pick-up" method.

(7) S. R. B. Cooke and M. Digre, *AIChE*, TP 2606, 2607, Mining Eng. No. 8 (1949).

(8) L. S. Foster, Technical Paper No. 2, Utah Engineering Experiment Station, 1928.

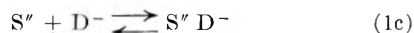
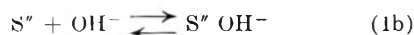
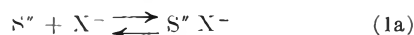
bubble even in pure water in the case of galena purified as described above. To determine the "best" definition of a "critical bubble pick-up" a series of tests were made in solutions of constant pH and ionic strength in which the ratio of collector to depressant was varied. The curve in Fig. 1 was obtained working at constant pH and constant depressant by varying the collector concentration. Each experimental point was obtained by removing the mineralized air bubble from the cell, drying the galena and weighing it. Incidentally, this test was also used to determine the approximate time for the attainment of equilibrium. In this test the weight of galena pick-up was measured as a function of time, other factors remaining constant, and found to reach a constant value within ten minutes in all cases, in agreement with the observations of Seidler.⁹

The pick-up shown by the vertical line in Fig. 1 namely 8 mg., was considered a satisfactory definition of the "critical bubble pick-up" because this point corresponded to the beginning of the region of rapid increase of weight as the ratio m_c/m_D was increased. Furthermore, this amount of pick-up was such that one could estimate it easily within relatively close limits, e.g., within 50% which corresponded to a relatively small error in the ratio m_c/m_D . By this means a standard visual method for determining the "critical bubble pick-up" point was established, thus enabling one to dispense with the tedious weighing method.

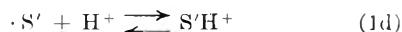
Figure 2 presents plots of the experimental data obtained in a comprehensive study of the system potassium *n*-amylxanthate-sodium sulfide-galena using the standardized visual inspection method for determining the "bubble pick-up" point. The data are plotted as m_c vs. m_D , both expressed in mg./liter, at constant pH. It was assumed in this work that the use of buffers in controlling pH and ionic strength would not interfere in the primary adsorption processes, but would assure against activity variations which otherwise might affect the results adversely. The tests covered a pH range of 5.7 to 13.3 and a concentration range up to 500 mg./liter for the collector and 150 mg./liter for the depressant.

Examination of "Ionic" Mechanism

The Wark "ionic" mechanism for the collector-depressant phenomena, while generally accepted for a number of years, has actually never been evaluated completely and objectively. There are, however, no apparent difficulties inherent in such an evaluation and it is thus worthwhile to undertake the evaluation here to bring out clearly the inherent weaknesses of the mechanism. For a single univalent depressant ion (D^-) system, Wark's mechanism involves the equilibria



where S'' is the electropositive site (the lead ion in galena). While the Wark discussion of this theory failed to include a consideration of the counter-ion adsorption, one must (on the assumption that all cations except hydrogen ion can be disregarded^{5,10}) also add the equilibrium equation for the counter-ion



where S' is the electronegative site (a surface sulfur ion in the case of galena). Cook and Nixon¹¹ believe that if an ionic mechanism is to apply, the counter-ions must occupy the compact double layer along with the anions in order to account for charge neutrality of the floated mineral and also

(9) P. Seidler, *Kolloid. Z.*, **68**, 89 (1934).

(10) H. Hagihara, *THIS JOURNAL*, **56**, 616 (1952).

(11) M. A. Cook and J. C. Nixon, *ibid.*, **54**, 445 (1950).

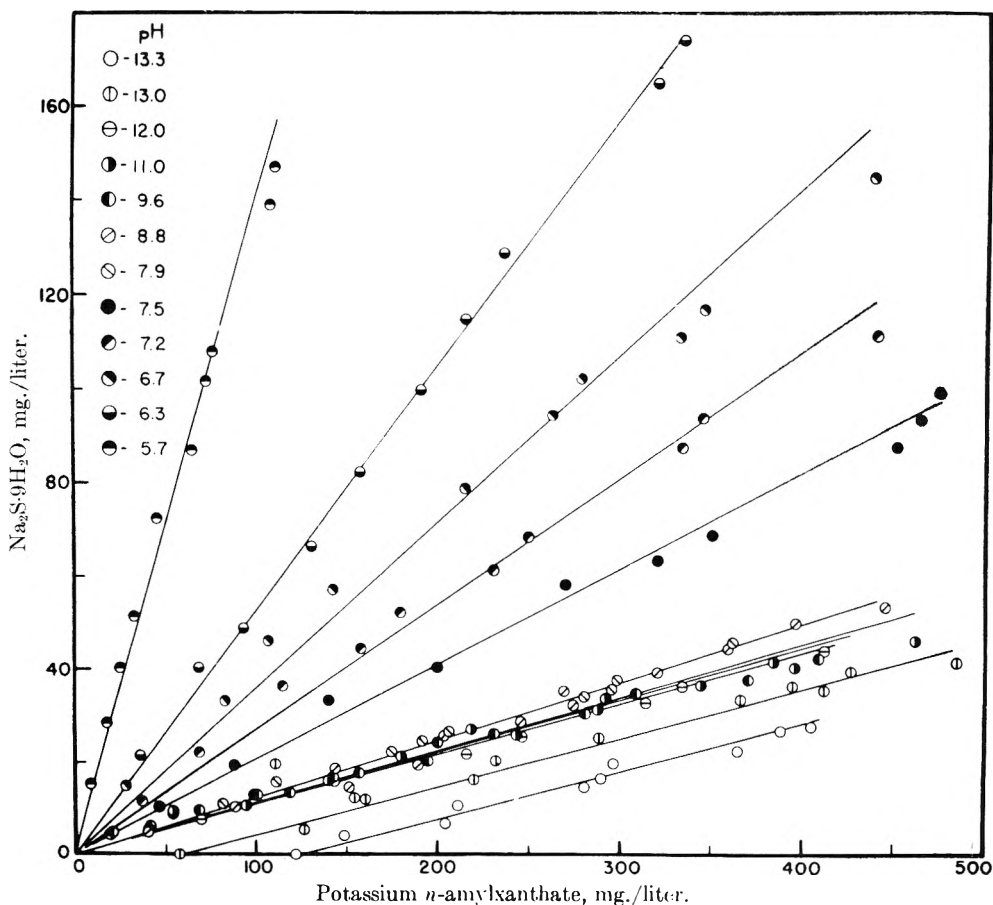


Fig. 2.—Experimental "bubble pick-up" data (galena-potassium *n*-amylxanthate-sodium sulfide).

the solution left behind. The condition for charge balance (for equal concentrations of S' and S'' sites) may be expressed by the equation

$$\phi = 1 - \theta_1'' - \theta_2'' - \theta_3'' = 1 - \theta' \quad (1e)$$

where ϕ is the fraction of each type of surface sites which remains unoccupied by collector and depressant ions (S''), or counter-ions (S'), θ_1'' , θ_2'' and θ_3'' are the fractions of the S'' sites occupied by X⁻, OH⁻, and D⁻, respectively, and θ' (= $\Sigma\theta_1'$) is the fraction of S' sites occupied by the counter-ion (H⁺).

The physical conditions of the "contact bubble" test and the "bubble pick-up" test both seem clearly to require the constancy of θ_1'' at the critical bubble contact point, *i.e.*

$$\theta_1'' = K' \quad (1f)$$

where K' is a constant. In other words the condition for air bubble attachment is determined by the presence on the surface of a certain fixed (critical) surface concentration of radicals responsible for the hydrophobic property, *e.g.*, the hydrocarbon radical. Of course, it is necessary to define what is meant by "bubble contact." It is possible, for example, that the investigators may define their critical "bubble contact" point differently. However, this will not present any serious difficulty as far as correlations are concerned so long as the data of each investigator are consistent. The equilibrium constants for reactions (1a)-(1d) are, respectively, defined as

$$K_1 = \theta_1''/(X^-)\phi \quad (1g)$$

$$K_2 = \theta_2''/(OH^-)\phi \quad (1h)$$

$$K_3 = \theta_3''/(D^-)\phi \quad (1i)$$

$$K_4 = \theta'/(H^+)\phi \quad (1j)$$

From equations (1e), (1h) and (1i), one obtains

$$\phi = (1 - \theta_1'')/(1 + y) \quad (1k)$$

where

$$y = K_2(OH^-) + K_3(D^-) \quad (1m)$$

Also, using equation (1j) with (1e) and (1k)

$$(H^+)K_4 = \frac{1 - \phi}{\phi} = \frac{y + K'}{1 - K'}$$

Substituting equation (k) in eq. (g) and eliminating y by means of eq. (m), one obtains the interesting relation

$$X^- = \frac{K'}{K_1} (1 + (H^+)K_4) \quad (2)$$

This equation implies that the critical X⁻ concentration is a function only of the hydrogen ion concentration, and D⁻ would then not act as a depressant at all! Furthermore, equation (2) is not in agreement with the observed "Barsky constant" (X⁻/OH⁻ = constant) in the absence of a specific depressant. The experimental facts are therefore incompatible with the Wark mechanism when one takes into consideration the requirements of charge neutrality, unless one denies the validity of the rather obvious relation (1f) assumed in the derivation of equation (2).

Proposed Mechanism

Since one can easily show that any double site mechanism is incompatible with the experimental data, the single site adsorption model involving both collector and depressants as free acids will now be investigated. The equilibria involved in this model are



The corresponding equilibrium constants are

$$K_1 = \frac{\theta_1}{\phi} \times \frac{1}{(\text{HX})} \quad (5)$$

$$K_2 = \frac{\theta_2}{\phi} \times \frac{1}{(\text{HD})} \quad (6)$$

where θ_1 is here the fraction of the surface sites covered by HX, θ_2 is the fraction of the surface sites covered by HD, and ϕ is the fraction of unoccupied surface sites given by the relation

$$\phi = 1 - \theta_1 - \theta_2 \quad (7)$$

Solving equation (6) for θ_2 , substituting into equation (7) and solving for ϕ one obtains

$$\phi = \frac{1 - \theta_1}{1 + K_2(\text{HD})} \quad (8)$$

Substituting (8) into equation (5)

$$K_1 = \frac{\theta_1}{1 - \theta_1} \times \frac{1 + K_2(\text{HD})}{(\text{HX})} \quad (9)$$

At the critical "bubble pick up" point the surface coverage θ_1 should be a constant, as discussed above, and

$$\theta_1/(1 - \theta_1) = K'' = \text{constant}$$

Equation (8) may then be written

$$K_1(\text{HX}) = K'' + K''K_2(\text{HD}) \quad (10)$$

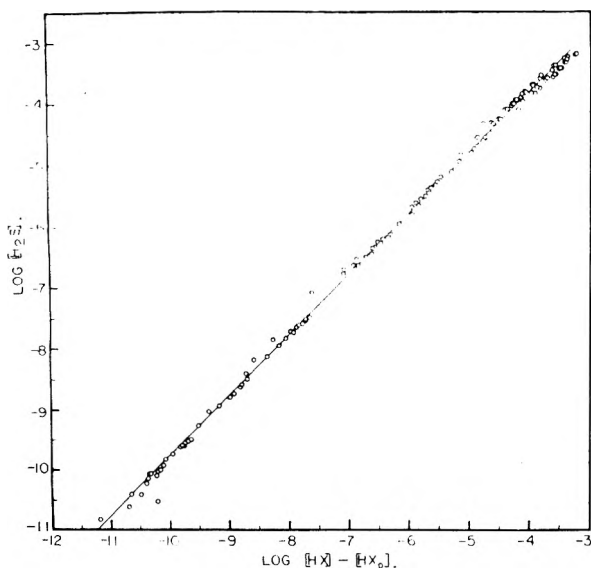


Fig. 3.—Experimental data of (Fig. 2) for the galena-*n*-amyl-anthate-sodium sulfide system plotted according to the single site free acid collector-free acid depressant adsorption mechanism.

Now, when $(\text{HD}) = 0$, $(\text{HX}) = (\text{HX}_0)$, and equation (10) becomes

$$K_1(\text{HX}_0) = K''$$

Hence

$$(\text{HX}) = (\text{HX}_0) + \frac{K''K_2}{K_1}(\text{HD}) \quad (11)$$

In logarithmic form

$$\log \{(\text{HX}) - (\text{HX}_0)\} = \log \frac{K''K_2}{K_1} + \log (\text{HD}) = \log B(\text{HD}) \quad (12)$$

where $B = K''K_2/K_1$. According to equation (12) a plot of $\log \{(\text{HX}) - (\text{HX}_0)\}$ vs. $\log (\text{HD})$ should give a straight line of unit slope. Figure 3 presents this plot for the data of Fig. 2, from which one will note that an excellent correlation is obtained.

Previously it has been conventional to plot experimental collector-depressant-mineral equilibrium data in terms of mg./l. of depressant vs. pH for constant collector concentrations. The following may be derived from equation (11).

$$m_D = \frac{(m_c - m_{c0})}{B'} \times \frac{K_D + (\text{H}^+)}{K_c + (\text{H}^+)} \quad (13)$$

where m_D is expressed as mg./l. of depressant salt, m_c as mg./l. of collector salt, m_{c0} is the collector salt concentration required for the critical free acid concentration (HX_0) , B' is $(K''K_2)/K_1$ in appropriate units, K_D is the dissociation constant of the depressant, and K_c is the dissociation constant of the collector. By means of equation (11) one may construct plots of depressant salt vs. pH

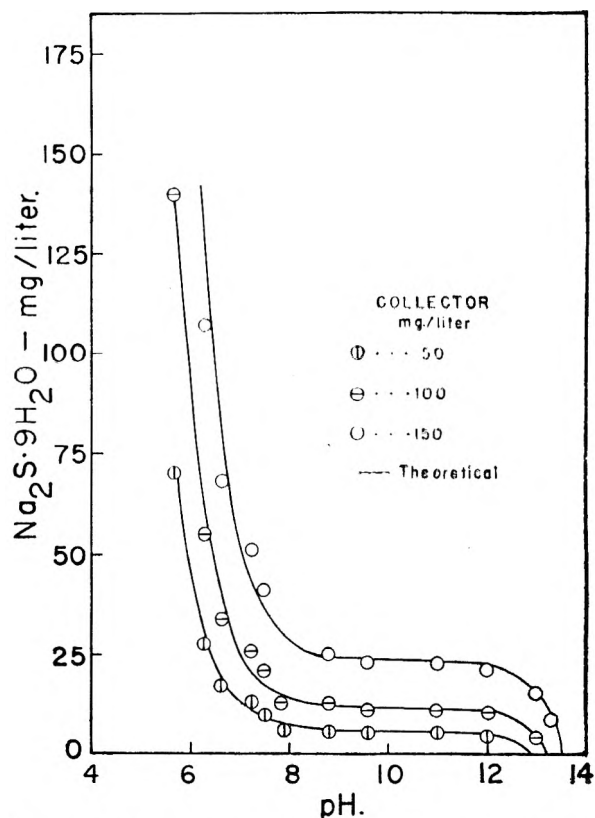


Fig. 4.—Depressant salt concentration vs. pH (galena-potassium *n*-amylxanthate-sodium sulfide).

TABLE I

ADSORPTION CONSTANTS AND ADSORPTION POTENTIALS FOR SEVERAL COLLECTORS AND DEPRESSANTS ON VARIOUS MINERALS

Mineral	Collector	Depressant	K_1	K_2	$-\Delta F^{\text{(cal.)}}$ collector	$-\Delta F^{\text{(cal.)}}$ depressant
Pyrite	Diethyl dithiophosphate	NaCN	4.67×10^7	2.95×10^6	10,600	8,900
Pyrite	Diethyl dithiocarbamate	NaCN	3.25×10^7	4.95×10^6	10,400	9,200
Pyrite	Ethyl xanthate	NaCN	6.1×10^{11}	2.72×10^6	16,200	8,800
Pyrite	<i>n</i> -Amyl xanthate	NaCN	8.06×10^9	7.31×10^6	13,700	9,500
Pyrite	Di- <i>n</i> -amyl dithiocarbamate	NaCN	8.13×10^7	4.56×10^6	10,900	9,200
Chalcopyrite	Ethyl xanthate	NaCN	1.21×10^{13}	1.37×10^7	18,000	9,800
Marcasite	Ethyl xanthate	NaCN	1.92×10^{12}	7.65×10^6	16,900	8,100
Bornite	Ethyl xanthate	NaCN	1.21×10^{16}	1.21×10^8	20,800	11,100
Tetrahedrite	Ethyl xanthate	NaCN	1.21×10^{16}	7.69×10^7	20,800	10,900
Covellite	Ethyl xanthate	NaCN	3.05×10^{14}	6.85×10^6	20,000	9,400
Galena	Ethyl xanthate	Na ₂ S·9H ₂ O	4.85×10^{11}	1.37×10^{10}	16,100	14,000
Activated sphalerite	Ethyl xanthate	Na ₂ S·9H ₂ O	3.85×10^{15}	1.22×10^{12}	20,100	16,700
Chalcopyrite	Ethyl xanthate	Na ₂ S·9H ₂ O		9.6×10^7		13,800
Bornite	Ethyl xanthate	Na ₂ S·9H ₂ O		1.53×10^{11}		15,400
Covellite	Ethyl xanthate	Na ₂ S·9H ₂ O		2.42×10^{10}		14,300
Pyrite	Ethyl xanthate	Na ₂ S·9H ₂ O		3.42×10^7		10,400
Galena	<i>n</i> -Amyl xanthate	Na ₂ S·9H ₂ O	3.32×10^{10}	1.86×10^{10}	14,500	14,200

for any desired concentration of collector. Figure 4 presents such plots for collector concentrations of 50, 100 and 200 mg./l. of potassium *n*-amyl-xanthate. The experimental points were taken at constant collector concentrations from Fig. 2.

Evaluation of K_1 , K_2 and K'' and Adsorption Potentials.—By substituting $K_1(\text{HX}_0)$ for K'' in equation (11), and solving for K_2 , one obtains

$$K_2 = \frac{(\text{HX}) - (\text{HX}_0)}{(\text{HX}_0)(\text{HD})} \quad (14)$$

Wadsworth, Conrady and Cook³ have shown in the case of ethyl xanthate and galena that zero contact angle corresponds to a surface coverage (θ) of 16% or less and that a 25° contact angle corresponds to approximately 50% surface coverage. On this basis, we have assumed a value of unity for K'' , that is, that our concentration of adsorbed collector for 8 mg. pick-up corresponds to roughly half coverage by collector molecules. By use of the value unity for K'' , K_1 becomes

$$K_1 \cong 1/(\text{HX}_0)$$

Since K_1 and K_2 are surface equilibrium constants, one may determine the free energy of adsorption (ΔF) for both the collector and the depressant by means of the equation

$$-\Delta F_i = RT \ln K_i \quad (15)$$

Consideration of Literature Data

The extensive data of Wark^{5,8} were analyzed by means of the equations and methods of the previous section. Equilibrium constants and the corresponding free energies computed from equation (15) are given in Table I. The values of the dissociation constants employed are listed in Table II. It is of interest to note that the values obtained for K_2 for NaCN on pyrite are practically the same

regardless of the collector involved in the system (see Table I). This indicates, in agreement with the proposed mechanism, that the adsorption potential for the depressant is independent of the collector used. This also applies to the collector since HX_0 is constant and independent of the depressant present in the system.

TABLE II

HYDROLYSIS CONSTANTS FOR COLLECTOR AND DEPRESSANT ACIDS

Acid	Dissociation constant
<i>n</i> -Amylxanthic	$1 \times 10^{-6.6}$
Ethylxanthic	$3 \times 10^{-3.6,11}$
Diethyl-dithiophosphoric	$2.3 \times 10^{-5.2}$
Diethyl-dithiocarbamic	$1.6 \times 10^{-7.11}$
Di- <i>n</i> -amyl-dithiocarbamic	$2 \times 10^{-9.11}$
Hydrothiosulfuric	$5.7 \times 10^{-8.12}$
Hydrocyanic	$7.2 \times 10^{-10.12}$

^a Value giving best fit of experimental data. Cook and Nixon¹¹ obtained the value 4.5×10^{-6} which is in fair agreement with our value. ^b References.

In general $\text{HX} \gg (\text{HX}_0)$ as long as HD is present in significant amounts, which is true along all of the depressant vs. pH curves of Wark. One may, therefore, write equation (14) for all practical purposes as

$$\log (\text{HX}) = \log B (\text{HD}) \quad (16)$$

From this equation it is seen that the log (HX) vs. log B (HD) plot should be a straight line of unit slope passing through the origin. This plot is presented in Fig. 5 for seventeen different collector-depressant-mineral systems including the one studied here. Values of B determined from the data in Tables I and II are also given in Fig. 5.

(12) N. A. Lange, "Handbook of Chemistry," 6th Ed., Handbook Publishers, Inc., Sandusky, Ohio, 1946.

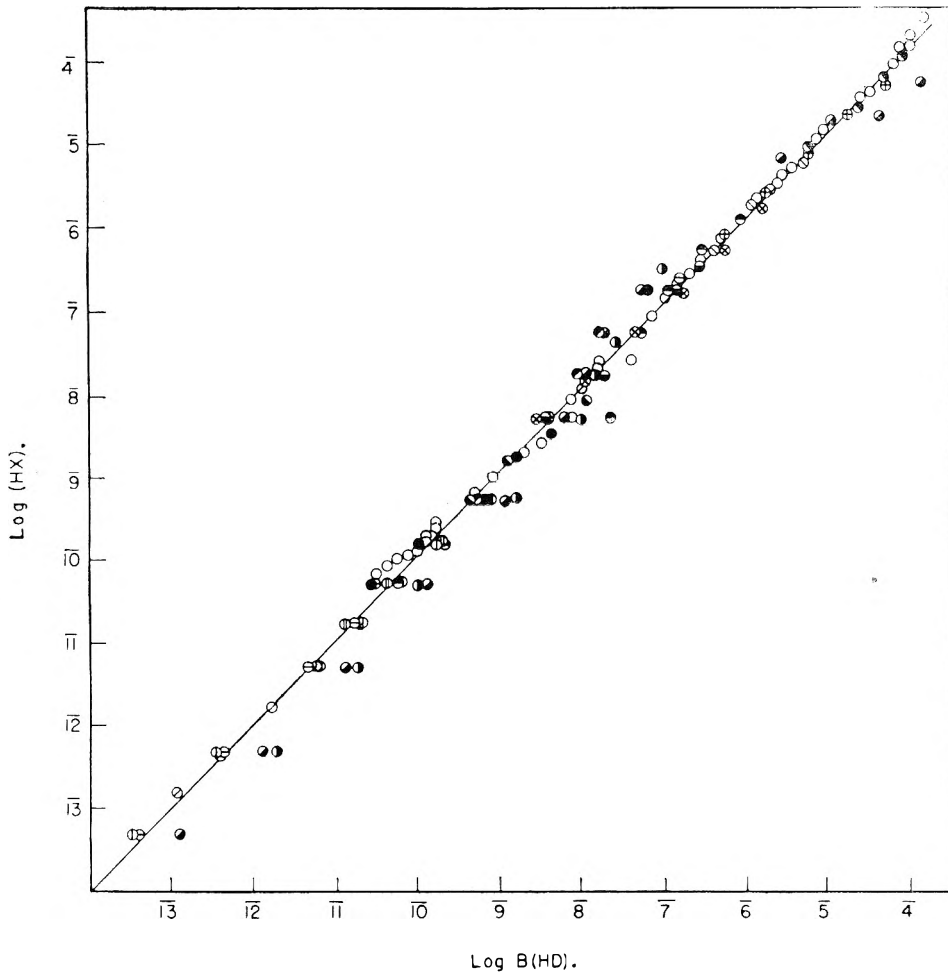


Fig. 5.—Correlation of literature data by hydrolytic adsorption mechanism:

System	B
● KEtX-NaCN-CHALCOPYRITE	1.24×10^{-6}
⊕ KEtX-NaCN-MARCASITE	5.31×10^{-7}
⊖ KEtX-NaCN-BORNITE	1.19×10^{-7}
⊗ KEtX-NaCN-TETRAHEDRITE	8.04×10^{-8}
⊙ KEtX-NaCN-COVELLITE	2.88×10^{-8}
○ KAmylX-Na ₂ S-GALENA (data of G. Last and Cook)	5.60×10^{-1}
⊗ KEtX-Na ₂ S-GALENA	2.96×10^{-2}
● KEtX-Na ₂ S-SPHALERITE (activated)	3.25×10^{-3}
● KEtX-Na ₂ S-CHALCOPYRITE	7.69×10^{-4}
● KEtX-Na ₂ S-BORNITE	2.15×10^{-4}
● KEtX-Na ₂ S-COVELLITE	1.10×10^{-4}
● KEtX-Na ₂ S-PYRITE	4.15×10^{-5}
● Diethyldithiophosphate-NaCN-PYRITE	7.02×10^{-2}
● Diethyldithiocarbamate-NaCN-PYRITE	1.52×10^{-1}
● KETX-NaCN-PYRITE	5.01×10^{-6}
⊗ KAmyl-NaCN-PYRITE	9.90×10^{-4}
⊕ Di-n-amylthiocarbamate-NaCN-PYRITE	5.73×10^{-2}

The agreement between theory and observation provides substantial support for the hypothesis of hydrolytic adsorption of both collector and depressant in metal sulfide flotation.

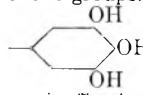
COLLECTOR-DEPRESSANT EQUILIBRIA IN FLOTATION. II. DEPRESSANT ACTION OF TANNIC ACID AND QUEBRACHO¹

BY GEORGE A. LAST AND MELVIN A. COOK

Department of Metallurgy, University of Utah, Salt Lake City, Utah

Received June 12, 1951

An experimental investigation of the systems galena-*n*-amyl xanthate-tannic acid and galena-*n*-amyl xanthate-quebracho was carried out, and the data interpreted by the single site model for hydrolytic (free acid) collector-depressant adsorption. These depressants are regarded as having two surface active groups capable of adsorbing on a galena surface, namely, the carboxyl and phenolic groups. It is assumed that not all the phenolic groups are active as depressants, but only the undis-

sociated radical . Some indications have been obtained which suggest that tannins in the colloidal form, i.e., as micelles, are ineffective as depressants for galena.

Part I² presented arguments that "ionic" depressants and collectors in metal sulfide flotation attach themselves to a mineral surface by means of single site adsorption of the neutral free acid molecules.³ Only a few studies have been carried out and very little is known about the actual mechanism by which colloidal depressants produce their effects upon a mineral surface. Bartsch⁴ showed that gelatine prevented the adsorption of oleic acid on chalcopyrite. However, Kellerman⁵ claimed that caprylic acid was adsorbed by galena even when flotation of the mineral was prevented by saponin. Thus, at the present time, it is not possible even to conclude that all colloidal depressants function by preventing the adsorption of the collector on the mineral surface.

This paper presents the results of an experimental investigation of the systems tannic acid-amyl xanthate-galena and quebracho-amyl xanthate-galena. It shows that the depressant properties of tannic acid and quebracho on galena may be interpreted by means of the free acid adsorption theory and in these cases at least the mechanism of depressant action is apparently the same as for the "ionic" depressants.

Experimental Procedure and Results.—The experimental method adopted for this study was the same as that used in part I, namely, the "bubble pick up" technique introduced by Cooke and Digré.⁶ All reagents used, except the quebracho, were of analytical reagent grade. The quebracho was the commercial quebracho extract. Ionic strength was maintained at 0.05 throughout all tests. The temperature of the solutions was maintained at 25 ± 0.1°. For a description of the apparatus, method of preparation of the galena, preparation of the solution, pH control, temperature control and experimental procedure see part I.²

Figures 1 and 2 show plots of the experimental data obtained in this investigation. The data are expressed in mg./l. units as total depressant (m_d) vs. total collector salt (m_c) at constant pH. Each curve of each figure connects points representing incipient floatability as shown by Fig. 1 of part I of this series of papers. Figure 1 gives the results for the tannic acid-xanthate-galena system and Fig. 2 those for quebracho-xanthate-galena system. Figures 3 and 4 are

(1) This paper comprises part of the dissertation submitted by G. A. Last in partial fulfillment of the requirements for the degree of Doctor of Philosophy, June, 1951. This investigation was supported by the Atomic Energy Commission.

(2) G. A. Last and M. A. Cook, *THIS JOURNAL*, **56**, 637 (1952).

(3) M. E. Wadsworth, R. E. Conrady and M. A. Cook, *ibid.*, **55**, 1219 (1951).

(4) O. Bartsch, *Kolloidchem. Beihefte*, **20**, 1 (1924).

(5) K. Kellermann, *Kolloid Z.*, **63**, 220 (1933).

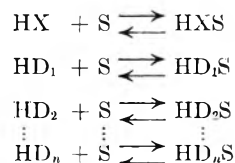
(6) S. R. B. Cooke and M. Digré, *AIMME*, TP 2606, TP 2607 Mining Eng. No. 8 (1948).

the low depressant-low collector portions of Figs. 1 and 2, respectively. These figures include the data which are important in the evaluation of the depressant mechanisms involved in this study.

Theoretical Considerations.—In part I it was shown, in the case of systems containing a single collector and a single depressant, that the equilibrium between collector and depressant may be expressed by the relationship

$$K_1[(HX) - (HX_0)] = K''K_2(HD) \quad (1)$$

where (HX) is the concentration of the collector free acid, (HX₀) is the critical collector free acid concentration to give "bubble pick up," (HD) is the depressant free acid concentration, K_1 and K_2 are the adsorption constants of HX and HD, respectively, and $K'' = \theta_{HX}/(1 - \theta_{HX})$ where θ_{HX} is the fraction of surface sites covered by the collector. In order to analyze data involving more than one depressant group, as will be the case with tannic acid and quebracho, it is necessary to develop a more general form of equation (1). Assuming that the collector and depressants follow the free acid single site adsorption mechanism, the equilibria may be written



where HX, HD₁, HD₂, ..., HD_n are the free acid collector and depressant molecules, S is the surface site, and HXS, HD₁S, HD₂S, ..., HD_nS are the filled surface sites. The equilibrium equations for the above reactions are

$$\begin{aligned} K_1(HX) &= \theta_{HX}/\phi \\ K_2(HD_1) &= \theta_{HD_1}/\phi \\ K_3(HD_2) &= \theta_{HD_2}/\phi \\ \vdots &\quad \quad \quad \vdots \\ K_{n+1}(HD_n) &= \theta_{HD_n}/\phi \end{aligned} \quad (2)$$

Hence

$$\sum_{i=1}^n K_{i+1}(HD_i) = \frac{1}{\phi} \sum_{i=1}^n \theta_{HD_i} \quad (3)$$

where (HD_i) is the concentration of the *i*th depressant free acid, K_{i+1} is its adsorption constant, θ_{HD_i} is the fraction of surface sites covered by

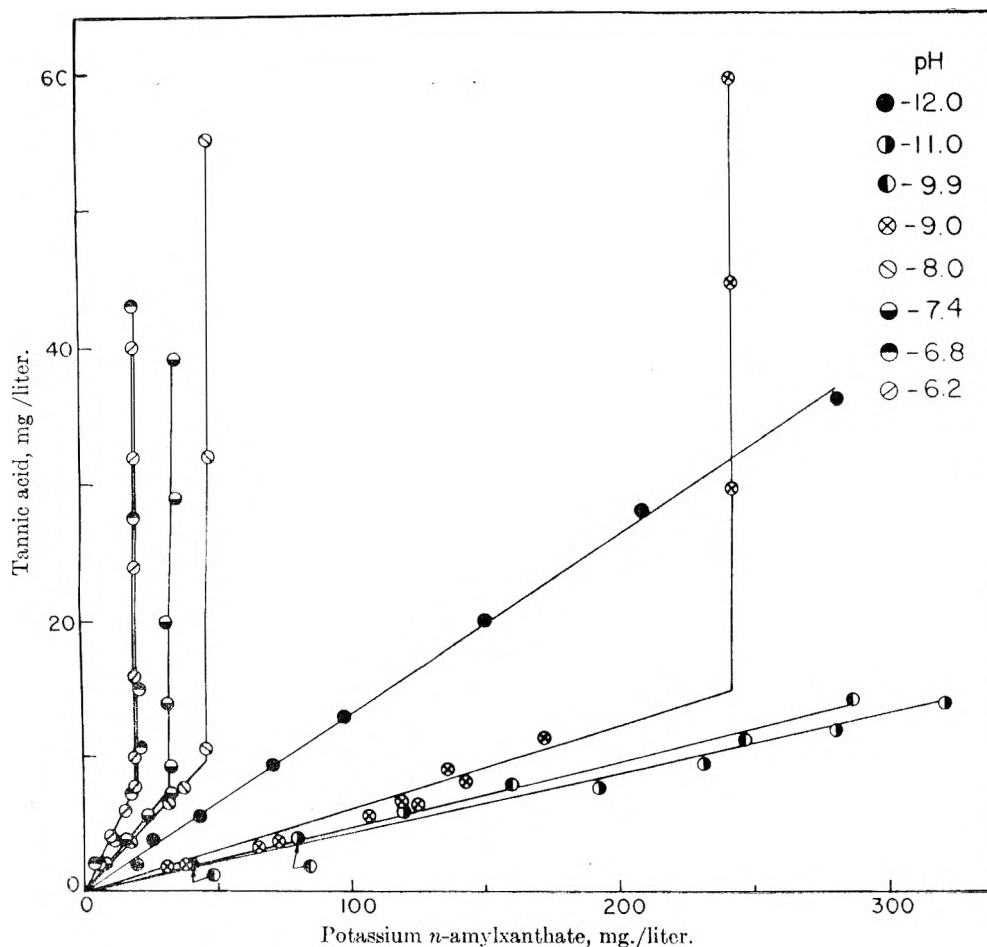


Fig. 1.—Experimental “bubble pickup” data (galena-potassium *n*-amyloxanthate-tannic acid); quebracho, mg./liter.

HD_i , and ϕ is the fraction of unoccupied surface sites. Thus one may write

$$\phi = 1 - \theta_{HX} - \theta_{HD_1} - \theta_{HD_2} \cdots \theta_{HD_n}$$

or

$$\phi = 1 - \theta_{HX} - \sum_1^n \theta_{HD_i} \quad (4)$$

Solving (3) for $\sum_1^n \theta_{HD_i}$, substituting into (4) and solving for ϕ or c obtains

$$\phi = \frac{1 - \theta_{HX}}{1 + \sum_1^n K_{i+1}(HD_i)} \quad (5)$$

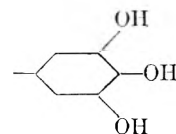
Substituting (5) in (2)

$$K_1 = \frac{\theta_{HX}}{c - \theta_{HX}} \times \frac{1 + \sum_1^n K_{i+1}(HD_i)}{(HX)} \quad (6)$$

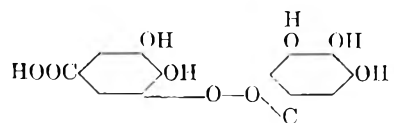
At the threshold of “bubble pick up” physical conditions of the test apparently impose the condition $\theta_{HX} = \text{constant}$, or $K'' = \theta_{HX}/(1 - \theta_{HX})$. In the absence of depressant, equation (6) reduces to $K_1 = K''/(HX_0)$ so that (setting $K'' = 1$ as before)

$$K_1[(HX) - (HX_0)] = \sum_1^n K_{i+1}(HD_i) \quad (7)$$

Analysis of Results.—The depressants (tannic acid and quebracho) used in this study are polybasic, *i.e.*, both the carboxyl and phenolic groups have acidic properties. The carboxyl group functions in the conventional manner, *i.e.*, in the neutral free acid form it is surface active and capable of adsorbing on a mineral surface. However, the phenolic groups are not all surface active. This is probably due to the manner in which they are associated in the molecule. The surface active group may be considered to be the radical



The tannic acid (*m*-digallic acid) used was one with the following structure⁷ (and contained 12% water).



Complete data on the dissociation constant of this

(7) Paul Karrer, “Organic Chemistry,” Elsevier Publishing Co., Inc., Amsterdam, 1947

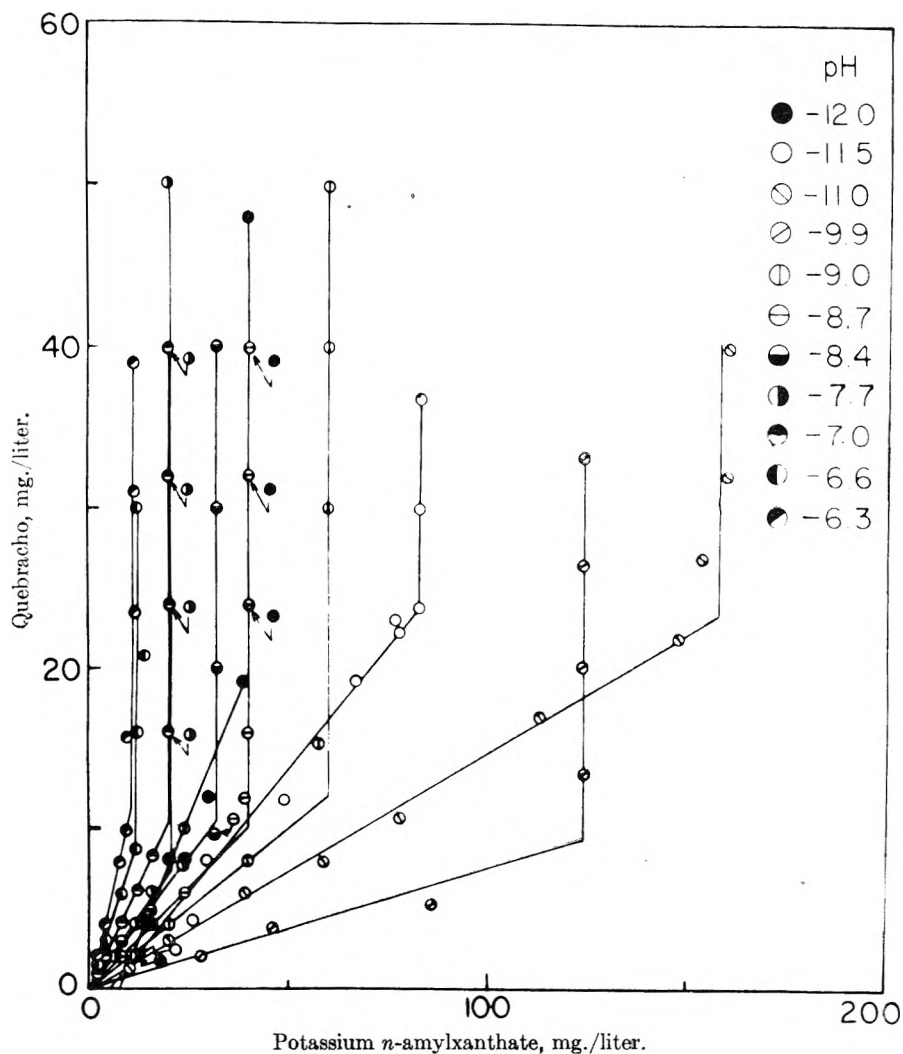
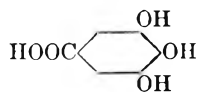
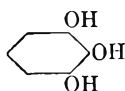


Fig. 2.—Experimental "bubble pickup" data (galena-potassium *n*-amylxanthate-quebracho).

compound are lacking. Sunthanker and Jatkar⁸ reported K_1 (carboxyl group) to be 1.32×10^{-5} . In order to obtain approximate values for K_2 and K_3 (dissociation constants of the first and second phenolic groups) we have taken known dissociation constants for similar radicals of compounds with the same type structures. Thus the dissociation constant of the first phenolic group of tannic acid should be of the order of magnitude of the dissociation constant of the first phenolic group of gallic acid



and the dissociation constant of the second phenolic group of tannic acid should be of the order of magnitude of the dissociation constant of the second phenolic group of pyrogallol



This comparison is substantiated by the close com-

(8) S. R. Sunthanker and S. K. K. Jatkar, *J. Indian Insti. Sci.*, **21A**, 209 (1938); *C. A.*, **33**, 507 (1939).

parison between the dissociation constant of the first phenolic group of gallic acid (1.41×10^{-9}) and the first phenolic group of pyrogallol (9.68×10^{-10}).⁹ From the above considerations the values of $K_2 = 1.41 \times 10^{-9}$ (dissociation constant of first phenolic group of gallic acid as determined by Abechandani and Jatkar⁹) and $K_3 = 2.30 \times 10^{-12}$ (dissociation constant of the second phenolic group of pyrogallol as determined by Abechandani and Jatkar) were used. For conformity with the terminology used in the derivation of equation⁵ and to avoid confusion with the adsorption constants, the dissociation constants of the depressants will henceforth be referred to as K_{d1} , K_{d2} , K_{d3} , i.e., $K_{d1} = 1.32 \times 10^{-5}$, $K_{d2} = 1.41 \times 10^{-9}$, and $K_{d3} = 2.30 \times 10^{-12}$.

Quebracho (along with oak and chestnut tannins) is one of the condensed tannins. The commercial quebracho extract contains about 80% of tannin plus small amounts of lactic, acetic and gallic acids.¹⁰ The molecular weights of the tannins in quebracho vary over a considerable range.

(9) C. T. Abechandani and S. K. K. Jatkar, *J. Indian Insti. Sci.*, **21A**, 417 (1938); *C. A.*, **33**, 3662 (1939).

(10) G. D. McLaughlin and E. R. Theis, "The Chemistry of Leather Manufacture," Reinhold Publishing Corp., New York, N. Y., 1945.

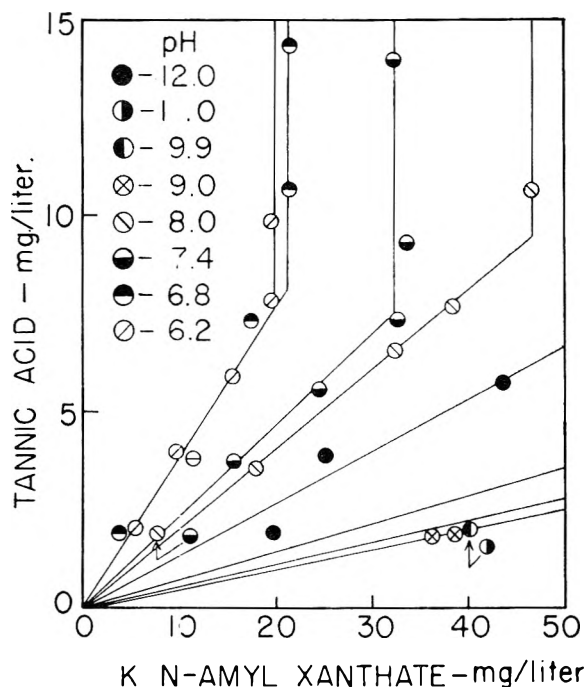


Fig. 3.—Low collector salt—low depressant salt portion of Fig. 1.

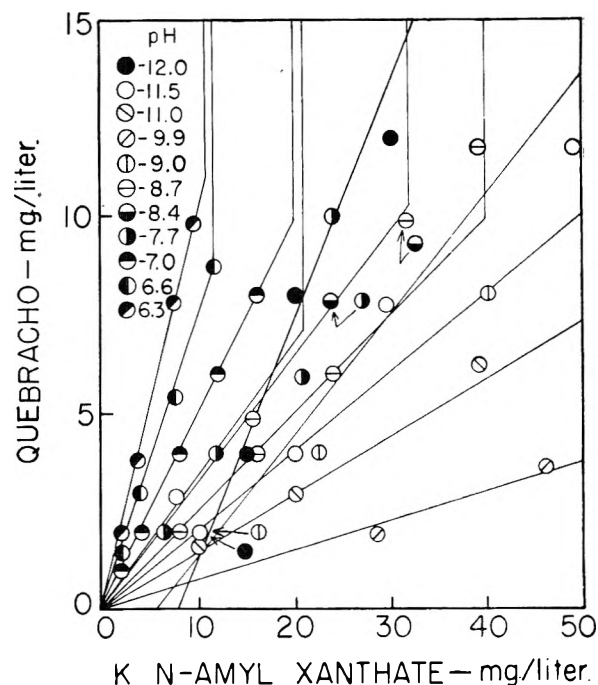


Fig. 4.—Low collector salt—low depressant salt portion of Fig. 2.

Douglas and Humphreys¹¹ found the molecular weight of quebracho to be 1159 before dialysis and 2421 after dialysis. Tests showed that considerable tannin passed through the cellophane dialysis membrane which would allow only the passage of molecules with molecular weights less than 500. Sokolov and Koyakova¹² found the dissociation constants for oak bark tannin to be $K_{d_1} = 6 \times 10^{-5}$ (carboxyl group) and $K_{d_2} = 1 \times 10^{-8}$ (phenolic group). The equivalent weights for these groups were found to be about 1800 for the carboxyl group and 300 for the phenolic group. Inasmuch as similar data were not available for quebracho, the above data were used here in the evaluation of the depressant action of commercial quebracho extract. The value of 4×10^{-12} for K_{d_3} (dissociation constant of second phenolic group), is the value for the best fit of the experimental curves as determined by trial of various values. The value 4.5×10^{-6} for the dissociation constant of *n*-amyl xanthate determined by Cook and Nixon¹³ was used. This differs slightly from the value used in part I (1.0×10^{-6}) but gives slightly better agreement in the present results than the value obtained independently in Part I. The difference, however, is practically insignificant. In the interest of consistency one should, of course, use either one value or the other. However, the tedious recalculations necessary to do this do not seem justified.

Since both tannic acid and quebracho contain two surface active groups, treating each group as though it were a separate acid, equation (7) reduces to

$$K_1[(HX) - (HX)_0] = K_2(HD_1) + K_3(HD_2) \quad (8)$$

This equation will apply in the case of tannic acid

(11) G. W. Douglas and F. E. Humphreys, *J. Intern. Soc. Leather Trades Chem.*, **21**, 378 (1937); *C. A.*, **31**, 72826 (1937).

(12) S. I. Sokolov and G. E. Koyakova, *Kolloid Z.*, **72**, 74 (1935).

(13) M. A. Cook and J. C. Nixon, *This Journal*, **54**, 445 (1950).

and quebracho if we consider the carboxyl and phenolic groups to function separately, *i.e.*, each group is independently in equilibrium with the mineral surface and may be treated as though it were a separate species. This assumption necessitates neglecting the absorbed molecules which is here justified because of negligible total adsorption for the particular conditions involved here. That is, the surface area of the sample was far too small compared with the total concentrations involved to remove an appreciable amount of solute by absorption. Under conditions of constant pH and by combining constants, equation 8 reduces to the following expression

$$K_a m_c + K_b = m_a \quad (9)$$

where K_a and K_b are functions of pH (K_b is usually negligible except at high pH values). The initial linear variation of collector with depressant seen in Figs. 1 and 2 bears out the relationship shown in equation (9). The sharp discontinuities in the (constant pH) curves of Figs. 1 and 2 are believed to be due to micelle formation, *i.e.*, any tannic acid or quebracho in excess of the concentration at the point of discontinuity is supposedly in the form of micelles and thus ineffective in changing the concentration of the real (free acid) depressant in solution. However, further investigation of micelle formation by an independent method would be of value. By using the relationship $(HA) = (m_a - (H^+))/(K + (H^+))$ where (HA) is the free acid concentration, m_a is the initial salt concentration, and K is the dissociation constant of the free acid, one obtains the following expressions (a), (b) and (c) for the corresponding terms in equation (8)

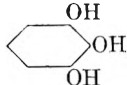
$$(a) \quad (HX) - (HX)_0 = \frac{m_c (H^+)}{K_c + (H^+)} - \frac{m_{c_0} (H^+)}{K_c + (H^+)} = \frac{(m_c - m_{c_0})(H^+)}{K_c + (H^+)} \quad (10)$$

where m_c is the added collector salt concentration, m_{c_0} is the collector salt concentration corresponding to (HX_0) and K_c is the dissociation constant of the collector free acid.

$$(b) \quad (HD_1) = \frac{m_{d_1}(H^+)}{K_{d_1} + (H^+)} \quad (11)$$

where m_{d_1} is the concentration of the carboxyl group associated with the added depressant and K_{d_1} is the dissociation constant of the carboxyl group.

$$(c) \quad (HD_2) = \frac{m_{d_2}(H^+)^2}{(K_{d_2} + (H^+))(K_{d_3} + (H^+))} \quad (12)$$

where m_{d_2} is the concentration of the  group associated with the added depressant and K_{d_2} and K_{d_3} are the dissociation constants of the above depressant group (considered here to be dibasic). Substituting (10), (11) and (12) into equation (8) there results the equation

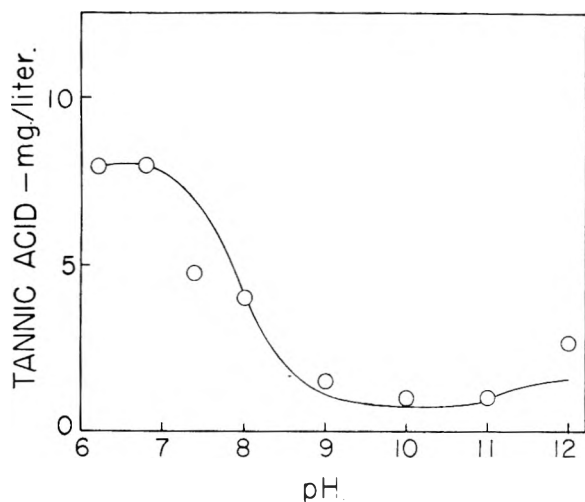


Fig. 5.—Theoretical depressant salt concentration vs. pH curve (galena-potassium *n*-amylxanthate-tannic acid)-potassium *n*-amyl xanthate = 20 mg./l.

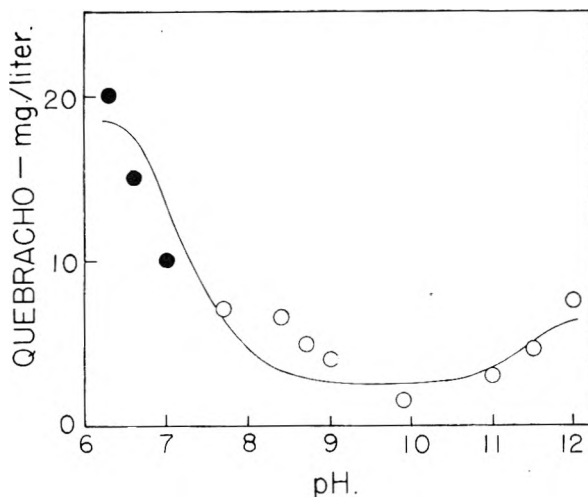


Fig. 6.—Theoretical depressant salt vs. pH curve (galena-potassium *n*-amylxanthate-quebracho)-potassium *n*-amylxanthate = 20 mg./l.

$$\frac{K_1(m_c - m_{c_0})(H^+)}{K_c + (H^+)} = \frac{K_2 m_{d_1}(H^+)}{K_{d_1} + (H^+)} + \frac{K_3 m_{d_2}(H^+)^2}{(K_{d_2} + (H^+))(K_{d_3} + (H^+))} \quad (13)$$

In equation (13) only the two constants K_2 and K_3 are unknown. These may be evaluated from two experimental points. (For the values of all constants see Table I).

In evaluating the data for tannic acid, the equivalent weights of the carboxyl and phenolic groups were taken as being the same as the molecular weight of the digallic acid used. In the case of quebracho the values of 3.3 meq./g. for the phenolic group and 0.55 meq./g. of the carboxyl group were

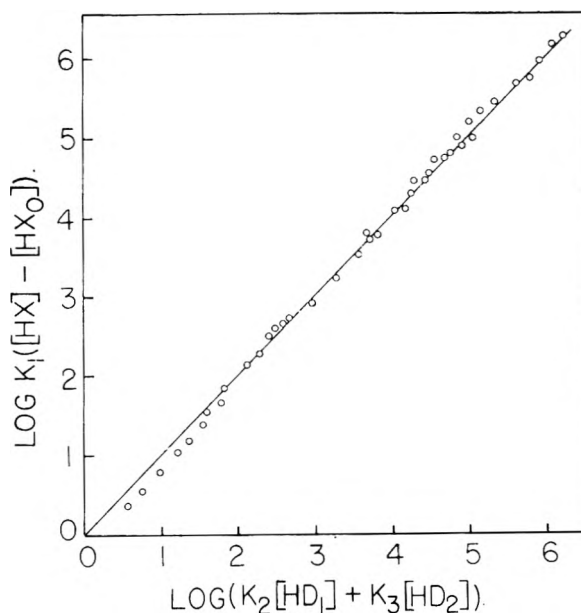


Fig. 7.—Experimental data (Fig. 1) plotted according to the single site free acid adsorption mechanism (galena-potassium *n*-amylxanthate-tannic acid).

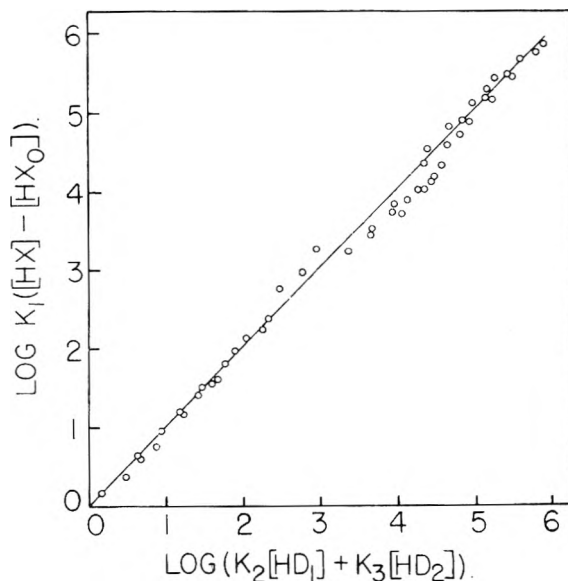


Fig. 8.—Experimental data (Fig. 2) plotted according to the single site free acid adsorption mechanism (galena-potassium *n*-amylxanthate-quebracho).

TABLE I

HYDROLYSIS CONSTANTS AND ADSORPTION CONSTANTS FOR TANNIC ACID, QUEBRACHO AND *n*-AMYL XANTHATE (ASSUMED IN THIS PAPER FOR PURPOSES OF CALCULATION AS OUTLINED IN THE TEXT)

Substance	Group	Dissociation constant	Adsorption constant
Tannic acid	Carboxyl	(K_{d_1}) 1.32×10^{-8}	(K_2) 1.8×10^{12}
	1st Phenolic	(K_{d_2}) 1.41×10^{-9}	(K_1) 1.8×10^9
	2nd Phenolic	(K_{d_3}) 2.30×10^{-11}	
Quebracho	Carboxyl	(K_{d_1}) 6×10^{-8}	(K_2) 1.5×10^{13}
	1st Phenolic	(K_{d_2}) 1×10^{-8}	(K_1) 3.5×10^9
	2nd Phenolic	(K_{d_3}) 4×10^{-11}	
<i>N</i> -Amyl xanthate		(K_a) 4.5×10^{-8}	(K_1) 1.5×10^{11}

employed.¹² Figures 5 and 6 are theoretical depressant vs. *pH* curves according to equation (13). The circles are data taken from Figs. 3 and 4. In Fig. 6 the solid circles indicate data obtained by extrapolation of the experimental data for the *pH* value indicated. The agreement between the experimental data and theory indicates the validity of the proposed free acid depressant mechanism for

tannic acid and quebracho. In Fig. 5 the disagreement between theory and experimental data at *pH* 12 may be largely corrected by increasing the value of K_{d_1} . In fact, such an increase in the magnitude of this constant is indicated by the author's value of the dissociation constant for the second phenolic group of the quebracho tannins.

In order to test all the data obtained in these two studies, it is necessary to employ a logarithmic form of equation (10), *i.e.*

$$\log K_1 ((HX) - (HX_0)) = \log (K_2(HD_1) + K_3(HD_2)) \quad (15)$$

According to equation (15) a straight line with a slope of unity passing through the origin should be obtained. Figures 7 and 8 show such plots using the data in Figs. 1 and 2. Only the data on the initial linear portion of the curves have been considered in this analysis. The excellent agreement between theory and data shown in Figs. 7 and 8 apparently substantiates the proposed mechanism of the depressant action of tannic acid and quebracho.

THE ROLE OF ADSORPTION IN THE REDUCTION OF ORGANIC MERCURY COMPOUNDS AT THE DROPPING MERCURY ELECTRODE

BY RUTH E. BENESCH AND REINHOLD BENESCH

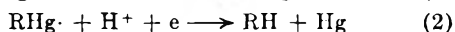
Department of Experimental Medicine, Northwestern University Medical School, Chicago, Illinois

Received June 27, 1961

It has been shown that the product resulting from the addition of one electron to certain organic mercury compounds is adsorbed at the dropping mercury electrode. The number of molecules adsorbed per unit area has been determined by several methods and the results were found to be in good agreement.

Introduction

It has been shown previously¹ that organic mercury compounds are reduced in two single electron steps at the dropping mercury electrode. The following reduction mechanism was proposed



Although this scheme was in agreement with most of the experimental facts, a number of observations could not be explained on the basis of this interpretation alone: (1) The wave-like irregularities on the first reduction wave above certain concentrations (Fig. 1). (2) The appearance of severe irregularities on the diffusion plateau of the first wave above certain concentrations, *e.g.*, 4×10^{-4} *M* in the case of phenylmercuric hydroxide (Fig. 2).

It was suspected that these phenomena might be due to adsorption of the organic mercury compounds or their reduction products at the surface of the mercury drop. Although surface active compounds are used widely in polarography for the suppression of maxima, cases in which the same compound is both surface active and electroactive have only rarely been encountered. One such example is methylene blue which was studied by Brdicka² who, on the basis of these investigations,

developed a general theory of polarographic adsorption waves.³ In the reduction of methylene blue a portion of the wave is shifted to more positive potentials forming a "pre-wave." This was ascribed to the adsorption of the reduction product, leuco methylene blue, at the electrode surface, so that the activity of the product is diminished by the free energy of adsorption. The height of this pre-wave is limited by the surface area of the mercury drop and therefore tends toward a constant value as the concentration is increased.

Experimental

The apparatus and methods used were essentially the same as those previously described.¹

The following experiments were carried out to determine whether the wave-like irregularity on the first wave (Fig. 1) was, in fact, a pre-wave caused by the adsorption of reduction products on the mercury surface:

(1) **Variation of the Height of the Pre-Wave (i_a) with Concentration.**—For these experiments the polarograms were spread over a narrow voltage span, *e.g.*, 0.5 volt (Fig. 3) so that sufficient separation of the pre-wave from the diffusion wave was obtained to permit accurate measurement of the height of the former. The results in Fig. 4 show that the height of the pre-wave varies logarithmically with concentration as would be expected for an adsorption wave.

(2) **Variation of i_a with the Height of the Mercury Reservoir above the Capillary Orifice (h).**—It is evident from the Ilkovic equation that the height of a diffusion wave (i_d) should vary with the square root of the height of the mer-

(1) R. Benesch and R. E. Benesch, *J. Am. Chem. Soc.*, **78**, 3391 (1951).

(2) R. Brdicka, *Z. Elektrochem.*, **48**, 278 (1942).

(3) R. Brdicka, *Collection Czechoslov. Chem. Commun.*, **12**, 522 (1947).

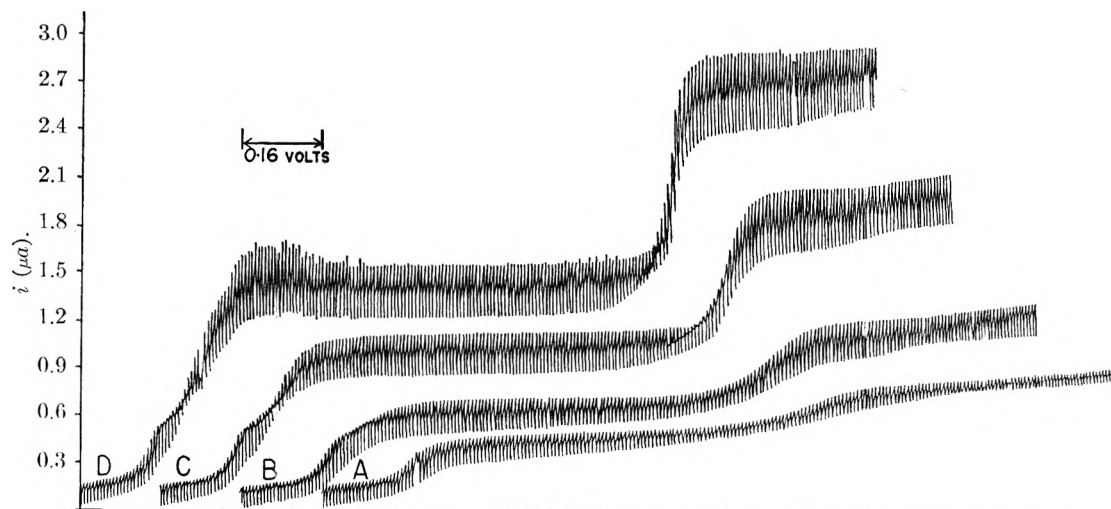


Fig. 1.—Polarograms of phenylmercuric hydroxide at various concentrations: A, $0.5 \times 10^{-4} M$; B, $1.0 \times 10^{-4} M$; C, $2.0 \times 10^{-4} M$; D, $3.0 \times 10^{-4} M$. Britton-Robinson buffer, $5 \times 10^{-2} M$, pH 5.0. KNO_3 , $1 \times 10^{-1} M$. All curves started at +0.2 volt.

cury reservoir above the capillary orifice ($h^{1/2}$). On the other hand, it can easily be shown² that the height of an adsorption wave (e.g., a pre-wave) should be directly proportional to h . As can be seen from Table I, experiments in which the height of the mercury reservoir was varied over a wide range yielded essentially constant values for $i_d/h^{1/2}$

and i_a/h , but not i_d/h and $i_a/h^{1/2}$. This again permits the conclusion that the pre-wave is indeed caused by adsorption.

(3) Effect of Temperature.—The temperature coefficient of the wave height provides another means of distinguishing between diffusion and adsorption waves, since the temperature coefficient of a diffusion current is generally about 1.6%

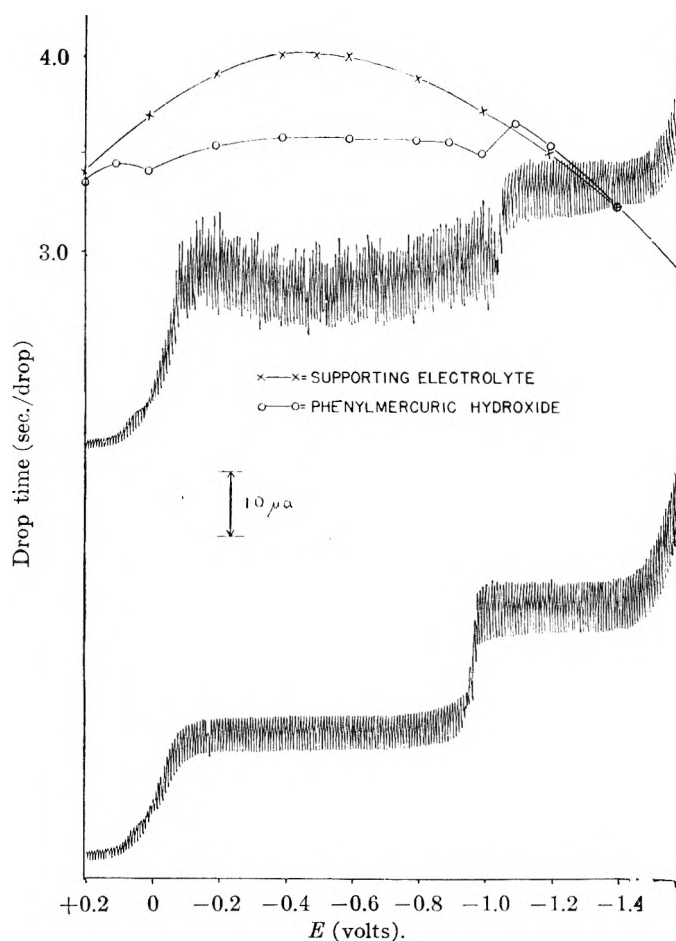


Fig. 2.—Effect of gelatin on the irregularities: upper polarogram: C_6H_5HgOH , $5 \times 10^{-4} M$; Britton-Robinson buffer, $5 \times 10^{-2} M$, pH 5.0; KNO_3 , $1 \times 10^{-1} M$. Lower polarogram: as above plus 0.01% gelatin.

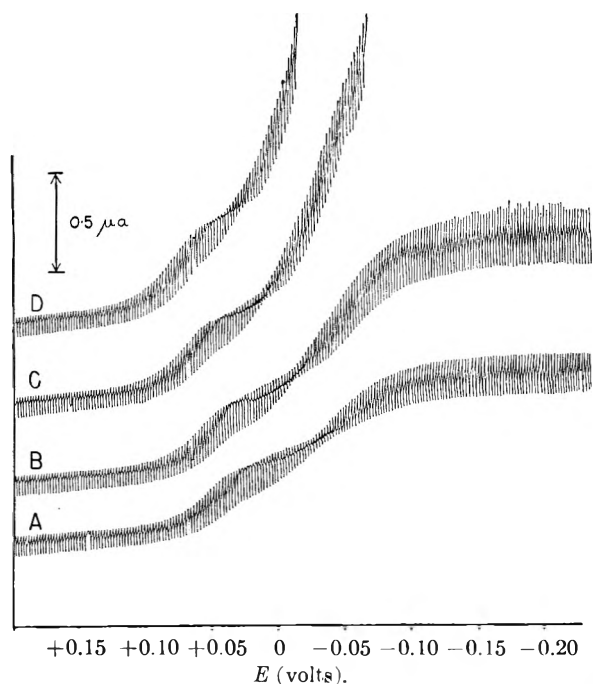


Fig. 3.—Effect of concentration on the height of the pre-wave: Britton-Robinson buffer, $5 \times 10^{-2} M$, pH 5.0; KNO_3 , $1 \times 10^{-1} M$; C_6H_5HgOH : A, $2.00 \times 10^{-4} M$; B, $3.00 \times 10^{-4} M$; C, $5.33 \times 10^{-4} M$; D, $10.00 \times 10^{-4} M$.

per degree, while that of an adsorption current is negligibly small. It was found that the temperature coefficient of the diffusion current was 1.6% per degree, while the height of the pre-wave has no significant temperature coefficient between 0 and 6°. This clearly demonstrates that the height of the pre-wave is not limited by diffusion and is compatible with the hypothesis that the pre-wave is due to adsorption.

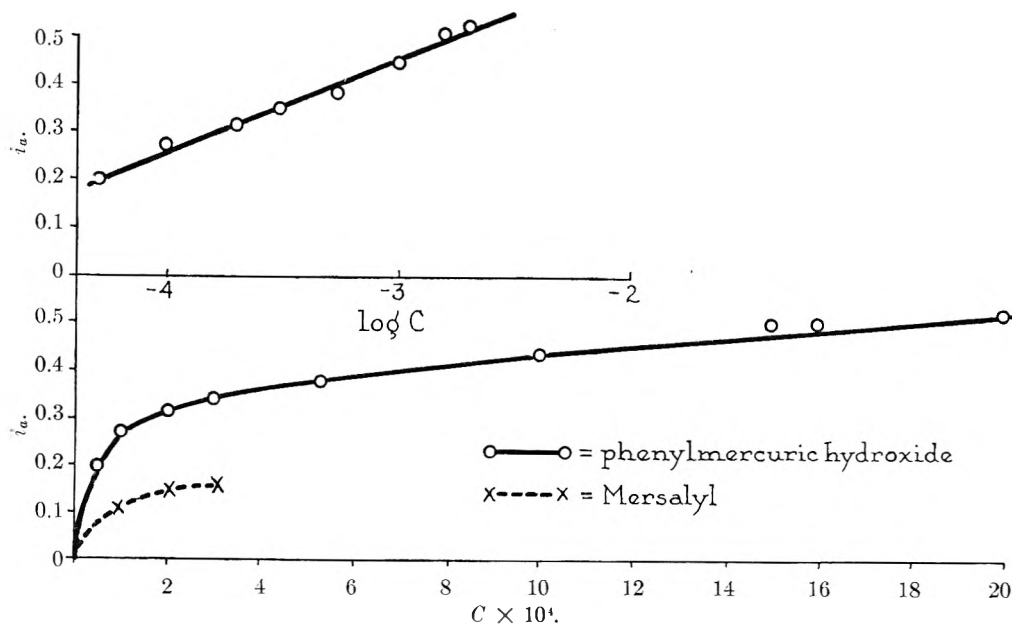


Fig. 4.—Relation between the height of the pre-wave and concentration: Britton-Robinson buffer, $5 \times 10^{-2} M$, pH 5.0; KNO_3 , $1 \times 10^{-1} M$.

(4) **Effect of Phenylmercuric Hydroxide on the Reversible Reduction Waves of Cadmium and Lead.**—When the dropping mercury electrode is coated with a surface active substance, some interference with the electrode reactions of other substances occurs, depending on the concentration of

TABLE I
EFFECT OF THE HEIGHT OF THE MERCURY RESERVOIR ON WAVE HEIGHTS

C_6H_5HgOH , $3 \times 10^{-4} M$; Britton-Robinson buffer, $5 \times 10^{-2} M$, pH 5.0; KNO_3 , $1 \times 10^{-1} M$

h (cm.)	$h^{1/2}$	i_a (μA)	i_a/h	$i_a/h^{1/2}$	i_d (μA)	$i_d/h^{1/2}$	i_d/h
80.8	8.99	0.40	0.00495	0.0444	1.19	0.132	0.0147
72.0	8.48	.36	.00500	.0425	1.13	.133	.0157
59.8	7.73	.31	.00517	.0401	1.02	.132	.0171
51.1	7.15	.26	.00509	.0364	0.91	.128	.0178
41.5	6.44	.21	.00506	.0326	0.82	.128	.0198

the surface active agent. Thus Kolthoff and Barnum⁴ found that the reduction wave of cystine was distorted in the presence of camphor in such a way that the upper portion of the wave was shifted to more negative potentials. As the concentration of camphor was increased, the whole wave was shifted to more negative potentials until, in saturated solutions of camphor, the cystine wave was displaced by as much as one volt to the potential at which camphor is desorbed from the mercury surface.

The occurrence of a pre-wave on the first reduction wave of the phenylmercuric compounds indicates that it is the product of this first reduction which is adsorbed at the mercury surface. This is also borne out by the electrocapillary curves to be discussed later. Interference with the waves of other ions would therefore be expected in the range of potentials between the end of the first and the beginning of the second wave, *i.e.*, between about -0.1 and -0.8 volt. Lead and cadmium were therefore chosen since their half-wave potentials are -0.4 and -0.6 volt, respectively, under the conditions used.

When a solution which was $2 \times 10^{-4} M$ in cadmium chloride and phenylmercuric hydroxide was electrolyzed in Britton-Robinson buffer at pH 5.0, the polarogram shown in Fig. 5 was obtained. It is clear that the cadmium wave is severely distorted so that only a small portion of it occurs at the usual potential, while the rest is continuous with the second reduction wave of phenylmercuric hydroxide. The effect on the lead wave was studied at pH 4.1 in 0.05 M acetate buffer with $3 \times 10^{-4} M$ phenylmercuric hydroxide and lead nitrate. The polarograms in Fig. 6 show that the reversible lead wave has become distorted in the presence of

the organic mercury compound and its half-wave potential shifted by 60 millivolts. These observations on the reversi-

(4) I. M. Kolthoff and C. Barnum, *J. Am. Chem. Soc.*, **63**, 520 (1941).

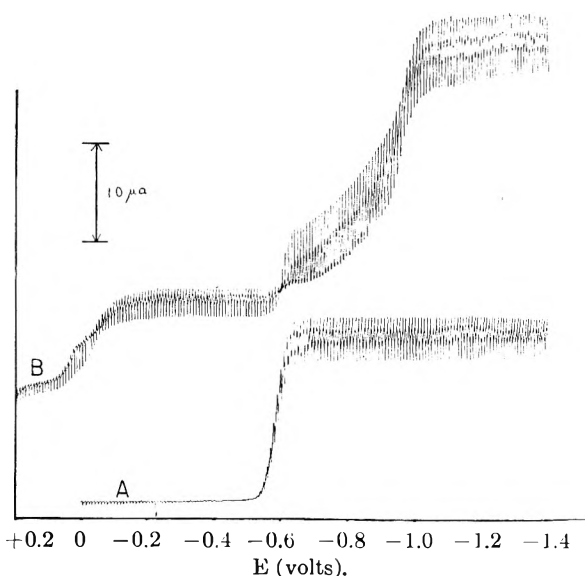


Fig. 5.—Effect of phenylmercuric hydroxide on the reduction wave of cadmium: solution B: CdCl_2 , $2 \times 10^{-4} M$; $\text{C}_6\text{H}_5\text{HgOH}$, $2 \times 10^{-4} M$; Britton-Robinson buffer, $5 \times 10^{-2} M$, pH 5.0; KNO_3 , $1 \times 10^{-1} M$. Solution A: identical with solution B but without $\text{C}_6\text{H}_5\text{HgOH}$.

ble cadmium and lead waves effectively demonstrate that the product of the first reduction of the phenylmercuric compounds is adsorbed on the dropping mercury electrode.

(5) Effect of Organic Mercury Compounds on the Electrocapillary Curve of Mercury.—Determination of the electrocapillary curves of mercury in the presence of organic mercury compounds were made on oxygen-free solutions of the compounds in Britton-Robinson buffers. The curves obtained with several concentrations of phenylmercuric hydroxide at pH 5.0 and 9.0 are shown in Fig. 7. Several

conclusions can be drawn from these curves: (a) The interfacial tension is lowered progressively by increasing concentrations of these compounds. (b) Increase of the concentration above $3 \times 10^{-4} M$ has no further effect on the interfacial tension. This may be compared with the curve relating the height of the pre-wave to concentration (Fig. 4) which flattens off at about the same concentration. (c) The range potentials over which the interfacial tension is lowered is more positive at pH 5.0 than at pH 9.0. This is well correlated with the shift of the reduction waves to more positive potentials with increasing hydrogen ion concentration. Furthermore, as can be seen from Fig. 8, there is a particularly striking correlation between the course of the second wave, *i.e.*, the complete destruction of the organic mercury compound to benzene and mercury, and the return of the drop times to normal values. The effect on the drop time is therefore limited to potentials at which the product resulting from the addition of one electron to the organic mercury compound is present at the electrode surface.

From all these lines of evidence it becomes clear that the pre-wave is indeed an adsorption wave. Adsorption therefore plays an important role in determining the polarographic behavior of organic mercury compounds. The previously postulated mechanism for the electroreduction of these compounds must thus be reinterpreted in the light of these findings. The reduction may then be pictured as follows:

As a result of the addition of the first electron to the organic mercury compound, RHg -free radicals are formed and this process is responsible for the formation of the first reduction wave. A portion of these radicals, limited by the surface area of the mercury, is adsorbed on the electrode, giving rise to the pre-wave. The free radicals then disproportionate to R_2Hg (*via* the unstable intermediate RHgHgR) which coats the electrode up to the potential at which, with the formation of the second reduction wave, the organic mercury compound is fully reduced with the addition of another electron.

An explanation can now be given for the severe irregularities which appear on the diffusion plateau of the first wave of the unsubstituted phenylmercuric compounds at concentrations greater than $3 \times 10^{-4} M$. This phenomenon is undoubtedly due to the coating of the electrode by the insoluble diphenylmercury. This interpretation is supported

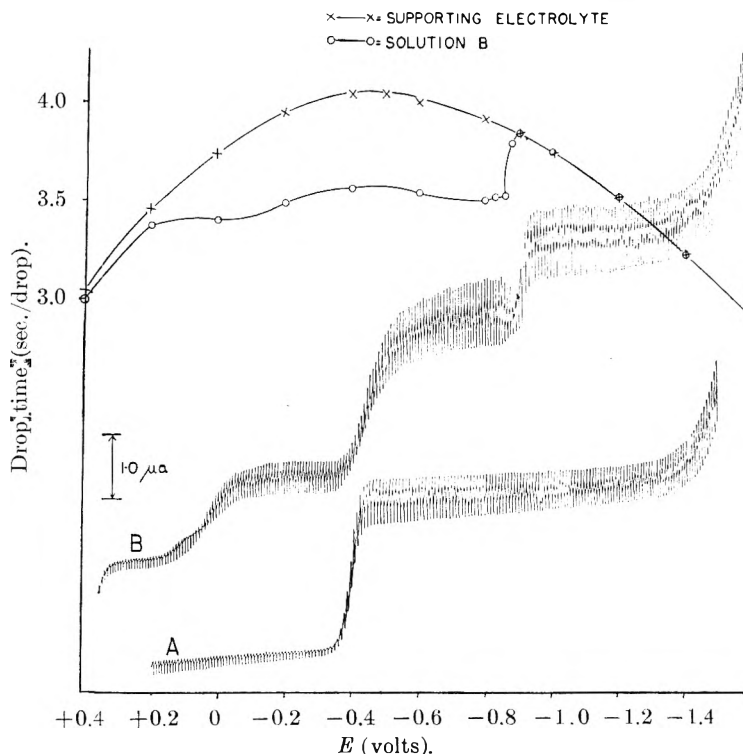


Fig. 6.—Effect of phenylmercuric hydroxide on the reduction wave of lead: Solution B: $\text{Pb}(\text{NO}_3)_2$, $3 \times 10^{-4} M$; $\text{C}_6\text{H}_5\text{HgOH}$, $3 \times 10^{-4} M$; acetate buffer, $5 \times 10^{-2} M$, pH 4.1; KNO_3 , $1 \times 10^{-1} M$. Solution A: Identical with solution B but without $\text{C}_6\text{H}_5\text{HgOH}$.

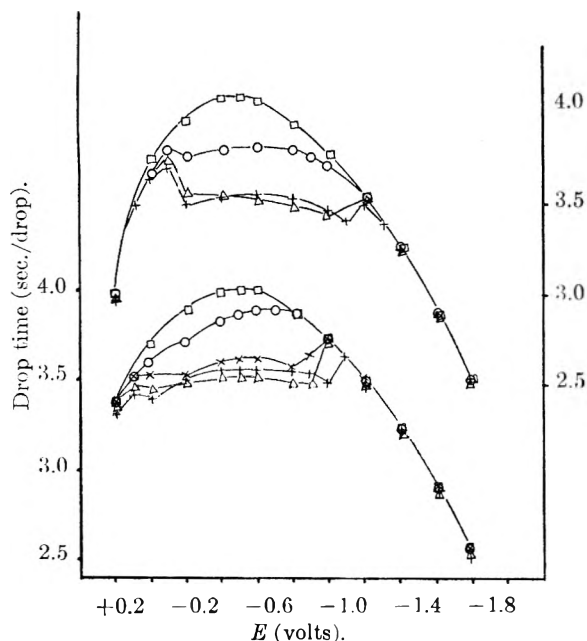


Fig. 7.—Electrocapillary curves in the presence of phenylmercuric hydroxide: Supporting electrolyte, Britton-Robinson buffer, $5 \times 10^{-2} M$; KNO_3 , $1 \times 10^{-1} M$; upper curves, pH 9.0; lower curves, pH 5.0. \square , supporting electrolyte; \circ , $1 \times 10^{-4} M$ phenylmercuric hydroxide; \times , $2 \times 10^{-4} M$ phenylmercuric hydroxide; Δ , $3 \times 10^{-4} M$ phenylmercuric hydroxide; $+$, $5 \times 10^{-4} M$ phenylmercuric hydroxide.

by the following facts: (a) The irregularities are sharply confined to the diffusion plateau of the first wave, *i.e.*, to the range of potentials over which the electrocapillary curve shows clear evidence of adsorption (Fig. 2). (b) They are observed only in the case of the unsubstituted phenylmercuric compounds where insoluble diphenylmercury is formed, but not in the case of *p*-chloromercuribenzoic acid, the dimer of which is soluble.

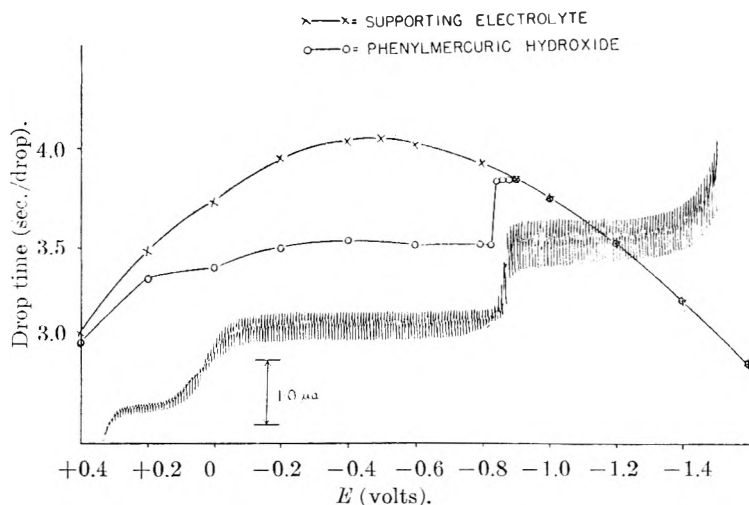


Fig. 8.—The effect of phenylmercuric hydroxide on the electrocapillary curve of mercury: C_6H_5HgOH , $3 \times 10^{-4} M$; acetate buffer, $5 \times 10^{-2} M$, pH 4.1; KNO_3 , $1 \times 10^{-1} M$.

Another unusual phenomenon, *i.e.*, the shift of the second reduction wave to more negative potentials with increasing concentration, has previously been ascribed to a competition between reduction and dimerization of the free radicals formed in the first reduction step.¹ Since adsorption of the free radicals on the mercury surface would tend to favor their dimerization, this argument receives further support from the additional facts reported here.

The detailed investigations on adsorption phenomena reported above, were carried out with phenylmercuric hydroxide. Pre-waves were, however, also observed on the first reduction waves of *o*- and *p*-chloromercuribenzoic acid as well as Mersalyl in alkaline solution. Drop time measurements in the presence of these compounds also gave clear evidence of adsorption. As would be expected, no pre-wave was discernible on the two-electron wave of Mersalyl in acid solution, since in this case the reduction proceeds without the intermediate formation of free radicals.

Calculation of the Number of Molecules Adsorbed per Unit Area of Mercury Surface

(1) **Direct Calculation from the Height of the Pre-Wave.**—The number of adsorbed molecules reduced per second is i_a/nF . The rate of increase of the mercury surface is $0.85 m^{2/3}t^{-1/3} \text{ cm.}^2/\text{sec.}$ ⁵ Hence the number of moles adsorbed per cm.^2 is

$$z = i_a/nF \cdot 0.85 m^{2/3}t^{-1/3}$$

On substitution of the following values: $i_a = 5.2 \times 10^{-7} \text{ amp.}$ (highest value in Fig. 4), $n = 1$, $m = 2.54 \times 10^{-3} \text{ g. per sec.}$, $t = 3.54 \text{ sec. per drop}$, the maximum number of adsorbed molecules is $z = 5.2 \times 10^{-10} \text{ mole cm.}^{-2} = 3.1 \times 10^{14} \text{ molecules cm.}^{-2}$, and the area occupied per molecule is 32 \AA.^2

The corresponding values for Mersalyl are: $i_a = 1.5 \times 10^{-7} \text{ amp.}$ (Fig. 4), $m = 2.54 \times 10^{-3} \text{ g. per sec.}$, $t = 3.70 \text{ sec. per drop}$. Therefore $z = 1.53 \times 10^{-10} \text{ mole cm.}^{-2} = 0.92 \times 10^{14} \text{ molecules cm.}^{-2}$, and the area per molecule is 109 \AA.^2 .

(2) **Calculation from the Langmuir Adsorption Isotherm.**—In order to avoid the rather arbitrary choice of a limiting value for i_a , the results were extrapolated according to the Langmuir adsorption isotherm

$$x/m = kzc/(1 + kc) \text{ or}$$

$$c/(x/m) = 1/kz + c/z$$

where x = number of moles adsorbed/ cm.^2 , m = area₁ of surface in cm.^2 , c = concentration of ad-

sorbable substance in the solution, z = maximum number of moles adsorbed/ cm.^2 , k = adsorption coefficient.

Although the concentration of adsorbable molecules (RHg· radicals) is not directly known, it is

(5) D. Ilkovic, *Collection Czechoslov. Chem. Commun.*, **6**, 498 (1934).

related to the concentration of electroactive substance (e.g., phenylmercuric hydroxide) by the proportionality factors of the Ilkovic equation. The concentration of phenylmercuric compound in the solution can therefore be used for c in the above equation, provided it is corrected for the amount removed from the solution by adsorption.⁶ This was done by multiplying the concentrations by $(i_d - i_a)/i_d \cdot x/m$, as has been seen above,⁵ is equal to $i_a/nF \cdot 0.85 m^{2/3} t^{-1/3}$. The results for phenylmercuric hydroxide are shown in Fig. 9. The value obtained for z is 6.0×10^{-10} mole per cm.²⁷ which corresponds to an area of 28 Å.² per molecule. This may be compared with the area of 32 Å.² obtained above.

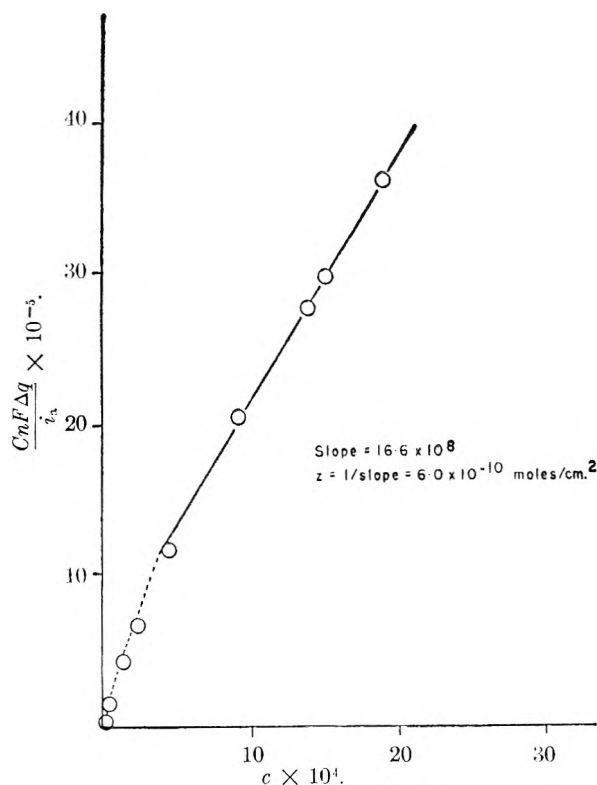


Fig. 9.—Relation between i_a and concentration plotted according to the Langmuir adsorption isotherm: C_6H_5HgOH ; Britton-Robinson buffer, $5 \times 10^{-2} M$, pH 5.0; KNO_3 , $1 \times 10^{-1} M$.

(3) **Calculation from the Gibbs Adsorption Isotherm.**—The number of molecules adsorbed was also calculated from the Gibbs adsorption equation. The drop times were determined as a function of concentration at -0.50 volt versus the saturated calomel electrode, since at this potential the concentration of unreduced phenylmercuric compound is zero and any adsorption can therefore be due only to the reduction product. The concentrations in the solution were corrected for depletion by adsorption as explained above. The results which are shown in Fig. 10 contain the values from two separate experiments to illustrate the reproducibility of the drop times. The best slope of the

(6) The necessity for this correction was kindly pointed out by P. Kivalo and H. A. Laitinen.

(7) The same value was obtained by extrapolating the results according to the method of Seatchard.⁸

(8) G. Seatchard, *Ann. N. Y. Acad. Sci.*, **51**, 660 (1949).

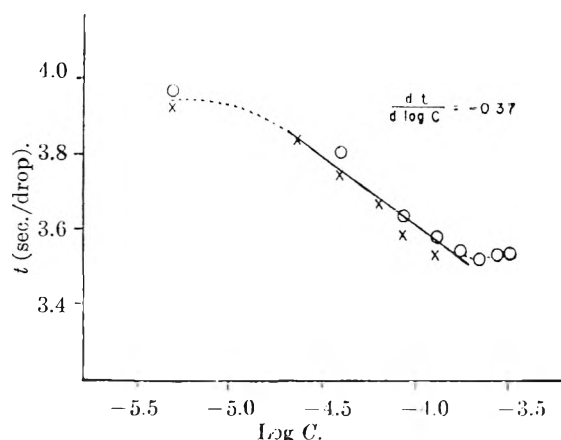


Fig. 10.—Variation of drop time with concentration: C_6H_5HgOH ; Britton-Robinson buffer, $5 \times 10^{-2} M$, pH 5.0; KNO_3 , $1 \times 10^{-1} M$.

straight line portion, corresponding to concentrations of phenylmercuric hydroxide from $0.75 \times 10^{-4} M$ to $2.50 \times 10^{-4} M$, was calculated by means of the regression equation

$$y = \bar{y} - \frac{S_{xy}}{S_x^2} (x - \bar{x})$$

The equation of the line was thus found to be

$$t = 2.14 - 0.37 \log c$$

The interfacial tension between mercury and water in the complete absence of oxygen is 427 dynes cm.⁻¹⁹ The drop time under these conditions was 4.03 seconds per drop. In view of the narrow limits of variation encountered, the correction factor for the conversion of drop time to surface tension is negligible.¹⁰ Therefore

$$\frac{d\gamma}{d \log c} = -0.37 \times \frac{427}{4.03}$$

and

$$\Gamma = 6.8 \times 10^{-10} \text{ mole cm.}^{-2} \text{ }^{11}$$

This value may be compared with: (1) 5.2×10^{-10} mole/cm.² from the "maximum" height of the pre-wave. (2) 6.0×10^{-10} mole/cm.² from the Langmuir adsorption isotherm. (3) 6.0×10^{-10} mole/cm.² from a molecular model of RHg. This was drawn to scale and the area measured with a planimeter. It is clear that all these values are in good agreement.

In conclusion it may be pointed out that the special advantages of the polarographic method in the study of adsorption phenomena are its relative experimental simplicity, its applicability to unstable molecules, such as free radicals, and the fact that the adsorbable substance is formed right at the surface of the adsorbing interface, so that diffusion toward that surface is not a limiting factor. The method is, however, limited to substances which are both electroactive and surface active and can, of course, only be applied to adsorption studies at a mercury/water interface.

Acknowledgment.—This investigation was supported by a research grant from the National Institutes of Health, U. S. Public Health Service.

(9) D. C. Henry and J. Jackson, *Nature*, **142**, 616 (1938).

(10) W. D. Harkins and F. E. Brown, "International Critical Tables," Vol. IV, McGraw-Hill Book Co., New York, N. Y., 1928.

(11) The use of the approximate form of the Gibbs equation seemed justified in view of the high ionic strength of the medium.

A STUDY OF THE FUNCTIONAL GROUPS OF CATION EXCHANGERS BY INFRARED ABSORPTION

By KENNETH T. WALDOCK¹ AND LAURENCE D. FRIZZELL²

Department of Chemistry, Northwestern University, Evanston, Illinois

Received June 27, 1951

Infrared analysis of the ion-exchangers; Zeo-Karb, Amberlite IR-1, Amberlite IR-100, Dowex-30 and Dowex-50, has established the presence of sulfonic acid groups in all of them and the presence of O—H groups, C=C groups and para groups. The O—H groups may be phenol groups but the evidence is not definite. The evidence for carboxyl groups in Zeo-Karb is also not beyond question. There is a structural similarity for Zeo-Karb, Amberlite IR-1 and Amberlite IR-100.

Introduction

The functional groups in cation exchange adsorbents and their source materials have been discussed in several papers.^{3,4-19} The presence of these groups has been generally inferred from the method used to prepare the exchanger. The identification of the functional groups by extracting the exchanger with solvents, such as ether, benzene, dioxane, and ethylene glycol has been tried but very small amounts of material were obtained. Sodium hydroxide solution and destructive distillation applied to the solid exchangers cause degradation and condensation that produce substances of uncertain relation to the original substances.

The interaction of infrared rays and matter can be recorded²⁰ as curves on coordinate paper, plotting wave length in microns *versus* absorption as optical density, $\log I_0/I$, and many types of bonds have a maximum absorption at particular wave lengths that are characteristic of them. This paper describes and discusses the use of infrared spectroscopy for the study of the functional groups of: Zeo-Karb, Amberlite IR-1, Amberlite IR-100, Dowex-30 and Dowex-50.

Experimental

A. Materials.—Measurements were made with a Beckmann infrared spectrophotometer model IR-2. Samples of the exchanger with adsorbed hydrogen ions or other cations were prepared as air-dried 20-40 mesh material.

The air-dried samples of the exchanger with adsorbed cation were ground to a fine powder in an agate mortar and then sufficient nujol was added to obtain a thin paste. The paste

was suspended in carbon tetrachloride and transferred to a plate of silver chloride. A thin, adherent film of solid exchanger in nujol was produced when the carbon tetrachloride evaporated and the film was dried over phosphorus pentoxide.

B. Infrared Spectra (1) Nujol.—The spectra from a thin film of nujol on a silver chloride plate are represented by curve 1, Fig. 1.

(2) **Pure Carbon.**—The spectra of pure sugar charcoal was obtained for comparison purposes. This is shown in curve 2, Fig. 1. The spectra from a sample of the sugar charcoal that had been in contact with 0.1 *N* ferric chloride solution more than 24 hours is shown in curve 3, Fig. 1.

(3) ***p*-Toluenesulfonic Acid.**—A film of *p*-toluenesulfonic acid was prepared by placing 1 ml. of a 10% solution of *p*-toluenesulfonic acid in water on a silver chloride plate and evaporating the water over phosphorus pentoxide. A film of the sodium salt of *p*-toluenesulfonic acid was similarly prepared. The spectra of these films are curves 1 and 2, respectively, Fig. 2.

(4) **Exchange Adsorbents.**—Films of hydrogen Zeo-Karb were prepared from a paste obtained by grinding hydrogen Zeo-Karb in water without nujol and from a paste obtained by grinding hydrogen Zeo-Karb in nujol. The spectra from these films are curves 1 and 2, respectively, Fig. 3. Curve 2A of Fig. 3 was prepared with an extrapolated base line and shows the approximate absorption due only to specific bonding.

The sodium form of Zeo-Karb was prepared by passing a 0.1 *M* sodium chloride solution at pH through the hydrogen form of the Zeo-Karb until equilibrium was attained. The spectra from a film prepared from water only is shown by curve 1, Fig. 4. The spectra from a film prepared with nujol, is shown in curve 2, Fig. 4, and the same spectra without the background is curve 2A, Fig. 4.

The spectra from films of the hydrogen form of Amberlite IR-1, Amberlite IR-100, Dowex-30 and Dowex-50, without the background, are shown in the labeled curves of Fig. 5.

Results and Discussion

The absorption wave lengths that might be expected in the materials studied are in Table I.²¹

TABLE I

WAVE LENGTHS OF ABSORPTION BANDS			
Wave lengths, μ groups	Wave lengths, μ groups		
2.70-3.35	O—H: stretching	3.20-3.35	C—H: aromatic
3.05-3.70	O—H: stretching	3.35-3.60	C—H: saturated
5.40-6.05	C=O: stretching	5.80-6.00	C=O: carboxylic
5.90-6.35	C=C: stretching	6.15-6.45	C=O: ionized acid
6.80-7.70	C—H: bending	5.80-6.05	C=O: aromatic ketone
6.90-8.35	O—H: bending		
7.70-11.10	C—O: stretching	6.15-6.35	C=C: aromatic
8.35-12.50	C—C: stretching	6.80-7.00	C—H: methyl
2.70-3.10	Water band	6.90-7.15	C—H: methylene
6.05-6.50	Carbon dioxide band	7.15-7.40	C—H: methyl or methylene
2.70-2.85	O—H: phenolic or alcoholic, non-bonded	7.95-8.70	Sulfonic acid or sulfonate ion
2.70-3.20	O—H: phenolic or alcoholic, hydrogen-bonded	8.85-9.10	Para grouping
2.90-3.25	O—H: sulfonic acid	9.15-9.90	Sulfonic acid or sulfonate ion
		9.70-10.00	Para grouping

(21) Barnes, Gore, Liddel and Williams, "Infrared Spectroscopy, Industrial Applications," Reinhold Publishing Corp., New York, N. Y., 1944.

- (1) Harpur College, Endicott, New York.
- (2) Merrimack College, Andover, Mass.
- (3) E. I. Akeroyd and G. Broughton, *THIS JOURNAL*, **42**, 343 (1938).
- (4) W. C. Bauman and J. Eichhorn, *J. Am. Chem. Soc.*, **69**, 2830 (1947).
- (5) H. E. Blyden, J. Gibson and H. L. Riley, "The Ultra Fine Structure of Coals and Cokes," British Coal Utilization Research Association, 1946, pp. 18, 176, 232.
- (6) K. Bolton, *J. Chem. Soc.*, 252 (1942).
- (7) W. A. Bone, *et al.*, *Proc. Roy. Soc. (London)*, **A110**, 537 (1926); **A127**, 481 (1930); **A148**, 492 (1936).
- (8) Dept. Sci. Ind. Res. British Fuel Res. Board Rept., No. 51 (1938).
- (9) J. F. Duncan and B. A. J. Lister, *J. Chem. Soc.*, 3285 (1949).
- (10) F. Fischer, and H. Schrader, *Brennstoff Chem.*, **2**, 37 (1921).
- (11) W. Fuchs, *Fuel*, **25**, 132 (1946).
- (12) Fuel Research Board Reports, No. 935-939.
- (13) R. Houwink, "Elasticity, Plasticity and Structure of Matter," Cambridge University Press, 1937.
- (14) U. Hofman, *Trans. Faraday Soc.*, **34**, 1017 (1938).
- (15) H. C. Howard, *THIS JOURNAL*, **40**, 1103 (1936).
- (16) R. J. Myers, J. W. Estes and F. J. Myers, *Ind. Eng. Chem.*, **42**, 697 (1951).
- (17) R. G. Randall, M. Benger and C. M. Grocock, *Proc. Roy. Soc. (London)*, **A165**, 432 (1938).
- (18) N. E. Topp and K. W. Pepper, *J. Chem. Soc.*, 3299 (1949).
- (19) H. F. Walton, *J. Frank Inst.*, **232**, 305 (1941).
- (20) H. F. Walton, *THIS JOURNAL*, **47**, 371 (1943).

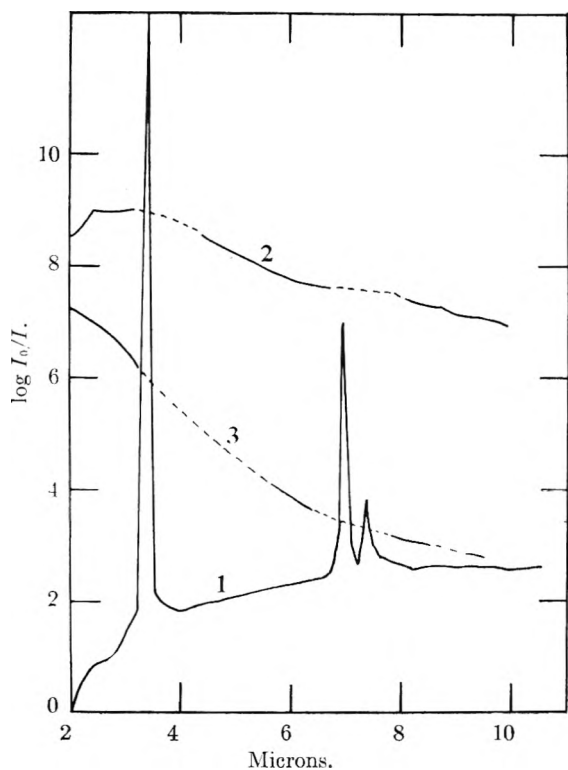


Fig. 1.—Absorption curves: curve 1, nujol; curves 2 and 3, sugar charcoal.

Absorption bands may be shifted in wave length by the presence of other bands.

The absorption spectra of nujol as curve 1, Fig. 1, shows absorption bands for C-H at λ 3.25, for $-\text{CH}_3$, $-\text{CH}_2-$ at λ 7.00 and for C- CH_3 at λ 7.35.

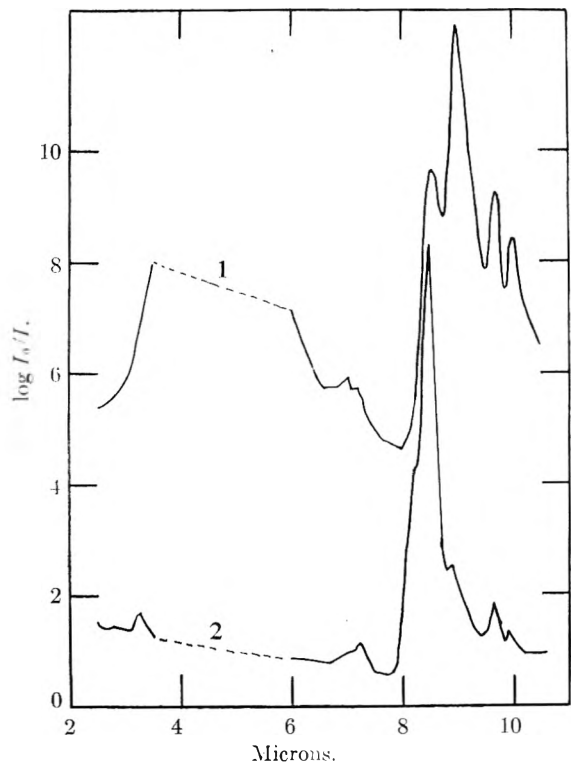


Fig. 2.—Absorption curves: curve 1, *p*-toluenesulfonic acid; curve 2, sodium *p*-toluenesulfonate.

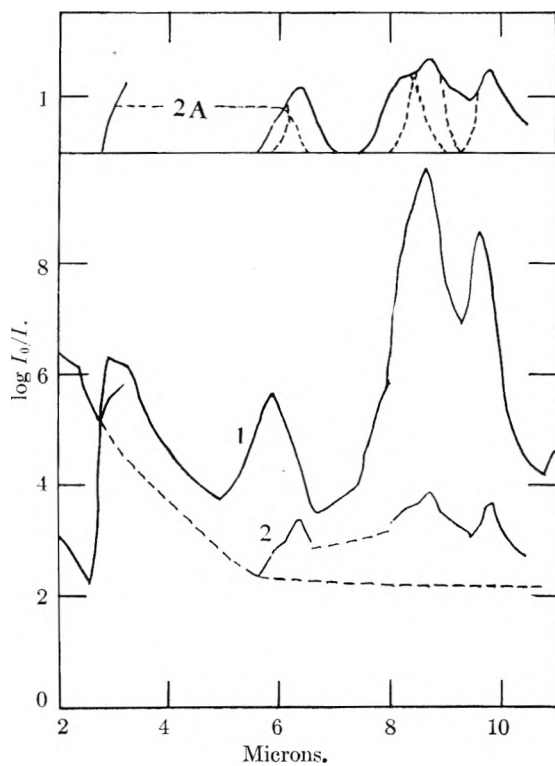


Fig. 3.—Absorption curves for hydrogen Zeo-Karb.

Only these three very distinct maxima occur for nujol.

The spectrum of sugar charcoal was obtained to have a knowledge of the possible background absorption and scattering of the exchanger. Zeo-Karb is prepared by treating coal with sulfuric acid and the other exchangers studied are from poly-

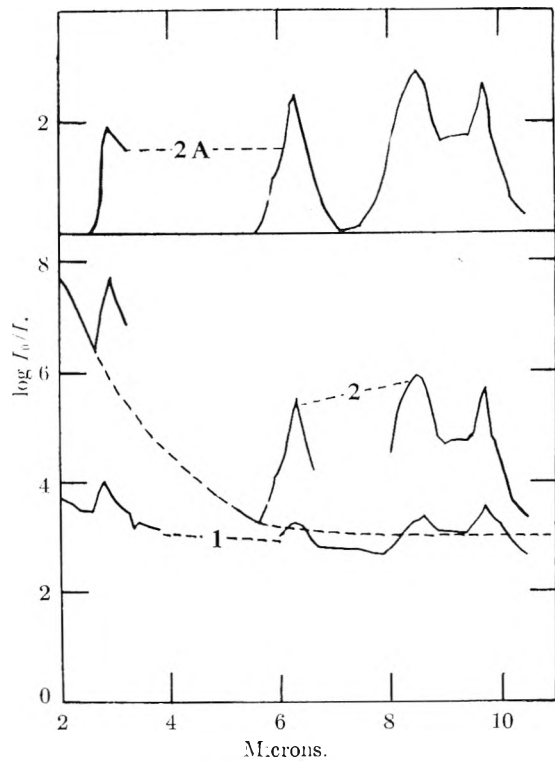


Fig. 4.—Absorption curves for sodium Zeo-Karb.

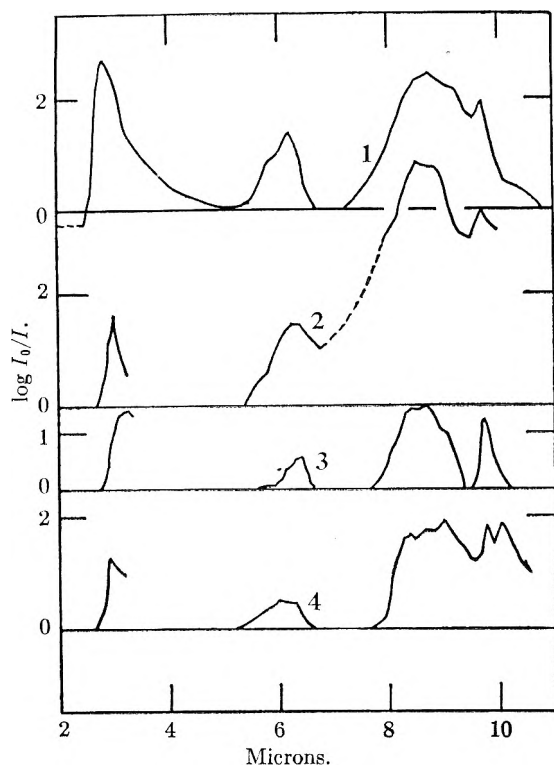


Fig. 5.—Absorption curves: curve 1, hydrogen Amberlite IR-1; curve 2, hydrogen Amberlite IR-100; curve 3, hydrogen Dowex-30; Curve 4, hydrogen Dowex-50.

mers consisting mainly of carbon with small amounts of hydrogen, oxygen and sulfur. The two curves for charcoal in Fig. 1 show no significant maxima and no particular difference indicating the absence of bands absorbing in the wave length region studied. Also, oxidation of the charcoal with ferric ions produced no evidence of special bonding caused by oxidation.

At the time this study was made, no absorption wave lengths were obtainable from published works for sulfonic groups. The curve for *p*-toluenesulfonic acid was therefore obtained for comparison purposes. The curve in Fig. 2 shows a wide band for O-H merging into the band for C-H in the region of three microns; a weak band for methyl C-H at 7.00 and at 7.20; a strong band for sulfonic at 8.55 and 9.65; and a strong band due to para grouping at 9.00 and at 10.00. The curve for the sodium salt of *p*-toluenesulfonic acid in Fig. 2 show all the bands present in curve 1, Fig. 2. Here the C-H absorption at 3.25 is distinct since the small O-H absorption at 2.80 is due to impurity. Particularly to be noticed is the much stronger absorption at 8.50 as compared with absorption at other wave lengths.

A consideration of the curves for nujol, charcoal and numerous curves for exchangers indicated that an accurate base line could not be constructed for the proportions of nujol and exchanger. An approximation can be made by extrapolation, considering the relative heights of the absorption maxima. The variations in the wave lengths of the maxima are probably caused by the influence of the dispersing agent and restricted motion such as hydrogen bridges. Many methods were tried to prepare a

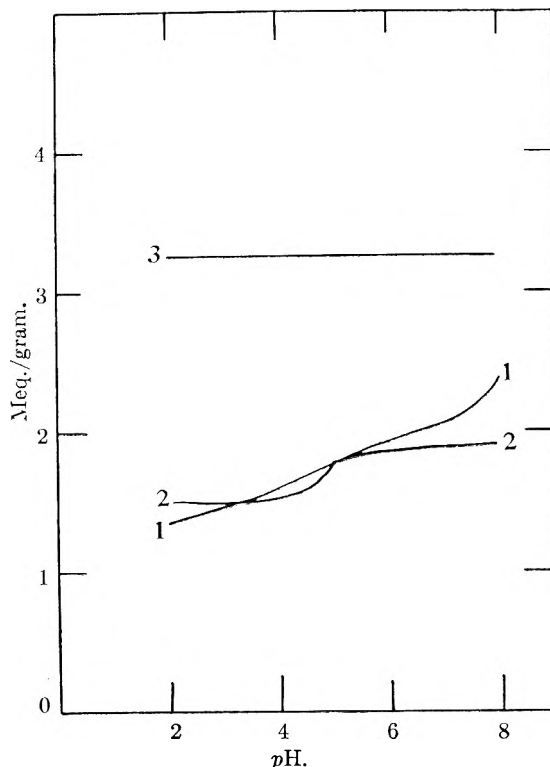


Fig. 6.—Cation capacity versus pH: curve 1, Zeo-Karb; curve 2, Amberlite IR-100; curve 3, Dowex-50.

film of solid only, but without success and the few curves shown represent many obtained.

The curves for hydrogen Zeo-Karb, prepared by two methods, are curves 1 and 2, Fig. 3. Curve 2A was prepared with an extrapolated base line from curves 1 and 2 and shows the approximate absorption due only to specific bonding.

These curves show a strong band for O-H at 2.90 indicating extensive hydrogen-bonding since it extends into the C-H band at 3.30. Also found is a band at 5.90 which could be ketonic or carboxylic C=O or both. This is seen to shift for the main part in the presence of nujol to a wave length of 6.35 indicative of ionized acid. The absorption at 8.7 and 9.7 are obviously due to sulfonic acid. The peak at 8.3 is probably due to a split in the peak at 8.7.

The curves for the sodium form of Zeo-Karb are in Fig. 4. Curve 1 is for the sample prepared in water and curve 2 is for the sample prepared in nujol. Curve 2A is curve 2 without the background. The maxima for the hydrogen Zeo-Karb are present in these curves. The sharp O-H peak at 2.80 strongly indicates non-bonded phenol, since carboxylic and sulfonic O-H should be missing at this pH and moreover absorb above this wave length to give a wider band as does water. The C=O peak at 6.30 agrees with the ionized carboxyl postulated in the hydrogen form. There is some indication of ketonic C=O at 5.90. Again the sulfonic absorption is present.

The inconclusive identification of the phenol group led to a titration of the hydrogen Zeo-Karb with 0.1 *N* sodium hydroxide solution. The very slow rate of reaction at pH greater than three made this unreliable for an accurate determination. However, the capacity of Zeo-Karb increases with

increasing pH beyond the capacity calculated for the sulfonic acid groups in it. This is shown in curve 1, Fig. 6, and confirms previous work.²⁰ The capacities for Amberlite IR-100 and Dowex-50 at several concentrations of hydrogen ions were measured for comparison and appear as curves 2 and 3, respectively, in Fig. 6. These curves confirm work reported^{10,18} since these results were obtained.

The curves for the hydrogen forms of Amberlite-IR-1, Amberlite IR-100, Dowex-30 and Dowex-50 in Fig. 5, show the same maxima for bands that occur in the curves from hydrogen Zeo-Karb and sodium Zeo-Karb, indicating a similar structure.

The curves from Zeo-Karb and the Amberlites are very similar. The curves from the Dowex exchangers are characterized by their lack of bands for a C=O group and the more numerous and narrow absorption bands in the region of sulfonic acid and aromatic groups. The curves for *p*-toluenesulfonic acid and Dowex-50 are similar in the portion from λ 8.0 to λ 10.0. In the Amberlite exchangers, the absorption at 6.25 is probably due to aromatic C=C rather than C=O since the latter should not be present according to the method of preparation.

This investigation was supported by a grant from the Abbott Fund of Northwestern University.

ADSORPTION OF OXYGEN ON SILVER

BY F. H. BUTTNER, E. R. FUNK AND H. UDIN

Metal Processing Laboratory, Massachusetts Institute of Technology, Cambridge, Mass.

Received July 2, 1951

The surface tension of solid silver, measured by the weighted wire method, was found to be 1140 ± 90 dynes per centimeter in the temperature range 870 to 945°. Measurements were made of the surface tension of solid silver in helium-oxygen atmospheres at several proportions and the surface tension was found to decrease linearly with the logarithm of the oxygen partial pressure. Using the data with the Gibbs adsorption isotherm indicate that oxygen chemisorbs to silver and that at 932° there are approximately 1.4 atoms of oxygen adsorbed per silver atom at the surface. There is little or no adsorbed oxygen on this chemisorbed layer.

This paper compares the results of recent experimental determinations of the surface tension of solid silver in pure helium and in an atmosphere of controlled helium-oxygen mixtures. From such determinations the adsorption of oxygen on silver is found.

Theoretical

The interfacial tension between two phases arises, according to Gibbs,¹ from the fact that an excess energy exists at the interface between two phases. Gibbs proves that this energy is a partial function of the interfacial area. The defining expression for the interfacial energy, γ , is then

$$\partial F / \partial A = \gamma$$

where $\partial F / \partial A$ is the rate of change of the free energy of the surface with changing surface area at constant temperature, pressure and composition of both phases. Gurney² has clarified the relation between surface energy and surface tension and shown that as long as thermodynamic equilibrium obtains between the surface and bulk phases, the two are equal in magnitude. γ may be properly termed surface tension since the long times and high temperatures of the work reported here ensure the required thermodynamic equilibrium.

Successful measurements of the surface tension of a solid metal were reported by Udin, Shaler and Wulff³ for copper. In their experimental procedure the contractile forces resulting from the surface tension in fine copper wires were opposed by a dead load suspended from the wire. By using

several wires each differently weighted, the resulting creep strain in these wires at high temperatures could be followed as a function of the applied load. At low loads the greater contractile force of surface tension caused the wire to shrink, while at higher applied loads the surface tension was overbalanced and the wires elongated. From the strain *versus* load plot, the value of the load which just balanced the surface tension was found.

For this balancing case, the sum of the surface tension forces acting along the wire axis must equal the applied dead load. The longitudinal force tending to shorten the wire is $2\pi r\gamma$. But also a hoop stress, γ/r , tends to decrease the radius and elongate the wire. The longitudinal component of this stress yields a force of $-\pi r\gamma$. The resultant contractile force is, by difference of these, $\pi r\gamma$ dynes. Equating this to the balancing dead load, w , then

$$w = \pi r\gamma \quad (1)$$

This analysis has assumed that the wire is a single crystal and that surface tension is isotropic with respect to surface orientation. But metallographic examination of the specimens after a test showed that the wires were not single crystals, but were made up of many grains with grain boundaries essentially perpendicular to the axis of the wire. Udin⁴ has made it clear that for a wire made up of these pancake grains, equation (1) must be modified for the energy of the grain boundaries. Each grain boundary, attempting to minimize its area, exerts a hoop stress on the wire, tending to elongate it. Thus

$$w = \pi r\gamma - (n/l)\pi r^2\gamma_g \quad (2)$$

(4) H. Udin, *ibid.*, **189**, 63 (1951).

(1) J. W. Gibbs, "Collected Works," Vol. I, Longmans, Green and Co. New York, N. Y., 1931.

(2) R. W. Gurney, *Proc. Phys. Soc.*, **358A**, 639 (1939).

(3) H. Udin, A. J. Shaler and J. Wulff, *Trans. AIME*, **185**, 186 (1949).

where η/l is the number of grain boundaries per unit length of the wire, and r is the radius. $\gamma_{g,b}$ is the grain boundary interfacial tension which Greenough⁵ has shown and further experiments confirmed to be one-third the tension of the free surface. Rewriting and combining terms equation (3) becomes then

$$w = \pi r \gamma \left[1 - \frac{\eta r}{l \beta} \right] \quad (3)$$

For the special case of the wires in our experiments, η/l is 60 ± 10 grain boundaries per centimeter and r is 0.0065 centimeter, so that the equation used to evaluate surface tension from the balancing load is then

$$w = \pi r \gamma [0.87] \quad (4)$$

$$\gamma = \frac{w}{\pi r (0.87)} \quad (5)$$

The applied stress for zero strain is merely the balancing load divided by the cross-sectional area of a wire, so

$$\gamma = \sigma_{\epsilon=0} l / 0.87 \quad (6)$$

where $\sigma_{\epsilon=0}$ is the applied stress for zero strain.

Experimental

The techniques and procedures devised for copper were used to measure the surface tension of solid silver. The silver wire was 0.00508 inch in diameter and was drawn from a vacuum cast billet of high purity silver. Careful metallographic examination did not reveal interior flaws or inclusions in the wire either prior to or following a test. The gage marks, approximately 1 centimeter apart, were cut into each wire specimen by rotating the wire against the edge of two spaced razor blades in a jig especially designed for this purpose. The weights were prepared by taking a length of this wire and melting it on a charcoal block. The end of the test specimen was thrust into the molten ball just as it solidified. In this way the weight was welded to the end of the wire. In all the runs 10 to 13 wires were used with end weights ranging from 0 to 120 mg.

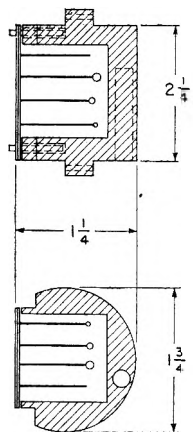


Fig. 1.—Silver cell with thermocouple well.

The wires were suspended from a silver cell cover and then the array was carefully transferred to a cylindrical silver cell. The cover closed but did not seal the cell. The cell, shown in Fig. 1, was then transferred to a platinum wound inconel tube furnace.

This furnace has three independent windings so that the temperature in a 6-inch hot zone could be held uniform to $\pm 2^\circ$. A Tagliabuc throttling pyrometer with manual droop compensation was used as a temperature control device.

The preliminary runs using this furnace were carried out in vacuum of 5×10^{-5} mm. at temperatures of 910 to 930°. The wires had so changed in diameter due to evaporation that no practical results could be obtained. All efforts to seal the wires more tightly in the cell while still leaving access to the vacuum chamber proved fruitless. The runs reported were therefore carried out in a purified helium atmosphere. A helium flow of 3 cc. per second was maintained throughout the run. The helium was purified by passing it through an activated charcoal trap held at liquid nitrogen temperatures.

In order to ascertain the effect of various partial pressures of oxygen on the surface tension of solid silver, a controlled amount of oxygen produced in a gas coulometer was admitted into the metered helium stream. This mixture

was passed through a Dry Ice and acetone trap to remove any water vapor before entering the furnace, see Fig. 2.

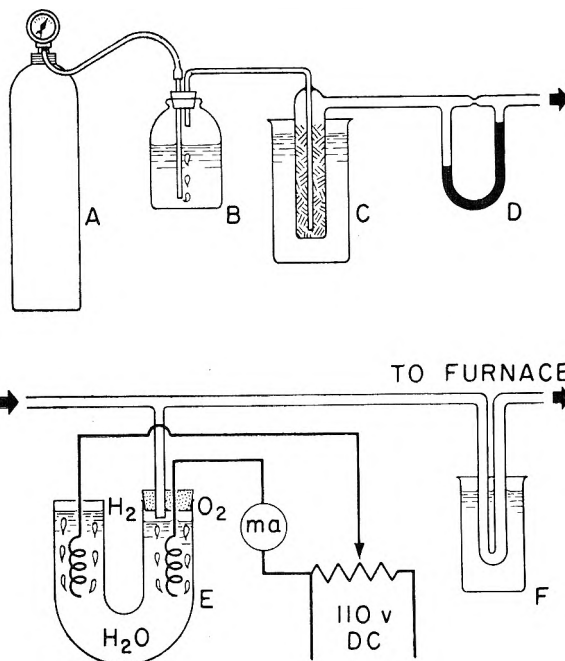


Fig. 2.—Atmosphere control system: A, helium tank; B, slight-flow meter; C, activated charcoal in liquid nitrogen; D, calibrated orifice manometer; E, gas coulometer; F, dry ice-acetone trap.

Due to the manipulation required for mounting, the wires were often slightly bent and cold worked. An anneal treatment of a few minutes at 600° was sufficient to allow straightening of the wires.

The specimens were washed in alcohol and ether to remove grease and dirt picked up from the air and returned to the furnace for a high temperature anneal. This anneal lasted one hour at 940°. The specimens were removed from the furnace after cooling and the gage length of each wire measured with a vertical traveling microscope with a screw accurate to ± 0.00015 cm. The array was returned to the furnace for the run which lasted up to 116 hours for the lower range of the test temperatures and as short as 18 hours for the highest temperature of 932°. Upon cooling the wires were removed from the furnace and the gage length again measured. The weights were clipped off at the weld and weighed to ± 0.1 mg.

It was always possible to count the number of grains in each wire after a test was completed. This can be done because where the grain boundary meets the free wire surface an equilibrium of surface forces exists. The groove angle established at the grain boundary (see Fig. 3) is distinctly

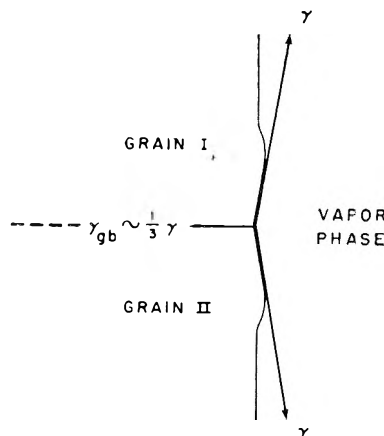


Fig. 3.—Formation of surface groove angles.

(5) A. P. Greenough, Report to Ministry, No. 52, London.

visible under diffuse oblique illumination at 50 magnifications. These grooves are often visible even after the short 940° anneal. A grain count on a number of specimens after the anneal and also after the test itself showed that the grain size established during the anneal remains essentially unchanged.

The surface tension for all runs was calculated from equation 6. A straight line fits the data for stresses between 0 and 4×10^5 dynes per cm.². A least square calculation was used to determine the most probable stress at zero strain. The necessary but small correction (0.15×10^5 dynes/cm.) to the ball weight for the weight of the wires between the lower gage mark and the weight was made.

TABLE I

Test number	Test temp., °C.	Duration of test, hr.	Oxygen partial pressure atmospheres	Log oxygen partial pressure	Surface tension, dynes/centimeter
22	938	18	Purified helium atmosphere		1110
23	941	29	Purified helium atmosphere		1150
24	923	18	Purified helium atmosphere		1190
25	906	26	Purified helium atmosphere		1265
26	923	36	Purified helium atmosphere		1115
27	907	50	Purified helium atmosphere		1210
28	907	108	Purified helium atmosphere		1215
29	Run lost				
30	924	64.5	Purified helium atmosphere		1005
31	876	116	Purified helium atmosphere		1045
32	938	59.5	Purified helium atmosphere		1070
33	935	36	0.2	-0.7	350
34	922	35.5	.2	-.7	560
35	912	46.5	.2	-.7	610
36	Run lost				
37	933	37.5	.1	-1	500
38	932	31	.01	-2	725
39	932	30	.001	-3	800
40	932	21	.0001	-4	1010
41	913	38	.01	-2	525
42	913	40	.001	-3	770
43	913	35.5	.0001	-4	1080

A summary of the experimental results is presented in Table I. Two typical strain-stress plots are given in Figs. 4 and 5.

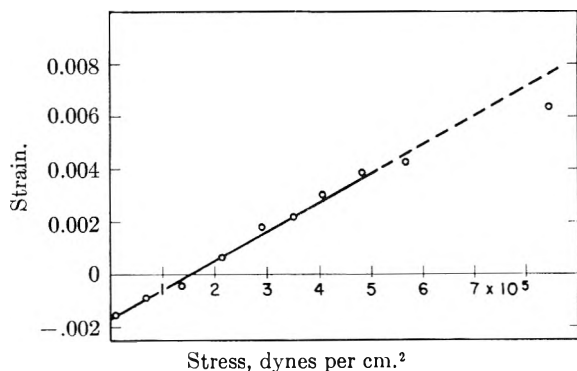


Fig. 4.—Strain-stress curves for Test No. 22.

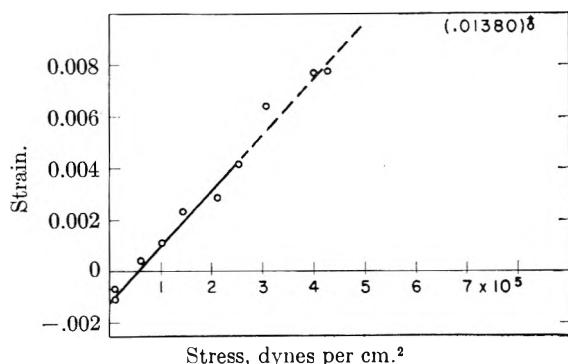


Fig. 5.—Strain-stress curves for Test No. 37.

Discussion of Results

Ten tests for surface tension of solid silver in a purified helium atmosphere were made at four different temperatures and various times. The average of the results is $\gamma = 1140 \pm 90$ dynes per cm. for the range 875 to 932°.

There is a trend toward higher surface tension at lower temperature in accordance with theoretical considerations, but the expected increase in the range of test temperatures is less than the uncertainty of the data. Therefore, no temperature coefficient for surface tension is reported.

Figure 6 summarizes the results of ten tests for the surface tension of silver in helium-oxygen admixtures. The data for 932° can be represented by

$$\gamma_{0_2} = 228 - 188 \log P_{0_2} \quad (7)$$

This equation is valid between 0.2 and 0.0001 atmosphere of oxygen and precise to ± 80 dynes per centimeter.

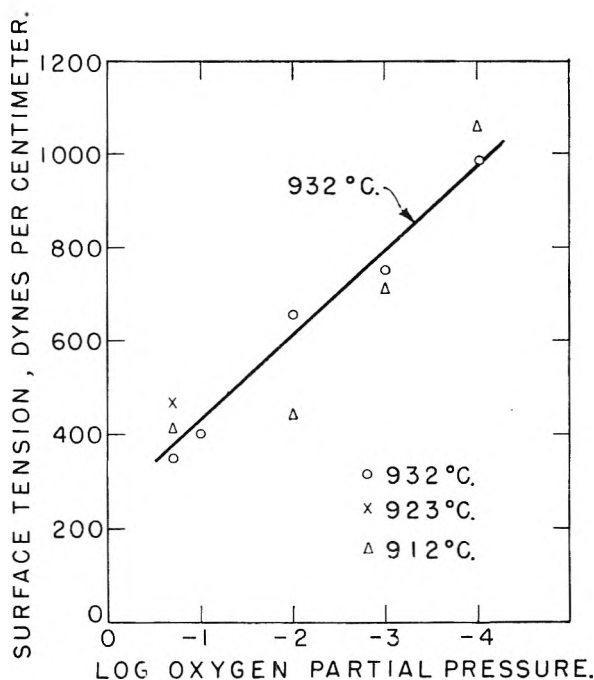


Fig. 6.—The oxygen partial pressure dependence of surface tension of solid silver. Straight line is least square plot for 932° points.

The amount of adsorption of oxygen on silver can be quantitatively related to the change in surface tension with the partial pressure of the surrounding gaseous phase by modifying the Gibbs Adsorption Isotherm. Although this equation has been used to find the adsorption of gases on liquid metals, it has never before been employed to find adsorption of gases on solid metals. That it can be used, however, is without question.⁶

For a solvent-solute system the Gibbs equation is

$$\Gamma = \frac{-C}{RT} \left(\frac{d\gamma}{dC} \right) T \quad (8)$$

where Γ is the surface excess or deficit of solute, and C is the concentration of solute in the bulk

(6) N. K. Adam, "The Physics and Chemistry of Surfaces," Oxford University Press, London, 1941.

phase. The concentration of oxygen in solid silver has been investigated by Sieverts and Hagenacker⁷ and Steacie and Johnson.⁸ These workers confirm that Sieverts' law holds for this system, *i.e.*, that

$$c = K\sqrt{P} \quad (9)$$

Differentiating (9) and substituting values of c and dc into equation (8) gives for the surface in the oxygen-silver system

$$\sigma = \frac{-2}{2.3RT} \left(\frac{d\gamma}{d \log P_{O_2}} \right) T \quad (10)$$

The change in surface tension with the logarithm of oxygen partial pressure can be obtained from Fig. 6 and is -188 . The surface excess at 930° is then

$$\Gamma = 1.98 \times 10^{18} \text{ atoms oxygen/cm.}^2$$

This figure can be more easily visualized by converting it to an excess oxygen surface concentration in atoms of oxygen per atom of silver. Assuming a close packed arrangement on the surface, a (111) face of silver will have 1.4 atoms of oxygen adsorbed per silver atom. A (110) face will have 1.65 atoms oxygen per silver atom. These values are uncertain by 15%.

The oxygen is undoubtedly chemisorbed to the silver surface. This conclusion is supported by the fact that the sorption is not, within the limits of the precision of the data, affected by a change in oxygen partial pressure.

While the adsorption isotherm gives the amount of adsorption, it says nothing about the form of the

(7) A. Sieverts and J. Hagenacker, *Phys. Chem.*, **68**, 125 (1909-10).

(8) E. W. R. Steacie and F. M. G. Johnson, *Proc. Roy. Soc. (London)*, **A112**, 429 (1926).

layer. However, it is certain that the chemisorbed layer does not have the thermodynamic properties of bulk silver oxide since bulk Ag_2O could only exist at the test temperature at an oxygen pressure of 1.7×10^4 atmospheres. One may speculate about the decomposition pressure of the surface film by observing that the oxygen partial pressure at which the presence of the oxygen becomes ineffective on the surface tension. Extrapolation of the line in Fig. 6 shows that in the vicinity of 10^{-5} atmospheres of oxygen the surface tension would become 1140, so that 10^{-5} appears to be a decomposition pressure of the surface film at 932° .

There have been no previous studies of adsorption of oxygen on silver at high temperatures reported in the literature. The results of this study are, however, in general qualitative with the results of Benton and Elgin⁹ who found that oxygen is chemisorbed on silver in the range 0 to 200° . Armbruster¹⁰ also studied the sorption of oxygen on silver and concluded that at 20° about 0.3×10^{15} molecules of oxygen adsorbed to silver per square centimeter and that adsorption increases with temperature. Thus the work of Armbruster provides an order of magnitude confirmation of the work presented in this paper.

Acknowledgment.—The authors are indebted to the Office of Naval Research for funds made available under contract number N5ori-07841 for equipment and supplies used in this research. We are also indebted to Prof. J. Wulff for his guidance and counsel.

(9) A. F. Benton and J. C. Elgin, *J. Am. Chem. Soc.*, **51**, 7 (1929).

(10) M. H. Armbruster, *ibid.*, **64**, 2515 (1942).

LOW VAPOR PRESSURE MEASUREMENT AND THERMAL TRANSPIRATION

BY S. CHU LIANG

Division of Chemistry, National Research Council, Ottawa, Canada

Received July 10, 1951

The thermomolecular pressure ratio, the R -factor, of ethylene has been measured and found that it can be fitted to the nitrogen values with the pressure shifting factor $f = 0.5$. The vapor pressure of ethylene at 77.5 and $90^\circ K$. has been measured. The results of Tickner and Lossing on methane, ethylene and acetylene have been corrected for the R -factor. The corrected values can be represented by an equation $\log p = A - B/T$. The constants A and B , and the applicable temperature range for each gas are given. A method is suggested by which f , and therefore the R , factor of one gas can be estimated from that of another.

Recently, Tickner and Lossing re-examined the vapor pressure data of hydrocarbons by means of a mass spectrometer for the purpose of providing some reliable values.^{1,2} Their effort will be defeated if the results so obtained are not corrected for the thermal transpiration effect. These authors being aware of such correction, used a connecting tube of large diameter (16 mm. i.d.), and contended that only the pressures below 0.01 mm. were uncertain. While it is so for some of the larger molecules, it is not so in the cases of methane and

acetylene. The present paper will treat the cases of these two gases and ethylene as examples and outline a method by which such a correction may be estimated without actually determining the effect for individual gases.

Experimental Part

Experimental work was carried out for ethylene to determine its vapor pressures at 77.5 and $90^\circ K$., and also to measure its thermomolecular pressure ratio R as a function of pressure p . The apparatus used was that of the relative method described elsewhere.³ The small tubing was a 1.6-mm. capillary and the large tubing was 32 mm. inside diameter. The ethylene used was withdrawn from a com-

(1) A. W. Tickner and F. P. Lossing, *J. Chem. Phys.*, **18**, 148 (1950).

(2) A. W. Tickner and F. P. Lossing, *This Journal*, **55**, 733 (1951).

(3) S. C. Liang, *J. Appl. Phys.*, **22**, 148 (1951).

mercial tank and purified by repeated operations of freezing the ethylene at 78°K., pumping off the residual gas and then reevaporizing the solid. The finally purified gas was found to be better than 99.9% pure by mass spectrometric analysis.

The *R*-value.—In the work with non-condensable gases, it was found that the *R vs. pd* curves of different gases could be reduced to a single curve by introducing a "pressure shifting factor" *f*, and the *f*-values for several gases were given by arbitrarily choosing $f_{N_2} = 1$. The present determination revealed that $R_{C_2H_4}$ fitted into this scheme very well with $f_{C_2H_4} = 0.5$. In other words, with the cold and warm ends at the same temperature differentials and tubing being of the same size, R_N at *p* is the same as $R_{C_2H_4}$ at 0.5 *p*. This is obviously because ethylene has larger cross-sectional area than nitrogen. The exact functional dependence of *f* on *r*, the radius of the gas molecule, is not known. However, in several instances we have found that the empirical relation

$$f_1/f_2 = 1 + 4 \left(\frac{r_1}{r_2} - 1 \right) \quad (1)$$

holds quite well. Table I gives the comparison of experimental values and that calculated from eq. (1) with *r* values compiled by Hirschfelder, Bird and Spatz⁴ from the viscosity data.

TABLE I
COMPARISON OF *f*-FACTORS

	Experimental ^a		Calcd. by eq. (1)
	I	II	
N ₂	1	1	1
A	1.25	1.30	1.3
H ₂	2.2	1.80	2.0
He	2.80	2.12	2.4
Ne	..	2.0	2.0

^a The experimental values were taken from Table VII, ref. 3, with neon value the unpublished work of the present author.

Considering the accuracy of the *r*-values, the agreements between the experimental and calculated values are excellent indeed with the exception of helium. With the aid of eq. (1), it is thus possible to estimate the *R*-factor for a given gas if its collisional diameter can be estimated from some other sources.

The Vapor Pressure.—The vapor pressure of ethylene has not before been measured experimentally at as low as 77.5°K. To serve as a double check, the pressure was measured simultaneously with two McLeod gages connected to the cold-bath by tubing of 1.6 and 32 mm. i.d., respectively. The 90°K. value was measured in the same manner. The readings from the two gages, as may be expected, are different; but become the same when corrected for. In Table II are summarized the experimental results.

TABLE II
VAPOR PRESSURE OF ETHYLENE

GAGE I (<i>d</i> = 1.6 mm.)			
	Experimental reading, mm.	<i>R</i> -Factor	Corrected pressure, mm.
77.5°K.	1.04×10^{-3}	0.51	$(0.53 \pm 0.01) \times 10^{-3}$
90°K.	0.036	0.82	0.030
GAGE II (<i>d</i> = 32 mm.)			
77.5°K.	0.77×10^{-3}	0.72	$(0.55 \pm 0.03) \times 10^{-3}$
90°K.	0.030	1.00	0.030

The importance of thermal transpiration is clearly illustrated. It is of interest to notice that the vapor pressure of ethylene at liquid nitrogen temperature has always been designated as 0.73×10^{-3} mm. The discussion obtained by correlating experimental data with this wrong value should therefore all be re-examined.

Discussion

The results of Tickner and Lossing on methane, ethylene and acetylene, corrected for the thermal

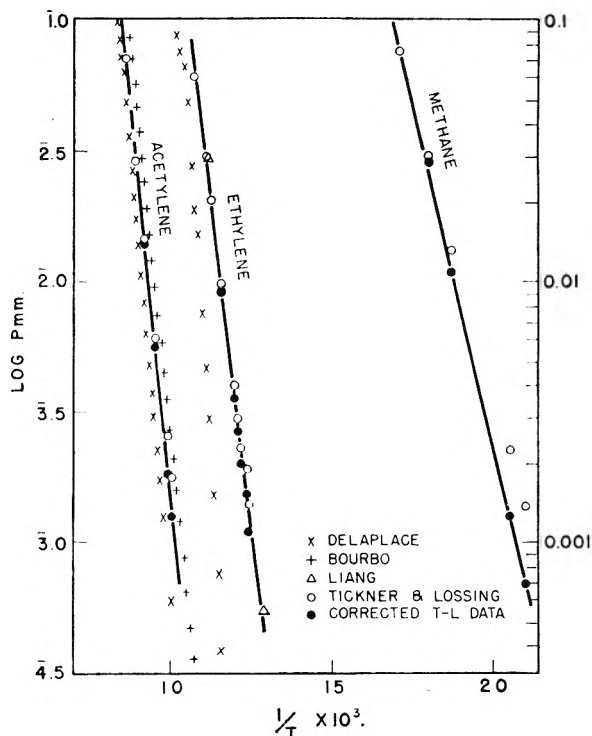


Fig. 1.—Vapor pressures of methane, ethane and ethylene: ×, Delaplace; +, Bourbo; Δ, Liang; O, Tickner and Lossing; ●, corrected T-L data.

transpiration effect, are plotted in Fig. 1 to compare with the uncorrected values and the values of other investigations. As the corrected values are believed to be the most reliable, for reasons to follow, and they can be represented by a straight line relationship

$$\log P \text{ mm.} = A - \frac{B}{T} \quad (2)$$

the constants *A* and *B* for all three gases are given in Table III.

TABLE III
CONSTANTS FOR VAPOR PRESSURE AND APPLICABLE TEMPERATURE

	Methane	Ethylene	Acetylene
A	7.655	9.526	9.630
B	515	998	1250
Highest applicable <i>T</i> , °K.	90	115	140

To use eq. (2) and Table IV, attention is called to the fact that they are only applicable up to a certain temperature and the highest applicable temperature for each gas is given in Table III as well.

Methane.—The vapor pressure of methane seems to be one of the least investigated. The data from the Bureau of Standards⁵ extend only down to 10 mm., below which Tickner and Lossing's work appears to be the only one. Equation (2) agrees with the Bureau of Standards value up to about 100 mm., above which the straight line takes a new slope.

Ethylene.—Within the temperature range where eq. (2) is applicable, the only other work is due to

(4) J. O. Hirschfelder, R. B. Bird and E. L. Spatz, *J. Chem. Phys.*, **16**, 975 (1948).

(5) National Bureau of Standards, A. P. I. Project 44, "Selected Values of Properties of Hydrocarbons." (1949).

Delaplace who calculated the vapor pressure by thermal conductivity.⁶ His data are also shown in Fig. 1. His values appear to be much too low as the temperature lowers. Inasmuch as his method is an indirect one, we incline to ignore his data.

Acetylene.—The vapor pressure of acetylene has attracted unusual attention. Aside from the data of Tickner and Lossing, Delaplace⁶ and Bourbo⁷ supply another two sets. The results of Delaplace again appear to be too low. The comparison between the results of Bourbo and the corrected values of Tickner and Lossing is of interest. The values plotted in Fig. 1 are taken from the table given by Bourbo. There is a small but definite difference between the T.-L. and Bourbo results. In terms of pressure, the two sets differ by a factor of 1.4 in the higher pressure region and 1.8 in the lower pressure region. In terms of temperature, the two sets differ by 2 degrees at all pressures. The temperatures recorded by T.-L. are accurate to $\pm 0.5^\circ$; if the Bourbo temperature scale is off by about 1° ,

(6) R. Delaplace, *Comp. rend.*, **204**, 493 (1937).

(7) P. S. Bourbo, *J. Phys. (U.S.S.R.)*, **7**, 286 (1943).

then the difference between the two can be accounted for by other experimental errors. Since we know the accuracy of T.-L. measurements, we choose their values as standard. While this is rather arbitrary, there is a somewhat side line evidence. Bourbo's data in such low pressure ranges fit exactly into the extrapolation of Stull's values⁸ which extend down to 10 mm. only. This is not the general behavior of other hydrocarbons which all exhibit a change of slope with temperature. The results of Tickner and Lossing, when corrected for R-effect, follow this general rule.

Other Gases.—The data of Tickner and Lossing on other gases, including carbon dioxide, may all need small corrections. However, owing to the low accuracy in their temperature measurements ($\pm 0.5^\circ$), the corrections are about the same as their experimental errors.

Acknowledgment.—The author is indebted to Drs. Tickner and Lossing for much of the detailed information about the vapor pressure measurements.

(8) D. Stull, *Ind. Eng. Chem.*, **39**, 517 (1947).

THE CATALYTIC ACTIVITY OF SOME REDUCED VANADATE SALTS

By C. S. ROHRER, R. C. CHRISTENA AND O. W. BROWN

Contribution No. 537 from the Department of Chemistry, Indiana University, Bloomington, Indiana

Received July 10, 1951

The optimum operating conditions for each of the catalysts are summarized in Table VIII for the reduction of nitronaphthalene to 1-naphthylamine. Of the catalysts studied copper gave the highest yields of the amine. Reduced nickel vanadate is too active for reduction to the amine giving appreciable amounts of the over reduction product, naphthalene. Small amounts of 1,2,5,6-dibenzophenazine were produced by the use of reduced copper vanadate and lead vanadate catalysts.

Many studies have been carried out on the properties of reduction catalysts, particularly on the metals prepared by the reduction of their oxides. These metals have been classified into various systems, in attempts to predict the best catalysts for hitherto unexplored systems. Many other investigations have been made on addition agents and their effects in modifying the activity or selectivity of these metal catalysts. On the other hand little has been reported as to the manner in which these catalysts may be altered by reduction from their salts. Studies are now being made on the classified effects of acid radicals as moderators or promoters on these reduced metal or reduced compound catalysts. Reports of the catalytic activity of copper chromate,¹ nickel tungstate² and cobalt molybdate³ in the reduction of nitro compounds to their respective amines have been published. This paper will deal with a systematic study of the variables concerned in obtaining the maximum activity of reduced nickel, copper and lead vanadates for the gas phase reduction of 1-nitronaphthalene to 1-naphthylamine. These cations were chosen as representatives from each of three groups, nickel being of extreme activity in the

reduction of nitrobenzene, even giving reduction within the benzene ring; copper, from those metals of moderate reducing activity; lead, of a group with considerably less activity.

Apparatus.—The apparatus was the type usually employed in such studies. A horizontal type electrically heated, metal block furnace containing a reaction tube of $1/2$ -inch iron pipe was employed. The furnace was thermostatically controlled, and temperatures were measured in the block and in the 10-inch catalyst bed at points one inch from each end. The feed was through a capillary tube with the rate regulated by a variable head of mercury. An oven thermostatically controlled at 77° was placed at the head of the furnace to contain the 1-nitronaphthalene feed tube, in order that the reagent be maintained as a liquid with a nearly constant viscosity. Hydrogen flow was measured in liters per hour through a calibrated flow meter.

Preparation of the Catalysts.—Copper oxide was prepared by the method of Brown and Henke.⁴ The salts were prepared by adding solutions of copper sulfate pentahydrate, nickel acetate tetrahydrate and lead acetate trihydrate to hot solutions of ammonium metavanadate. Vanadium pentoxide was prepared by adding glacial acetic acid to a boiling solution of ammonium metavanadate. Each of the above precipitated compounds was washed repeatedly with distilled water except that the nickel vanadate, which is appreciably soluble, was washed with ethyl alcohol. The compounds were then dried overnight at 145° .

Ten grams of a compound prepared as above, was evenly distributed in a ten-inch bed in the cold catalyst furnace and reduced under a stream of 14.5 liters of hydrogen per hour.

(1) H. A. Doyal and O. W. Brown, *This Journal*, **36**, 1549 (1932).

(2) C. S. Rohrer, J. Rooley and O. W. Brown, *ibid.*, **55**, 211 (1951).

(3) F. A. Griffiths and O. W. Brown, *ibid.*, **42**, 107 (1938).

(4) O. W. Brown and C. O. Henke, *ibid.*, **26**, 715 (1922); F. A. Madenwald, C. O. Henke and O. W. Brown, *ibid.*, **31**, 862 (1927).

One hour was required to bring the copper oxide to 296°, nickel vanadate to 304° and copper vanadate to 302°, while two hours were required to bring lead vanadate to 425° and one hour and forty minutes were required to bring the vanadium pentoxide up to 407°. Each was maintained at its respective temperature for one additional hour.

Discussion

Copper Catalyst.—Copper was shown by Sabatier⁵ to have a high degree of selectivity in the complete conversion of the nitro group to the amine, without reduction in the benzene ring. For the purpose of comparing the activity of a catalyst in the reduction of 1-nitronaphthalene to 1-naphthylamine with that of nitrobenzene to aniline, copper was studied first.

Figure 1 curve 5 shows the effect of the operating temperature on the percentage conversion to amine. The operating conditions for the construction of this curve were 8 liters of hydrogen per hour, a rate of 1-nitronaphthalene of 4.5 to 5.0 g. per hour over 10 g. of copper oxide reduced to copper. The temperature of approximately 256° for maximum conversion agrees well with the 260° reported by Brown and Henke⁴ for the reduction of nitrobenzene.

The rate of flow of hydrogen giving the maximum yield is seen from Table I to be 432% of the theoretical where a conversion of 99.9% was observed. Analytical results became inconsistent at lower flow due to the difficulty of sweeping the catalyst free of the reaction product.

As with nitrobenzene⁴ copper is seen to give practically complete conversion of 1-nitronaphthalene to the amine with practically no decomposition or by-products.

TABLE I

Catalyst, 10 g. copper oxide reduced; temperature of catalyst, 256°; reactant rate, 4.5 to 5.0 g. per hour

Liters per hour of hydrogen	Hydrogen % of theory	Yield of amine, Wt. %
8	432	99.9
16	864	99.4
24	1296	98.4

Reduced Vanadium Pentoxide Catalyst.—This catalyst was difficult to work with due to its extremely short life. After four or five runs the yields dropped about 10%. For this reason the points shown in Fig. 1 curve 4 do not represent averages of two or more determinations as do the other data in the paper; however, on the other catalysts single runs were very seldom in error by more than 1 or 2%. For the same reason only qualitative determinations on the rate of flow of hydrogen and 1-nitronaphthalene were made. The temperature of 374° for the maximum conversion to the amine, Fig. 1 curve 5, lies between the 365° reported by Brown and Henke⁶ and 403° reported by Doyal and Brown¹ who reduced nitrobenzene to aniline over reduced vanadium pentoxide. The operating conditions for this curve were 14.5 liters per hour of hydrogen and 5.9 to 6.7 g. per hour of 1-nitronaphthalene over 10 g. of vanadium pentoxide reduced.

(5) Paul Sabatier, "Catalysis in Organic Chemistry," D. Van Nostrand Co., Inc., New York, N. Y., 1922.

(6) O. W. Brown and C. O. Henke, *THIS JOURNAL*, **26**, 272 (1922).

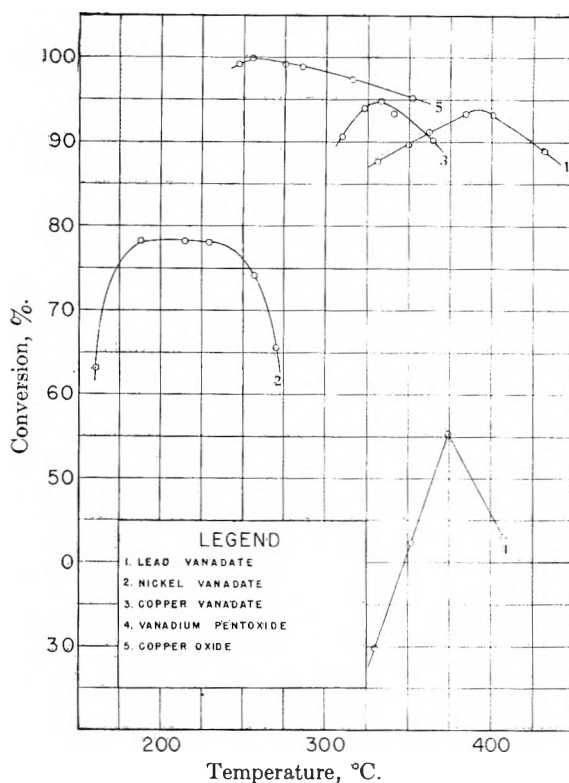


Fig. 1.—Conversion, % vs. °C.: 1, lead vanadate; 2, nickel vanadate; 3, copper vanadate; 4, vanadium pentoxide; 5, copper oxide.

Reduced Nickel Vanadate Catalyst.—The optimum temperature for the reduction of the nitro group over this catalyst is seen from Fig. 1 curve 2 to be between about 185 to 235°. The operating conditions for determining the points on this curve were 18.5 liters of hydrogen per hour, 4.5 to 6 g. of 1-nitronaphthalene per hour over catalyst obtained from 10 g. of nickel vanadate. The temperature chosen for the optimum on further experiments was therefore 210°.

Table II shows a ratio of hydrogen to the nitro compound of from 703 to 1000% of the stoichiometrically required amounts to give a maximum yield of the amine.

TABLE II

Catalyst, 10 g. of nickel vanadate reduced; temperature of catalyst, 210°; reactant rate, 4.5 to 6 g. per hour

Liters per hour of hydrogen	Hydrogen, % of theory	Yield of amine, Wt. %
2.8	150	67
4.0	216	73
13.0	703	79
18.5	1000	79
25.3	1368	78
3.16	1708	75

Obtaining quantitative results over this catalyst was extremely difficult since one is operating at temperatures approximately 95° below the boiling point of 1-naphthylamine and attempts to sweep the catalyst clean of the adsorbed reactant rendered results accurate to little better than $\pm 1\%$. In determining the optimum rate of flow of the reactant, then, one can conclude from the data of Table

III only that the yield of amine changes little with rates from 5.3 to 12 g. per hour.

TABLE III

Catalyst, 10 g. of nickel vanadate reduced; temperature of catalyst, 210°; rate of hydrogen, 18.5 liters per hour.

Reactant rate, g. per hour	Yield of amine, Wt. %
5.3	77
8.7	78
12.2	78
18.1	75

This catalyst was too active for reduction to the amine as seen by the appearance of beautiful white leaflets of naphthalene in the condenser.

The optimum temperature for reduction lies between that reported by Brown and Henke¹ for nickel in the reduction of nitrobenzene at 192° and the approximately 375° here reported for the reduction over reduced vanadium pentoxide.

Reduced Copper Vanadate.—The reduction temperature found to give a maximum yield of amine was 333°, Fig. 1 curve 3. The operating conditions for the construction of this curve were 16 liters of hydrogen per hour, 2.0 to 2.2 g. per hour of 1-nitronaphthalene over 10 g. of copper vanadate reduced. Table IV shows a maximum for the rate feed to be 2 g. per hour or less. From the results on individual runs this curve appears to level off at rates below 2 g. per hour, however the difficulty of duplicating made it impractical to carry the rate lower, and 2 g. per hour was taken as the optimum.

TABLE IV

Catalyst, 10 g. copper vanadate reduced; temperature of catalyst, 333°; rate of hydrogen, 16 liters per hour

Reactant rate, g. per hour	Yield of amine, wt. %
2.0	94.8
5.1	88.9
6.7	79.5
15.6	58.0
23.8	49.2

Table V shows 16 liters per hour as the optimum rate of flow of hydrogen; however, there was no detectable difference in rates of from 14 to 18 liters per hour.

TABLE V

Catalyst, 10 g. copper vanadate reduced; temperature of catalyst, 333°; reactant rate, 2.0 to 2.2 g. per hour

Liters per hour of hydrogen	Hydrogen, % of theory	Yield of amine, wt. %
8	432	89.9
16	864	94.8
24	1296	91.6

At temperatures well above the optimum naphthalene appeared in small quantities. Also occurring as a by-product was 1,2,5,6-dibenzophenazine. It occurred in amounts as great as 3.5% on a new catalyst but decreased to about 1% or less as the

activity for the amine formation increased. Low rates of hydrogen also increased the yield of the dibenzophenazine.

Reduced Lead Vanadate.—From Fig. 1 curve 1 it is seen that the temperature for maximum conversion is approximately 392°. The operating conditions for the points listed on this curve were 18 liters of hydrogen per hour, and 2.0 to 2.2 g. of 1-nitronaphthalene per hour over 10 g. of lead vanadate reduced.

The maximum yields of amine occur at hydrogen rates of from 16 to 18, or more, liters per hour and proved to be approximately constant over this range, Table VI.

TABLE VI

Catalyst, 10 g. lead vanadate reduced; temperature of catalyst, 362°; reactant rate, 2.0 to 2.2 g. per hour

Liters per hour of hydrogen	Hydrogen, % of theory	Yield of amine, wt. %
8	432	84.7
16	864	91.1
18	972	91.1
24	1296	90.7
32	1728	85.9

Due to the difficulty in controlling very low rates of feed, Table VII terminates with a level maximum yield of amine from between 2.1 and 1.4 g. per hour.

TABLE VII

Catalyst, 10 g. lead vanadate reduced; temperature of catalyst, 362°; rate of hydrogen, 18 liters per hour

Reactant rate, g. per hour	Yield of amine, wt. %
1.4	91.1
2.1	91.1
4.1	88.7
5.9	85.3
7.8	80.5
8.7	80.0

Brown and his co-workers¹ found the optimum of 308° for the reduction of nitrobenzene over lead. While experiments in this Laboratory on other compound catalysts have not confirmed this behavior, it is of interest to notice that each of the three compound catalysts reported in this paper have optimum temperatures for the reduction of the nitro group lying between that for the reduced oxide of the cation and that for reduced vanadium pentoxide.

As with the copper vanadate a few per cent. of 1,2,5,6-dibenzophenazine occurred, the yields increasing with lower temperatures, low hydrogen rates, and the newness of the catalyst.

TABLE VIII

Catalyst	Tempera- ture, °C.	Hydro- gen, % of theory	Reactant rate, g. per hour	Yield of amine, wt. %
Copper	256	432		99.9
Nickel vanadate	210	1000	5.0-12.0	78.2
Copper vanadate	333	864	2.0- 2.2	94.8
Lead vanadate	392	974	1.4- 2.0	93.3
Vanadium pentoxide	374	55.4

PREFERENTIAL CAPILLARY ADSORPTION OF WATER FROM SOLUTIONS OF ALCOHOLS BY SILICA GEL¹

BY F. E. BARTELL AND D. JOSEPH DONAHUE

University of Michigan, Ann Arbor, Michigan

Received July 13, 1951

The isotherms for the adsorption of water from *n*-butyl, *n*-amyl, *n*-hexyl, and heptyl alcohols at 0, 25, and 45° were determined by means of the Karl Fischer method of water analysis and the amounts adsorbed were plotted against the reduced concentrations. The Brunauer, Emmett and Teller equation was applied to the adsorption data and the physical significance of the BET constants $(x/m)_m$, n and c' were examined. The value of $(x/m)_m$ per unit area was shown to be at least partially dependent upon the solubility of the solute in the solvent. The values of n and c' appear in these cases to represent the physical significance implied by the BET theory. From the isotherms it was observed that at reasonably high reduced concentrations a process analogous to capillary condensation in gases must have occurred which caused an apparently large increase in the amount adsorbed. Evidence was presented which indicated that the rapid increase in apparent adsorption resulted from separation of a water rich phase in the capillaries. Study of the dehydrating ability of silica gel has shown that the effectiveness of the dehydration increases rapidly with the decrease of the solubility of the water in the solvent. Evidence in support of the preferential adsorption theory of membrane semi-permeability has been presented. The large apparent adsorption of water observed in the high concentration region of the isotherms gives strong support to this theory. It was found that water displaced other components from the capillaries of a hydrophilic gel. This would prevent the passage of other components through the capillaries and in a continuous gel membrane would result in a membrane which would be semi-permeable or nearly semi-permeable to water only.

Recent work on adsorption in this Laboratory² showed that the Brunauer, Emmett and Teller (B.E.T.) equation represents multi-molecular adsorption from binary liquid solution as well as it represents adsorption from gaseous systems. In that study, as has been the case in most studies of adsorption from solutions, different solutes were adsorbed from a given solvent. It seemed desirable that a similar study be made of the adsorption of a given solute from different solvents. By conducting such experiments at different temperatures further information could be obtained as to the general applicability of the B.E.T. equation to adsorption from solution.

The isotherms for the adsorption of vapors by highly porous adsorbents, such as silica gel, normally show a rapid increase in apparent adsorption in the intermediate, or higher, pressure region. This rapid increase in apparent adsorption is a result of capillary condensation of the vapor within the pores of the adsorbent. It seemed possible that adsorption of a solute from solution with such a porous adsorbent might tend to give analogous effects and might at least give some interesting and perhaps previously unobserved results. Highly porous silica gel appeared to be a logical choice for the adsorbent and water an ideal choice for the solute. Solvents for these systems should be liquids with which water would have limited solubility; accordingly some of the higher alcohols were selected. It was believed that adsorption data obtained with such systems would furnish worthwhile information concerning the specific effect of the solvent. Of special importance would be information relating to the dehydrating properties of silica gel when used with various organic liquid systems in which the solubility of water was limited. The data also should show the extent to which water is preferentially adsorbed within the capillaries of the gel. Such information should

be valuable in a study of the semi-permeability of membranes. The object of this investigation was therefore to obtain isotherms for the adsorption of water from organic solutions by silica gel and to consider the fundamental significance of the data obtained.

Experimental

Analysis of Water.—The Karl Fischer method for the determination of water was used in the adsorption studies as also in the solubility measurements. The apparatus used is illustrated in Fig. 1. The end-point of the direct titration was detected by means of the potentiometric method. The circuit as described by Kieselbach³ was used in conjunction with platinum and tungsten electrodes.

The Karl Fischer reagent was prepared and standardized daily with a solution of water in methanol by the method of Mitchell and Smith.⁴

Materials

Liquids.—During the purification of the alcohols no attempt was made to remove the last trace of water since all of the solutions were analyzed for their water content prior to use. A four-foot packed column was used for all of the fractional distillations. Eimer and Amend best grade *n*-butyl alcohol and Eastman Kodak Co. best grade *n*-heptyl alcohol were fractionally distilled. Eastman practical grade *n*-hexyl alcohol was fractionally distilled twice. Eastman practical grade *n*-amyl alcohol was purified by the method previously employed in this Laboratory.² The water used was distilled water which had been redistilled from an alkaline permanganate solution.

Silica Gel.—Eimer and Amend silicon tetrachloride was distilled and the middle fraction was again distilled into twice distilled water until the rapidly stirred solution showed a blue tinge. After the solution had set to a gel it was heated in an oven at 55 to 75° for 15 days in order to remove most of the water and acid from the silica. It was then heated to 230° and washed. The heating and washing was repeated until all of the hydrogen chloride was removed. The gel was finally activated at 300°.

Procedures

The specific surface area of silica gel was determined by the Brunauer, Emmett and Teller method⁵ using adsorption of nitrogen at liquid nitrogen temperatures. This area was found to be 455 sq. m./g.

The Kelvin radius was calculated from the adsorption isotherm of ethyl alcohol obtained with this gel. This deter-

(1) The data in this paper were taken from a portion of a thesis by D. Joseph Donahue, submitted to the School of Graduate Studies of the University of Michigan in partial fulfillment of the requirements for the Ph.D. degree, June, 1951.

(2) R. S. Hansen, Y. Fu and F. E. Bartell, *This Journal*, **53**, 769 (1949).

(3) R. Kieselbach, *Ind. Eng. Chem., Anal. Ed.*, **18**, 726 (1946).

(4) J. Mitchell and D. M. Smith, "Aquametry," Interscience Publishers, Inc., New York, N. Y., 1948.

(5) S. Brunauer, P. H. Emmett and E. Teller, *J. Am. Chem. Soc.*, **60**, 309 (1938).

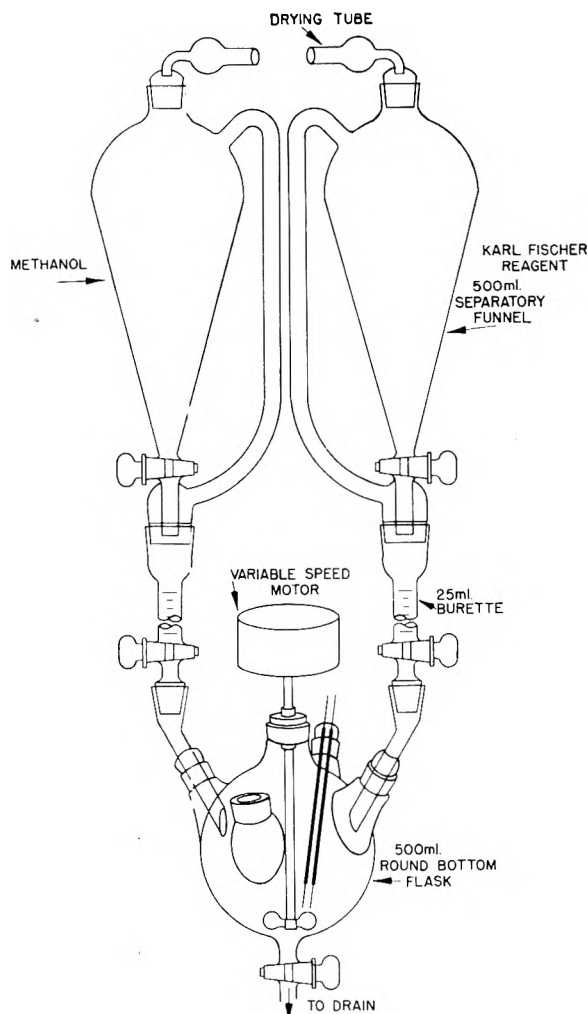


Fig. 1.

mination was made with a modified McBain and Bakr type gravimetric gas adsorption apparatus which was described by Bartell and Dobay.⁶ The Kelvin radius was found to be 41 Å. From the amount of ethyl alcohol adsorbed at the saturated vapor pressure the pore volume of the gel was calculated to be 0.99 ml./g.

For the determination of solubility, alcohol with excess water was shaken mechanically in a constant temperature-bath at $25.0 \pm 0.1^\circ$ and at $45.0 \pm 0.1^\circ$ for 48 hours. Similar solutions were subjected to intermittent shaking in an insulated ice-bath held at 0° . Samples of the saturated alcohol phases were pipetted into the titration flask and analyzed. Each value reported is the average of at least four determinations. The densities of the saturated phases were determined at these same temperatures. The data are recorded in Table I.

In the determination of the adsorption data the initial solutions were made up to approximately the desired strength volumetrically and were analyzed for water content with Karl Fischer reagent. In general, for each determination approximately 1 g. of silica gel was weighed into a 10-ml. glass stoppered erlenmeyer adsorption flask and 5 ml. of the analyzed solution was added. In the region of high reduced concentrations successively smaller samples, down to 0.05 g., of silica gel were used with the same volume of liquid. After sealing, the flasks were submerged to their necks in a water-bath at $25.0 \pm 0.1^\circ$, or at $45.0 \pm 0.1^\circ$ and mechanically shaken for 48 hours. The data for the 0° isotherms were obtained by supporting the flasks in an insulated ice-bath and shaking them intermittently over a period of 48 hours. Following the shaking period samples of the liquid

(6) F. E. Bartell and D. G. Dobay, *J. Am. Chem. Soc.*, **72**, 4388 (1950).

TABLE I
THE SOLUBILITY OF WATER IN THE DIFFERENT ALCOHOLS
AND THE DENSITIES OF THE SOLUTIONS

Alcohol	Temperature, °C.	Density saturated alcohol phase, g./ml.	Solubility of water in the alcohols Molar, moles/l.	Mole fraction
<i>n</i> -Butyl	0	0.8594	8.50	0.471
	25	.8432	9.15	.500
	45	.8282	9.50	.515
<i>n</i> -Amyl	0	.8502	4.28	.328
	25	.8325	4.75	.357
	45	.8174	5.00	.377
<i>n</i> -Hexyl	0	.8454	2.80	.265
	25	.8284	3.07	.288
	45	.8121	3.20	.303
<i>n</i> -Heptyl	0	.8450	2.30	.250
	25	.8268	2.46	.267
	45	.8117	2.53	.277

were pipetted directly from the adsorption flasks in the thermostats into the Karl Fischer titration assembly where they were analyzed.

The isotherms for the adsorption of water by silica gel from *n*-butyl, *n*-amyl, *n*-hexyl and *n*-heptyl alcohol solutions were constructed for 0 , 25 and 45° . The surface excess of the solute at equilibrium was calculated from the change in concentration of a known volume of bulk liquid during the adsorption process. Thus

$$x/m = (c_i - c_f) V = \text{millimoles solute adsorbed per gram of adsorbent}$$

and

$$x/ms = \text{millimoles adsorbed per unit area of adsorbent surface}$$

where c_i and c_f are the initial and final concentrations of the bulk solution of volume V , and m is the number of grams of

TABLE II
ADSORPTION OF WATER FROM *n*-BUTYL ALCOHOL BY SILICA GEL.

x/m , milli- moles/g.	0°		25°		45°	
	c/c_0		c/c_0		c/c_0	
0.62	0.034		0.59	0.033	0.49	0.032
0.96	.069		1.15	.102	0.78	.071
1.12	.102		1.60	.169	1.03	.105
1.95	.276		2.13	.277	1.95	.240
2.97	.453		3.36	.489	3.00	.398
3.10	.512		4.55	.688	4.90	.652
4.04	.638		4.89	.707	5.95	.707
5.55	.797		6.10	.768	6.61	.743
6.23	.831		7.26	.820	7.45	.757
7.55	.855		10.51	.840	8.53	.788

TABLE III
ADSORPTION OF WATER FROM *n*-AMYL ALCOHOL BY SILICA GEL.

x/m , milli- moles/g.	0°		25°		45°	
	c/c_0		c/c_0		c/c_0	
0.67	0.050		0.58	0.048	0.31	0.039
0.90	.079		0.69	.068	0.51	.070
1.49	.198		1.11	.135	1.07	.135
1.73	.272		1.58	.226	1.65	.240
2.19	.366		1.75	.259	1.95	.281
3.45	.641		2.34	.377	2.80	.443
4.51	.821		2.80	.485	3.50	.494
5.56	.841		4.06	.688	4.68	.683
7.97	.900		4.85	.773	5.60	.779
11.50	.932		11.80	.881	7.52	.829

TABLE IV
ADSORPTION OF WATER FROM *n*-HEXYL ALCOHOL BY SILICA GEL

0°		25°		45°	
<i>x/m</i> , milli- moles/g.	<i>c/c</i> ₀	<i>x/m</i> , milli- moles/g.	<i>c/c</i> ₀	<i>x/m</i> , milli- moles/g.	<i>c/c</i> ₀
0.58	0.050	0.39	0.035	0.32	0.048
.80	.088	.50	.049	0.63	.088
.94	.128	.94	.118	1.50	.248
1.40	.239	1.43	.226	1.99	.364
1.95	.370	1.93	.354	2.56	.445
2.81	.602	2.57	.486	2.82	.511
3.41	.677	3.36	.650	4.18	.685
4.84	.840	4.62	.780	5.14	.760
5.89	.875	6.70	.854	8.00	.815
9.11	.934	12.00	.915	9.24	.830

TABLE V
ADSORPTION OF WATER FROM *n*-HEPTYL ALCOHOL BY SILICA GEL

0°		25°		45°	
<i>x/m</i> , milli- moles/g.	<i>c/c</i> ₀	<i>x/m</i> , milli- moles/g.	<i>c/c</i> ₀	<i>x/m</i> , milli- moles/g.	<i>c/c</i> ₀
0.87	0.080	0.65	0.065	0.54	0.056
1.10	.122	.84	.094	0.76	.082
1.52	.226	.97	.110	1.19	.161
1.84	.319	1.29	.203	1.80	.287
2.30	.488	1.83	.340	2.10	.349
2.52	.538	2.52	.485	3.07	.516
3.51	.728	3.39	.631	3.44	.557
3.87	.773	4.21	.774	3.80	.660
4.86	.860	5.40	.852	5.26	.790
6.00	.915	11.50	.926	9.72	.842

the adsorbent having a surface area of *s* sq. cm. Tables II-V give the apparent adsorption values, *x/m*, in millimoles per gram together with the equilibrium reduced concentration values, *c/c*₀. These results are represented graphically in Figs. 2-5.

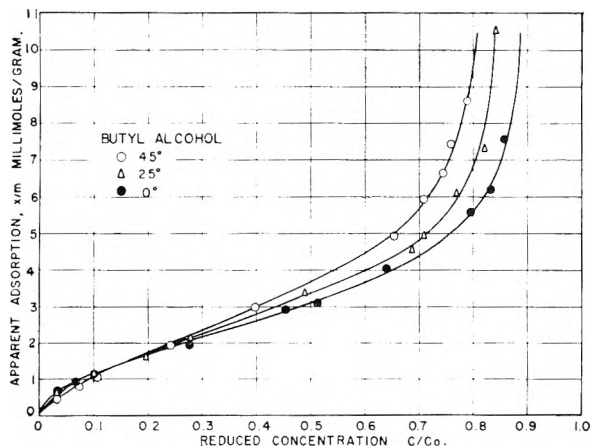


Fig. 2.

Discussion of Results

Multimolecular Adsorption from Solution.—The BET equation was found to represent multimolecular adsorption of water from solutions of alcohols as well as it represents gaseous adsorption. The equilibrium adsorption data were plotted to conform with the linear form of the equation and the values of (*x/m*)_m (the apparent number of millimoles of adsorbate in a monolayer per gram of ad-

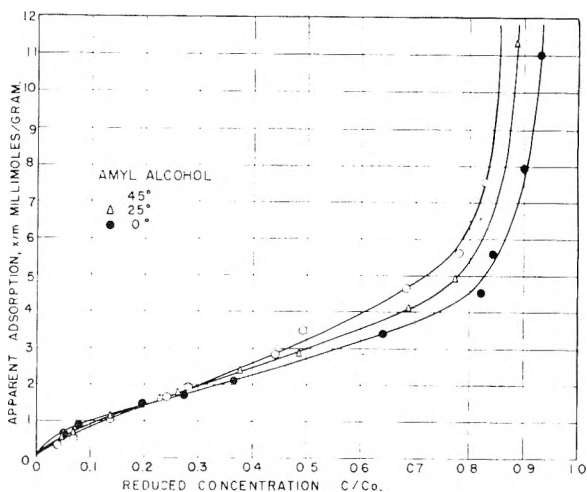


Fig. 3.

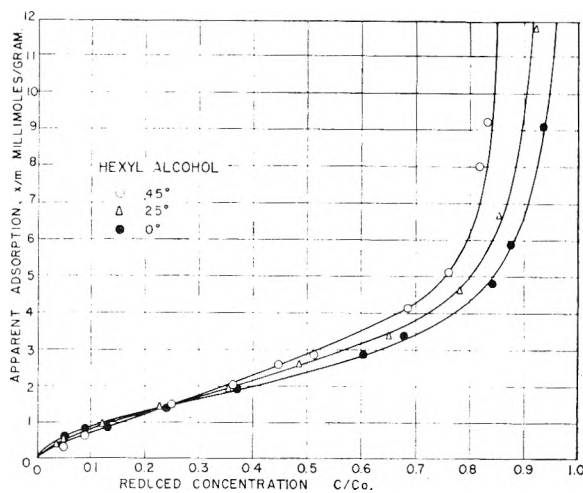


Fig. 4.

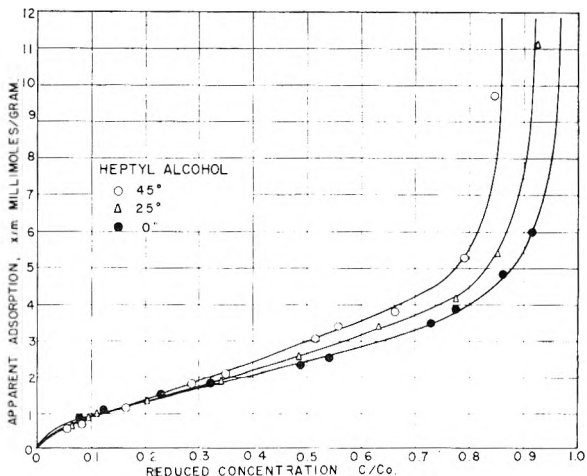


Fig. 5.

sorbent) and *c'* (a constant related to the heat of adsorption) were calculated from the slope and intercept of the line. The value of *n* (number of layers adsorbed) was determined by the method of Joyner, Weinberger and Montgomery.⁷ The values of these constants are summarized in Table VI.

(7) L. G. Joyner, E. B. Weinberger and C. W. Montgomery, *J. Am. Chem. Soc.*, **67**, 2182 (1945).

TABLE VI
 CONSTANTS OF THE BET EQUATION

Alcohol	Temperature, °C.	$(x/m)_m$, millimoles/g.	n	c'	$E_1 - E_L$, kcal./mole
<i>n</i> -Butyl	0	1.75	6	15.4	1.48
	25	1.91	6	10.5	1.39
	45	2.24	6	6.9	1.22
<i>n</i> -Amyl	0	1.54	6	12.7	1.38
	25	1.79	6	7.9	1.22
	45	1.97	6	5.6	1.09
<i>n</i> -Hexyl	0	1.29	6	15.2	1.48
	25	1.51	6	8.5	1.26
	45	1.73	6	5.6	1.09
<i>n</i> -Heptyl	0	1.30	6	18.7	1.59
	25	1.48	6	10.7	1.40
	45	1.72	6	7.5	1.28

Hansen, Fu and Bartell² found that $(x/m)_m$ was a function of the surface area of the adsorbent. They calculated the area each solute molecule would occupy on the adsorbent if $(x/m)_m$ millimoles of that solute per gram of adsorbent were distributed uniformly in a monolayer on the surface of the adsorbent. This area for each solute was found to be identical for the adsorption of the solute on different adsorbents. The fact that the same area values were obtained for each of given solutes against different adsorbents indicates that $(x/m)_m$ must be significantly related to the surface area and not to the physical structure of the solids.

The systems used in the present adsorption study were identical in all respects except for the alcohols which differed in structure by the number of methylene groups in their hydrocarbon chains. The similar nature of the different systems makes it possible to study the effect of the limited solubility of the solute on $(x/m)_m$, the apparent limiting number of millimoles of adsorbate in a monolayer per unit area of surface. One can compare the surface concentrations of the solute corresponding to an adsorption of $(x/m)_m$ with the concentrations of the saturated solutions of water in the alcohols both of which can be expressed in the same units. The surface concentrations appearing in Table VII are based on the assumption that the surface layer has a thickness which is equal to the length of the

 TABLE VII
 SURFACE CONCENTRATIONS

Alcohol	Temperature, °C.	Concentration saturated solution, moles/liter	Surface concentration at $(x/m)_m$, moles/liter
<i>n</i> -Butyl	0	8.50	7.35
	25	9.15	8.06
	45	9.50	9.65
<i>n</i> -Amyl	0	4.28	5.00
	25	4.75	6.00
	45	5.00	6.68
<i>n</i> -Hexyl	0	2.80	3.56
	25	3.07	4.28
	45	3.20	4.92
<i>n</i> -Heptyl	0	2.30	3.13
	25	2.46	3.60
	45	2.53	4.21

alcohol molecules. The lengths of the molecules were calculated from their cross sectional areas and their molar volumes. These data show that a change in the solubility of the solute brought about by the substitution of one solvent for another or by the alteration of the temperature results in a change of the surface concentration in the same direction and of similar relative magnitude as that of the solubility. It is thus evident that the apparent number of millimoles of adsorbate in a monolayer per unit area of surface is affected by the solubility of the solute.

Although the exact physical significance of n is not altogether clear its value appears in general to be related to the number of layers adsorbed. If n is directly related to the number of layers adsorbed then a small variation in the nature of the solvent or a small change of temperature would be expected to have little effect on n . This is in agreement with the results obtained for the adsorption of water from solution since n was found to have a value of six for all the isotherms determined. Hansen, Fu and Bartell⁴ and also Thomas⁸ found that for different solid-solution systems n had values ranging from one to four. The water used as solute in this investigation has molecules much smaller than those of the organic solutes used by the other investigators; therefore, the adsorption forces should extend through a greater number of layers of adsorbed water than of the adsorbed organic solutes. Water is also capable of strong hydrogen bond formation and the lower oriented layers should be more capable of attracting further layers than would the oriented layers of an organic solute. It is thus logical that water molecules should give a greater value of n than would the larger less polar organic molecules.

In the derivation of the BET equation for gases c' was defined as $c' = eE_1 - E_L/RT$, where E_1 is the heat of adsorption of the first layer and E_L is the heat of adsorption of the subsequent layers. The term E_L for adsorption from solutions should presumably be quite small owing to the fact that most of the available forces have been satisfied by the wetting of the solid by the bulk liquid and by the adsorption of the first layer. This would mean that the quantity $E_1 - E_L$ for adsorption from solution is a measure of the heat of adsorption of the solute. Hansen, Fu and Bartell² and Thomas⁸ found the BET heat of adsorption of organic solutes from solution by carbon to be approximately 2.5 kcal./mole while this heat for the adsorption of water from solution was found to be approximately 1.5 kcal./mole, Table VI. The displacement of a loosely bound water molecule from hydrophobic carbon by an organic liquid should be expected to liberate more energy than the displacement of a polar alcohol molecule from silica gel by water. Thus the values of the heats of adsorption obtained from the BET equation correspond with the physical picture of adsorption.

Capillary Condensation from Solution.—Although equations derived specifically for the physical adsorption of gases, such as the BET and the Langmuir equations, apply equally well to adsorp-

(8) T. L. Thomas, Thesis, University of Michigan (1948).

tion from solution, no case of capillary condensation of adsorbates from solution has, to our knowledge, ever been reported but such a process could conceivably occur in solutions should suitable conditions exist. In gaseous adsorption processes capillary condensation may be detected by the hysteresis effects which occur but since hysteresis effects cannot similarly be detected in the process of adsorption from solution, capillary condensation from solution could only be detected by a marked increase in the slope of the isotherm. Few if any complete isotherms for the adsorption of partially miscible solutes from solution by an adsorbent having pores suitable for the detection of capillary condensation from solution have been determined. The systems used in this investigation were chosen because they were believed to have suitable properties for the detection of capillary condensation from solution should it occur in the pores of the silica gel. An inspection of the isotherms, Figs. 2-5, reveals that as one increases the reduced concentration above approximately 0.8 the equilibrium amount adsorbed by the gel increases extremely rapidly. This is similar to the increase observed on corresponding isotherms obtained when capillary condensation occurs from the vapor phase with the same gel. This indicates that capillary condensation of a type actually does occur from solution. Even before this phenomenon begins the silica gel has adsorbed 4 to 6 millimoles of water per gram of gel. This amount of water distributed uniformly throughout the bulk solutions in the pores would produce solutions having concentrations greater than the concentrations of the saturated solutions of water in the alcohols. From the bulk solutions of still higher concentrations values of x/m as large as 25 millimoles of water per gram of silica gel were obtained and on a few occasions values even higher than this were obtained. The distribution of 25 millimoles of water uniformly throughout the bulk solutions in the capillaries would produce solutions having concentrations greater than 0.8 mole fraction of water. The higher x/m values may indicate that the solution within the capillaries approaches pure water. The experimental error in the determination of x/m is greater in the region of high reduced concentrations but the data never-

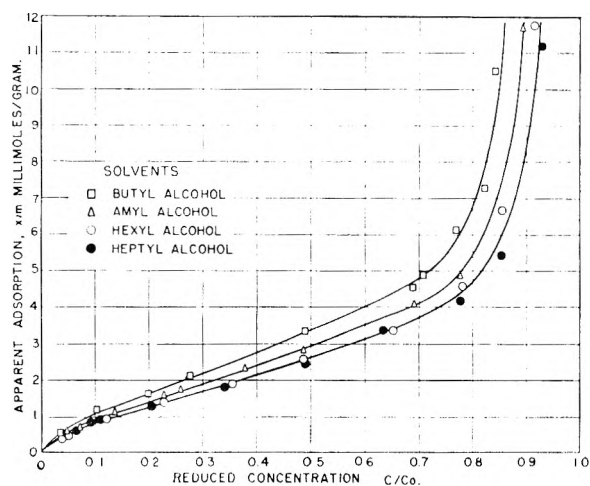


Fig. 6.

theless definitely show that the capillaries must have filled with a solution of high water content.

The process of this phase separation is probably comparable to that of the capillary condensation of gases. The concentration of the solute in the surface phase becomes quite high even at low reduced concentrations. As water is absorbed it probably begins to separate as a distinct phase which would be separated from the bulk liquid by a highly curved interface. The equilibrium across this interface should be shifted from that for the same two-phase system having an interface with a large radius of curvature. It is presumably this shift of equilibrium conditions which allows the water rich phase to continue to separate and to fill the capillaries.

Figure 7 is a plot of the data for the adsorption of water from *n*-butyl alcohol at 25° in the linear form of the BET equation in which the number of layers adsorbed is set equal to infinity. It will be observed that the adsorption in the intermediate region is less than is predicted by the theory. This type of deviation can be noted in nearly all cases of adsorption of gases and of solutes from solution. As the concentration is increased a point is reached at which the experimental curve crosses the theoretical curve into the region which shows that a greater amount has been adsorbed than is predicted by the BET theory for an infinite number of layers. This indicates that something other than physical adsorption alone caused this rapid increase in apparent adsorption. Curves of this nature were obtained by Bartell and Dobay⁷ for the vapor adsorption of aliphatic amines by silica gel which had a similar structure. They attributed this excessive adsorption to condensation of vapor in the capillaries. It is thus evident there exists in adsorption from solutions a phenomenon which is analogous to capillary condensation in gaseous adsorption. The occurrence of this phenomenon results in the filling of the capillaries of the silica gel with a solution of high water content.

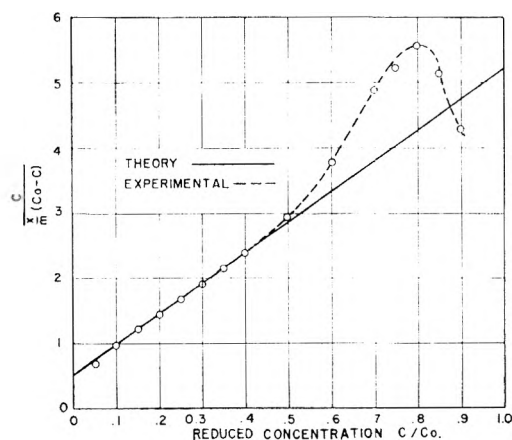


Fig. 7.

Dehydration with Silica Gel.—Although silica gel has been used as a dehydrating agent, both in industry and in research laboratories, but few fundamental studies of the adsorption of water from solution by silica gel have been made, and very little information is available on this subject. One

of the purposes of this investigation was to study the effectiveness of dehydration by silica gel from different solvents. For the purpose of comparison the four 25° isotherms have been plotted together on the same scale in Fig. 6. It is of interest to note that when one compares the isotherms for the ascending homologous series they are found to approach the same shape and for the higher members the isotherms become practically identical. If solvents representing still higher members of the series were to be used, it is believed that all the resulting isotherms would be approximately the same as those of the two higher alcohols. This would indicate that the amount of water adsorbed is a function of the reduced concentration of water and is largely independent of the total amount or molar concentration of the water present in the solution. The efficiency of water removal therefore increases rapidly as the solubility of the water in the liquid is decreased. It is apparent from the isotherms that silica gel would be a relatively poor dehydrating agent in the alcohol solutions studied but that it would be an excellent dehydrating agent for the removal of water from hydrocarbons and other liquids in which water is relatively insoluble.

Preferential Adsorption and Membrane Semi-permeability.—The results obtained in this investigation tend to support the theory that semi-permeability of osmotic membranes is the result of preferential adsorption. While it had previously been shown that water is adsorbed by osmotic membrane materials⁹⁻¹⁰ and that water tends to displace other liquids (or solutes) from the pores of hydrophilic solids,¹¹ there have, heretofore, been no quantitative data to indicate the extent to which water is preferentially adsorbed within the capillaries of such porous materials.

It seemed reasonable to assume that since a partially dehydrated silica gel adsorbs water preferentially from an aqueous solution the framework of the original non-dehydrated gel should likewise give preferential adsorption of water and, further, that if the pores formed within the gel structure were sufficiently small, a membrane of the gel should give osmotic effects.

To test this view an osmotic cell was prepared by using a small glass cylinder about 2 cm. in diameter and 4 cm. in depth. A piece of fine nylon cloth, to serve as a membrane support, was placed over one end of the cylinder followed by

a piece of waterproof cellophane (which later could be removed). These were held in place by a rubber band and constituted the bottom of the cell. A solution of "silicic acid" prepared by bringing together equal volumes of 1.15 sp. gr. sodium silicate solution and 6 *N* hydrochloric acid solution was poured into the cell to the depth of about 1 cm. and allowed to stand for a few hours, during which time it formed a firm gelatinous membrane.

For an osmotic experiment¹² a pure liquid, or an aqueous solution, was put into the cell. A one-hole stopper carrying a glass outlet tube (approx. 2 mm. i.d.) was inserted into the top of the cell and forced against the solution until the solution had risen in the glass tube a few centimeters above the stopper. The cellophane was removed from the bottom of the cell after which the cell was placed in a beaker containing about 400 ml. of water and lowered until the height of the liquid in the tube was at the water surface level. The temperature was maintained at approximately 25°.

In a series of osmotic experiments *n*-butyl, *n*-amyl, *n*-hexyl and *n*-heptyl alcohols were used. In one set of experiments water saturated solutions were used while in another set the pure alcohols were used. Osmotic effects were obtained in every case; within 24 hours the liquids in the different outlet tubes rose to heights ranging from 4 to 8 cm. For a given set of experiments the different alcohols gave effects of the same order of magnitude. Interestingly enough, very similar results were obtained when pure alcohol and when water-saturated solutions of alcohol were used in the cells. This should not be surprising for the cases of the higher alcohols when one considers that as soon as water begins to pass through the membrane the alcohol in contact with it at once becomes saturated and soon there exists immediately above the membrane an alcohol-saturated water phase and above this a water-saturated alcohol phase. After a few hours the menisci between phases rose to such heights that two liquid phases could readily be observed. Although water was preferentially adsorbed the membranes were not strictly semi-permeable; some alcohol was found to have passed through to the water compartments.¹³ Perhaps a denser gel with still finer pores would have been more nearly semi-permeable.

In another experiment a molar solution of sucrose produced a measurable hydrostatic pressure within a few hours. After four days the liquid in the tube had risen 7 to 8 cm. No trace of sugar was detected in the outer water. Against solutions of sugar the membrane appeared to be semi-permeable.

In still other experiments salt solutions were used. Aluminum chloride, 3 *N*, caused the liquid in the outlet tube to rise to a height of over 30 cm. in 48 hours. Tests showed that in this case aluminum chloride had diffused through the membrane into the water compartment. Water apparently was not preferentially adsorbed by the membrane from the solution of this electrolyte to as great an extent as from the sugar solution.

The results cited above are admittedly very qualitative in nature; nevertheless, they do show that hydrated silica gel membranes can function as osmotic membranes and tend further to strengthen the theory that membrane semi-permeability is the result of preferential adsorption of the solvent within the pores of the membrane.

(9) (a) J. Mathieu, *Ann. Physik.*, **9**, 340 (1902); (b) F. Tinker, *Proc. Roy. Soc. (London)*, **92A**, 357 (1916); **93A**, 268 (1917).

(10) H. B. Weiser, *This Journal*, **34**, 1826 (1930).

(11) F. E. Bartell and H. J. Osterhof, *Colloid Symposium Monograph*, **IV**, 234 (1926).

(12) The experimental work described herein was carried out by Mr. Lowell Schleicher whose assistance we wish hereby to acknowledge.

(13) In the experiments with the alcohols there was evidence that the framework of the gel tended to contract somewhat; this may have resulted in a leak between membrane and cell wall.

PRECIPITATION OF COLLOIDAL FERRIC OXIDE BY CORROSION INHIBITOR IONS

By W. D. ROBERTSON

Hammond Metallurgical Laboratory, Yale University, New Haven, Connecticut

Received July 17, 1951

The relative precipitating power with respect to a ferric oxide sol of anions employed as corrosion inhibitors has been determined. It is concluded that the colloidal precipitating power of anions is not a significant factor in the corrosion inhibition mechanism.

Introduction

Several proposals have been made regarding a possible connection between the relative precipitating power of various anions with respect to the positive ferric oxide sol and the pronounced effect of the same ions on the corrosion rate of iron.^{1,2} However, sufficiently extensive data for an adequate evaluation of the proposed correlation has not been available, particularly with regard to ions that markedly inhibit corrosion.

For the present purpose, the ions may be divided into three general classes in accordance with their effect on the corrosion rate: the accelerators, of which chloride is typical; sulfate and nitrate which have a less pronounced accelerating effect; and the inhibitors typified by chromate. Recently, nitrite³ and molybdate and tungstate⁴ have been added to the class of inhibitors. Thus, there is available a reasonably large group of anions of different charge whose general effect on corrosion rate is known and, since the effects of the various classes of ions are so greatly divergent, a correlation between their relative precipitating power and their effect on corrosion rate should be readily apparent. For example, chloride and nitrite are, respectively, an accelerator and an inhibitor but both are univalent anions; similarly, sulfate is a moderate accelerator whereas other divalent anions, chromate, molybdate and tungstate, are efficient inhibitors. If the rate of corrosion in solutions of these ions is directly related to their precipitating power, it may be anticipated that nitrite would fall in the class of divalent ions and presumably the mechanism of inhibition would then involve the precipitation of hydrated ferric oxide in contact with the reacting iron surface, inhibiting subsequent reaction. Alternatively, if the precipitation values of nitrite and sulfate are similar to other univalent and divalent anions, respectively, it may be concluded that colloidal considerations are not a predominant part of the corrosion or inhibition mechanism.

The following experiments were undertaken to obtain the necessary data with which to evaluate the proposed hypothesis.

Experimental Procedure

In view of the fact that only relative precipitating power of the ions was required for direct comparison, a commer-

(1) J. Newton Friend, *Carnegie Scholarship Memoirs*, **21**, 125 (1922).

(2) W. D. Robertson, "Encyclopedia of Chemical Technology," **4**, 487 (1949).

(3) A. Wachter and S. S. Smith, *Ind. Eng. Chem.*, **35**, 358 (1943); A. Wachter, *ibid.*, **37**, 749 (1945).

(4) W. D. Robertson, *J. (and Trans.) Electrochem. Soc.*, **98**, 94 (1951).

cially available, dialyzed 5% ferric oxide sol was used (Eimer and Amend So-D-12).

A stock solution containing 2 g. per liter of Fe_2O_3 was prepared by dilution and the pH adjusted to 5.0 ± 0.1 by dropwise addition of 0.1 M sodium hydroxide. The initial pH of the solution, 2.90, was increased to limit polymerization of the molybdate and tungstate ions and, to maintain the relative character of the experiment, all precipitations were carried out at constant pH as measured by the glass electrode. Subsequent experiments to determine the effect of the hydroxyl ion alone indicated that precipitation does not occur below pH 6.5.

Twenty milliliters of the stock solution and 20 ml. of a solution of the sodium salt of the precipitating ion were mixed in a reproducible manner in a container which was patterned after Weiser⁵ but more conveniently made entirely of glass from standard taper (45/50) Pyrex joints. Following inversion of the container, the resulting solution was poured into a test-tube and allowed to stand for 24 hours. Successive tests with bracketing concentrations resulted in a narrow range of ion concentration above and below the precipitation values given in Table I. In the event of questionable completeness of precipitation, the apparently clear supernatant liquid was pipetted out and tested with an excess of sodium sulfate.

The criterion of precipitation adopted was the appearance of a narrow band of clear solution (less than 1 mm.) at the top of the tube in 24 hours. In a series of ten tubes containing increasing concentrations of the precipitating ion, the distinction between (by definition) incomplete precipitation indicated by flocculation without clarification at the top of the tube and definite clarification was readily observed and verified by successive bracketing of concentrations for the purpose of narrowing the precipitation range.

Results

The values obtained are presented in Table I, together with those of Weiser and Middleton⁵ for comparison. It should be noted that the

TABLE I
PRECIPITATION VALUES FOR Fe_2O_3 SOL, 1 G. PER LITER, AT pH 5.0

Ions	Precipitation value (millimoles/liter)	
	This work	Weiser and Middleton
PO_4^{3-}	0.23	...
WO_4^{2-}	.33	...
CrO_4^{2-}	.36	0.650
$\text{Cr}_2\text{O}_7^{2-}$375
MnO_4^{2-}	.38	...
SO_4^{2-}	.40	.437
(OH ⁻)	(.73) pH 6.5	...
IO_3^-	...	0.900
NO_2^-	15.5	...
Cl^-	16.5	103.0
ClO_4^-	102.0	...
ClO_3^-	...	115.6
NO_3^-	...	131.2

(5) H. B. Weiser and E. B. Middleton, *This Journal*, **24**, 30 (1920).

comparison of the two sets of data, obtained with sols prepared in a different manner, is only indicative of similar trends; however, with the exception of the chloride ion, the correspondence between the two sets of data is good. The variation obtainable between univalent ions and the clear distinction between univalent and divalent ions is again demonstrated.

Conclusions

It is apparent from the data that nitrite, molybdate, tungstate and chromate fall in their respective class of univalent and divalent ions with respect to precipitating power; in other words, there is nothing distinctive about the inhibitor ions that

would indicate that their colloidal properties are involved in the inhibitor mechanism. The fact that sulfate, a moderate accelerator, and nitrite, an efficient inhibitor, have precipitation values characteristic of their charge apparently means that precipitation of colloidally dispersed corrosion products is not directly involved, otherwise chloride and sulfate should both be inhibitors or, alternatively, nitrite should be an accelerator.

Acknowledgment.—This work was done while the author was associated with the Institute for the Study of Metals, University of Chicago, and was in part supported by Army Air Force Contract #AF 33 (038) - 6534.

BOOK REVIEW

College Chemistry. By LINUS PAULING, Professor of Chemistry in the California Institute of Technology W. H. Freeman and Company, San Francisco, Calif. 1950. x + 705 pp. 213 figs. 37 tables. 16 × 24 cm. Price, \$4.50.

In this book—one might almost say edition—the illuminating and unconventional approach of Pauling's "General Chemistry" is still there, although in a more diluted form. The treatment of fundamentals is clear and adequate, although the occasional obscure sentences of "General Chemistry" have been not quite completely eliminated. At first glance the two books appear almost identical, but in "College Chemistry" the order of chapters has been changed—for example the treatment of gases and gas laws is now considered much earlier—and material shifted around between chapters; the contents have been expanded by addition of more factual matter on metallurgy, manufacturing processes, chemistry of the common elements, biochemistry and photography including color photography. The printing of the book and also the illustrations have been improved and there are very few misprints.

The main reason given for publishing "College Chemis-

try" is, it seems, the need for a freshman text "written in a more slowly paced and less mathematical form." The attempt to achieve a slower pace seems to have been made in the main, by the omission of paragraphs on more sophisticated topics, except in one or two chapters, such as the one on gases and gas laws, where a certain amount of rewriting has been done; many of the chapters, however, including the first five or so, have virtually the same wording as in "General Chemistry." The writing in a less mathematical form appears to consist in omitting the use of calculus in rate equations, thus bringing the book into line with most conventional freshman texts. A pity. In this reviewer's opinion it is questionable whether the average or subaverage freshman, to whom it seems popular to cater these days, will find the present book so much easier to understand than "General Chemistry" that its existence is justified. There is no doubt, however, that Prof. Pauling's "College Chemistry" is one of the best freshman texts available at the present time.

DEPARTMENT OF CHEMISTRY
HARVARD UNIVERSITY
CAMBRIDGE 38, MASSACHUSETTS

GEOFFREY WILKINSON

Now available.....

1950 ACS SPECIFICATIONS

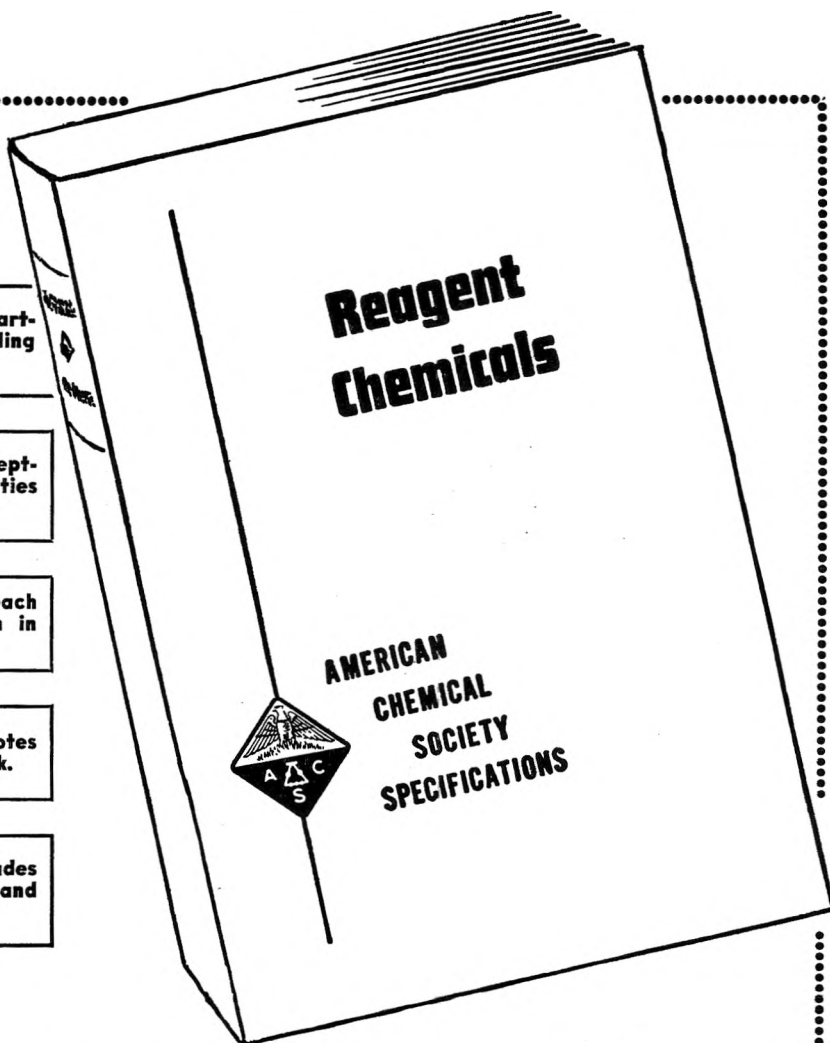
177 Reagents described, starting with acetic acid and ending with zinc sulfate.

Important properties and acceptable limits of usual impurities given for each reagent.

Approved test method for each property and impurity given in detail.

Convenient space for your notes provided throughout the book.

Total page count of 406 includes 30 pages of introduction and other pertinent material.



Price of the book in cloth binding \$5.00 postpaid.

SEND ORDERS TO:

**SPECIAL PUBLICATIONS DEPARTMENT
AMERICAN CHEMICAL SOCIETY
1155—16th Street, N.W., Washington 6, D.C.**

INDEXES

PUBLISHED BY
THE
AMERICAN
CHEMICAL SOCIETY

27-Year Collective Formula Index to Chemical Abstracts

Over half a million organic and inorganic compounds listed and thoroughly cross referenced for 1920 - 1946. In 2 volumes of about 1000 pages each.

Paper bound \$80.00 Cloth bound \$85.00

10-Year Numerical Patent Index to Chemical Abstracts

Over 143,000 entries classified by countries in numerical order with volume and page references to Chemical Abstracts for 1937 - 1946. Contains 182 pages.

Cloth bound \$6.50

Decennial Indexes to Chemical Abstracts

Complete subject and author indexes to Chemical Abstracts for the 10-year periods of 1917 - 1926, 1927 - 1936, and 1937 - 1946.

2nd Decennial Index (1917 - 1926) . . . Paper bound . . . \$ 50.00

3rd Decennial Index (1927 - 1936) . . . Paper bound . . . \$150.60

4th Decennial Index (1937 - 1946) . . . Paper bound . . . \$120.60

(Foreign postage on the Decennial Indexes is extra.)

Order from:

Special Publications Department

American Chemical Society

1155 - 16th St., N.W., Washington 6, D.C.